

Lib

AGARDograph 122

AGARDograph 122

# AGARD

ADVISORY GROUP FOR AEROSPACE RESEARCH & DEVELOPMENT

ORGANIZATION DU TRAITE DE L'ATLANTIQUE NORD

## Selected Topics In Electrofluid Dynamic Energy Conversion

*Editors*

Maurice Lawson      Frank Wattendorf

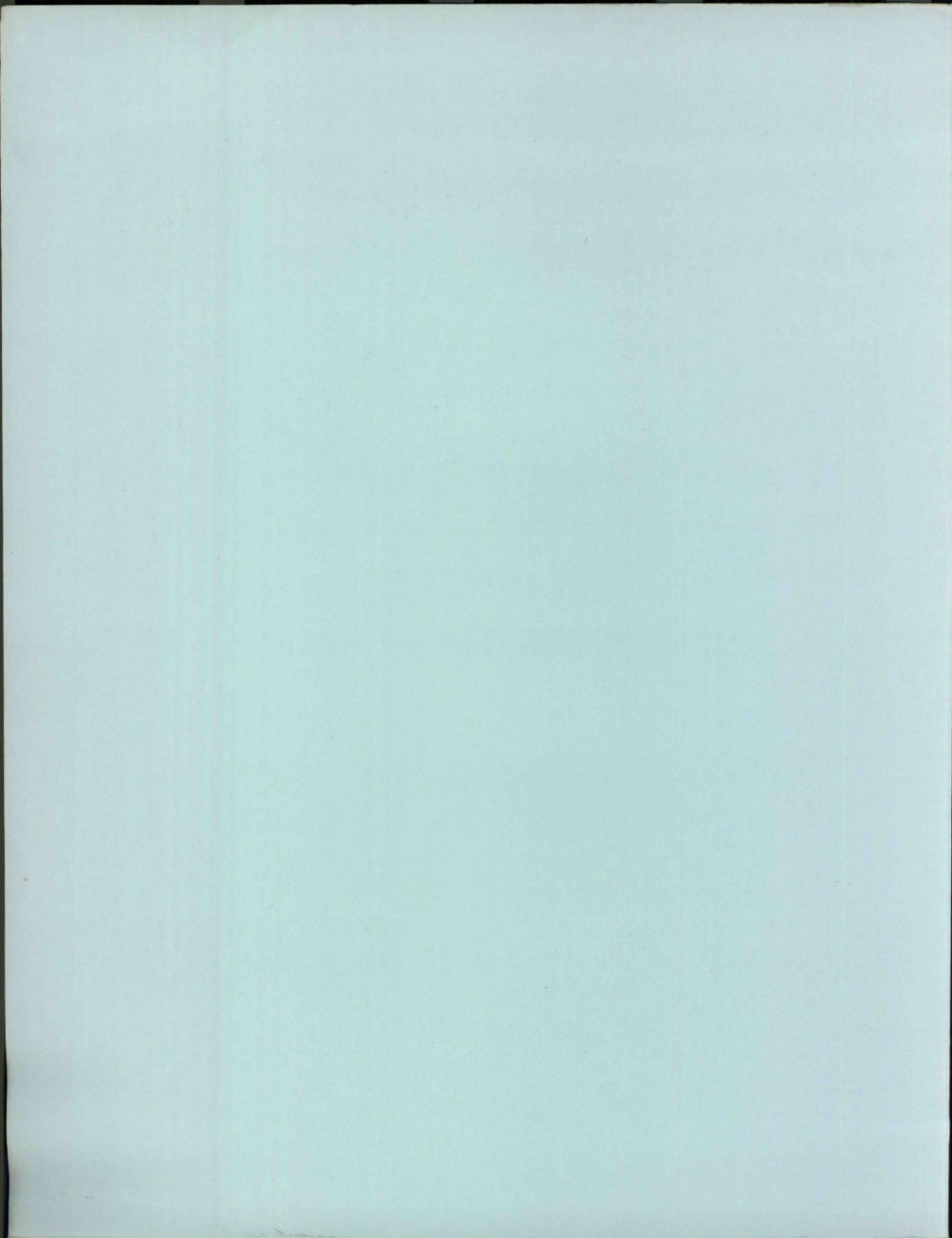


DECEMBER 1968



NORTH ATLANTIC TREATY ORGANIZATION





NORTH ATLANTIC TREATY ORGANIZATION  
ADVISORY GROUP FOR AEROSPACE RESEARCH AND DEVELOPMENT  
(ORGANIZATION DU TRAITE DE L'ATLANTIQUE NORD)

SELECTED TOPICS  
IN  
ELECTROFLUID DYNAMIC ENERGY CONVERSION

EDITORS

MAURICE LAWSON

FRANK WATTENDORF

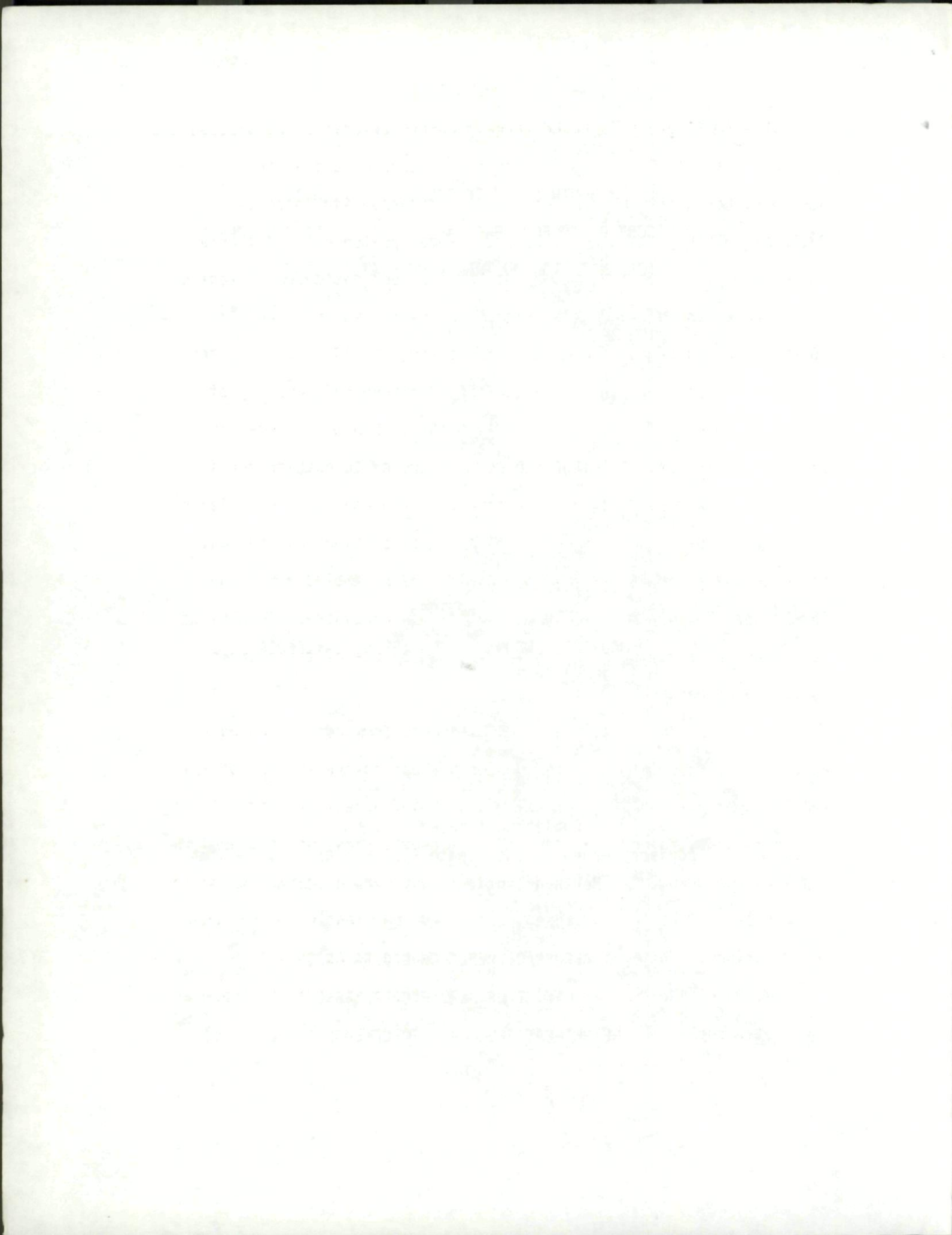
DECEMBER 1968

Published for and on behalf of  
Advisory Group for Aerospace Research and Development  
North Atlantic Treaty Organization

by

AEROSPACE RESEARCH LABORATORIES  
OFFICE OF AEROSPACE RESEARCH  
WRIGHT-PATTERSON AIR FORCE BASE, OHIO

538.4:533.95



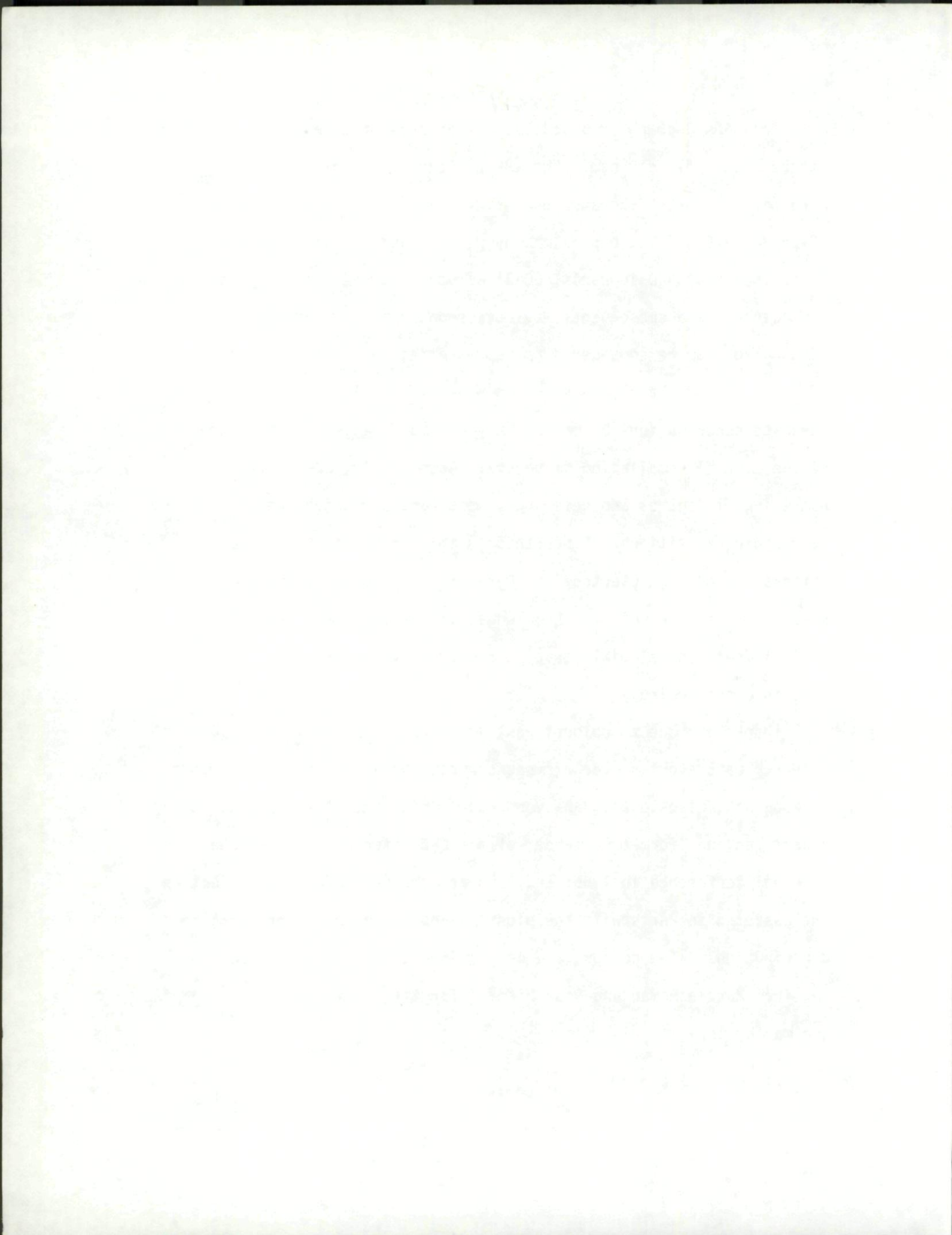
## PREFACE

This AGARDograph is based largely on presentations and discussions at the Electrofluid Dynamic "Workshop" Conference held at the Aerospace Research Laboratories, Wright-Patterson Air Force Base, Ohio, 23-25 May, 1966. The papers, however, were updated at an editorial conference at AGARD in Paris, 30-31 October 1967, attended by most of the authors; and subsequently by correspondence; so that the AGARDograph can be considered as representing the 1968 state of the art.

The editors have endeavored to preserve the individuality of the separate contributions by making only minimum changes, in the interest of the overall compilation of papers. Accordingly, each author's numbering of figures and references were kept unchanged, which leads to certain repetitions. Since this is the first time that so many different papers on Electrofluid Dynamics are assembled under the same cover, to the editors' knowledge, it was considered appropriate to include a general bibliography, prepared by one of the authors, Captain John Decaire.

Thanks are due to Colonel Paul Atkinson, Commander, Aerospace Research Laboratories, for his sponsorship and active support of this AGARDograph; also to Dr. Hans von Ohain, Chief Scientist, and Colonel Robert Fontana, former Commander of the Laboratories, who convened the original Conference in 1966; and to Jean Fabri and Jean-Pierre Contzen who assisted in Paris with the planning and coordination of European contributions. The editors are deeply indebted to Captain John Decaire, Marcia Homan and Rose Michael for their assistance in preparing the master copy.

The Editors



## SUMMARY

Electrofluid dynamic (EFD) energy conversion processes have only in recent years received renewed interest as an area of research. EFD processes are of particular interest for directly converting fluid dynamic energy into electrical energy without the use of moving parts.

This AGARDograph is based largely on presentation of EFD research or related research being conducted in each NATO nation represented at the Electrofluid Dynamic "Workshop" Conference which was held at the Aerospace Research Laboratories, Wright-Patterson Air Force Base, Ohio, 23-25 May 1966; subsequently, many of the papers were updated at an editorial conference held at AGARD, Paris, 30-31 October 1967, while others still later, were updated by correspondence.

## CONTENTS

PREFACE- - - - - The Editors	ii
GENERAL SUMMARY- - - - -	iii
NOTATION - - - - -	iv
INTRODUCTION - - - - - Frank Wattendorf	1
THE ROLE OF ELECTROFLUID DYNAMICS IN THE FIELD OF DIRECT ENERGY CONVERSION - - - - - Hans Pabst von Ohain	5
ELECTROFLUID DYNAMIC ENERGY CONVERSION PROCESSES CHARACTERISTICS AND RESEARCH AREAS - - - - - Maurice O. Lawson	15
EFFECTS OF ELECTRODE GEOMETRY      SIMILARITY AND SCALING LAWS IN EFD ENERGY CONVERSION PROCESSES	
I.   FUNDAMENTAL CONSIDERATIONS- - - - - John A. Decaire	35
II.   EXPERIMENTAL RESULTS - - - - - James R. Wifall	65
WORKING MEDIA FOR ELECTROFLUID DYNAMIC GENERATORS- - - - - Michael Hawes	97
SOME ANALYTICAL TREATMENTS OF EFD PROCESSES- - - - - John E. Minardi	125
SOME REMARKS ON EFD ENERGY CONVERSION- - - - - Jean-Pierre Contzen	181



DESIGN AND CONSTRUCTION OF A 3-MW MAGNETOGASDYNAMIC POWER GENERATION FACILITY AT THE UNIVERSITY OF TORONTO INSTITUTE OF AEROSPACE STUDIES - - - - -	189
S. J. Townsend	
PLASMA RESEARCH IN DENMARK - - - - -	203
K. Refslund	
COMMENTS ON ELECTROFLUID DYNAMICS AND RELATED RESEARCH IN FRANCE - - -	207
Jean Fabri	
THE ELECTROFLUID DYNAMIC ENERGY CONVERTER WITH SPACE CHARGE NEUTRALIZATION - - - - -	211
E. M. Knoernschild and P. E. Schoeck	
COMMENTS ON ELECTROFLUID DYNAMICS AND RELATED RESEARCHES IN ITALY- - -	235
L. G. Napolitano	
INTEREST AND PROGRESS IN ELECTROFLUID DYNAMICS AND RELATED RESEARCHES IN ENGLAND - - - - -	245
R. G. Voysey	
BIBLIOGRAPHY - - - - -	253

## NOTATION (ARL PAPERS)

- $a^*$  = Speed at Mach unity  
 $E_a$  = Applied electric field  
 $E$  = Electric field strength  
 $E_b$  = Breakdown electric field strength  
 $E_{b,n}$  = Breakdown electric field strength under normal atmospheric conditions  
 $E_h$  = Electric field strength at the exit electrode  
 $E_l$  = Electric field strength at the entrance electrode  
 $E_x$  = Electric field strength at station (x)  
 $E_{sc}$  = Electric field strength due to space charge  
 $h$  = Distance between the two parallel plane electrodes  
 $i$  = Current density in amperes per unit flow area  
 $I$  = Total electric current at collector electrode  
 $k$  = Mobility of colloids or ions in a working substance  
 $k_n$  = Mobility under normal atmospheric conditions  
 $K$  = Figure of merit of the working substance, equal to  $\epsilon/\rho k^2$   
 $K_n$  = Figure of merit of a gaseous working substance under normal atmospheric conditions  
 $L$  = Fluid kinetic power  
 $L_d$  = Power loss per unit flow area due to aerodynamic drag  
 $L_e$  = Electric power output per unit flow area  
 $L_f$  = Power extracted from the working substance per unit flow area by the interaction effects between the electric field and the ions in the working substance  
 $M$  = Mach number  
 $\theta$  =  $4\epsilon/\rho k^2$   
 $P_n$  = Pressure of working gas under normal atmospheric conditions  
 $P_p$  = Pressure of primary flow  
 $P_s$  = Pressure of secondary flow  $v_i$

- $P_{t,1}/P_{t,2}$  = Total pressure ratio between entrance and exit electrode due to the electric field
- $\Delta P_e$  = Electrical total pressure drop
- $\Delta P_{Tot} = P_{t,1} - P_{t,2}$
- $R$  = Dimensionless ratio  $r/h$
- $R_a$  = Inner radius of attractor electrode or initial charge cloud radius
- $R_i$  = Radius of charge cloud at entrance to conversion duct
- $R_1$  = Resistance
- $R_o$  = Radius of charge cloud at exit of conversion duct
- $S$  = Ratio of drift velocity to fluid velocity
- $V$  or  $\phi$  = Electrical potential between the electrodes
- $V$  = Attractor voltage
- $v$  = Speed of the working substance between the electrodes
- $v_d$  = Drift velocity, equal to  $kE$
- $v_{e,x}$  = Speed of the electric charges at station (x)
- $v_{d,x}$  = Drift speed of the charged colloids or ions relative to the working substance at station (x)
- $v_{d,1}$  = Drift speed of the ions or charged colloids at station (x = 0)
- $x$  or  $z$  = Distance of observation point from the entrance electrode
- $\alpha$  = Geometric scaling factor or ratio of applied field to dielectric strength
- $\beta = E_1/E_b$
- $\gamma = E_h/E_1$  or ratio of specific heats
- $\epsilon = 8.9 \times 10^{-12} \frac{\text{amp sec}}{\text{volt met}}$  ; dielectric constant for vacuum and gas
- $\mu = \text{Ratio of fluid velocity to maximum possible drift velocity, } v/kE_b$
- $\eta_t$  = Complete cycle efficiency of heat into electrical energy
- $\eta_{th}$  = Efficiency of conversion of heat into fluid dynamic energy

- $\eta$  or  $\eta_{st}$  = Electrical stage efficiency in conversion of fluid dynamic energy into electrical energy  
 $\theta$  = Angle of growth of charge cloud  
 $\lambda$  = Ratio of drift speed at entrance electrode to twice the speed of the working substance =  $\frac{v_{d,1}}{2v} = \frac{kE_1}{2v}$   
 $\xi$  = Overall drag loss coefficient of grid electrodes  
 $\rho$  = Mass density of working substance or dimensionless ratio,  $\rho_e/\rho_{e0}$   
 $\rho_g$  = Mass density of the working substance  
 $\rho_{e,0}$  = Initial charge density  
 $\rho_{e,x}$  = Electric charge density at station (x)  
 $\rho_n$  = Mass density of a working gas under normal atmospheric conditions  
 $Z$  = Dimensionless ratio,  $z/h$

#### Subscripts

- $n$  = Standard conditions  
 $e$  = Refers to charge  
 $0$  = Initial conditions  
 $z$  = Axial component

## INTRODUCTION

FRANK WATTENDORF

VICE CHAIRMAN, AGARD

The purpose of this introduction is to give a brief review of events leading up to the preparation of this AGARDograph.

In comparison with the major effort over many years in Magneto-fluid Dynamics (MFD), the field Electrofluid Dynamics (EFD) is relatively unexplored but advancing rapidly.\* Therefore, it is an appropriate subject for AGARD interest.

In the EFD process, ions or charged particles in a rapidly moving fluid stream are carried against an opposing potential field, thus losing fluid energy while building up electrical potential. Electrostatic forces on the ions or charged particles are preponderant, and magnetic effects negligible. Potential is high and current is low.

In the MFD process, on the other hand, magnetic effects predominate, potential is low and current high, in comparison to EFD. It is seen that EFD and MFD are complementary, rather than competitive. In fact both can be thought of as portions of the broad area of electromagnetic effects in fluid flow, which might be called "Electromagnetic Fluid Dynamics" or EMFD.

\*Although many other expressions such as MHD, MGD, MPD, EGD, EHD, etc., are found in the literature, the expressions MFD and EFD were adopted following discussions between the editors and Dr. von Ohain with Dr. von Karman at ARL in 1962. Dr. von Karman pointed out that fluid dynamics was a more general term which included the concepts both of hydrodynamics and gas dynamics.

AGARD interest in EFD was stimulated when the Aerospace Research Laboratories (ARL) participated in the AGARD Energy Conversion Symposium in Cannes, France, in March 1964, presenting a group of five papers. Encouraged by the interest expressed by other countries, Colonel Robert Fontana, at that time Commander of ARL, proposed a small working conference on the subject at ARL in May of 1966, to acquaint other countries with the research in progress at ARL, including important research areas for the future, with the objective of stimulating research activities in other countries. In response, Belgium, Canada, France, Denmark, Germany, Italy, The Netherlands, and the United Kingdom nominated experts to attend the conference and the European Office of Air Research issued invitational travel orders under the "Window on Science" program to five European participants. (The representatives of Denmark and The Netherlands were unable to attend.)

In the conference which met at ARL 23-25 May 1966, the first part was devoted to a general review of electrofluid dynamics, followed by presentations in depth of the research in progress and planned at ARL, with special emphasis on the areas of promising research. The remainder of the conference was devoted to presentations and comments by the visiting experts on research in their respective countries in fields having a bearing on electrofluid dynamics, followed by general discussion and exchange of views. The participants were enthusiastic and recommended that a follow-up conference be convened when new material became available.

At a subsequent meeting of the AGARD Propulsion and Energetics Panel, Colonel Paul G. Atkinson, Commander, Aerospace Research Laboratories, and a member of the Panel, proposed an AGARDograph on Electrofluid Dynamic Energy Conversion, utilizing the material presented at the meeting in May of 1966 at ARL as background. This was accepted by the AGARD Panel.

Since the field is advancing rapidly, it is desirable to have the AGARDograph as up to date as possible. For this reason, an editorial conference was held at AGARD in Paris on 30 and 31 October 1967, to update the material for the AGARDograph. The meeting was attended by the authors from Belgium, France, Germany and Italy, also by an editorial team from the Aerospace Research Laboratories and by the Vice Chairman, Executive of the Propulsion and Energetics Panel, and the Scientific Publications Officer of AGARD.

The participants in the editorial meeting wished the fact stressed in the foreword that the papers did not attempt to cover the field of EFD as a whole. Whereas some of the papers were original technical contributions, others represented comments on related activities in the author's own country. Subsequent to this meeting there was further updating accomplished by correspondence.

Throughout this AGARDograph there has been a concerted attempt at emphasizing areas of promising research. It is hoped therefore, that it will serve as a stimulant to research throughout the NATO nations, and will lead to further conferences on electrical phenomena in fluid dynamics.

THE ROLE OF ELECTROFLUID DYNAMICS IN THE FIELD OF  
DIRECT ENERGY CONVERSION

Summary

Although relatively unexplored among the many direct energy conversion processes, electrofluid dynamics (EFD) promises performance characteristics complementary to other processes in the overall energy conversion spectrum. The high potential, low current density electrical power of EFD devices has several natural applications. Moreover, virtually unlimited application possibilities will open up with the development of compact, inexpensive power conditioning apparatus.



THE ROLE OF ELECTROFLUID DYNAMICS IN THE FIELD OF  
DIRECT ENERGY CONVERSION

Hans von Ohain  
Aerospace Research Laboratories  
Office of Aerospace Research  
United States Air Force  
Wright-Patterson Air Force Base, Ohio

Research in the field of direct energy conversion has received a greatly increased emphasis during recent years. This broad research area is of interdisciplinary nature, being concerned with combined effects and phenomena of nearly all physical sciences, particularly of Physical Chemistry, Thermodynamics, Fluid Physics, and Electrodynamics.

While the various direct energy conversion processes differ greatly from each other in nature, they all have one overall characteristic in common; namely, the transmutation of the energy released by the energy source into useful electrical energy without employing rotating or reciprocating machinery. The energy source may be solar, chemical or nuclear.

Typical examples of such direct energy conversion processes are electric batteries, including fuel cells; solar cells; thermo-electric and thermionic converters; and processes by which fluid dynamic energy is directly converted into electrical energy. All of these direct energy conversion processes have, in one way or another, limitations

with respect to

- .power output range
- .power-to-weight ratio
- .operational voltage range
- .adaptability to environmental conditions
- .suitability for open or closed cycles
- .suitability for specific types of primary energy sources

For this reason, a great diversity of direct energy conversion processes is needed to satisfy the broad spectrum of power requirements; and, consequently, these various direct energy conversion processes, in general, do not compete with each other, but rather complement each other.

The major reason for the great emphasis on research and development in the field of direct energy conversion lies in the elimination of machinery with moving mechanical parts. This promises the following potential advantages: prolonged endurance, increased reliability, higher temperatures of working media, and lower manufacturing cost. Potential characteristics like these are very attractive for many application areas, such as power and propulsion for air and space vehicles, ground power for unattended areas, and finally, commercial applications aiming at improved overall efficiencies and reduced capital cost.

This paper is concerned with electrofluid dynamic processes, and where these processes may fit in the overall energy conversion spectrum. Electrofluid dynamic (EFD) energy conversion can be considered

as one category of direct conversion processes from fluid dynamic energy into electrical energy. The other category is magnetofluid dynamic (MFD) energy conversion.

In MFD processes, fluid dynamic energy is directly converted into electrical energy by passing an electrically conductive working medium through a magnetic field.

In EFD processes, magnetic field effects are insignificant and the predominant field-fluid interactions are of an electrostatic nature. In these processes, fluid dynamic energy is directly converted into electrical energy by passing an electrically insulating carrier medium containing electric charges of one polarity through an electrostatic field. Such a process can be considered as a fluid dynamic Van de Graaff generator.

Major world-wide research efforts are focused upon MFD processes. EFD processes, on the other hand, are in a relatively unexplored state, probably because initial investigations revealed quite discouraging performance characteristics. In the Aerospace Research Laboratories, with the active participation of Dr. Frank Wattendorf, theoretical investigations on EFD energy conversion processes were conducted, beginning in 1959. Results of these studies indicated some promising avenues for obtaining compact and light weight EFD converters with favorable performance characteristics over a very wide power output range, from as low as a kilowatt up to megawatts.

The fundamental characteristics of MFD and EFD conversion

processes employing gaseous working media are summarized in a qualitative manner in Table I.

MFD processes require high degrees of ionization of the working medium, of the order  $10^{-2}$  -  $10^{-1}$  charges per neutral. In EFD processes, however, the ratio of elementary charges to neutral molecules is extremely low, of the order  $10^{-8}$  and smaller.

To obtain sufficiently high conductivity values, temperatures in MFD processes must be high enough for thermal ionization of the working gas or seed component. Thus, static temperature levels are of the order of magnitude 2000°K and higher. EFD processes operate at much lower temperatures -- from below ordinary room temperatures on up to temperatures at which thermal breakdown processes (decomposition, ionization, etc.) become significant.

MFD processes promise attractive performance characteristics provided that the working medium has a high ratio of conductivity to mass density. Correspondingly, gas density levels are usually low. Static pressure levels are of the order of atmospheric pressure. The static pressures in EFD processes may be 20-30 times normal atmospheric pressure. Coupled with the large temperature difference, then, gas densities in EFD are in general about two orders of magnitude higher than those of MFD processes.

The basic electrical characteristics are also quite different. In MFD, current densities are several amperes/centimeter<sup>2</sup>; potential gradients are in the range 10-100 volts/centimeter; and output

potentials range from a few volts to a few ten thousands of volts, mainly depending on the size of the MFD generator. In EFD, current densities correspond to only a few milliamperes/centimeter<sup>2</sup>; however, potential gradients are of the order of 100,000 volts/centimeter and output potentials range from hundreds of thousands to millions of volts, depending on the length of the conversion channel.

Due to the opposite current-potential relationships, the power densities (electrical power output per unit area of flow channel) are not greatly different for the two processes, being only slightly higher in MFD processes. However, MFD channels tend toward large sizes with powers of several megawatts, whereas EFD channels tend toward smaller sizes with powers in the kilowatts regime. Moreover, with multi-channel configurations, the power outputs of EFD processes can be extended up to several megawatts.

Because of difficulties associated with the high temperature requirement, gaseous MFD processes look attractive primarily for open cycle applications utilizing combustion products. Since the temperature levels in EFD processes are considerably lower, closed, as well as open cycles, appear to be feasible for several basic energy sources: solar, chemical, and nuclear.

As mentioned previously, the general characteristics clearly illustrate that MFD and EFD conversion processes do not compete with each other, but rather complement each other in almost all respects. Indeed, the potential of EFD processes with regard to both small and large powers, both closed and open cycles, and all types of basic energy sources,

points toward many attractive application areas. Several possibilities which might be envisioned are listed in Table II. For example, such areas as electric propulsion, fluid dynamic Van de Graaffs, and large power burst type systems are natural applications for EFD generators, while other areas, such as air and space vehicle power, will require the development of compact, inexpensive power conditioning equipment.

At the present time, however, EFD research is still in the early stages of exploration and much remains to be learned before EFD processes reach a state of practical development. This will be made evident in subsequent papers which will treat EFD processes and associated research in detail.

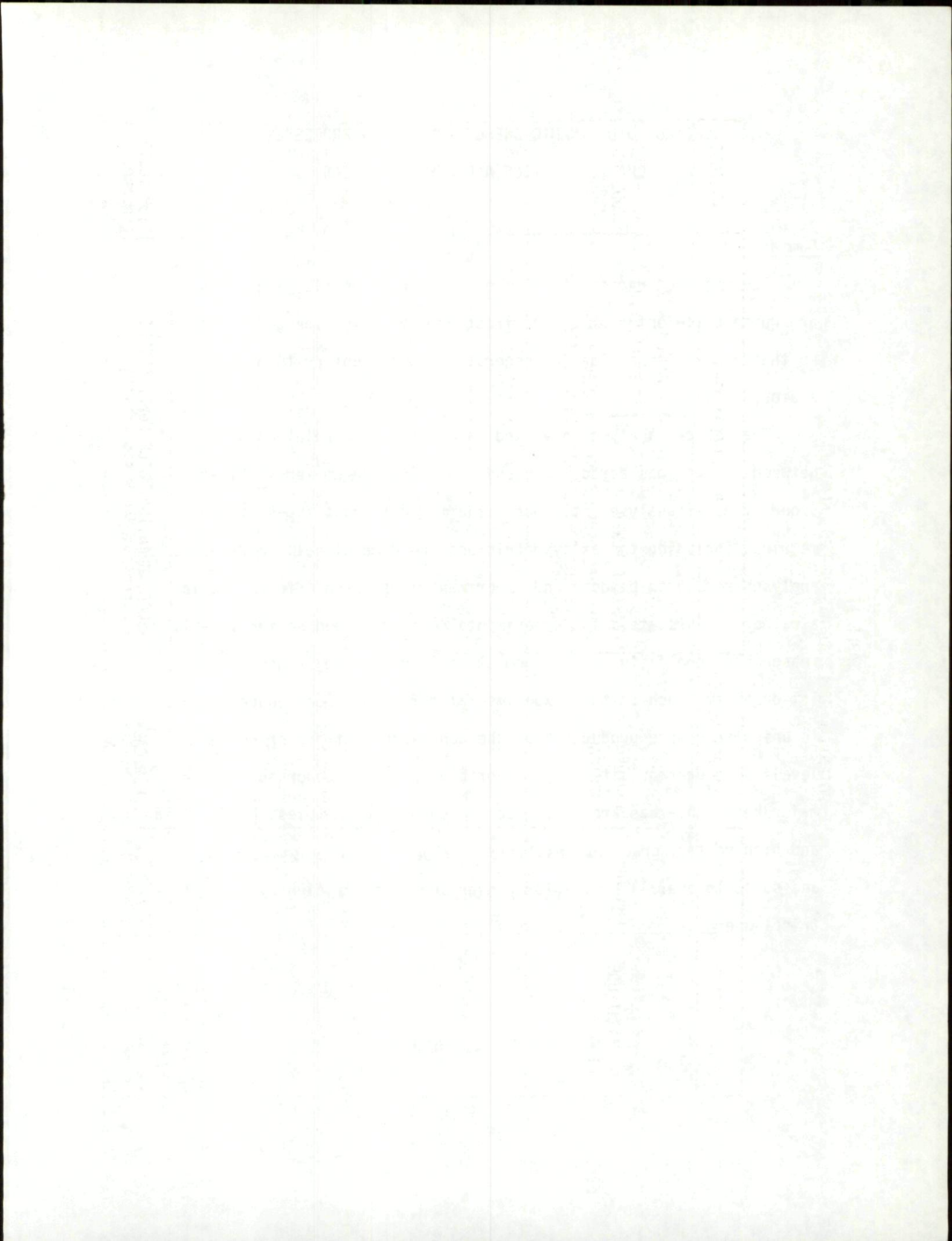
**TABLE I**  
**DIRECT ENERGY CONVERSION PROCESSES FROM FLUID DYNAMIC INTO**  
**ELECTRICAL ENERGY**

<b>BASIC PROCESS</b>	<u><b>MFD</b></u> PASSING AN ELECTRICALLY CONDUCTIVE WORKING MEDIUM THROUGH A MAGNETIC FIELD	<u><b>EFD</b></u> PASSING AN ELECTRICALLY INSULATING CARRIER MEDIUM CONTAINING ELECTRIC CHARGES OF ONE POLARITY THROUGH AN ELECTROSTATIC FIELD
IONIZATION DEGREE	HIGH	LOW
TEMPERATURE	HIGH	LOW
GAS DENSITY	LOW	HIGH
CURRENT DENSITY	HIGH	LOW
POTENTIAL GRADIENT	$\leq 10^2 \frac{\text{VOLT}}{\text{CM}}$	$\approx 10^5 \frac{\text{VOLT}}{\text{CM}}$
POTENTIAL	$\leq 10^4$ VOLTS	$\approx 10^5$ VOLTS
POWER FLUX	$\approx 10 \frac{\text{KW}}{\text{CM}^2}$	$\approx 1 \frac{\text{KW}}{\text{CM}^2}$
POWER OUTPUT RANGE	$\geq 1$ MEGAWATT	$\geq 1$ KILOWATT
MOST SUITABLE ENERGY SOURCE	CHEMICAL	CHEMICAL, SOLAR, ISOTOPE NUCLEAR REACTOR
MOST SUITABLE CYCLE	OPEN	CLOSED, OPEN

TABLE II  
 POTENTIAL APPLICATIONS OF EFD ENERGY  
 CONVERSION PROCESSES

POWER OUTPUT	CYCLE	ENERGY SOURCE	APPLICATION AREA	VOLTAGE
FRACTION KW TO 0. MAGNITUDE 10 KW	RANKINE	<ul style="list-style-type: none"> <li>• SOLAR</li> <li>• ISOTOPE</li> <li>• CHEMICAL</li> </ul>	<ul style="list-style-type: none"> <li>• TELECOMMUNICATION</li> <li>• POWER FOR REMOTE AREAS</li> <li>• VEHICLE POWER</li> <li>• ELECTRIC PROPULSION (COLLOIDAL) FOR ATTITUDE CONTROL AND MINOR ORBITAL CORRECTIONS</li> </ul>	WITH POWER CONDITIONING  0. MAGNI- TUDE $10^5$ VOLTS
0. MAGNITUDE 100 KW to 1000 KW	RANKINE	• NUCLEAR REACTOR	ELECTRIC PROPULSION (COLLOIDAL) FOR SCOUT VEHICLES	0. MAGNI- TUDE $10^5$ VOLTS
	OPEN (OPEN G.T.)	<ul style="list-style-type: none"> <li>• CHEMICAL</li> <li>• (NUCLEAR)</li> </ul>	<ul style="list-style-type: none"> <li>• MOBILE MILITARY POWER</li> <li>• POWER FOR REMOTE AREAS</li> <li>• STANDBY EQUIPMENT</li> </ul>	
	CLOSED CYCLE	<ul style="list-style-type: none"> <li>• FAN OR COMPRESSOR ACTUATED BY ELECTRICAL OR CHEMICAL ENERGY</li> </ul>	<ul style="list-style-type: none"> <li>• FLUID DYNAMIC VAN DE GRAAFF FOR RESEARCH</li> </ul>	
0. MAGNITUDE 10 MW AND ABOVE	OPEN G.T.	<ul style="list-style-type: none"> <li>• CHEMICAL</li> <li>• (NUCLEAR)</li> </ul>	• HIGH POWER STANDBY	$\sim 5 \cdot 10^5$ VOLTS
	STORAGE BLOWDOWN	• CHEMICAL	• SHORT DURATION, HIGH POWER OUTPUT (HYPERSONIC FLOW SIMULATION)	$10^6$ VOLTS AND ABOVE





ELECTROFLUID DYNAMIC ENERGY CONVERSION PROCESSES  
CHARACTERISTICS AND RESEARCH AREAS

Summary

The major characteristics of electrofluid dynamic generators are quite different from other direct energy conversion generators so that an important class of generators complementary to other generators is promised.

Theoretical analyses have indicated the basic relationships between the various aerodynamic and electrical parameters. First order types of analyses have been made for different types of geometries, including the axisymmetric and two dimensional. More exact analyses remain to be done and experimental research efforts are in a rather early state. The experimental data obtained so far establish reasonably good faith in the theoretically predicted trends and relationships. Much of this experimental effort has been concentrated in unipolar charge production, as the achievement of proper current levels is a prerequisite for a favorably operating generator. Other major research areas are electrode and channel geometries, high voltage and high voltage gradient insulation, properties of working fluids and suitable overall cycles for converting heat efficiently into electrical energy.

ELECTROFLUID DYNAMIC ENERGY CONVERSION PROCESSES  
CHARACTERISTICS AND RESEARCH AREAS

Maurice O. Lawson  
Aerospace Research Laboratories  
Office of Aerospace Research  
United States Air Force  
Wright-Patterson Air Force Base, Ohio

Introduction

Electrofluid dynamic (EFD) and Magnetofluid Dynamic (MFD) processes represent two general approaches to the direct conversion between fluid dynamic energy and electrical energy (conversion accomplished without any moving mechanical parts). Although both approaches have been established for many years, research efforts in these two fields have been greatly unbalanced. MFD power generation has been extensively investigated during the last two decades. The area of EFD power generation, on the other hand, has received scant attention through the years, and has only in recent years been reviewed and found to be an attractive field deserving further research.

The Basic EFD Generator Process

The basic electrofluid dynamic (EFD) process, while being quite realistic, is far simpler than the corresponding model of the MFD process. A schematic view of the basic EFD generator channel is shown in Figure 1. It consists of three basic sections: the charge production, energy conversion, and charge collection sections. Upstream of the grounded inlet electrode, charges of one sign (positive or negative)

are seeded into the flowing gas, e.g., by corona discharge, as shown, which will be described later. These charges are viscously coupled to the neutral gas molecules and are transported downstream through the energy conversion section against the electrostatic field of the collector (electrode) section. Because of the external load, charges will accumulate on the collector until a steady neutralizing current occurs. This process is analogous to a Van de Graaff generator in that the flowing gas performs the function of the mechanically driven belt, with the essential differences being that the coupling of the charges to the moving element is viscous rather than rigid and that far larger electrostatic fields are utilized. Since the speed of the gas can be far higher than the speed of a belt, power densities obtainable with EFD processes can be far higher than those of conventional Van de Graaff generators.

The unipolar charges for the EFD generator process can be generated in many ways; for instance, by the previously mentioned corona discharge method, which is illustrated in Figure 1. The attractor electrode which is charged to a high electrical potential, induces corona discharge at the grounded corona electrode. Thereby, separation of the positive and negative charges occur in a local region and ions of one polarity are introduced into the general stream. These ions tend to migrate to the attractor electrode; however, due to the high speed of the gas, the ions over a large range of current level are driven away from the attractor electrode and are carried through the conversion section into the collector

electrode. In the case of ions being the charge carriers, the maximum current is limited by charges appearing at the attractor. This type of limitation is shown to be nonexistent when the gas contains a vapor which condenses around the ions, forming very small, singly charged droplets. In this case, at some attractor voltage, the condition of spark-over (electric breakdown) between the attractor and the needle electrode through the charged flow, limits the current.

Since for normal generator operating conditions the charges do not come in contact with the attractor electrode, the attractor current is zero. Hence, the sustaining of the electric field between the attractor and corona electrode does not require an electric power input. The necessary energy for the current production process corresponds to a drop in total head of the working gas as it passes through the attractor-corona electrode configuration. In this sense, fluid dynamic power, rather than electrical power, is consumed for the generation of the charges. The power required for producing the charges is a minute fraction, on the order of  $10^{-4}$ , of the possible useful electrical power output.

Within the conversion section it is important that the charges do not contact the insulator wall, otherwise, electric breakdown may occur prematurely, limiting the design potential. Following the conversion section, the charge collection process is facilitated by diffusing the flow since longer dwell times are provided for a given collector length. In some cases, a neutralizing corona discharge within the initial portion of the collector is used to aid the collection process.

### Major Characteristics of the Generator Process

Table I itemizes the major characteristics of EFD energy conversion processes. A high output voltage on the order of 100,000 volts and higher, is perhaps most characteristic of this energy conversion process. Highest power densities are achieved with field strengths in the conversion section approaching the dielectric strength of the gas as well as when the dielectric strength is very high, corresponding to very high gas densities. For instance, air has a dielectric strength of about three million volts per meter at normal conditions, and at twenty atmospheres, has approximately 60 million volts per meter, so that a channel one centimeter in length can readily withstand a hundred thousand volts.

The characteristic of low electric current density results from relatively low transport speeds of the charges which correspond approximately to the gas velocities (in comparison to electron speeds in vacuum), as well as to space charge effects. The self-generated field of the charge is limited in principle to the dielectric strength of the gas; and further, may be more strongly limited by the current production means itself. In the author's paper, [1], it is shown that corona discharge into high speed gas flows can produce current densities which are compatible with the electric current requirements and the scaling characteristics (geometry and pressure) of EFD generators.

The very high number of neutral molecules per elementary charge, order of magnitude  $10^8$ , is primarily an effect of space charge. Moreover, if the available energy per neutral molecule is approximately

1/100 of an electron volt, then to transport one elementary electric charge against a potential of, for example  $10^5$  volts, the combined fluid dynamic energy of a great number of neutral molecules of the working gas is required, on the order of  $10^7$ .

The characteristic value of power density is on the order of one kilowatt per square centimeter -- the value depending principally on the desired efficiency, the gas or working medium properties, and the geometry of the channel.

A favorable power-to-weight ratio of the process is indicated because of the extremely high power output per unit volume of the conversion section. This high power per unit volume of the conversion section comes about because of the relatively short conversion lengths (order of 10 centimeters) and the power density of 1 kilowatt per  $\text{cm}^2$ . In addition, no magnets are needed.

The EFD process is primarily suited for relatively low values of power levels; however, by paralleling channels, a wide range of power can be covered, from on the order of kilowatts to megawatts.

The characteristic of very low total pressure ratio across the conversion section represents a difficulty in achieving a favorable overall thermodynamic cycle. In contrast to an impulse turbine where the total pressure ratio may be very high, e.g., ten, the total pressure ratio across an EFD channel may be less than 1.05, see Table 2. As one sees from the table, the power density may however be quite appreciable, nearly a kilowatt per square centimeter. However, as indicated by the very small total pressure ratio, the per cent of total enthalpy

removed from the flow is very small. Two major concepts are being investigated to achieve a favorable thermodynamic cycle. One is multistaging and the other is a special two fluid cycle, where one fluid is favorable for the EFD generator process and the other is favorable for the thermodynamic cycle of converting heat into directed motion energy [2].

The last major characteristic of EFD processes considered here is the non-stringent temperature requirement. Gas temperatures in the conversion duct are below thermal molecular instability values, so that the gas is a good insulator. Thus, closed cycles are feasible, including the application of nuclear or isotope heat sources. Such a generator system, with an absence of moving parts and lack of extreme temperatures, promises characteristics of high power-to-weight ratio, simplicity, reliability, and long lifetime which are so desirable for space as well as other remote area and infrequently serviced applications.

#### Research Areas

The characteristics of EFD generator processes outlined above, including application to closed cycles, warrant further expanded research. Fundamental research in the following areas is required.

#### Unipolar Charge Generation

The objective is to generate sufficient numbers of unipolar charges in very dense, high-speed flows. Presently, a corona discharge, described earlier, is primarily used by EFD investigators.



For the case of ion charge carriers, actual current values have adequately corresponded to theoretical predictions. In the case of aerosol charge carriers which are produced by adding a small amount of vapor such as water or alcohol to the working gas, and expanding the gas-vapor mixture through the attractor nozzle whereby the ions, provided by the corona discharge, act as condensation nuclei for the vapor; the values of current achieved at pressures below 40 atmospheres stagnation pressure have agreed adequately with predicted values. Above this pressure, currents, as well as permissible maximum attractor voltages, have not scaled linearly with pressure but have substantively departed from a linear increase. To extend this method up to approximately 100 atmospheres is an important area being pursued.

Some work in electrohydrodynamic spraying has been investigated as a means of producing charged aerosols [3]. Essentially, the electrode geometry appears as in Figure 1 except that the corona electrode is replaced by a capillary tube. As a liquid is expelled through the end of the tube into the gas stream in the presence of a very high electric field (highest electric field can be obtained in the subsonic flow immediately upstream of the throat for a supersonic nozzle), the liquid is inductively charged and breaks up into small droplets. Droplets produced by this method generally exhibit a much higher and more nonuniform range of charge-to-mass ratios than do condensation droplets. Values of current produced so far by this

method have not exceeded those by condensation around ions even for the above 40 atmosphere pressure regime; however, only initial research has been conducted with this charging process.

Other approaches to generate low mobility charge carriers should be investigated, such as contact ionization and ionizing of existing solid particles. In the presently investigated methods of charge production, the total field structure, electric and flow, both inside and outside the nozzle, should be considered to arrive at the highest possible charge densities over the entire range of operating conditions of interest for EFD purposes.

#### Electric Field Structures

Electric field structures is an important research area. The combined effects of the fields due to the electrodes and the charged particles associated with their motion and density are, in the general case, not amenable to explicit solutions. In the case of ions, where the charges are very mobile, there is a rapid expansion of the ion cloud as it passes through the channel. In the case of aerosols when the influence of the electric field on the charge motion is negligible, turbulent mixing will control the spreading of the charges. The latter case, that of aerosol charge carriers, is fortunately the more interesting one for the realization of efficient high power density generators. In this case one may adopt a charge spreading angle according to the gas flow properties and determine the corresponding charge density distribution and thus be able with the aid of high

speed computers to solve for the electric field structure for given generator channel geometries. This kind of investigation is being included in the research of Mr. John Minardi, which is reported in this AGARDograph.

#### Geometry Effects

Theoretical analyses giving explicit solutions are, fortunately possible for the one dimensional, or broad channel case. However, simplified analyses have shown that the performance characteristics of EFD channels are sensitive to the channel geometry, in particular, to the length-to-height ratio of the conversion section, as well as to whether the channel is axisymmetric or two dimensional. The latter channel configuration has, inherently, about one-half of the frictional losses for the same electrical power as has the axisymmetric. Also, an extremely important research area is the effect of the charging, shielding (entrance electrode to the conversion channel), and collecting electrodes, since these strongly influence the overall electric field structure -- a field structure without any significant peaks being desirable in order to be able to load the channel maximally with respect to the extraction of electric power.

#### Working Media

Theory has shown that some of the major desirable properties of EFD working media are high dielectric strength, low molecular weight, and low mobility of the charges. Working medium characteristics for high power and highest efficiency using ions as the charge carriers,

are a high figure of merit (low mass density and mobility,  $\epsilon/\rho k^2$ ), as well as a suitable dielectric strength. For the use of charged aerosols, a high dielectric strength is required; and again a low molecular weight (high speed of sound) is favorable with respect to power density. This area has been first experimentally investigated with the above working media characteristics in mind by Mr. Michael Hawes, as reported in this AGARDograph. He has investigated certain special gas mixtures, formulated with regard to application as EFD working media. However, much more work needs to be done in this area.

#### Similarity and Scaling Laws

Theoretical scaling laws of performance characteristics with working media pressure level and generator size should be experimentally examined. Deviation from the scaling laws are expected and should be determined. Some results have been obtained for the ion corona charge production process, but more work needs to be done, especially for the complete generator configurations.

#### Overall Cycles

The characteristic of low pressure ratio per generator stage, as previously discussed, presents a major problem in the incorporation of EFD generators into an overall conversion cycle of heat into electrical energy. In such a cycle, heat is transformed into fluid dynamic energy which, in turn, is directly transformed by the EFD process into electrical energy. The wasted heat, that is, the heat energy not transformed into electrical energy, must be rejected. The efficiency,  $\eta_t$ , of a

complete cycle from heat into electrical energy is as follows:  $\eta_t = \eta_{th} \cdot \eta_{st}$  where  $\eta_{th}$  is the efficiency of the conversion from heat into fluid dynamic energy and  $\eta_{st}$  is the efficiency of the direct conversion from fluid dynamic energy into electrical energy. However, as Table 1 shows, the pressure ratios of one stage EFD generators are extremely low. Two major approaches to this problem have been proposed. One is to stage in series, and requires from a favorable efficiency standpoint, very low subsonic high density flows, and charged particles of negligible mobility. However, the charge production technique commonly used for aerosol production by condensation around ions is not applicable due to the lack of an appreciable expansion with the corresponding high supersaturation of the vapor. Electrohydrodynamic spray charging needs further research before it can provide adequate current and charge droplets of only low mobility which is necessary for subsonic flow generators. Also, conditioning of the working gas to remove excessive liquid would be necessary every ten stages or so.

The second major approach, which is being investigated by the Aerospace Research Laboratories, is to employ a special cycle. The previous consideration showed that, to obtain favorable performance characteristics of EFD energy conversion processes, special properties of the working substance are required. These properties may be incompatible with those required for a working medium to transform heat efficiently into fluid dynamic energy. Also, the pressure ratio characteristics of an efficient EFD energy conversion process are incompatible

with the pressure ratio requirements for effective conversion from heat into fluid dynamic energy. These difficulties can be overcome by employing two loops with two working media, one for the thermodynamic process to transform heat into fluid dynamic energy; the other for the EFD process to transform fluid dynamic energy into electrical energy. In such a two-component, two-loop system, the conflicting requirements of the thermodynamic and the EFD conversion process are essentially uncoupled, and favorable conditions can be provided for each individual process. The EFD process may employ a low molecular weight gas of high dielectric strength, which recirculates in the pressurized EFD loop with a subsonic Mach number through the conversion section. [2] The thermodynamic process may use a vapor, preferably of much higher molecular weight than that of the EFD working medium, and may employ, for example, a super-heated Rankine cycle of high pressure ratio. Energy transfer from the thermodynamic to the EFD working medium can be accomplished by an injector process. By such a process, energy can be transferred efficiently if the speeds between the working media are not too different. For example, the speed of the thermodynamic working medium should be less than twice the speed of the EFD working medium. This requirement does not conflict with the requirement of a high expansion pressure ratio of the thermodynamic working medium if the molecular weight is sufficiently high in comparison to that of the EFD working medium. The volume flow of the recirculating EFD working medium can be far larger than that of the thermodynamic medium

since the power required for sustaining the recirculation of the EFD working medium is only a fraction of the kinetic power in the conversion section; the balance of the kinetic power is available for EFD electrical power extraction. To complete the thermodynamic loop, the condensed thermodynamic working fluid is separated from the EFD working medium and returned to the boiler. In some cases, the thermodynamic working medium may be utilized not only for the energization of the EFD working medium, but also for forming charged aerosols by condensation around ions in the EFD working medium. Research is needed in low pressure ratio (high secondary volume flow) injector processes, as more efficient injector processes will result in higher power density and/or more efficient EFD generators.

#### Alternating Current Power

Inasmuch as the charge generation methods outlined in the preceding are mostly independent of the polarity to the attractor nozzle the direct generation of high voltage, alternating current power is possible by applying a properly biased alternating potential to the attractor electrode. Of course, there will be a decrease in power density relative to DC operation. Exploratory research in this field was promising [4]. In this early work a major problem was the low frequency limitation due to the output capacitance of the generator being high in comparison to the current level achieved.

A second possibility lies in the field of power conditioning, where the power is produced as high voltage DC and is then converted

into power with more readily usable characteristics. Some degree of such power conditioning is necessary in almost all direct energy conversion devices. Utility power systems have found high voltage DC (500-800 kilovolts) transmission desirable in some long distance applications. Present inverters use mercury arc tubes which have excessive bulk and much too high capacities for the present state of EFD power generation. More compact solid state inverters are under development, however, and may be available when EFD systems have progressed to a state of practical application.

#### Space Charge Neutralization

In this concept charges of one polarity are confined to the conversion section while charges of the opposite polarity are transported through this region against a retarding field to a higher potential. Thus, the conversion section would be near gross neutrality condition at all times and the severe limitation on current due to space charge effects would be alleviated. For example, electrons might be confined to spiralling motions by a transverse magnetic field while positive ions pass through the conversion duct. This concept was discussed by Dr. E. Knoernschild in a colloquium at Wright-Patterson Air Force Base in 1961 and is a subject of a paper in this AGARDograph. Such a generator would have characteristics of both MFD and EFD generators. The entire field of such hybrid systems is open to exploration.



References

1. Maurice O. Lawson, "Ion Generation by Corona Discharge for Electrofluid Dynamic Energy Conversion Processes", AGARDograph 81.
2. Hans von Ohain and Frank L. Wattendorf, "Potentialities of Direct Electrofluid Dynamic Energy Conversion Processes For Power Generation", AGARDograph 81.
3. Krishan Kant Joshi, "Electrical Charging of Liquid Sprays in High Pressure Gas Flows for Electrofluid Dynamic Processes", International Electron Devices Meeting, October 18-20, 1967, Washington, D.C.
4. J. Paul Sutherland and John W. Storr, "The Electrical Characteristics of an Electrofluid Dynamic Generator for an Alternating Input", GA/Phys 63-11,12, August 1963, Air Force Institute of Technology

TABLE I  
CHARACTERISTICS OF ELECTROFLUIDDYNAMIC  
ENERGY CONVERSION PROCESSES

30

- HIGH OUTPUT VOLTAGE  $\sim 10^5$  VOLTS AND ABOVE
- LOW ELECTRIC CURRENT DENSITY
- VERY HIGH NUMBER OF NEUTRAL MOLECULES PER ELEMENTARY CHARGE, ORDER OF MAGNITUDE  $\sim 10^8$
- POWER OUTPUT  $\sim 1 \text{ KW/CM}^2$
- FAVORABLE POWER-TO-WEIGHT RATIO
- BROAD RANGE OF POWER OUTPUT
- VERY LOW TOTAL PRESSURE RATIO ACROSS CONVERSION SECTION
- NON-STRINGENT TEMPERATURE REQUIREMENTS


# TABLE II


## SOME PERFORMANCE VALUES OF VISCOUS EFD PROCESSES

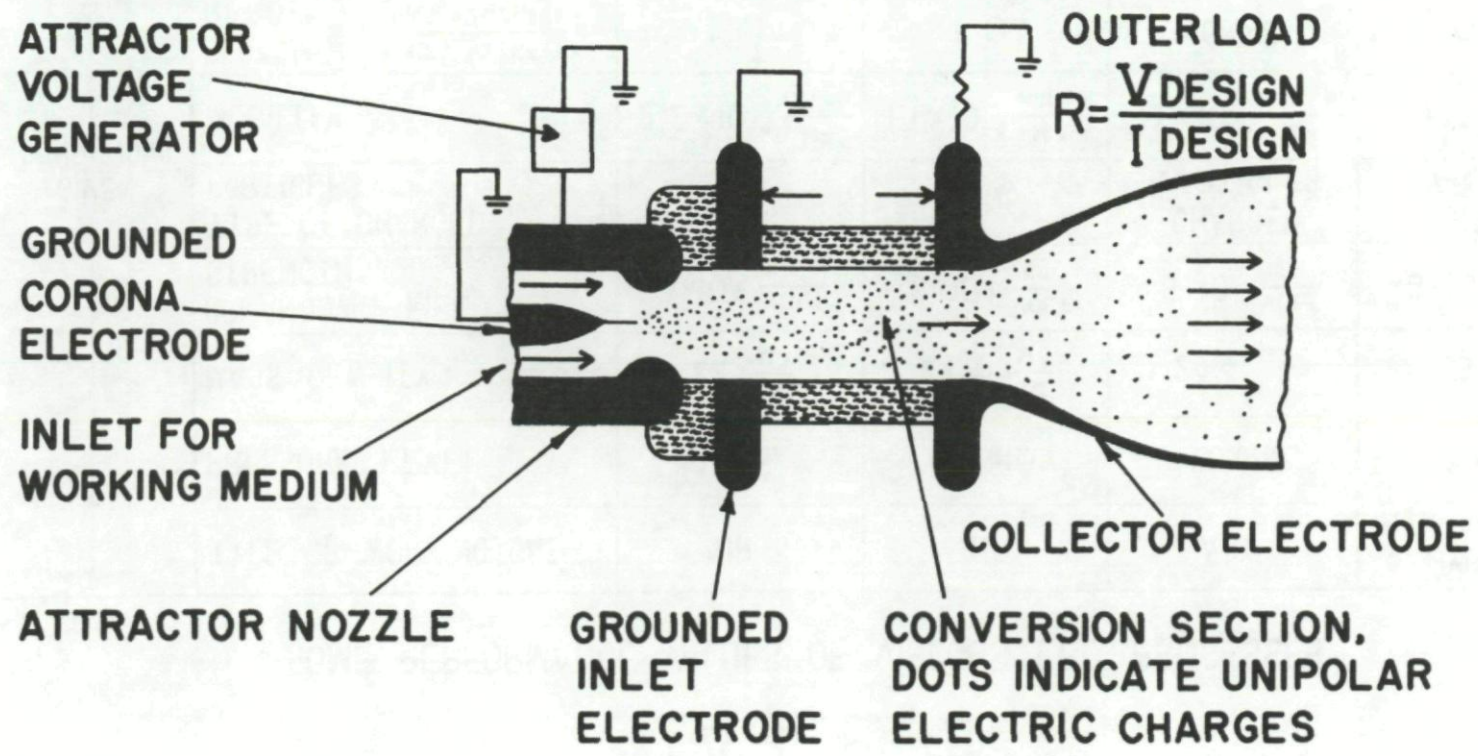
GIVEN CONDITIONS	TYPE OF WORKING GAS	AIR	AIR	AIR	HYDROGEN WITH ADDITIVES
	PRESSURE LEVEL	1 atm.	20 atm.	20 atm.	20 atm.
	MASS DENSITY	$1.22 \frac{\text{KG}}{\text{M}^3}$	$24.4 \frac{\text{KG}}{\text{M}^3}$	$24.4 \frac{\text{KG}}{\text{M}^3}$	$1.9 \frac{\text{KG}}{\text{M}^3}$
	BREAKDOWN FIELD STRENGTH	$3 \cdot 10^4 \frac{\text{VOLT}}{\text{cm}}$	$6 \cdot 10^5 \frac{\text{VOLT}}{\text{cm}}$	$6 \cdot 10^5 \frac{\text{VOLT}}{\text{cm}}$	$\sim 6 \cdot 10^5 \frac{\text{VOLT}}{\text{cm}}$
	TYPE OF CHARGED PARTICLES	IONS	IONS	CHARGED PARTICLES	CHARGED PARTICLES
	MOBILITY	$2.2 \times 10^{-4} \frac{\text{M}^2}{\text{volt sec.}}$	$1.1 \times 10^{-5} \frac{\text{M}^2}{\text{volt sec.}}$	$1 \times 10^{-8} \frac{\text{M}^2}{\text{volt sec.}}$	$2.5 \times 10^{-8} \frac{\text{M}^2}{\text{volt sec.}}$
	SLIP RATIO $S = \frac{\text{DRIFT VELOCITY}}{\text{GAS VELOCITY}}$	1.0	1.0	.002	.002
	VELOCITY OF WORKING GAS	$250 \frac{\text{M}}{\text{SEC.}}$	$250 \frac{\text{M}}{\text{SEC.}}$	$250 \frac{\text{M}}{\text{SEC.}}$	$470 \frac{\text{M}}{\text{SEC.}}$
	DRAG COEFFICIENT ( $\xi$ ) OF CONVERSION SECTION	$\frac{3}{100}$	$\frac{3}{100}$	$\frac{3}{100}$	$\frac{3}{100}$
RESULTING PERFORMANCE VALUES	SPECIFIC POWER OUTPUT	$.05 \frac{\text{WATT}}{\text{cm}^2}$	$20 \frac{\text{WATT}}{\text{cm}^2}$	$400 \frac{\text{WATT}}{\text{cm}^2}$	$750 \frac{\text{WATT}}{\text{cm}^2}$
	STAGE EFFICIENCY	0.2%	3%	41%	74%
	PRESSURE DROP ÉLECTRIC + DRAG	.01 atm	.2 atm	.40 atm	.22 atm
	PRESSURE RATIO	1.01	1.01	1.02	1.01

# FIGURE I.

## ILLUSTRATION OF ELECTROFLUIDDYNAMIC ENERGY CONVERSION PROCESS (FLUID DYNAMIC VAN DE GRAAFF)

 INDICATES ELECTRICAL INSULATOR

 INDICATES ELECTRICAL CONDUCTOR



RECORDS OF THE PHYSICS

DEPARTMENT OF THE UNIVERSITY OF CALIFORNIA

AT BERKELEY, CALIFORNIA

1911-1912

BY

W. H. WYLLIE

PHYSICIAN

AND

LECTURER

IN

PHYSICS

UNIVERSITY OF CALIFORNIA

BERKELEY, CALIF.

1912

PRINTED BY

UNIVERSITY OF CALIFORNIA

BERKELEY, CALIF.

1912

NO. 1

1912

1912

1912

1912

EFFECTS OF ELECTRODE GEOMETRY SIMILARITY AND  
SCALING LAWS IN EFD ENERGY CONVERSION PROCESSES

Part I: Fundamental Considerations

Summary

Attractive performance characteristics are possible with viscous EFD processes which employ electrode and channel configurations corresponding to small aerodynamic drag losses, and which utilize pressurized gases of low molecular weight and high dielectric strength containing unipolar charged particles. Basically however, EFD processes are low pressure ratio processes inconsistent with a high overall conversion efficiency from heat into electricity. To overcome this incompatibility, ARL is exploring a special two-loop, two-fluid cycle. Successful operation of this concept requires the ability to seed the working medium with charge densities which are the highest possible consistent with fundamental channel limitations. A corona discharge is being investigated for charge seeding.

EFFECTS ON ELECTRODE GEOMETRY SIMILARITY AND  
SCALING LAWS IN EFD ENERGY CONVERSION PROCESSES

Part I: Fundamental Considerations

John A. Decaire  
Aerospace Research Laboratories  
Office of Aerospace Research  
United States Air Force  
Wright-Patterson Air Force Base, Ohio

Introduction

Electric power generation by means of electrofluid dynamic (EFD) processes has been under experimental investigation at the Aerospace Research Laboratories (ARL) since 1963. This paper presents the major aspects of this EFD research effort. The present part reviews the fundamental physical and theoretical considerations of viscous EFD energy conversion processes and outlines the special two-fluid, two-loop cycle being considered at ARL. A detailed description of the experimental generator and associated unipolar charge generation process (a corona discharge) is included. Experimental data will be presented and discussed in Part II.

Basic Relationships

The operation of the basic single stage EFD power generator entails three phases --unipolar charge generation, charge transport, and charge neutralization --illustrated in Figure 1. A realistic physical model of the EFD process is simple and straightforward for two main reasons. First, magnetic field effects are negligible; the major effects are generated by electrostatic fields only. Secondly, the working gas is at relatively high density levels and can be characterized by a few macroscopic parameters --temperature, pressure, mo-

lecular weight, breakdown field strength, and charge mobility. Figure 2 illustrates the relationships between the various aerodynamic and electrical parameters for a typical observation point,  $(x,r)$ , in an axisymmetric conversion section.

The electric field,  $E$ , is the vector sum of the applied field due to the difference in potential between the inlet and collector electrodes (usually assumed axial and uniform) and the field due to the space charge which has both an axial and a radial component. A major limiting condition to be considered is that the field intensity must always be less than that corresponding to electrical breakdown of the gas. The breakdown field strength of a gas,  $E_b$ , is not a fundamental physical property and varies with the particular electrodes and electrode gap under consideration, however, most dielectric gases can be characterized by a reasonably valid engineering value for  $E_b$ . For many of these gases,  $E_b$  is nearly linearly proportional to the density level over a wide range above normal atmospheric density.

$$E_b \approx E_{b,n} \frac{\rho}{\rho_n} \quad (1)$$

where the subscript,  $n$ , refers to normal atmospheric conditions. Table I lists typical values of  $E_{b,n}$  for several gases.

The charges naturally tend to move in the direction of the electric field relative to the gas flow with a drift velocity,  $v_d$ , described by the product of the charge mobility,  $k$ , and the local field intensity.

$$\vec{v}_d(x,r) = k\vec{E}(x,r) \quad (2)$$



The resulting transport velocity of the charges,  $v_e$ , is given by the vector sum of the fluid velocity,  $v$ , and the charge drift velocity.

$$\vec{v}_e(x,r) = \vec{v}(x,r) + \vec{v}_d(x,r) \quad (3)$$

Throughout the EFD conversion channel, the transport velocity of the charges must be finite and in the downstream direction, a limiting condition being that the axial component of the fluid velocity must exceed the axial drift velocity of the charges.

$$v_x(x,r) > kE_x(x,r) \quad (4)$$

The radial drift of the charges under the influence of the space charge field must also be limited. Electrical breakdown due to charge deposition on insulator surfaces is an experimentally well-known high voltage phenomenon. To avoid these surface breakdown effects, the charges should not contact the conversion channel walls except within the collector electrode.

The property of charge mobility is a measure of the effectiveness of the viscous coupling mechanism. A low value of mobility indicates a strong coupling interaction. In any specific gas, the magnitude of the charge mobility depends strongly on the size and charge of the particles employed. Typically quoted values for positive and negative molecular ions are listed for several gases in Table I. For many gases, the ion mobility is inversely proportional to the density over a wide range of density levels.

$$k \cong k_n \frac{\rho_n}{\rho} \quad (5)$$

Figure 3a shows mobility values calculated for singly charged particles in air as a function of pressure with the particle diameter,  $d$ , as the curve parameter (Ref. 1). The mobility of very small particles,  $d \approx 0.02$  microns, is governed mainly by molecular interactions and is nearly inversely proportional to the pressure as expected from equation (5). With increasing particle diameter, the mobility becomes less dependent on the pressure level, and for diameters greater than about one micron, the mobility is nearly independent of the pressure. Moreover, the rapid decrease in the mobility with increasing particle size indicates the desirability of using charged aerosol particles in viscous EFD processes (Ref. 9). Drift velocities of singly-charged particles in air at normal breakdown field strength values are shown in Figure 3b.

#### Scaling Characteristics

The basic equations for the various performance parameters - charge density,  $\rho_e$ ; current density,  $i$ ; total current,  $I$ ; and potential,  $V$  - are listed in Figure 2. Subject to the limiting conditions outlined above, these basic equations lead to scaling characteristics with respect to changes in channel size and operating pressure level which are generally valid for viscous EFD processes. These scaling relationships are listed in Figure 4 (Ref. 7).

Figure 4A: The power density,  $L_e$ , is the product of the potential and average current density and thus represents the electrical power

output per unit area of flow channel. Holding all other conditions constant, scaling of all the linear dimensions of the channel and electrodes by a constant factor,  $\alpha$ , does not change the power density. Therefore, cylindrical conversion ducts of a specified length-to-diameter ratio can be scaled up to increase the power level whenever an increased output potential is allowable. A power increase at constant potential requires an increase in the number of conversion ducts.

Figure 4B: If the temperature, velocity, and geometry are unchanged while the pressure level of the working gas is increased from atmospheric pressure,  $P_n$ , to pressure,  $P$ , the electric power output is proportional to the square of the increased operating pressure level. Therefore, high working pressure levels are desirable in the range over which equations (1) and (5) remain valid.

#### Performance Characteristics

Using the basic relationships and limiting conditions, the aerodynamic and electrical performance can be determined if the geometry and boundary conditions are specified; however, the general equations are not amenable to explicit solution. One case that can be solved explicitly is when the conversion section is very large in comparison to the length. In this case, the radial components and end effects become negligible and the problem is essentially one-dimensional. This one-dimensional case has been analyzed by several investigators (Ref. 2, 6, 7, 10, 12, 13). Some solutions which have been obtained are shown in Table II (Ref. 7). These equations contain the maximizing condition that the electric field inten-

sity at the collector electrode is zero which corresponds to the maximum allowable charge densities without field reversal. A constant gas velocity is also assumed, that is, compressibility effects are small.

The left column contains the ion case in which the slip between the charges and gas molecules has a significant influence on the performance. This slip is characterized by a parameter,  $s$ , defined as the ratio of the drift velocity at the entrance electrode (position of highest value) to the gas velocity. Possible values of  $s$  lie between zero and one. Whenever  $v < kE_b$ , the maximum field strength is limited by the gas velocity as in equation (4). If  $v > kE_b$ , the field strength at the entrance electrode can be made to approach the breakdown field strength. The power density then, is the highest possible consistent with both space charge and electrical breakdown limitations. In the case of negligible mobility charge carriers (right column), the gas velocity and electric field are completely uncoupled and the field strength may theoretically always approach the breakdown field strength of the gas.

The electrical pressure drop,  $\Delta P_e$ , listed in Table II, is the total pressure drop across the conversion channel due to the body force imposed on the gas by the interaction of the space charges and electric field.

$$\Delta P_e = \int_0^h \rho_e \vec{E} \cdot d\vec{x} \quad (6)$$

where  $h$  is the length of the channel. The product,  $\Delta P_e \cdot v$ , represents, for incompressible flow, the total energy change per unit cross-sectional area due to the charge-field interaction and includes both the useful out-

put power density,  $L_e$ , and the energy density lost as joule heating due to the slip between the charges and working gas.

An added energy loss mechanism for the EFD process is aerodynamic drag. The energy per unit area of flow channel  $\Delta P_{\text{drag}} \cdot v$ , lost by this mechanism may be expressed as (Ref. 6)

$$\Delta P_{\text{drag}} \cdot v = \xi \cdot \rho \frac{v^2}{2} \cdot v \quad (7)$$

where  $\xi$  represents an overall drag loss coefficient for the conversion section and electrodes.

The stage efficiency,  $\eta_{\text{st}}$  (bottom row of Table II), is defined as the ratio of electrical power output to the total consumed fluid dynamic energy,

$$\eta_{\text{st}} = \frac{L_e}{\Delta P_e \cdot v + \Delta P_{\text{drag}} \cdot v} \quad (8)$$

This efficiency definition is analogous to the stage efficiency used in turbomachinery whereby the exiting kinetic energy is not considered a loss. For the ion case, the dimensionless quantity,  $\epsilon/\rho k^2$ , in the denominator depends only on the nature and state of the carrier gas and can be considered a figure of merit for the gas in analogy to the figure of merit used in magnetofluid dynamics - the ratio of conductivity to mass density. The figure of merit, denoted as  $K$ , is proportional to the ratio of electrical pressure to dynamic pressure. Similarly, in the negligible slip case, the quantity,  $\epsilon E_b^2 / \rho v^2$ , is linearly proportional to the ratio of electrical pressure to dynamic pressure for incompressible flow conditions. For constant Mach numbers,  $\epsilon E_b^2$  serves as an efficiency

figure of merit for the gas. Considering constant Mach numbers, the products  $Ka^*$  and  $E_b^2 a^*$  represent figures of merit for power for the slip and non-slip cases respectively (where  $a^*$  is the sonic velocity at Mach 1 flow condition).

#### Numerical Performance Values

Numerical evaluation of the equations in Table II show a surprisingly wide span of potential EFD performance capabilities. These range from extremely poor to highly attractive depending on the value of the drag coefficient and physical properties and pressure level of the working gas. Table III shows numerical values for four different cases assuming a favorable drag coefficient of three per cent.

The first case treats air under atmospheric pressure containing negative ions. Resulting performance values are many orders of magnitude too low for any normally conceivable application. The performance is greatly improved when the air is pressurized to 20 atmospheres (second case), however, the values are still too low to be considered for practical applications. Utilizing charged particles ( $d \approx 0.1$  microns) rather than ions (third case), the performance values begin to look quite attractive. The fourth case is based upon a low molecular weight gas such as hydrogen, again pressurized to 20 atmospheres and containing charged particles. An additional assumption is that trace amounts of suitable additives raise the dielectric strength to approximately equal that of air. In this case, very attractive values of power density and stage efficiency are predicted. Moreover, theoretical analyses of axisymmetric channels indicate that power

densities for the negligible slip case should be two to five times greater than those of the one-dimensional channels (Ref. 7).

These numerical results show that very favorable power densities and conversion efficiencies become possible with viscous EFD processes which employ electrode and channel configurations corresponding to a small drag loss, and which utilize pressurized gases of low molecular weight and high dielectric strength containing unipolar charged particles. As can be seen from the bottom row of Table III however, the pressure ratios of EFD channels are extremely low which makes it difficult to employ a one-stage viscous EFD process directly into an overall cycle of reasonable thermal efficiency.

#### ARL RESEARCH

The low pressure ratio of the EFD process represents a problem when the overall conversion from heat into electricity is considered. In such a cycle, a thermodynamic process transforms heat into fluid dynamic energy which, in turn, is directly transformed into electrical energy by the EFD process. A high conversion efficiency of heat into fluid dynamic energy requires a high pressure ratio. This requirement, however, as shown above, is incompatible with the pressure ratio characteristics of an efficient EFD energy conversion process. The various EFD research efforts differ primarily around the method proposed to resolve this incompatibility. Approaches which have been suggested and are being investigated are "slender channel" geometries (Ref. 3,4), multi-staging in series (Ref.2,6), and special cycles (Ref 6, 14).

The Aerospace Research Laboratories is considering the development of a special cycle to permit effective coupling between a one-stage EFD power generator and a high pressure ratio thermodynamic process. This concept employs two loops with two working media, one for the thermodynamic process to transform heat into fluid dynamic energy, and the other for the EFD process to transform fluid dynamic energy into electrical energy. In such a two-component, two-loop system, the conflicting requirements of the thermodynamic and the EFD conversion process are essentially uncoupled, and favorable conditions can be provided for each individual process. The EFD process may employ a light molecular weight gas of high dielectric strength, which recirculates in the pressurized EFD loop with a suitable speed through the conversion section. The thermodynamic process may use a steam, preferably of much higher molecular weight than that of the EFD working medium, and may employ, for example, a super-heated Rankine cycle of high pressure ratio. Energy transfer from the thermodynamic to the EFD working medium can be accomplished by an injector process (Figure 5). By such a process, energy can be transferred efficiently if the speeds between the working media are not too different. For example, the speed of the thermodynamic working medium should be about twice the speed of the EFD working medium (Ref. 14). This requirement does not conflict with the requirement of a high expansion pressure ratio of the thermodynamic working medium, if the molecular weight is sufficiently high in comparison to that of the EFD working medium. The mass flow of the thermodynamic medium will be smaller than that of the recirculating EFD working medium, since the power required for sustaining the recircula-



tion of the EFD working medium is only a fraction of the kinetic power in the conversion section. To complete the thermodynamic loop, the condensed thermodynamic working substance is separated from the EFD working medium and returned to the boiler. In some cases, the thermodynamic working medium may be utilized not only for the energization of the EFD working medium, but also for forming charged aerosols by condensation around ions in the EFD working medium.

Successful operation of the ARL concept requires high output potentials - 1/2 to 1 million volts - and charge densities which are the maximum possible consistent with the basic channel limitations. The method of generating sufficient densities of unipolar charges, therefore, represents a key research area and a large portion of ARL's research effort to date has been concerned with charge production.

#### Corona Charging Process

The charging process presently being used by ARL and most other investigators in EFD, is a corona discharge from a slender needle electrode centered on the axis of an attractor nozzle electrode. This configuration is schematically illustrated in Figure 1. When a high electric potential is applied to the attractor electrode, a very intense field is produced in the immediate vicinity of the needle point. Ionization of the gas occurs locally in this region with subsequent charge separation by ions flowing toward the electrode of opposite polarity. As the working gas flows over the electrodes, those ions which have moved radially outward into the weaker field region become viscously coupled to the

neutral gas molecules and are swept downstream into the conversion section. Charged aerosol particles are commonly produced by free condensation. A small mass fraction of a vapor such as water is added to the flow of primary working gas. The gas-vapor mixture is then strongly expanded with accompanying supersaturation of the vapor in the region of the corona. Ions from the corona act as condensation nuclei for the vapor component resulting in charged droplets which are carried by the primary gas.

The nature of the corona discharge is quite complex and the charge producing characteristics of the attractor nozzle-corona needle electrode configuration depend strongly on the specific conditions: physical properties, pressure, temperature, and velocity of the working gas; geometry, size, and material of the electrodes; and magnitude and polarity of the applied attractor potential. Maximum charge production is limited by space charge effects and spark breakdown between the electrodes. Under the proper conditions, almost all of the charges are transported downstream and a negligible number flow to the attractor electrode. This is the desirable operating regime for EFD processes since no input electric power is used to obtain charge separation, rather the small amount of energy needed for charge separation is supplied by the working gas. In this case, several side conditions rather than the corona process may determine the current which can be generated. The major side conditions are: The charge cloud must not touch the attractor electrode which insures that all the charges are carried downstream; the charges have a drift velocity relative to the gas flow and hence, the transport speed is

fractionally smaller than the gas speed; and the field strength due to the space charges cannot exceed the breakdown field strength of the gas. A theoretical analysis has been done by Lawson (Ref. 8) which predicts the similarity and scaling relationships and maximum current levels to be expected from the corona electrode configuration when these side conditions are the controlling factor, that is, the corona is assumed to always be capable of supplying a sufficient number of ions within these limits\*. The equations for the maximum current level are for ions,

$$I_i = \frac{\pi \epsilon v^2 R_a}{k_n} \frac{\rho}{\rho_n} \quad (9)$$

and for charged aerosol particles,

$$I_p = 2\pi \epsilon v R_a E_{b,n} \frac{\rho}{\rho_n} \quad (10)$$

where  $R_a$  refers to the radius of the attractor electrode.

From equations (9) and (10) the current generated by the corona process is expected to be linearly proportional to a geometric scaling factor and to the operating pressure level as was the current for the conversion channel (Figure 4). Lawson (Ref. 8) has shown that the current magnitudes predicted by these equations are within the requirements of the EFD channel. For example, assuming air at stagnation conditions of 80 atmospheres and 25°C, a 1/8 inch attractor radius, and Mach 2 flow, results in predicted currents of 2.4 and 6 milliamperes for ions and

---

\*This assumption is expected to hold better for the case of negative point corona since the current yields and spark breakdown voltages are higher than a corresponding positive point (15). Moreover, the negative point operates over a much wider range of pressures (15).

charged particles, respectively\*. Experimental values are expected to be somewhat less than those predicted values since the theory did not make any allowance for externally applied fields; indeed, preliminary experimental currents are about half of the theoretical values.

### Experimental Generator

Experimental research is being conducted on a test rig which was designed and built at ARL in 1963 (Ref. 5). This rig operates as a recirculating ejector and, therefore, simulates closed cycle operation of the two-fluid, two-loop concept except that one working fluid is used throughout the system. Schematic operation of the test rig is shown in Figure 5. High pressure gas is expanded supersonically through an ejector nozzle and drives a recirculating flow in a closed duct system. An amount of gas equal to the input mass flow rate is bled out of the system to maintain steady flow conditions. The relative pressure levels between input and recirculating flows is regulated by means of a throttle valve placed in the bleed line. The ejector nozzle serves a dual purpose as the attractor electrode for the corona process.

Figure 6 shows the overall construction of the ARL test generator. From the ejector, the gas flows through the conversion section, the diffuser, and an insulator duct with conducting liner; is turned 180° by two elbows; and returns to the ejector chamber through an insulator duct and a tee. Bleed gas is taken through either of two lines: an

---

\*The relative current levels of particles to ions varies inversely with the gas velocity

$$\left[ \frac{I_p}{I_k} = \frac{2k_n E_{b,n}}{v} \right]$$

insulator duct which bleeds boundary layer air from the perforated diffuser or through a junction of the tee in the return path. The insulator material used throughout the rig is a resin impregnated fiberglass which has the mechanical strength necessary to contain the high pressure, as well as adequate electrical properties. All electrodes are made of stainless steel to prevent corrosive effects, while the ducting elbows and tee are cast steel.

The recirculating path length is approximately 12 feet and is primarily of a 2 inch inside diameter. The actual energy conversion section occupies only a very small portion of this overall length. For convenience, the walls of the diffuser and lined insulator duct are used to provide a long charge collecting surface. However, the long insulator ducts are used mainly as a simple and inexpensive outlet for the high voltage of the EFD process. Aluminum shields prevent corona losses from the sharp edges of bolts, flanges, etc. To improve the resistance to surface breakdown phenomena, the conversion section and insulator ducts are enclosed by a high pressure jacket, and insulator disks have been mounted transverse to the duct axis to increase the external surface path length.

A more detailed view of the electrode and conversion section assembly is shown in Figure 7. All major components—nozzle, needle, ground plate, conversion duct, and diffuser—are designed to be easily interchanged over a wide range of sizes and shapes. The ground plate electrode which serves as the entrance to the conversion section shields the nozzle

needle ionizer combination from the high electric fields in the conversion region, and allows a constant charge production at varying collector potentials. A small gap is left between the insulator conversion duct and the ground plate to alleviate charge leakage and surface breakdown through the boundary layer which had been experienced in earlier channel designs.

The test generator is designed as a basic research tool rather than a generator with specified performance characteristics. Intended research includes fundamental EFD channel flow phenomena and the testing and verification of the theoretically predicted trends and relationships which have been outlined above. Using air as the primary working fluid, experimental tests have encompassed a wide range of electrode and channel configurations and operating pressure levels. As mentioned, the research effort to date has concentrated mainly on the area of charge generation by the corona process. Specific results of the various tests are presented and discussed in Part II of this paper.

References

1. John A. Decaire, "Effects of Partial Condensation Around Ions in Electrofluid Dynamic Energy Conversion Processes", ARL Report 66-0187, Wright-Patterson Air Force Base (1966).
2. Meredith C. Gourdine, "Power Generation by Means of the Electric Wind", JPL Technical Report 32-6 (April 1960).
3. Meredith C. Gourdine and B. Kahn, "A Basic Study of Slender Channel Electrogas dynamics", ARL Report 63-205, Wright-Patterson Air Force Base (November 1963).
4. Meredith C. Gourdine and B. Kahn, "Electrogasdynamic Power Generation", AIAA Journal, Vol. 2 Nr 8, 1423-1427 (August 1964).
5. Michael Hawes, "Experimental Techniques in Electrofluid Dynamic Energy Conversion Research", ARL Report 64-77, Wright-Patterson Air Force Base (1964).
6. Maurice O. Lawson, Hans J.P. von Ohain, and Frank Wattendorf, "Performance Potentialities of Direct Energy Conversion Processes Between Electrostatic and Fluid Dynamic Energy", ARL Report 178, Wright-Patterson Air Force Base (December 1961)
7. Maurice O. Lawson, "Performance Characteristics of Electrofluid Dynamic Energy Conversion Processes Employing Viscous Coupling", ARL Report 64-74, Wright Patterson Air Force Base (October 1964).
8. Maurice O. Lawson, "Ion Generation by Corona Discharge for Electrofluid Dynamic Energy Conversion Processes", ARL Report 64-76, Wright-Patterson Air Force Base (October 1964).
9. Alvin M. Marks, "Heat-Electrical Power Conversion Through the Medium of a Charged Aerosol", U.S. Patent Nr 2,638,555 (1953).
10. Alvin M. Marks, et.al., "Charged Aerosol Energy Converter", AIAA Journal, Vol 2, Nr 1, 45-51 (January 1964).
11. Marks Polarized Corporation, Final Report on Contract N0w 63-0225-C, Bureau of Naval Weapons, Washington, D.C. (1963).
12. John M. Smith, "Theoretical Study of the Electrohydrodynamic Generator", G.E. Space Sciences Laboratory, R615D192 (November 1961).
13. Otmar M. Stuetzer, "Ion Transport High Voltage Generators", The Review of Scientific Instruments, Vol 32, Nr 1, pp 16-22 (Jan 1961).

14. Hans J.P. von Ohain and Frank Wattendorf, "Potentialities of Direct Electrofluid Dynamic Energy Conversion Processes for Power Generation", ARL Report 64-73, Wright-Patterson Air Force Base (October 1964)
15. J.M.Meek and J.D.Craggs, "Electrical Breakdown of Gases", Oxford at the Clarendon Press (1953)



TABLE I  
CHARACTERISTICS OF DIELECTRIC GASES

Gas	Ion Mobility ( $\text{cm}^2/\text{volt-sec}$ )		Relative Dielectric Strength $E_{b,n}/E_{b,n}(\text{air})^*$
	k(+)	k(-)	
Air	1.7	2.2	1.00
Hydrogen	6.4	10.	0.67
Helium	6.1	7.6	~0.2
Carbon Dioxide	0.9	1.2	0.9
Sulfur Dioxide	0.5	0.5	1.9
Steam ( $\text{H}_2\text{O}$ )	0.85	0.82	~1.
Ammonia	0.7	0.77	~1.2
Chloroform	0.23	0.2	4.2

\*  $E_{b,n}(\text{air}) \sim 30,000$  volts/cm

TABLE II  
PERFORMANCE CHARACTERISTICS OF VISCOUS EFD  
ENERGY CONVERSION PROCESSES

k = ion mobility; h = electrode distance; v = gas velocity; E<sub>1</sub> = entrance field strength  
 (Contains maximizing condition, E(h) = 0)

	Slip between ions and working medium $s = \frac{kE_1}{v}$	Negligible slip (charged particles) s → 0
Current Density	$i = \frac{\epsilon v^2}{2hk_n} s(2-s) \frac{\rho}{\rho_n}$	$i = \frac{\epsilon v E_{b,n}}{h} \frac{\rho}{\rho_n}$
Potential	$V = \frac{hv}{k_n} \frac{s(1-\frac{2}{3}s)}{(2-s)} \frac{\rho}{\rho_n}$	$V = \frac{hE_{b,n}}{2} \frac{\rho}{\rho_n}$
Maximum Power Density	$L_e = iV = \frac{\epsilon v^3}{2k_n^2} s^2(1-\frac{2}{3}s) \frac{\rho}{\rho_n}$	$L_e = iV = \frac{\epsilon v E_{b,n}^2}{2} \frac{\rho}{\rho_n}$
Electrical Pressure Drop	$\Delta P_e = \frac{\epsilon E_1^2}{2} = \frac{\epsilon v^2}{2k_n^2} s^2 \frac{\rho}{\rho_n}$	$\Delta P_e = \frac{\epsilon E_{b,n}^2}{2} \frac{\rho}{\rho_n}$
Stage Efficiency	$\eta_{st} = \frac{1 - \frac{2}{3}s}{1 + \xi \frac{\rho_n k_n^2}{\epsilon} \frac{1}{s^2} \frac{\rho_n}{\rho}}$	$\eta_{st} = \frac{i}{1 + \xi \frac{\rho_n v^2}{\epsilon E_{b,n}^2} \frac{\rho_n}{\rho}}$

# TABLE III

## SOME PERFORMANCE VALUES OF VISCOUS EFD PROCESSES

GIVEN CONDITIONS	TYPE OF WORKING GAS	AIR	AIR	AIR	HYDROGEN WITH ADDITIVES
	PRESSURE LEVEL	1 atm.	20 atm.	20 atm.	20 atm.
	MASS DENSITY	$1.22 \frac{\text{KG}}{\text{M}^3}$	$24.4 \frac{\text{KG}}{\text{M}^3}$	$24.4 \frac{\text{KG}}{\text{M}^3}$	$1.9 \frac{\text{KG}}{\text{M}^3}$
	BREAKDOWN FIELD STRENGTH	$3 \cdot 10^4 \frac{\text{VOLT}}{\text{cm}}$	$6 \cdot 10^5 \frac{\text{VOLT}}{\text{cm}}$	$6 \cdot 10^5 \frac{\text{VOLT}}{\text{cm}}$	$\sim 6 \cdot 10^5 \frac{\text{VOLT}}{\text{cm}}$
	TYPE OF CHARGED PARTICLES	IONS	IONS	CHARGED PARTICLES	CHARGED PARTICLES
	MOBILITY	$2.2 \times 10^{-4} \frac{\text{M}^2}{\text{volt sec.}}$	$1.1 \times 10^{-5} \frac{\text{M}^2}{\text{volt sec.}}$	$1 \times 10^{-8} \frac{\text{M}^2}{\text{volt sec.}}$	$2.5 \times 10^{-8} \frac{\text{M}^2}{\text{volt sec.}}$
	SLIP RATIO $S = \frac{\text{DRIFT VELOCITY}}{\text{GAS VELOCITY}}$	1.0	1.0	.002	.002
	VELOCITY OF WORKING GAS	$250 \frac{\text{M}}{\text{SEC.}}$	$250 \frac{\text{M}}{\text{SEC.}}$	$250 \frac{\text{M}}{\text{SEC.}}$	$470 \frac{\text{M}}{\text{SEC.}}$
	DRAG COEFFICIENT ( $\xi$ ) OF CONVERSION SECTION	$\frac{3}{100}$	$\frac{3}{100}$	$\frac{3}{100}$	$\frac{3}{100}$
RESULTING PERFORMANCE VALUES	SPECIFIC POWER OUTPUT	$.05 \frac{\text{WATT}}{\text{cm}^2}$	$20 \frac{\text{WATT}}{\text{cm}^2}$	$400 \frac{\text{WATT}}{\text{cm}^2}$	$750 \frac{\text{WATT}}{\text{cm}^2}$
	STAGE EFFICIENCY	0.2%	3%	41%	74%
	PRESSURE DROP ÉLECTRIC + DRAG	.01 atm	.2 atm	.40 atm	.22 atm
	PRESSURE RATIO	1.01	1.01	1.02	1.01

FIGURE 1

# ILLUSTRATION OF ELECTROFLUIDDYNAMIC ENERGY CONVERSION PROCESS (FLUID DYNAMIC VAN DE GRAAFF)

 INDICATES ELECTRICAL INSULATOR

 INDICATES ELECTRICAL CONDUCTOR

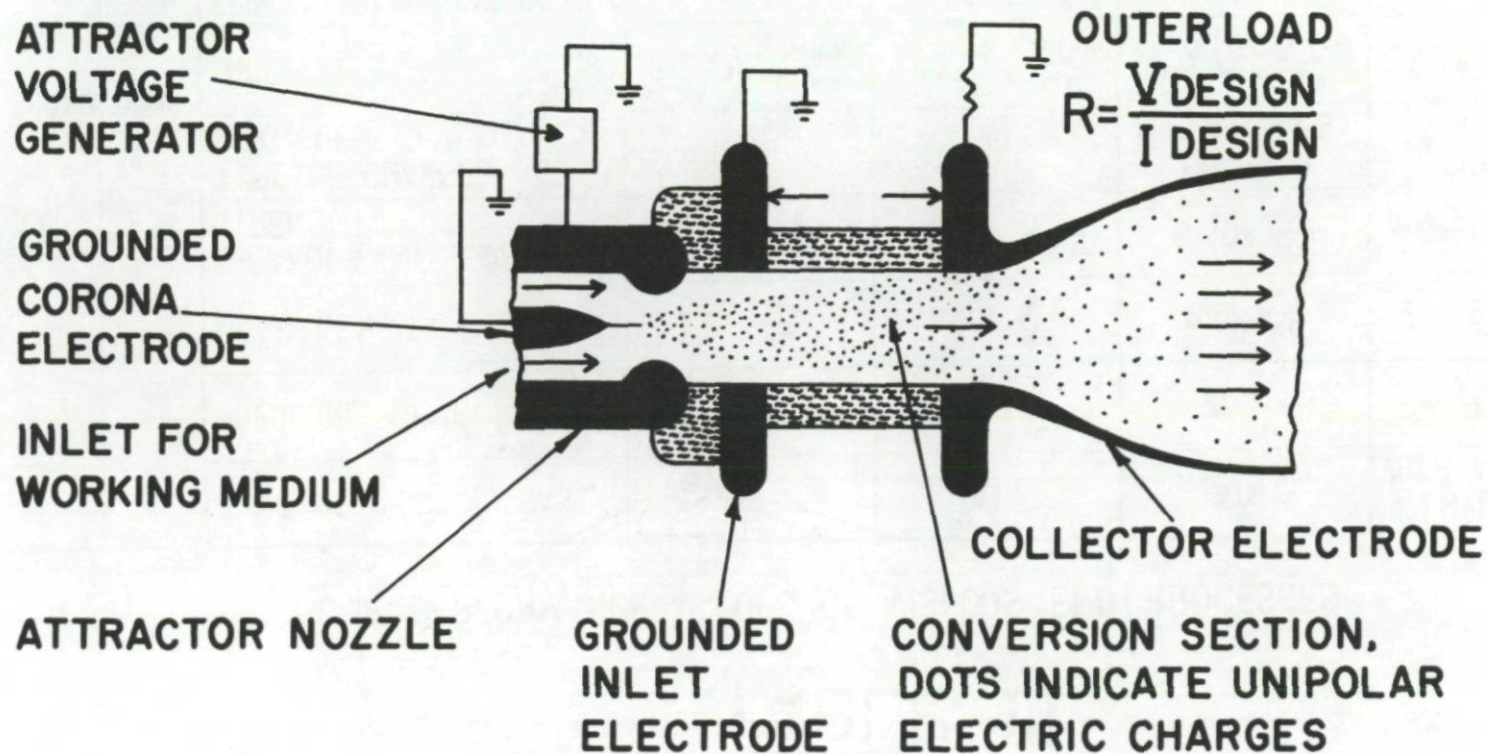
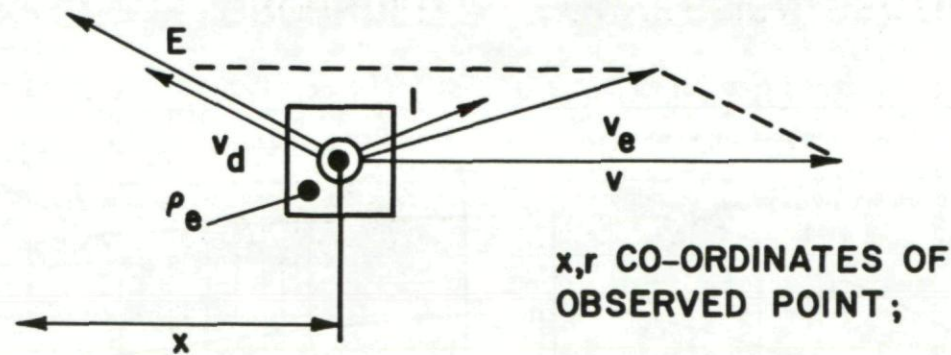


FIGURE 2

RELATIONS BETWEEN ELECTRICAL AND VELOCITY FIELDS



$\vec{v}(x,r)$  = VELOCITY OF DIELECTRIC WORKING MEDIUM;

$\vec{E}(x,r)$  = ELECTRIC FIELD STRENGTH DUE TO COLLECTOR POTENTIAL (V) AND SPACE CHARGE;

$\vec{v}_d(x,r) = k\vec{E}(x,r)$  = DRIFT VELOCITY OF CHARGED PARTICLES RELATIVE TO WORKING MEDIUM;  $k$  = MOBILITY;

$\vec{v}_e(x,r) = \vec{v}(x,r) + \vec{v}_d(x,r)$  = TRANSPORT VELOCITY OF CHARGED PARTICLES

$\rho_e(x,r) = \epsilon \operatorname{div} \vec{E}(x,r)$  = ELECTRIC CHARGE DENSITY;

$\vec{i}(x,r) = \rho_e(x,r) \cdot \vec{v}_e(x,r)$  = ELECTRIC CURRENT DENSITY;

$V = \int_0^h \vec{E}(x,r) \cdot d\vec{x}$  = ELECTRIC POTENTIAL (independent of  $r$ )

THROUGHOUT THE CONVERSION SECTION:

$v_x(x,r) > kE_x(x,r)$  (CHARGES TRANSPORTED TO COLLECTOR)

$E(x,r) < E_b$  ( $E_b$  = BREAKDOWN FIELD STRENGTH)

$I = 2\pi\epsilon \int_0^R \vec{i}(x,r) \cdot r dr$  = ELECTRIC CURRENT, INDEPENDENT OF  $x$   
(no charges deposited on walls)

FIGURE 3

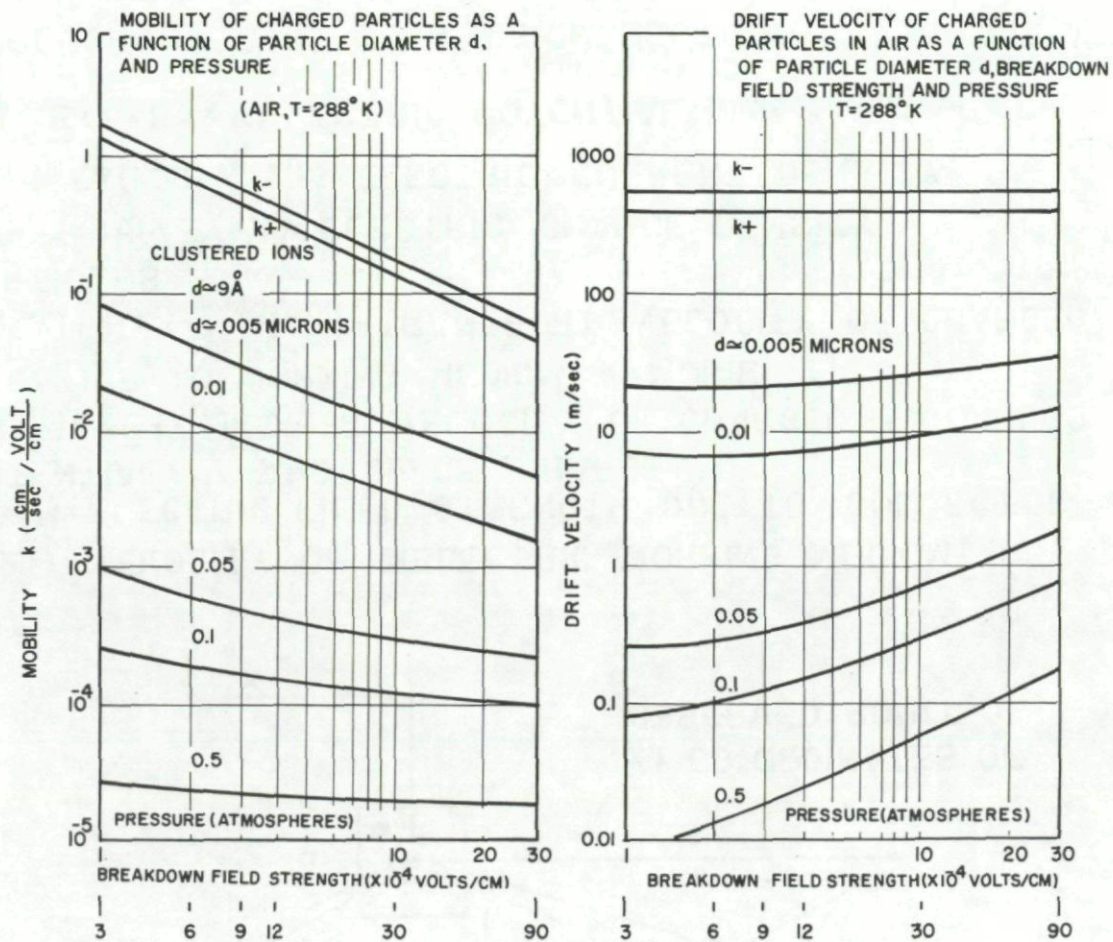


FIGURE 4

SCALING CHARACTERISTICS

A) GEOMETRIC SCALING, SCALING FACTOR  $\alpha$ :

(VELOCITY AND PHYSICAL PROPERTIES OF FLUID MEDIUM UNCHANGED)

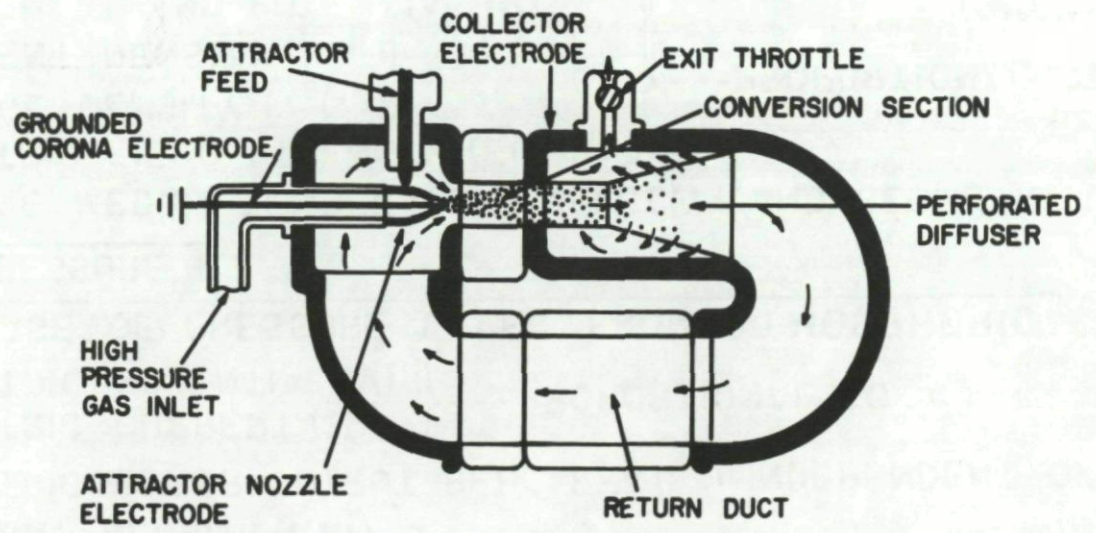
- a) CHARGE DENSITY ( $\rho_e(x,r)$ )  
CURRENT DENSITY ( $i(x,r)$ ) } ---- INVERSELY PROPORTIONAL TO  $\alpha$
- b) ELECTRIC POWER OUTPUT PER AREA ( $L_e$ ) INDEPENDENT OF  $\alpha$
- c) ELECTRIC CURRENT (I)  
ELECTRIC POTENTIAL (V) } --- PROPORTIONAL TO  $\alpha$

B) INCREASE OF PRESSURE LEVEL FROM ATMOSPHERIC PRESSURE  $P_N$   
TO PRESSURE P:

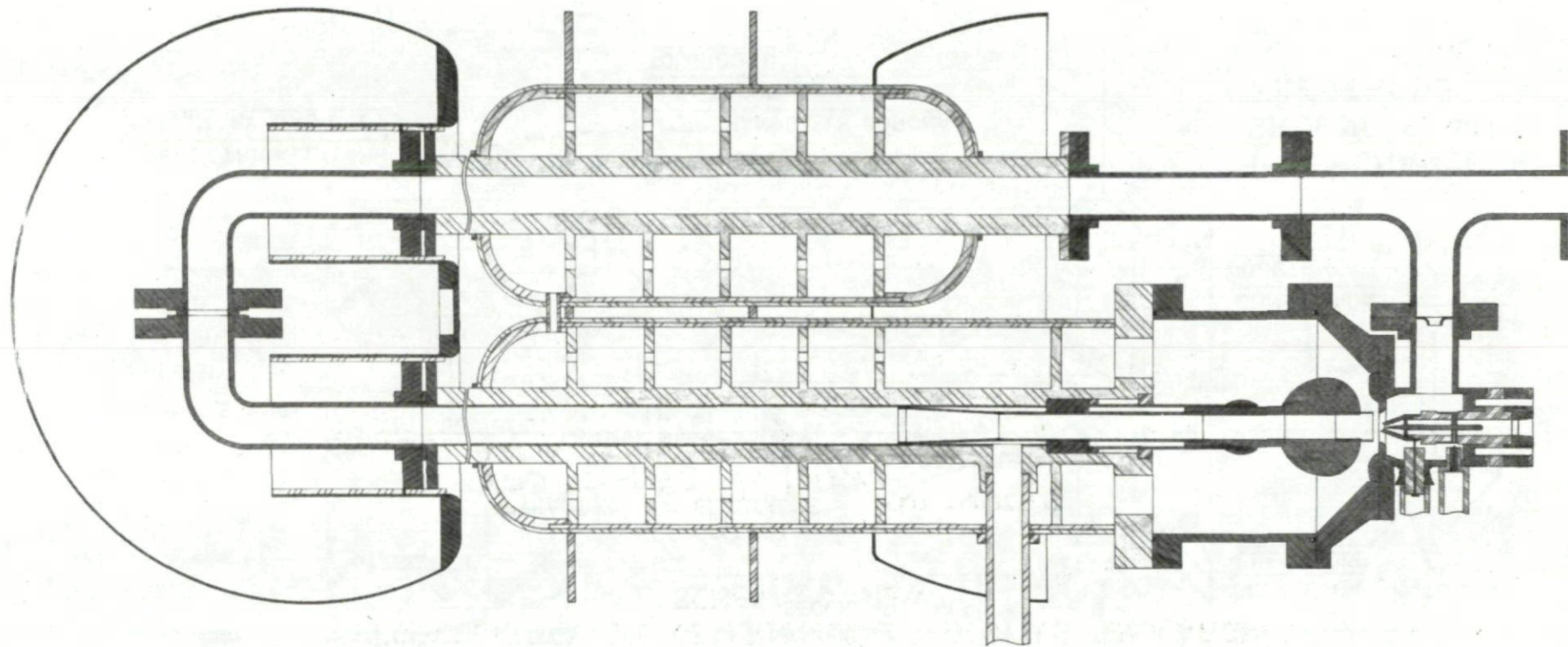
(WORKING MEDIUM, TEMPERATURE, VELOCITY, AND GEOMETRY UNCHANGED)

- d) ELECTRIC FIELD STRENGTH ( $E(x,r)$ )  
CHARGE DENSITY ( $\rho_e(x,r)$ )  
CURRENT DENSITY ( $i(x,r)$ )  
CURRENT (I) AND POTENTIAL (V) } --- PROPORTIONAL TO  $P/P_N$
- b) TRANSPORT VELOCITY ( $v_e$ ), DRIFT VELOCITY ( $v_d$ )  
OF IONS OR CHARGED COLLOIDS OF VERY  
SMALL DIAMETER (BELOW  $\frac{2}{100}$  MICRON) } --- INDEPENDENT OF  $P/P_N$
- c) ELECTRIC POWER OUTPUT (I·V) --- PROPORTIONAL TO  $(P/P_N)^2$

FIGURE 5  
RECIRCULATORY EFD GENERATOR, (CLOSED CYCLE SIMULATION)  
SCHEMATIC VIEW



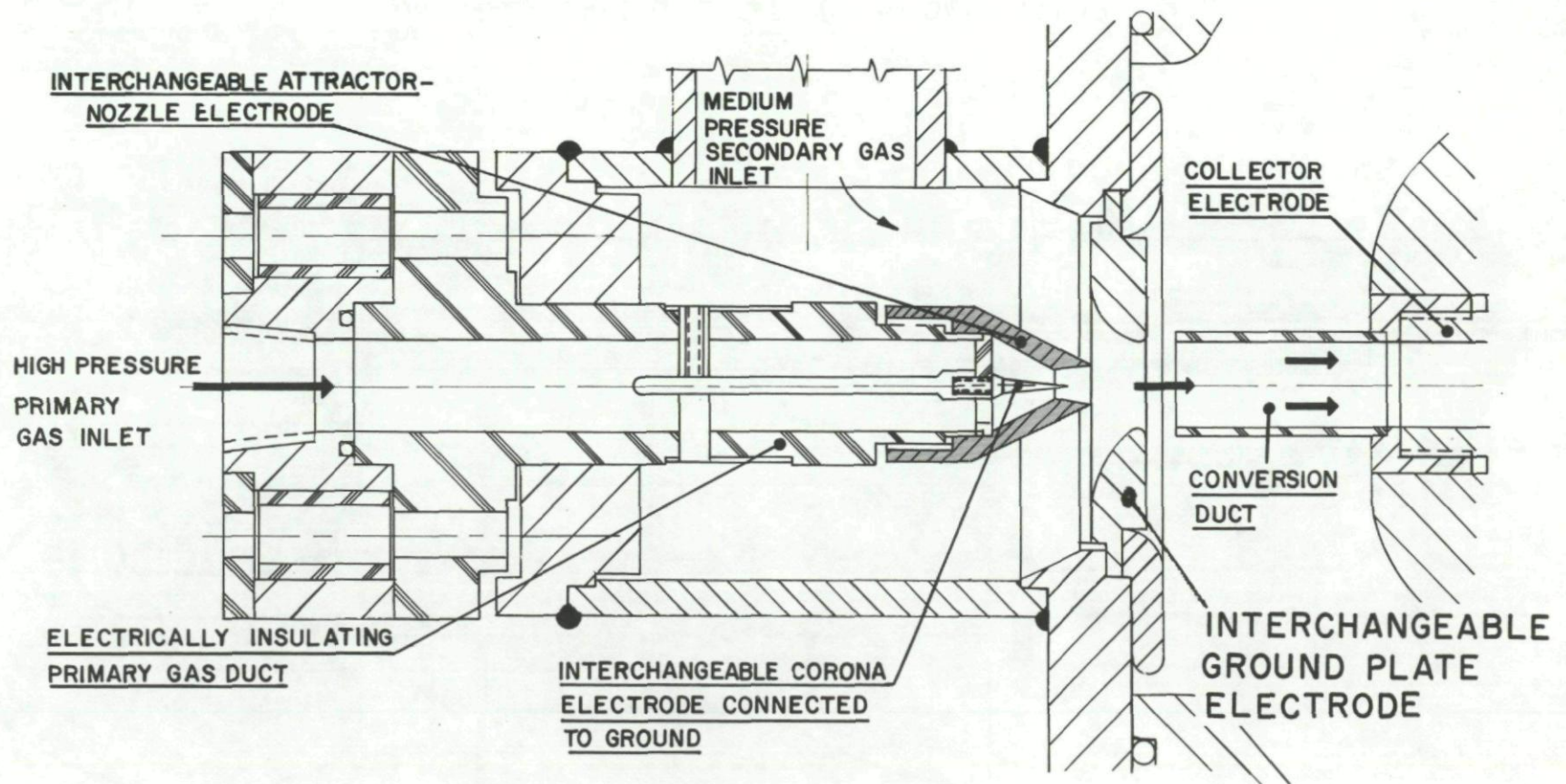




 INSULATOR  
 CONDUCTOR

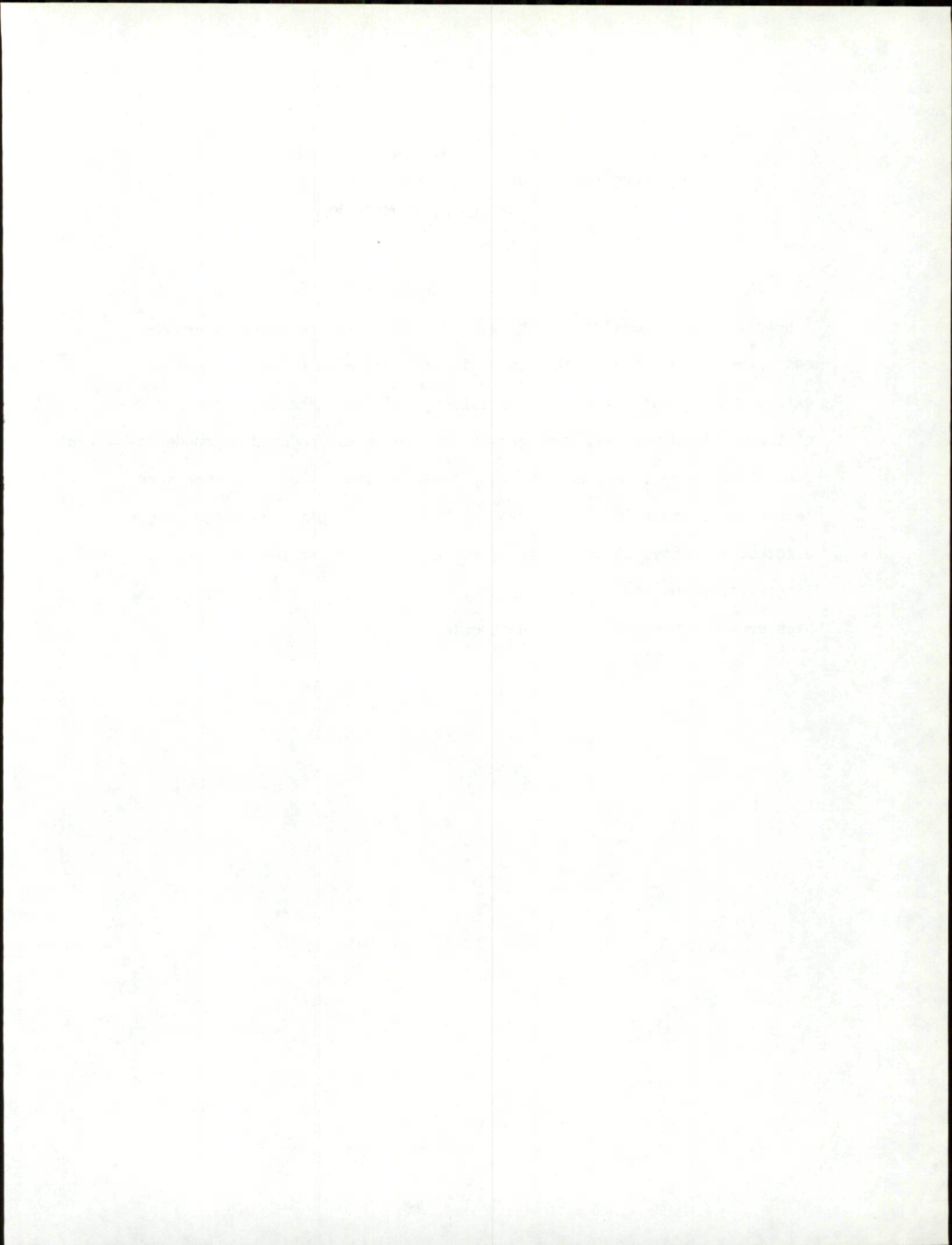
ARL EXPERIMENTAL EFD GENERATOR

FIGURE 6



TYPICAL ELECTRODE CONFIGURATION OF EFD TEST RIG

FIGURE 7



EFFECTS OF ELECTRODE GEOMETRY SIMILARITY AND  
SCALING LAWS IN EFD ENERGY CONVERSION PROCESSES

Part II: Experimental Results

Summary

The ion currents generated with a sharp needle electrode increase linearly with increasing primary air pressure level up to about 40 atmospheres. The linear variation of ion current with total pressure is extended up to the maximum test pressure of 80 atmospheres by the use of the nailhead needles. Charged aerosol currents produced by condensation of water vapor around ions vary linearly with inlet total pressure levels up to about 30 atmospheres for both the sharp and nailhead needle electrodes. Above 30 atmospheres, the aerosol current fell off from a linear variation with total pressure. Future tests will investigate the high pressure aerosol current production.

EFFECTS OF ELECTRODE GEOMETRY SIMILARITY AND  
SCALING LAWS IN EFD ENERGY CONVERSION PROCESSES

Part II: Experimental Results

James R. Wifall  
Aerospace Research Laboratories  
Office of Aerospace Research  
United States Air Force  
Wright-Patterson Air Force Base, Ohio

Introduction

The major experimental effort in electrofluid dynamics(EFD) at ARL has been in charge production. This effort was conducted on the test rig described in Part I and shown in Figure 6. The overall test set-up is schematically shown in Figure 8. Pressurized dry air (-65°F dew-point) at approximately 200 atm is supplied from the ARL bottle farm. The pressure to the generator is accurately controlled by pressure regulators on the test stand. Three heaters in the air lines permit the addition of up to 240 KW of energy. A water injection system permits the addition of small flow rates of water to control the relative humidity of the air. The measured parameters of the input (primary) air include stagnation temperature and pressure, flow rate of water added, and the air mass flow rate. In the generator, the temperature and pressure of the recirculating (secondary) air, needle, ground plate, collector and attractor currents, attractor voltage, and collector potential were recorded. The test generator (Figure 7) provided for many variations, some of which are the nozzle throat diameter, design Mach number and position, needle size, shape and position, conversion section diameter and length, ground plate shape and diameter, and collector diameter and position. Almost all

of the tests were run with a positive potential on the attractor which provides negative ions as the charge carriers and a negative collector potential. Since the generator had a limited voltage capability due to external breakdown of the fiberglas insulation, most of the tests were run with the collector grounded, similar to a short circuit generator test.

#### Current Characteristics

A typical current versus attractor voltage characteristic for the test generator is shown in Figure 9. The ion current characteristic for increasing attractor voltage can be divided into three regimes. The first regime shows the current increasing nearly linearly with increasing attractor voltage. In this regime, the current lost to the ground plate and attractor is negligible and all the current produced at the needle is collected on the collector. Continued increase in the attractor voltage results in a second regime in which the needle current still increases nearly linearly but there is an appreciable attractor and ground plate current. Since for the conservation of current, the needle current must equal the sum of the attractor ground plate and collector currents, the collector current is decreased from the linear increase and may level off. Continued increase of the attractor voltage in the third regime results in an abrupt increase in needle and attractor currents corresponding to spark breakdown between these electrodes. Certain operating conditions and/or geometries may minimize the second regime and the characteristic may go directly from the first regime to the third regime. Since any current not going to the collector is a loss, and in order to

compare test results, we have picked the operating point which is considered the maximum current as that point at which the attractor current reaches 30 micro amperes or there is spark breakdown between the needle and attractor electrodes. Throughout the rest of this paper, any reference to maximum needle current will refer to either of these conditions. This is actually the maximum current that can be transported to the collector.

#### Influence of Pressure

Both the primary (input) and secondary (recirculating loop) pressure could be varied. The primary pressure was varied from 10 to 80 atm. The variations with pressure are really variations with density, but since the temperature was kept constant, it is more convenient to discuss the effect of pressure variations. The effect of this variation on the maximum needle current and corresponding attractor voltage is shown in Figure 10. In this case, the secondary pressure was kept at 1/5 the primary pressure. The maximum needle current and corresponding attractor voltage increase nearly linearly with increasing primary pressure up to about 50 atmospheres. Over 50 atmospheres, the current no longer increases and becomes quite erratic. The corresponding attractor voltage also falls off from the linear increase expected. The probable reason for this departure from Lawson's theory (Ref. 8) is that the limiting side conditions assumed in the theory no longer apply. The limitation on current production at these higher pressures occurs with a spark breakdown rather than an excessive attractor current, thus indicating that it may be the corona process itself which provides

the current limitation. The sharp needle at 80 atmospheres requires a very high attractor voltage (almost 100 KV).

In order to increase the current linearly with pressure up to 80 atm., a unique needle electrode configuration was designed as shown in Figure 11. The configuration was changed from a sharp point to a needle with a sharp edged disk (called a nailhead needle) providing the corona edge. As the supersonic flow passes over the corona edges, there is a local low pressure regime due to the expansion fan at the edge. This low pressure regime is favorable to the corona mechanism. Figure 12 shows the dependence of the maximum current and corresponding attractor voltage on the pressure level. With the nailhead needle, the current increases linearly throughout the entire range of pressure tested and the corresponding attractor voltage is approximately 1/2 that required for the sharp needle. It should also be noted that the current level is slightly higher over the low pressure regime. The needles shown in Figure 13 are all considered to be nailhead needles since in each case the corona edge is the edge of a disk which also produces a low pressure region and in all cases the maximum current varies linearly with primary pressure over the entire pressure range. The results for all needles thus far have been essentially the same with only a slight variation in magnitude.

Another pressure variation which influences the maximum needle current is the expansion ratio, i.e., the pressure ratio across the nozzle. This was controlled by keeping the primary pressure constant and varying the secondary pressure. Figure 14 shows the maximum current and



corresponding attractor voltage for the nailhead and sharp needles as a function of the expansion ratio. The maximum needle current for the nailhead needle rises nearly linearly with a decreasing ratio. The current reaches a maximum at a ratio between 6 and 7 and then drops off. The corresponding attractor voltage curve for the nailhead needle rises smoothly with decreasing ratio over the entire range. The curves for the sharp needle are similar in shape with the maximum needle current occurring at an expansion ratio of 5. In all cases, the peak current occurs at a ratio between 3 and 7 and in most cases between 5 and 7. One interesting characteristic of the sharp needle curves is that they are both made up of straight lines with different slopes. This change in slope occurs at the design pressure ratio (8) of the nozzle.

#### Scaling Relationships

Part I discussed some of the scaling relationships that Lawson (Ref. 8) has derived. One of the relationships was that the maximum current is directly proportional to the geometric scaling factor  $\alpha$ , i.e., if all the dimensions are varied by some factor  $\alpha$  then the maximum current should also vary by the factor  $\alpha$ . To check this scaling relationship, a series of scaling configurations were designed which are shown in Figure 15. These configurations are photographic reductions of the largest geometry which has a Mach 2 nozzle with a 5/16" diameter throat, a 1 1/4" diameter ground plate, and a 1 1/4" diameter conversion section 1" long. The configurations were reduced to nozzle throat diameter of 1/4", 3/16", and 1/8". Figure 16 shows the sharp and nailhead needles used in the scaling tests. Scaled versions of these needles

were used for the scaling tests. The scaling configurations were run at various pressures, with the results averaged as shown in Figure 17. The maximum current and corresponding attractor voltage for each configuration has been normalized by the values obtained for the 5/16" configuration, therefore, the scaling factor  $\alpha$ , for the 5/16" configuration is 1, for the 1/4" configuration 0.8 and so forth. Curve "a" shows the scaling relationship of current for the sharp needle. As can be seen from the curve, the maximum needle current ( $I_{\max}$ ) and corresponding attractor voltage ( $V_{\max}$ ) does not correspond to the linear scaling relationship that was predicted. The smaller configurations do considerably better than expected from the linear scaling relationship. This deviation is not completely understood but is probably due to high voltage effects, non-uniform fields and the departure of the gas from the linear breakdown relationship. As a point of interest, the attractor voltage ( $V$ ) was forced to follow the linear relationship. In this case, the needle current ( $I$ ) also closely follows the linear scaling relationship. The two nailhead needles gave similar results and the combined results are shown in Curve "b". Again, the smaller geometries do better than would be expected from the theory. As before, if the attractor voltage is forced to follow the linear relationship, then the current also closely follows the linear variation. The high current values at the smaller geometries is an added indication that small sizes should be used to obtain the highest current densities.

Another of the geometric variables is the ratio of the nailhead diameter to the nozzle throat diameter. The effect of this ratio on

the maximum needle current and corresponding attractor voltage is shown in Figure 18. In this case, the nozzle diameter was fixed and the size of the nailhead varied. The maximum current is only slightly dependent on the ratio although there is a maximum at a ratio of about one half. It should be noted that the attractor voltage decreases nearly linearly with an increasing ratio. As a point of interest, the sharp needle results are plotted at the left of the graph. Since the current depends to a great extent on the actual geometry of the needle and attractor, Figure 18 should only be used to indicate trends.

Another of the geometrical variables, which may depend a great deal on particular geometry, is the axial position of the needle within the nozzle. As the corona edge or point is moved upstream in the nozzle toward the throat, the conditions for the corona process change greatly and the maximum current then depends on the interaction of several effects. Among these are: a decreasing distance between the attractor and corona electrodes; a decreasing velocity and corresponding increasing pressure; an increased area of the attractor electrode seen by the charges and therefore, a greater chance for them to flow to this electrode; and a change in the field concentration on the corona electrode which may lead to a component tending to pull the ions downstream. The effect of axial needle position in the nozzle on the maximum current is shown in Figure 19. The area between the exit plane and throat is of primary interest as there is a substantial decrease in current outside of this area. The effects of both the sharp needle and nailhead needle are plotted. It should be noted that the maximum current

from the nailhead needle is more dependent on position than is the sharp needle, although in both cases the maximum occurs slightly upstream of the exit plane. Figure 20 shows the same curves with the corresponding attractor voltage added. It can be seen that the attractor voltage for the sharp needle is relatively independent of position which would tend to indicate that the various effects compensate for changing needle position. For the nailhead needle, the attractor voltage curve is similar to the maximum current curve. But as will be discussed later, it may be desirable when running with a counter voltage on the collector to operate with the needle upstream of the position of maximum current to help compensate for the less than total shielding of the ground plate.

#### Charged Aerosol Particles

The feasibility of producing charged aerosol particles by the free condensation method described in Part I has been demonstrated by ARL and several other investigators at relatively low pressure levels, that is, below 15 atmospheres. ARL is currently in the process of extending this investigation up to 80 atmospheres primary pressure. It should be stressed that the use of aerosol particles as charge carriers is relatively unexplored. The following discussion refers only to the preliminary results from the tests using the aerosol particles as the charge carriers. Figure 21 shows a typical current-voltage characteristic for air with water added to provide 10% relative humidity. In this case, the current increases nearly linearly with increasing attractor voltage up to the point of spark break-down between the needle

and attractor electrodes. All the current is carried to the collector and the ground plate and attractor current are negligible. Also, the maximum current is the current at the point of spark breakdown between the needle and attractor electrodes. The effect of primary pressure on the maximum current is shown in Figure 22. The maximum current increases nearly linearly with increasing pressure up to about 30 atmospheres and above this pressure the maximum current falls off from the expected linear increase. This reduction in maximum current may be due to the shielding of the needle electrode by a dense cloud of low mobility charge carriers close to the corona edge, although the real reason for this may be more basic, such as differences in the condensation process at high pressures. Comparing the aerosol carriers with ions (Figure 23) it should be noted that at low pressures, the aerosol carriers are considerably better than the ions, as predicted by theory, however, at the higher pressures, the ions are slightly better than the charged aerosols at the present time. Also, the corresponding attractor voltage required is slightly higher for the aerosol case. The high pressure charged aerosol particle generation is a major area for future work, since the present current performance level of the charged aerosol particles is less than that for the ion carriers.

The scaling trend for current for aerosol charge carriers is shown in Figure 24. The conversion section geometries were modified to make them more favorable for future power tests on aerosol particle carriers. The channel diameters were reduced by a factor of  $3/4$  and the length increased by a factor of  $2 \frac{1}{2}$ . The current has been normalized by the

current for the 5/16" geometry and the sizes by 5/16". As in the ion case, the smaller sizes do considerably better than the linear relationship predicted by theory. Also, it should be noted that the current does scale linearly when the corresponding attractor voltage is forced to follow a linear variation.

The effect of needle position within the nozzle with aerosol particles is shown in Figure 25, also, plotted again are the results with ion current (from Figure 19). The position for maximum current with ions was slightly upstream of the exit plane, however, with aerosol particles, the needle position for maximum current occurs farther upstream near the throat. Also, it should be noted that the effect of position is less important for aerosol particles than for ion carriers. Experiments indicate that it is more favorable to make charged aerosol particles by condensing the vapor around the charge than by adding the charges to aerosol particles. In the latter case, there is even evidence that a mixture of ions and aerosol particles result. This explains why it is more favorable to produce the charges slightly down stream of the throat before the condensation occurs.

The present generator is limited by the insulation to 400,000 volts and therefore, very few power tests have been made. At this voltage, surface breakdown and sparkover are observed on the outside insulations. Figure 26 shows a power characteristic with ion carriers. The attractor voltage was kept constant at 45,000 volts and the load consisted of a 460 megohm resistor bank in parallel with a variable air gap. Plotted is current versus collector potential. As the collector potential is increased, the

needle current drops slightly. This is due to the ground plate not completely shielding the current producing section. Also, as the collector potential increases, there is an increase in ground plate and attractor current which results in a sizable drop in collector current. At lower current levels, it is possible to run up to maximum collector potential with negligible attractor and ground plate currents. Figure 27 shows a similar test using aerosol particle carriers. In this case, there is no decrease in current level with increasing collector potential and there is negligible attractor and ground plate currents.

# ARL EXPERIMENTAL SETUP

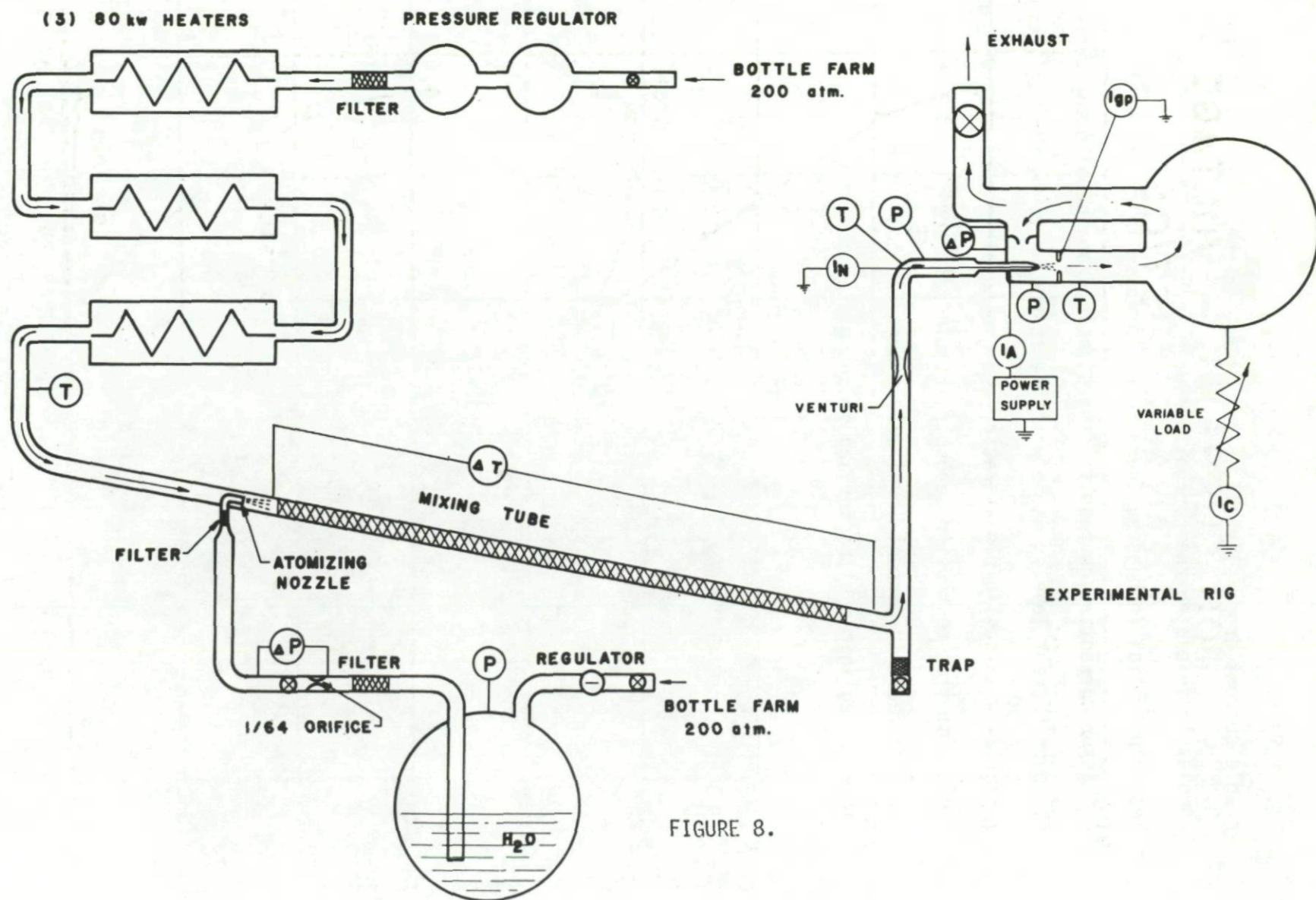


FIGURE 8.



# ION CURRENT - VOLTAGE CHARACTERISTICS

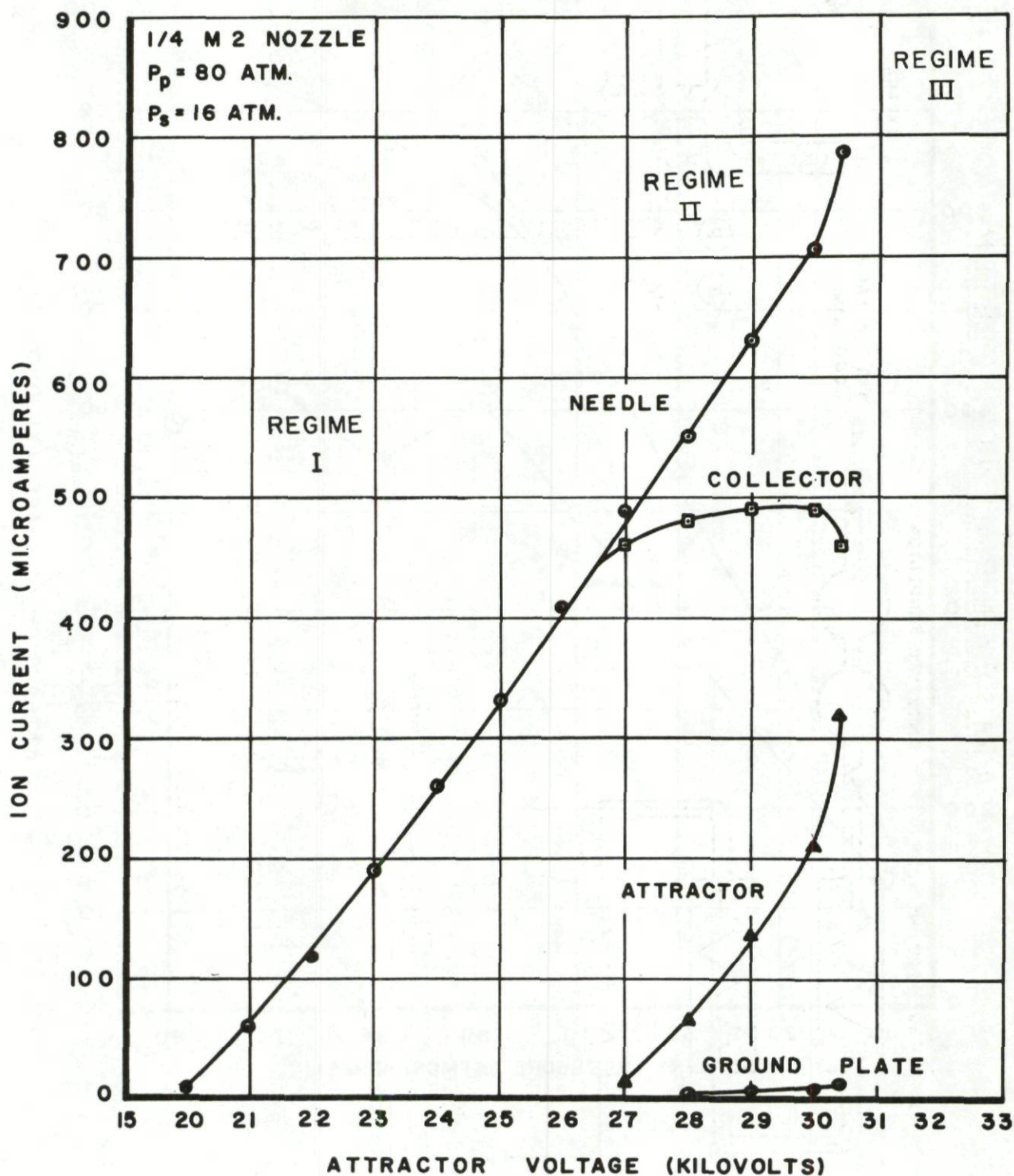


Figure 9

### ION CURRENT and VOLTAGE versus STAGNATION PRESSURE

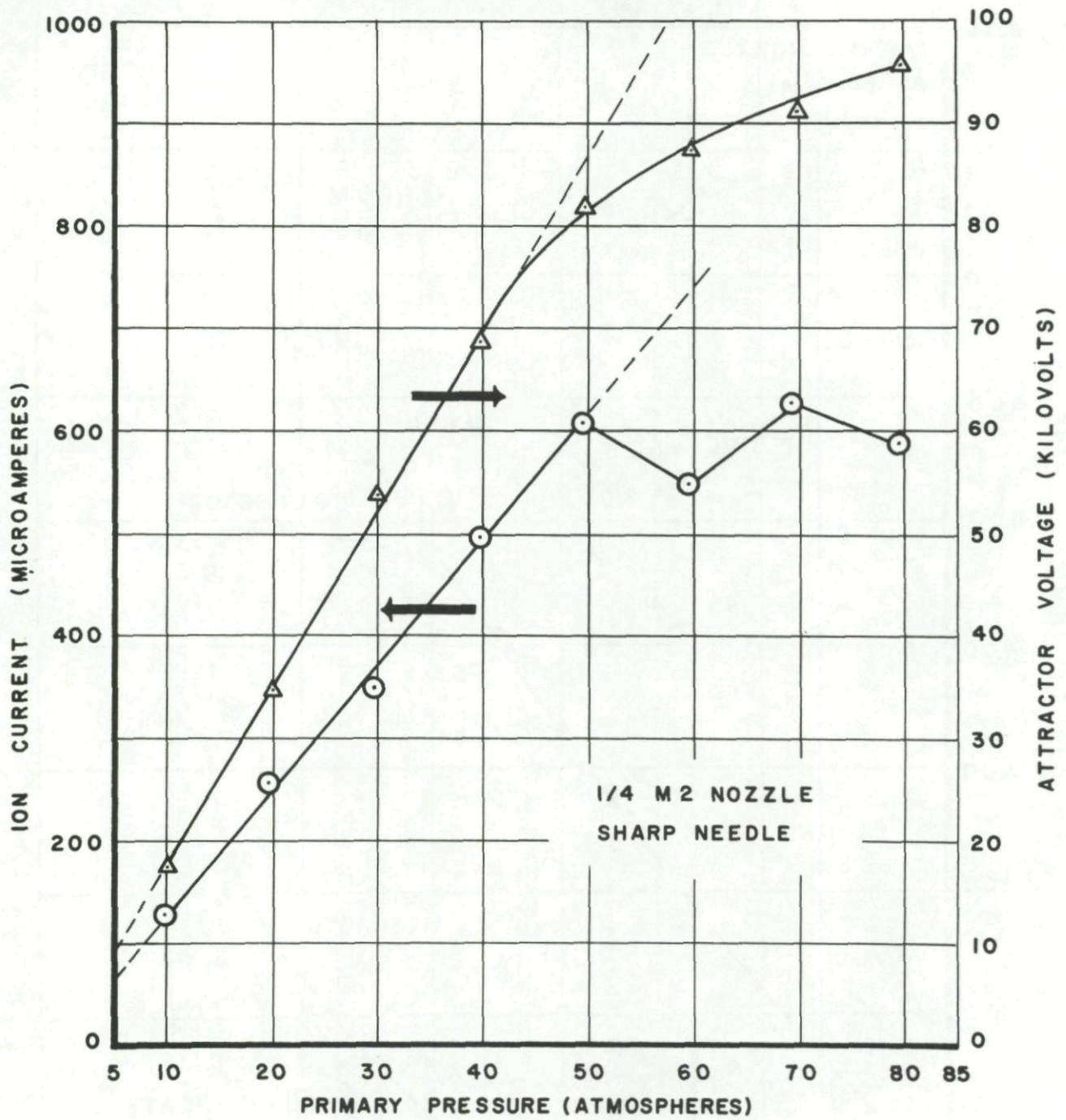


Figure 10

# NAILHEAD      NEEDLE

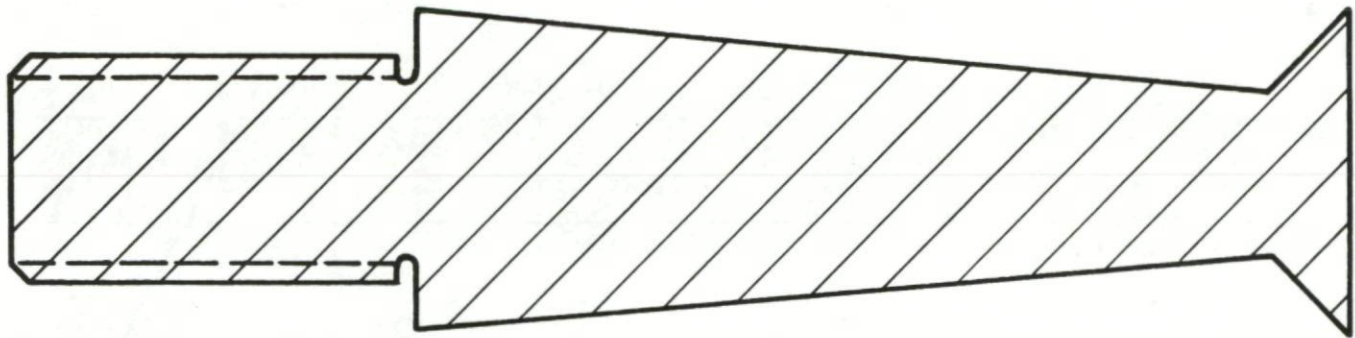


FIGURE 11.

# ION CURRENT and VOLTAGE versus STAGNATION PRESSURE

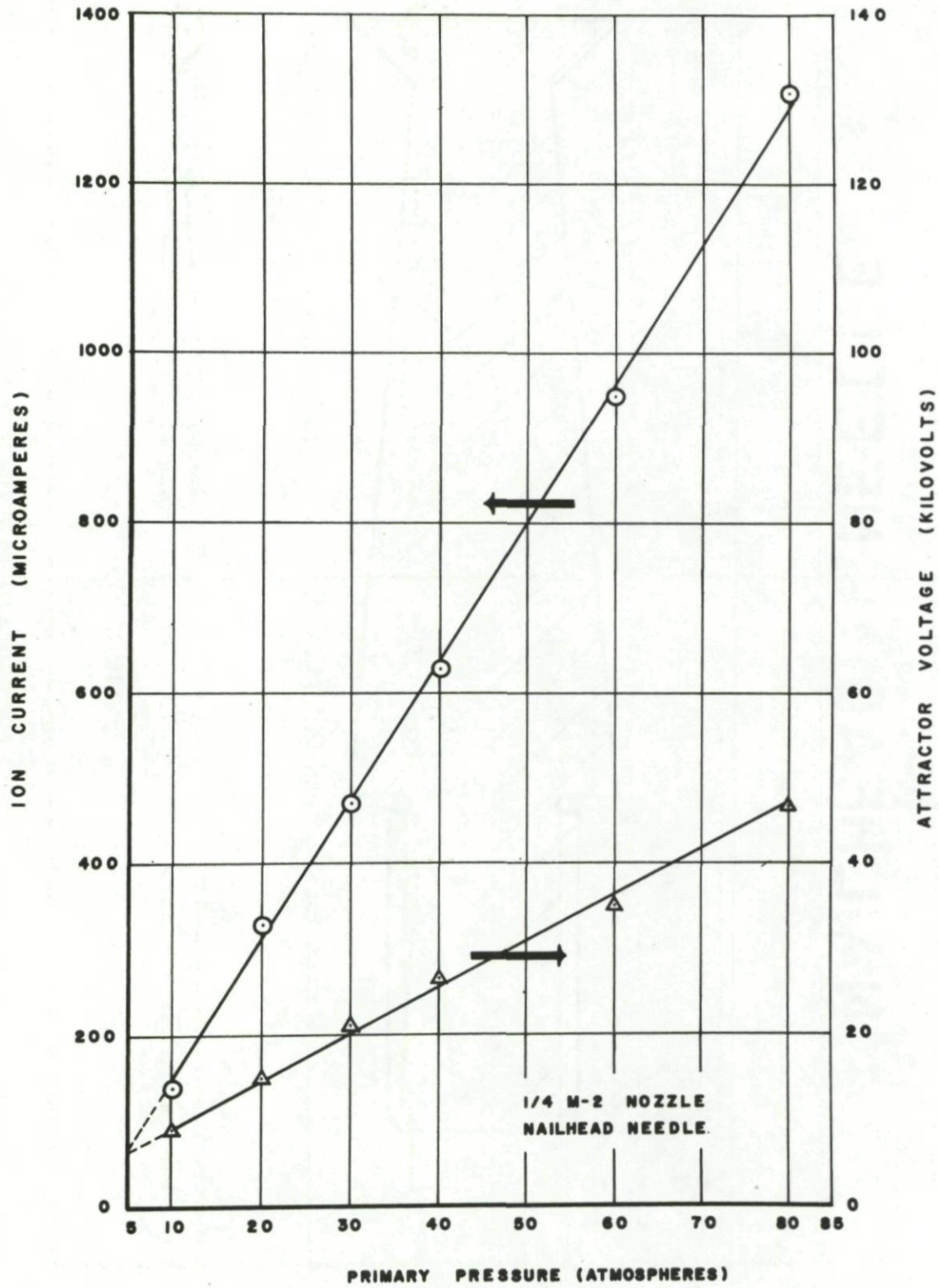
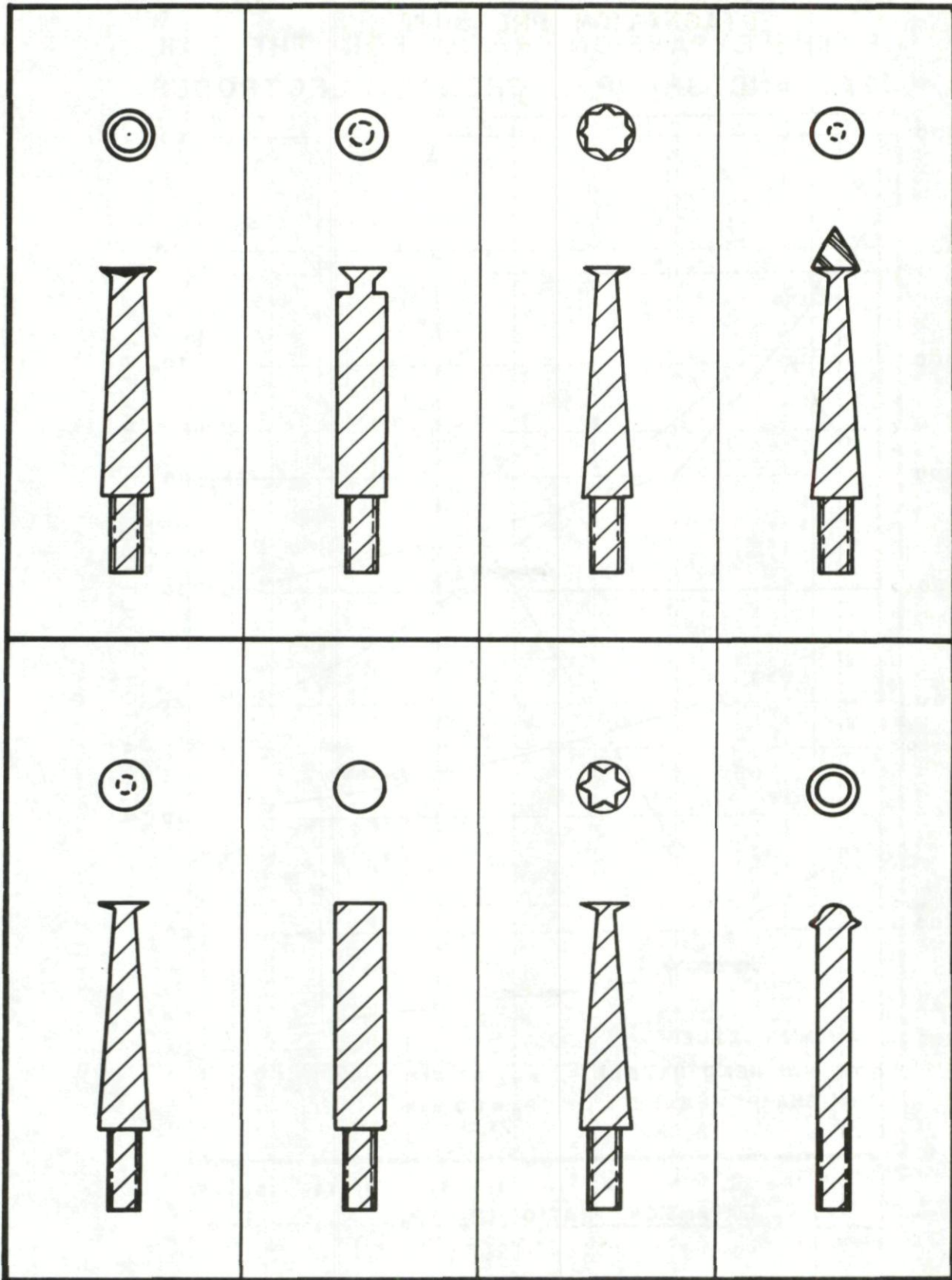


Figure 12



**NAILHEAD NEEDLES**  
FIGURE 13

# ION CURRENT & VOLTAGE AS A FUNCTION OF THE EXPANSION RATIO FOR THE NAIL HEAD AND SHARP CORONA ELECTRODES

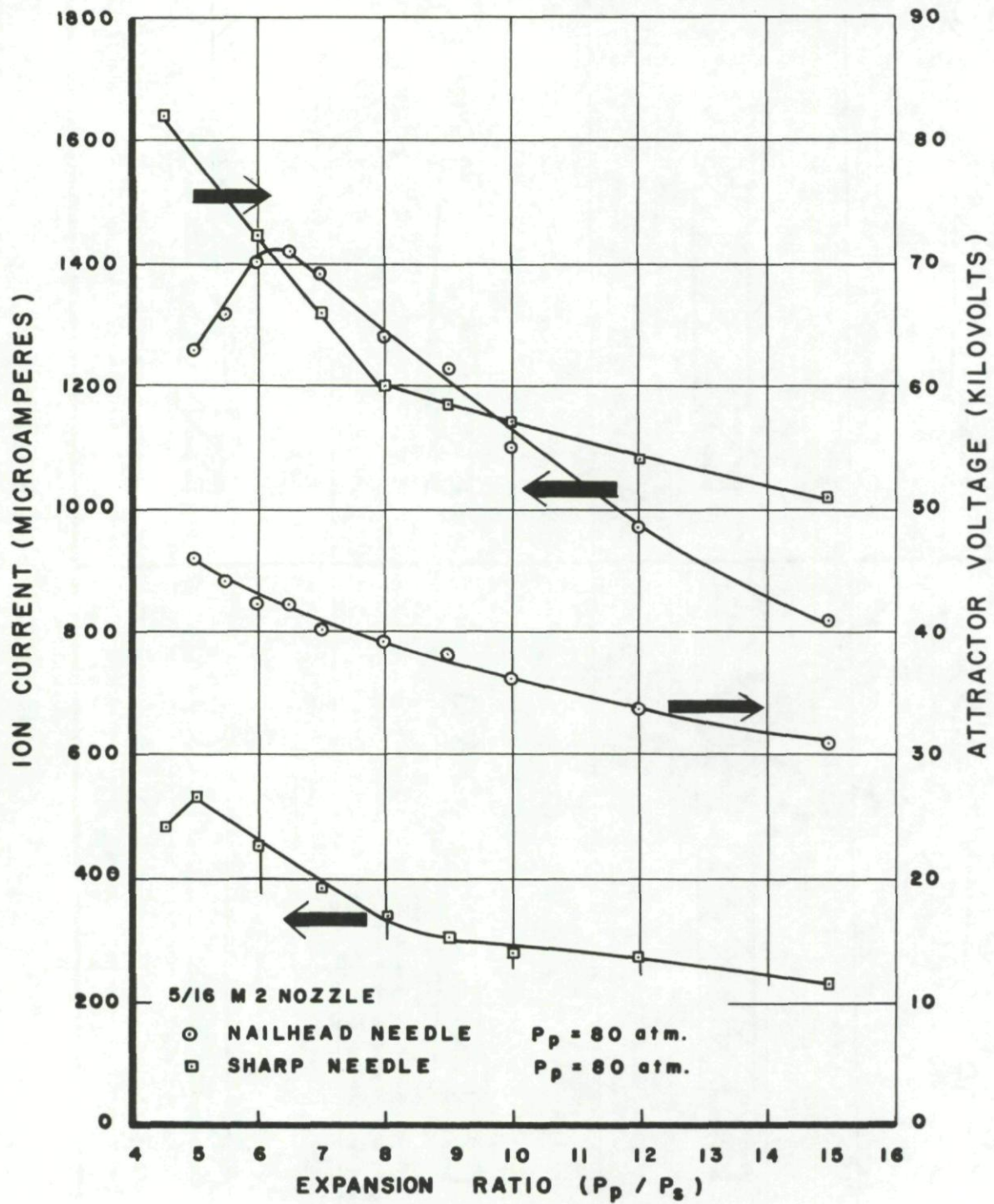


FIGURE 14

# GEOMETRIC SCALING CONFIGURATION

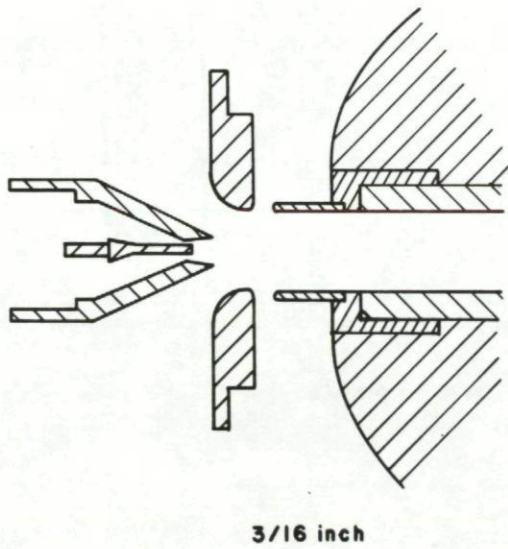
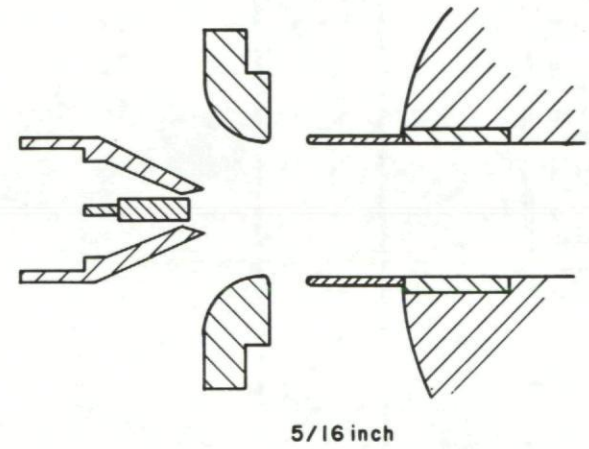
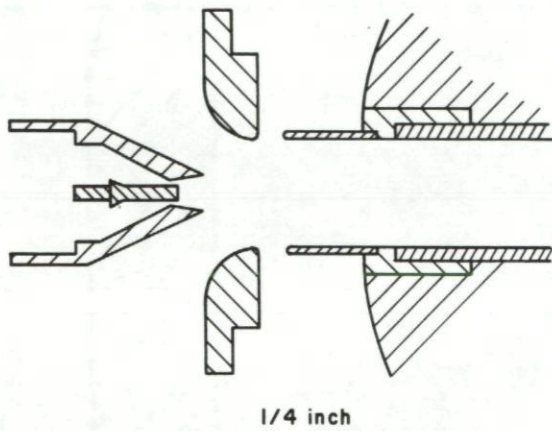
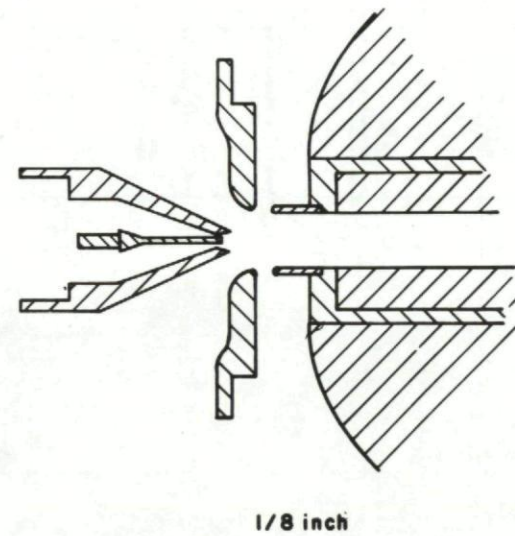


FIGURE 15



SCALING

NEEDLES

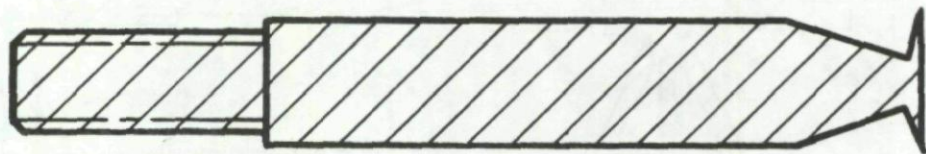
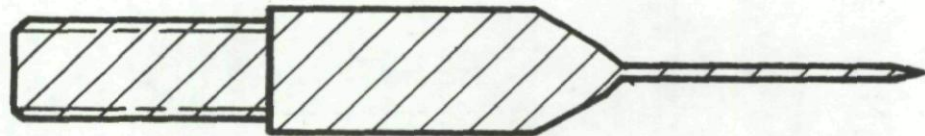
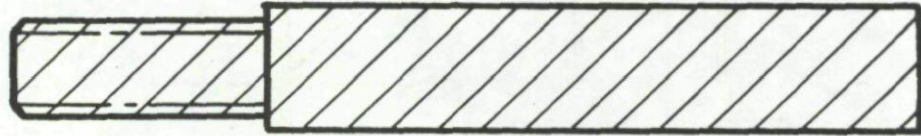
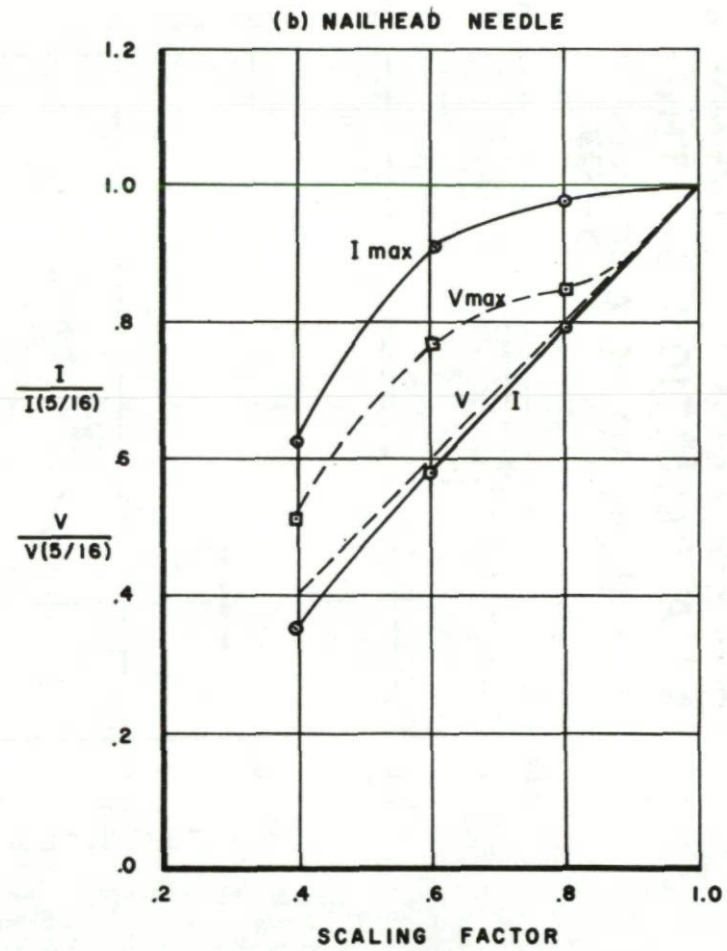
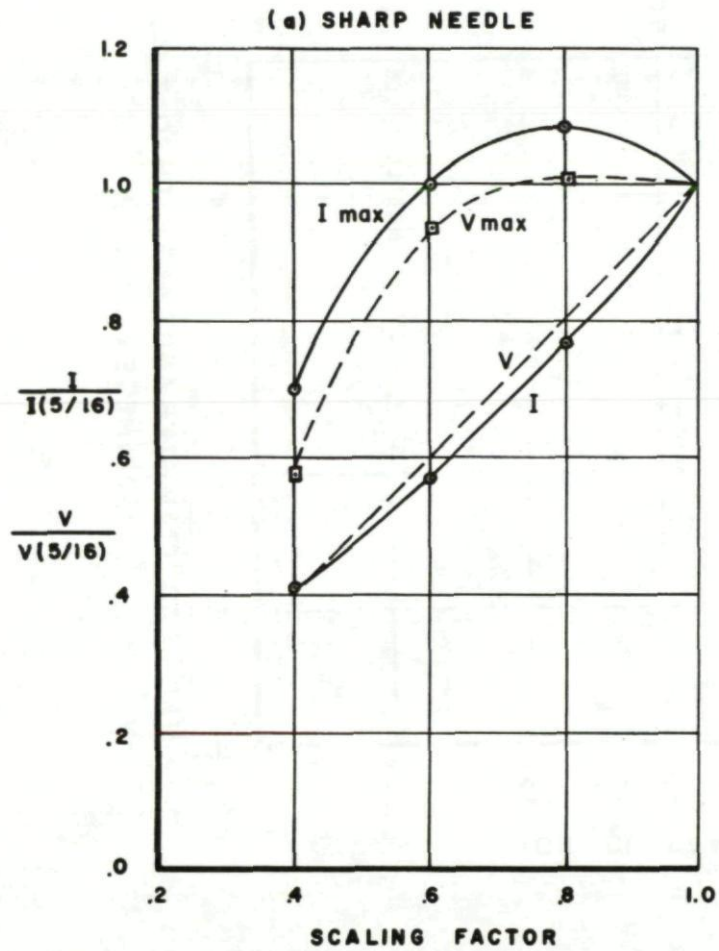


FIGURE 16



# GEOMETRIC SCALING RESULTS (ION CURRENT)

Figure 17



# ION CURRENT and VOLTAGE AS A FUNCTION OF THE NAILHEAD DIAMETER

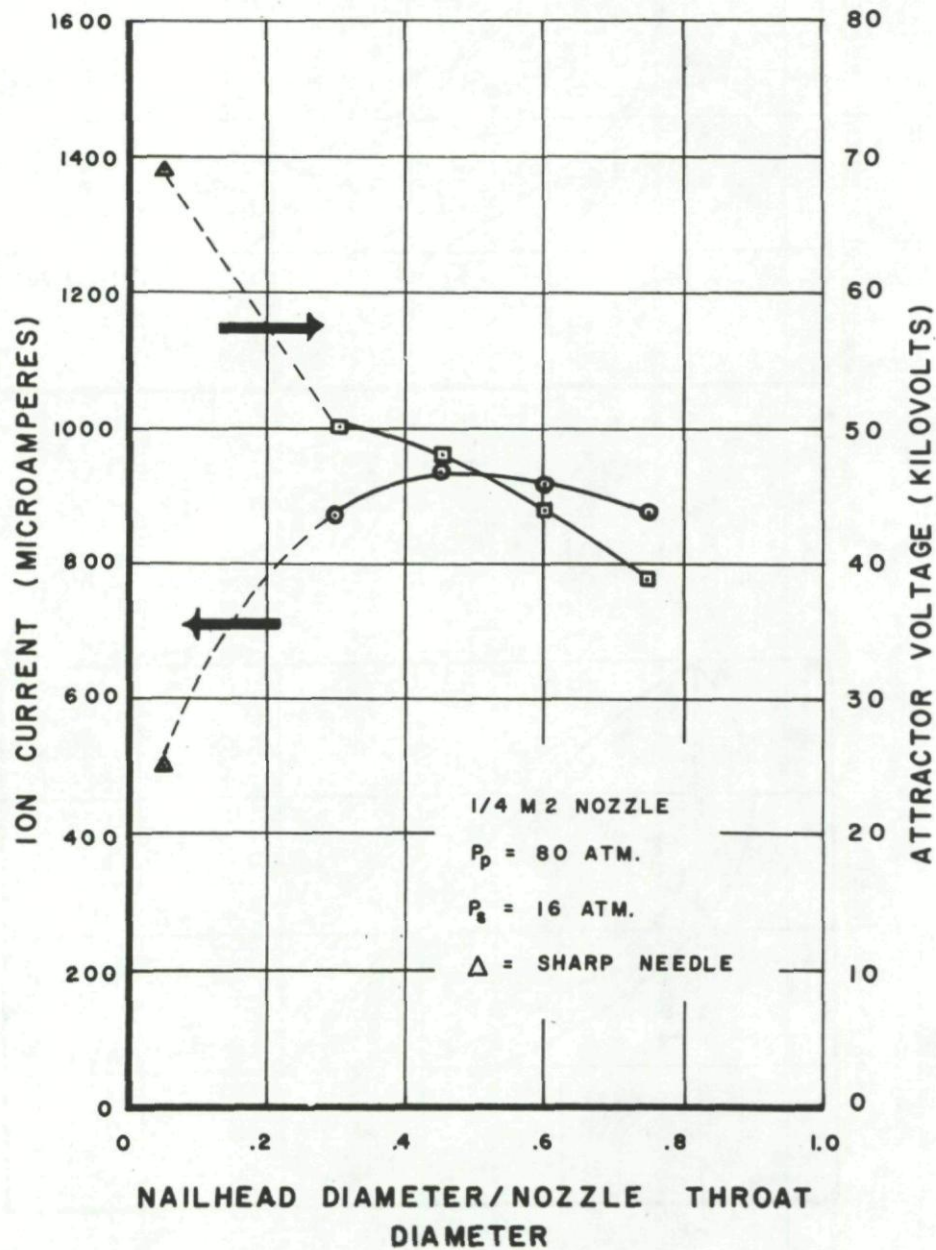


Figure 18

# ION CURRENT AS A FUNCTION OF THE NEEDLE POSITION IN NOZZLE <sup>87</sup>

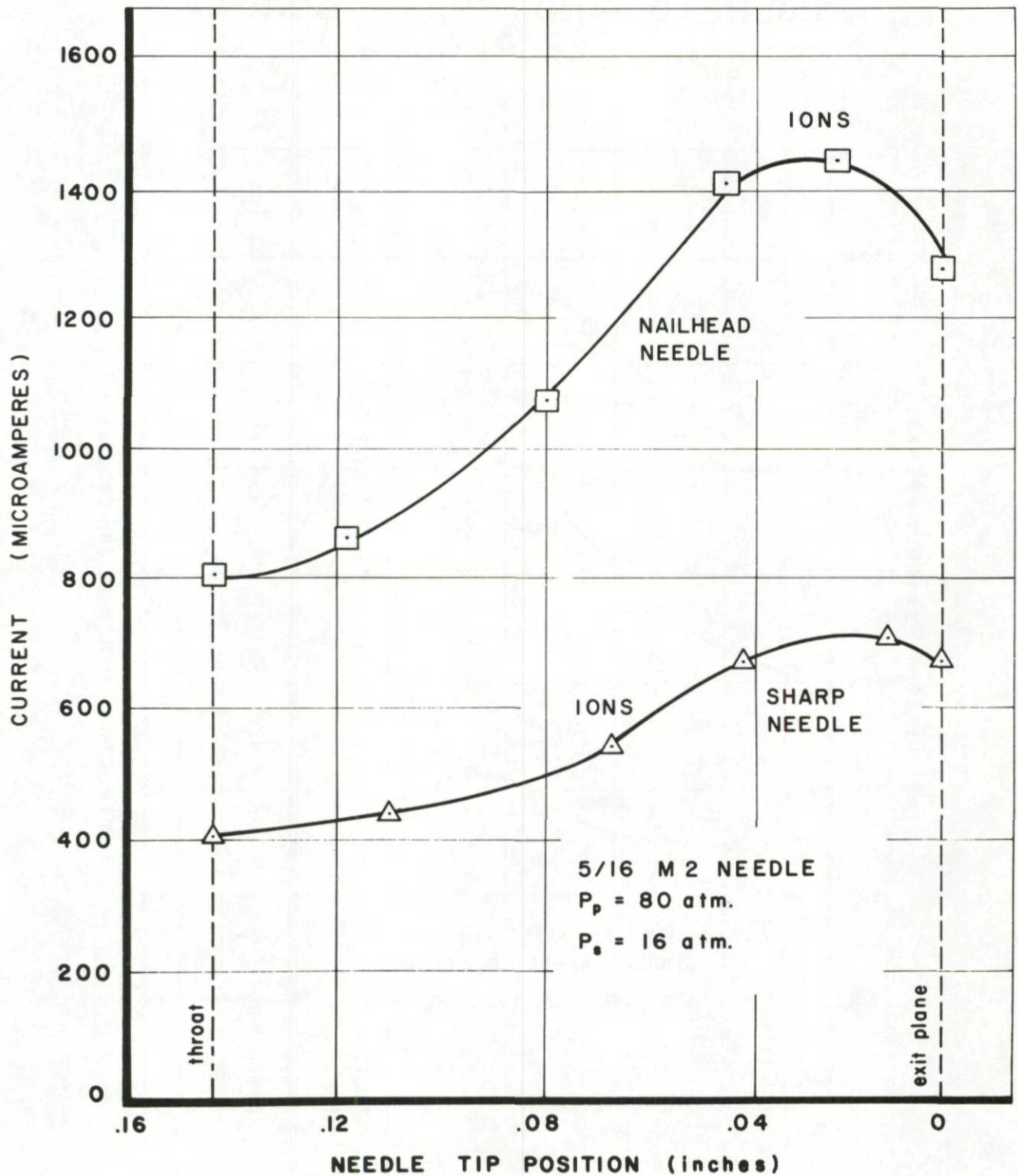


FIGURE 19

# ION CURRENT & VOLTAGE AS A FUNCTION OF THE NEEDLE POSITION IN NOZZLE FOR THE NAILHEAD AND SHARP CORONA ELECTRODES

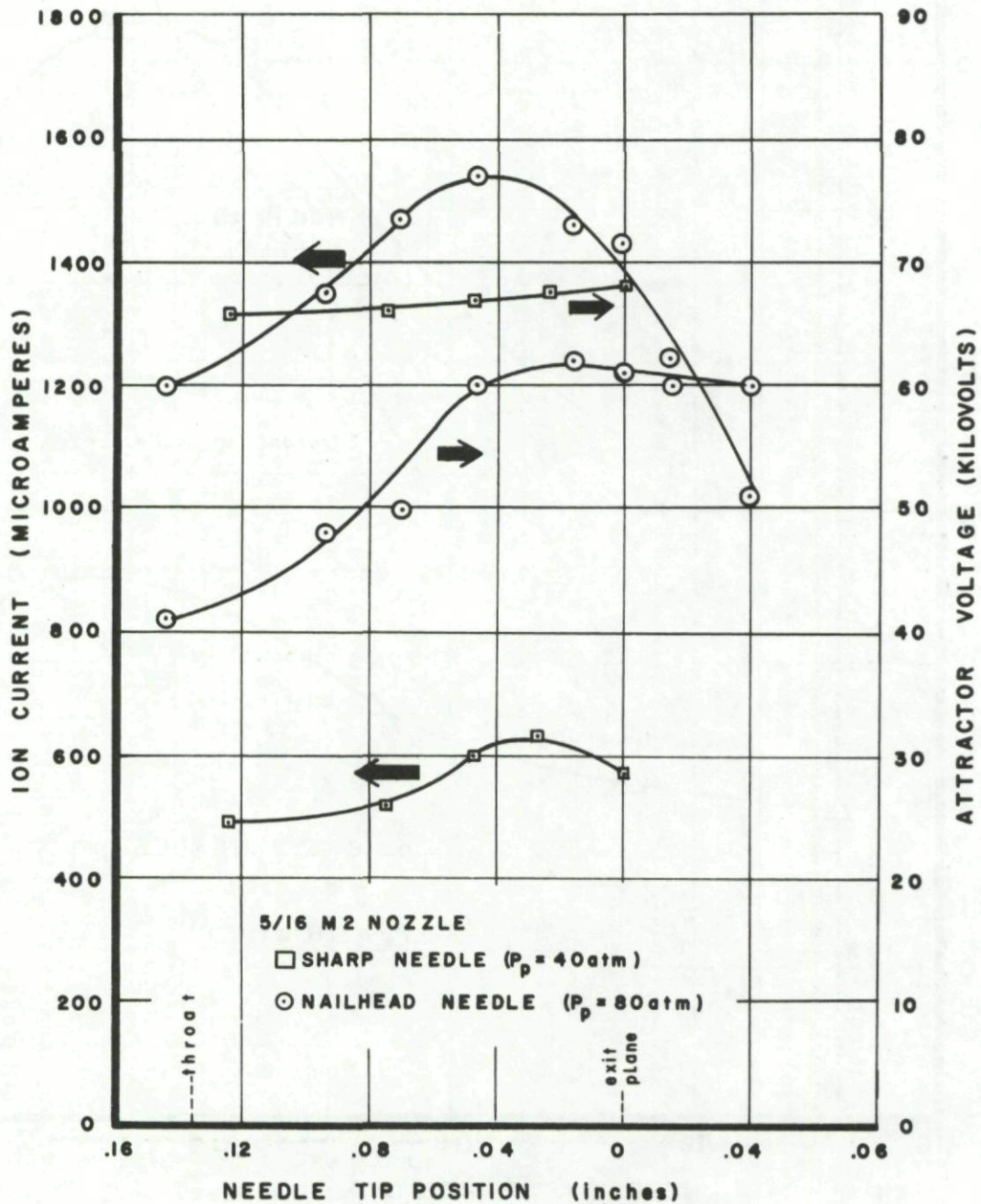


Figure 20

## AEROSOL CURRENT VOLTAGE CHARACTERISTIC

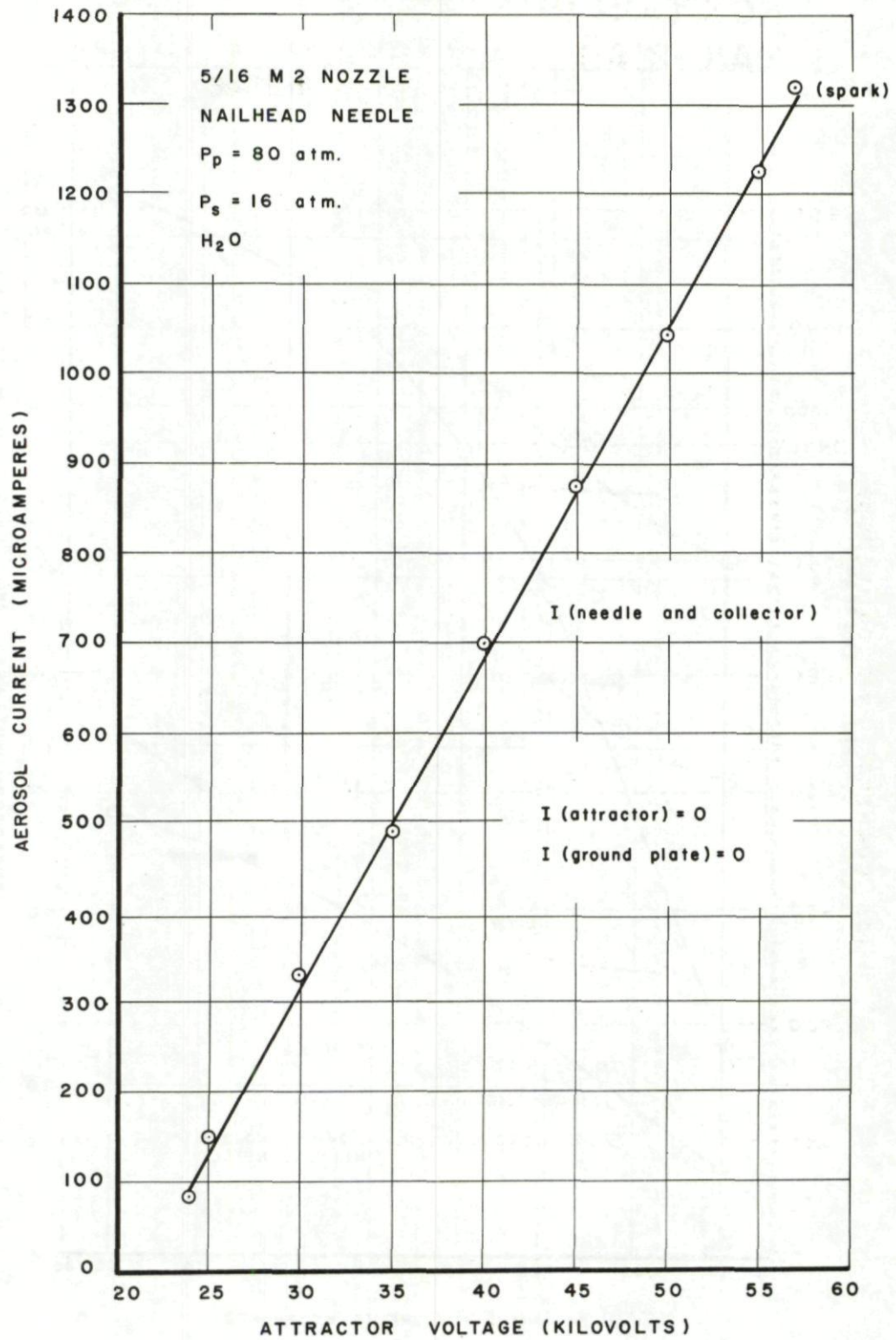


Figure 2f

## AEROSOL CURRENT and VOLTAGE versus STAGNATION PRESSURE

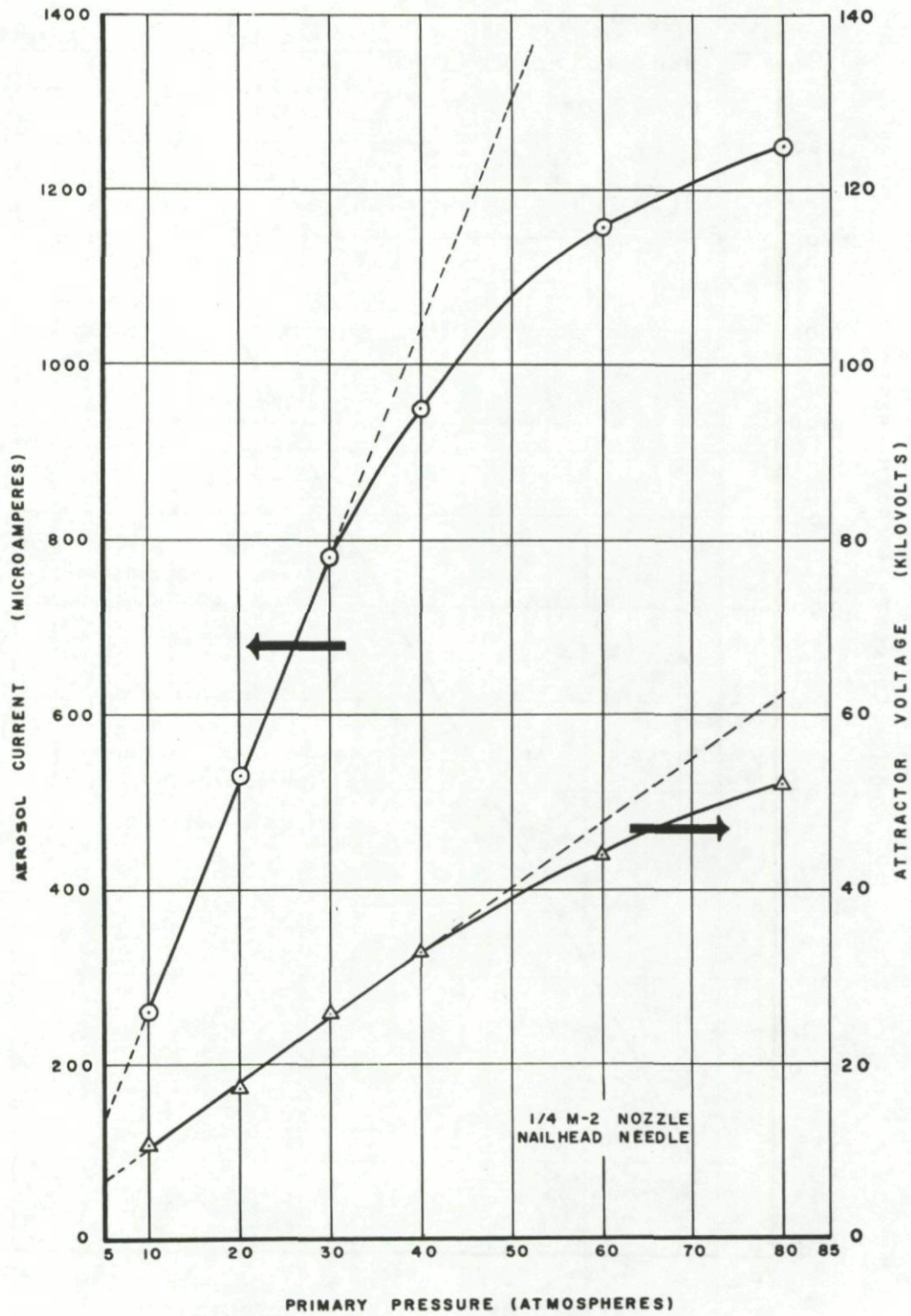
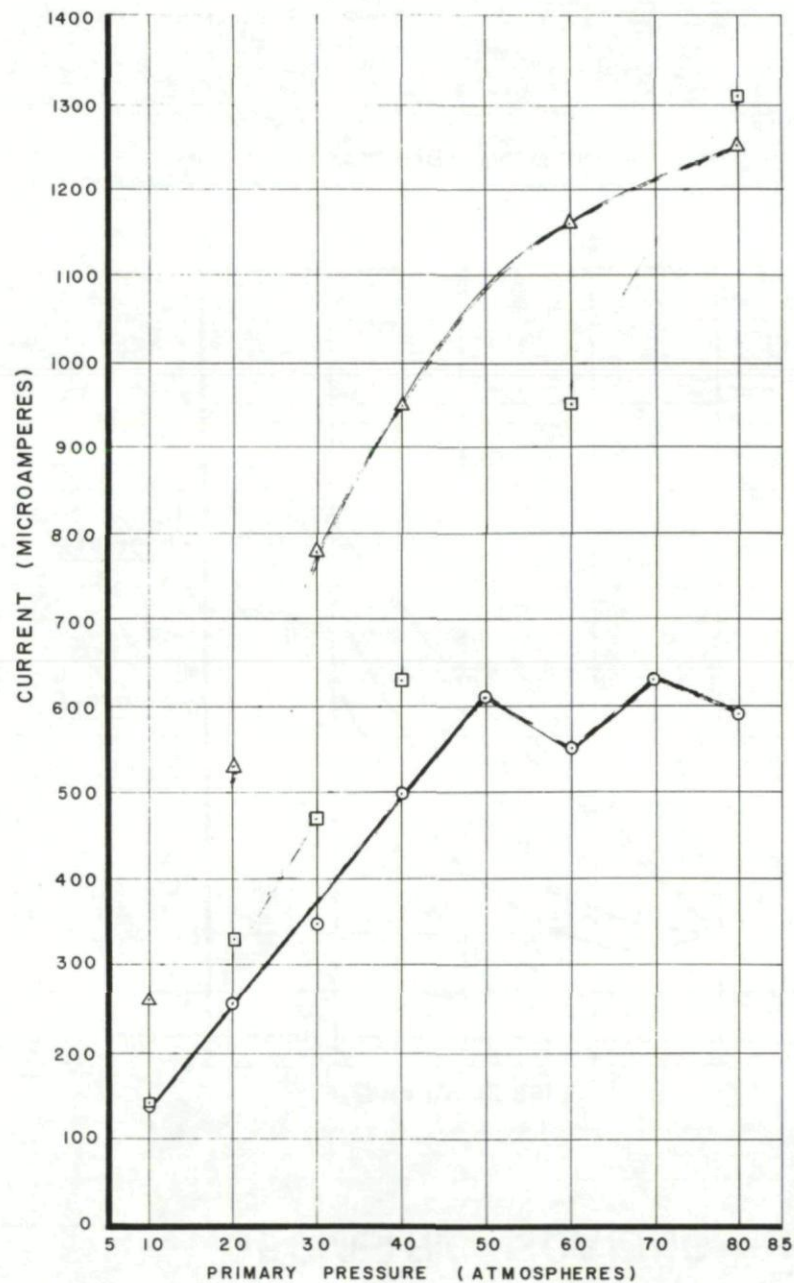


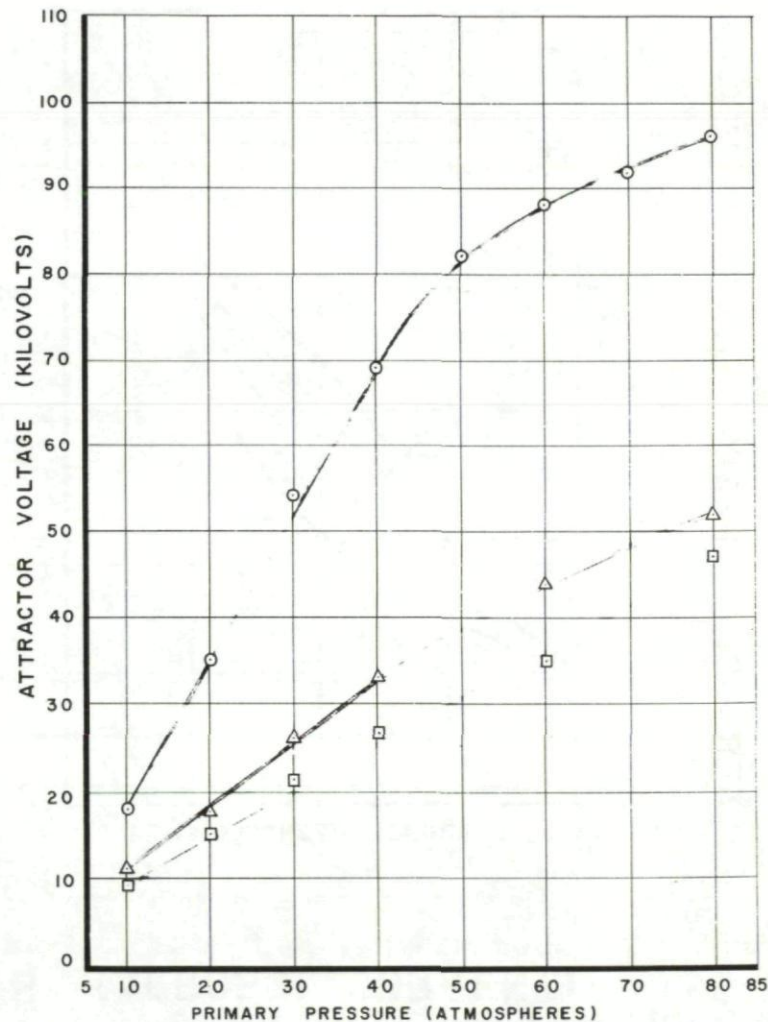
Figure 22

# CORONA CURRENT AND VOLTAGE vs. OPERATING PRESSURE

Figure 23

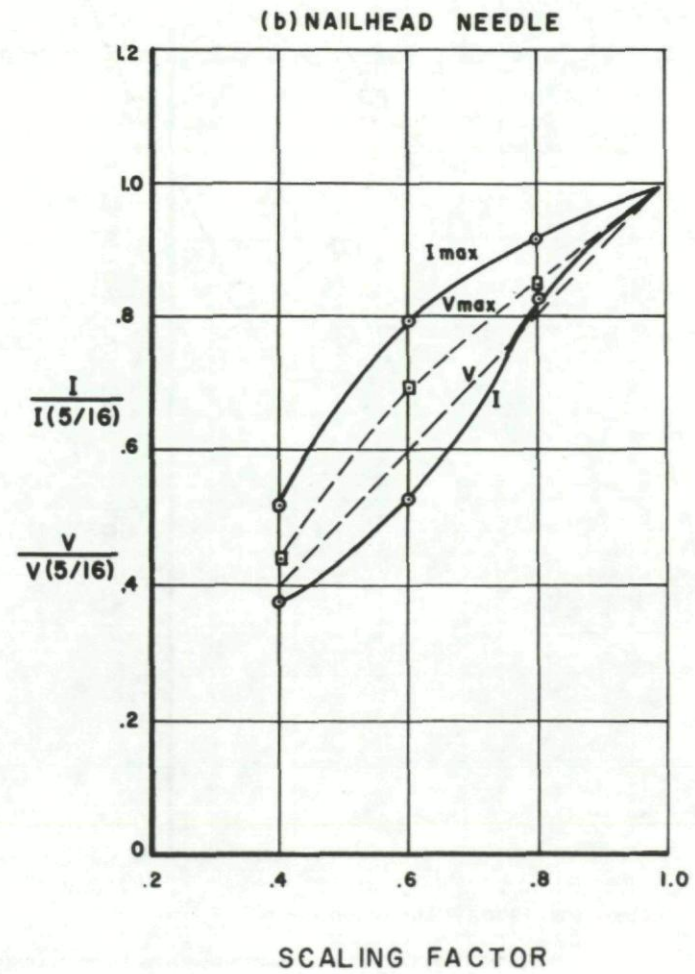
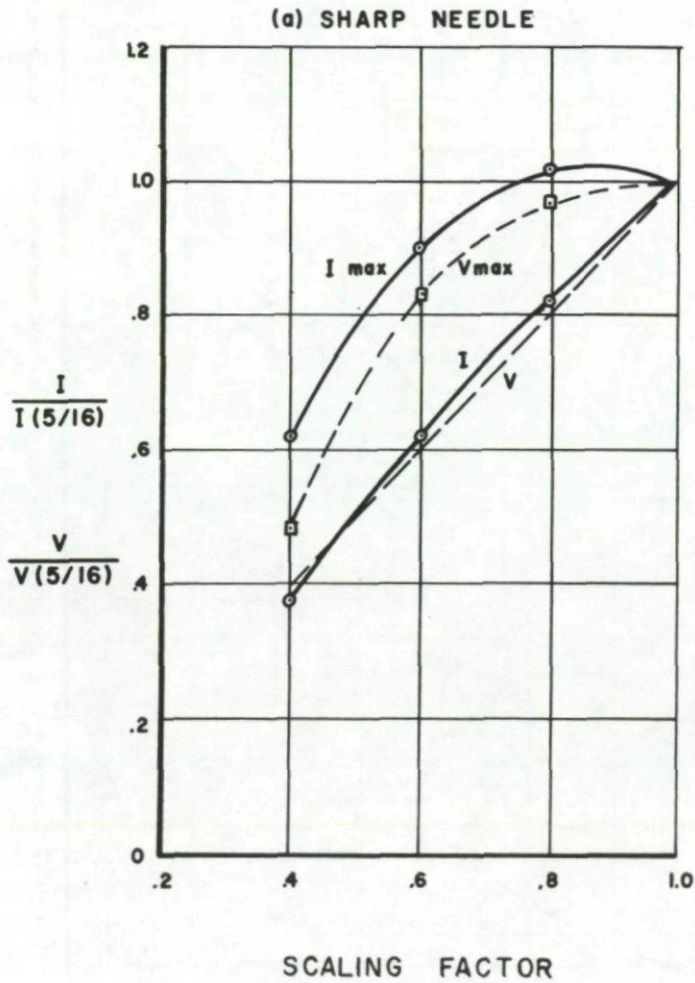


- — ○ SHARP NEEDLE (IONS)
- — □ NAILHEAD NEEDLE (IONS)
- △ — △ NAILHEAD NEEDLE (AEROSOL)



# GEOMETRIC SCALING RESULTS (AEROSOL CURRENT)

Figure 24





# CURRENT AS A FUNCTION OF THE NEEDLE POSITION IN NOZZLE

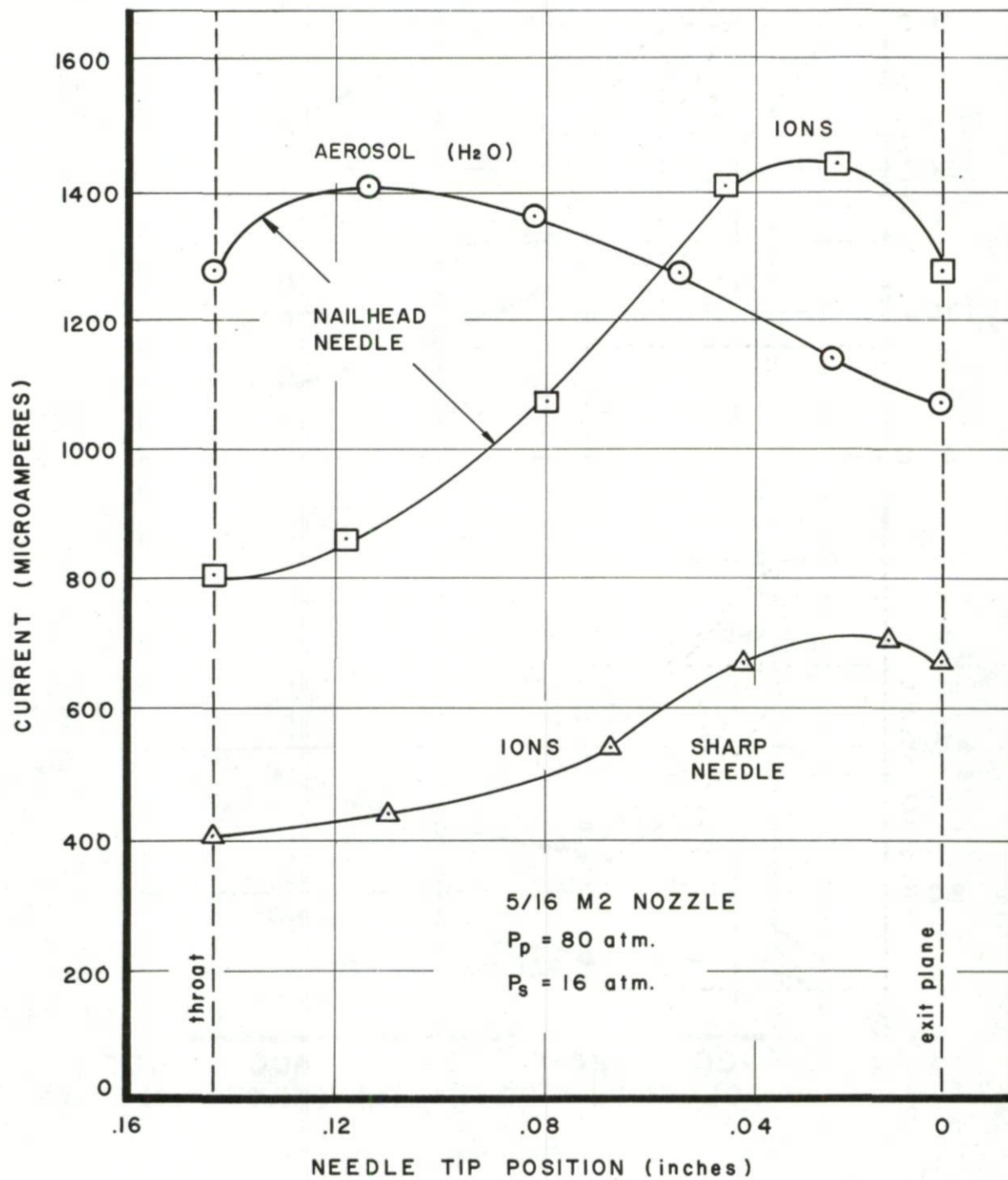


Figure 25

# ION CURRENT versus COLLECTOR POTENTIAL

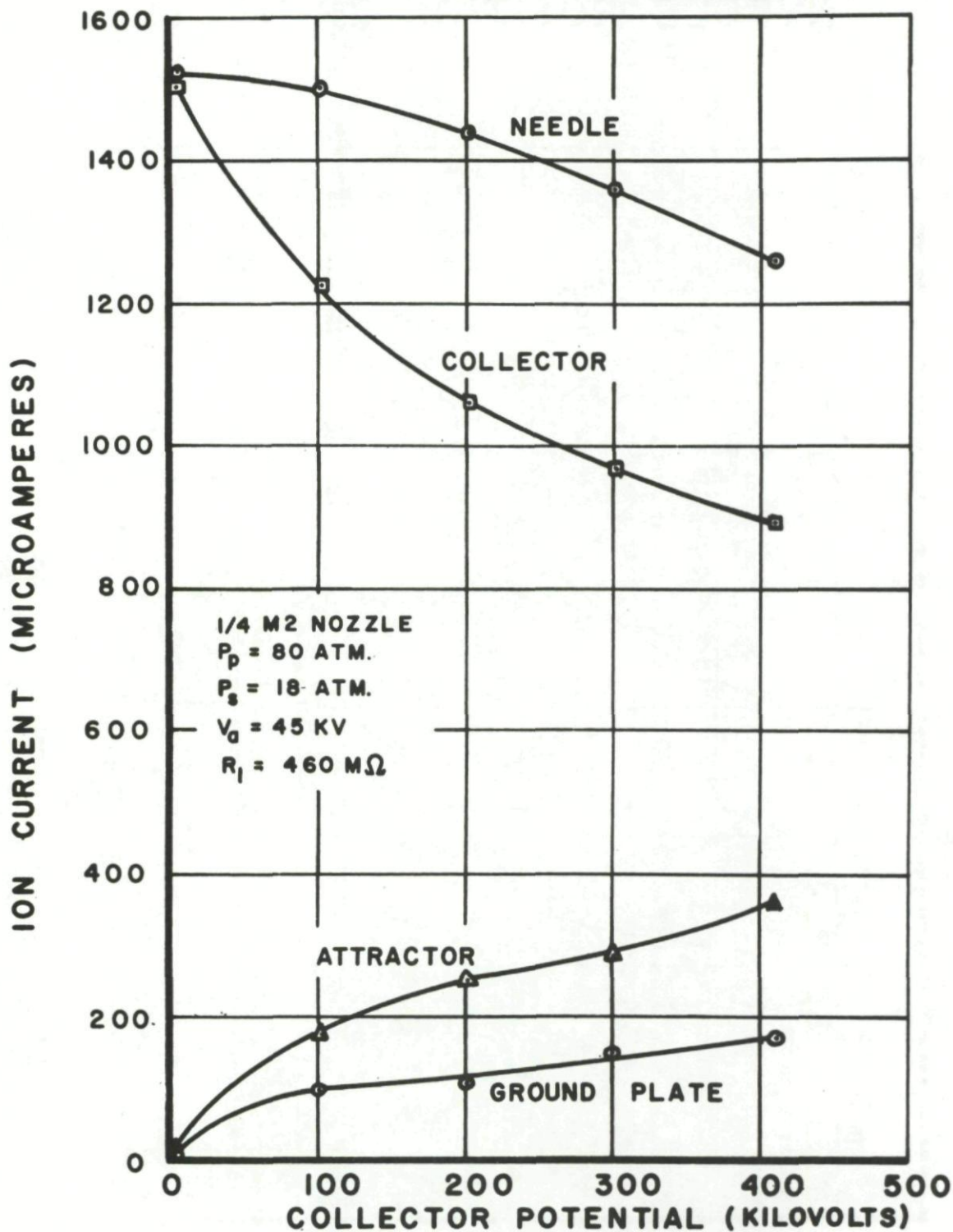


Figure 26

# AEROSOL CURRENT versus COLLECTOR POTENTIAL

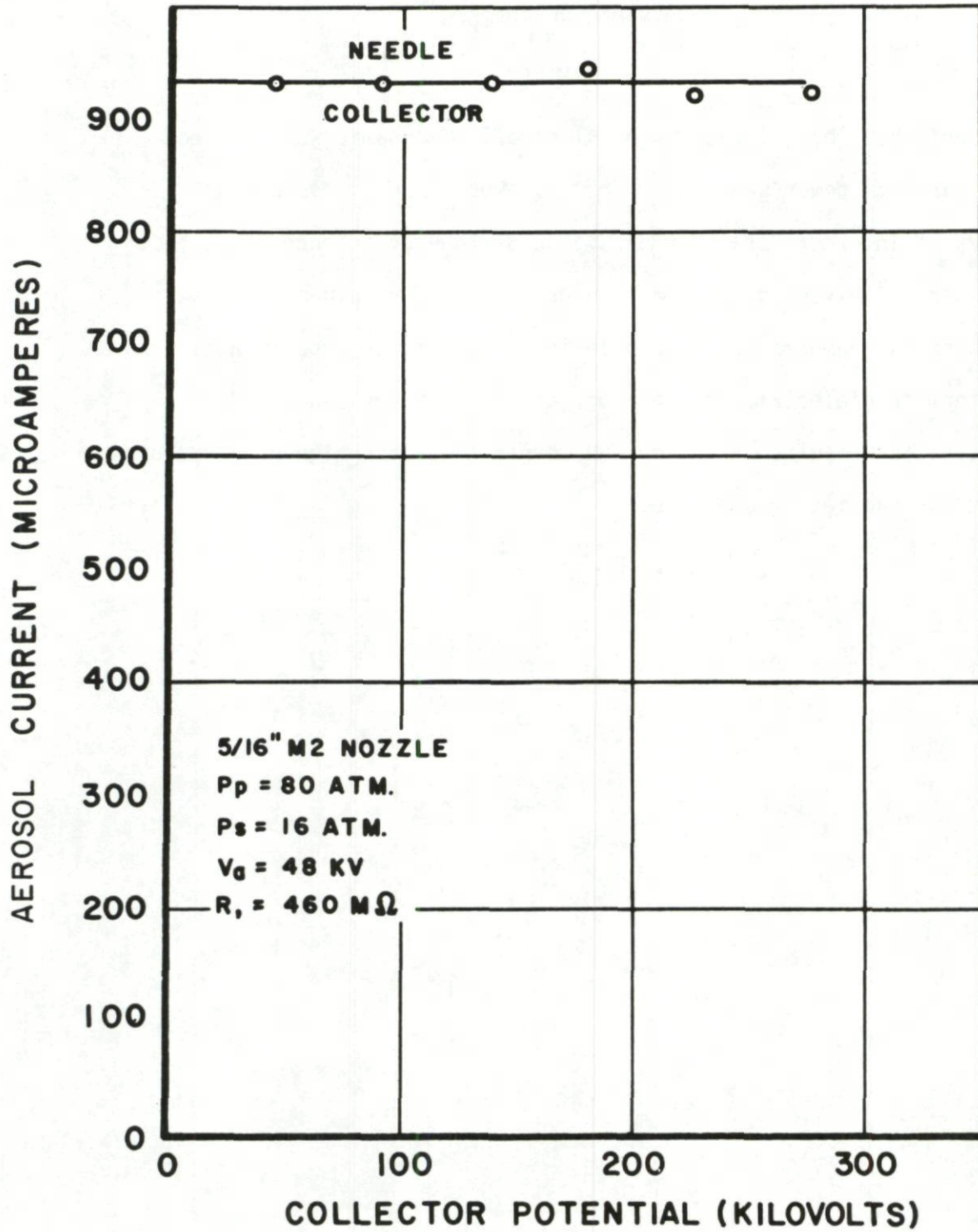


Figure 27

## WORKING MEDIA FOR ELECTROFLUID

## DYNAMIC GENERATORS

## Summary

Desirable characteristics of electrofluid dynamic Working Media with regard to power generation are reviewed. The dimensionless numbers of interest for power density and stage efficiency are cited. Since special mixtures of gases can provide better values of these dimensionless numbers than a single gas or vapor, an experimental program to determine dielectric strength of gas mixtures was conducted. Investigation results are given and comparisons with high pressure air as the working medium are made.

WORKING MEDIA FOR ELECTROFLUID  
DYNAMIC GENERATORS

Michael Hawes  
Aerospace Research Laboratories  
Office of Aerospace Research  
United States Air Force  
Wright-Patterson Air Force Base, Ohio

INTRODUCTION

The preceding papers have presented the overall concept of the electrofluid dynamic direct energy conversion process and some of the experimental results obtained. Although the theoretical analysis indicates some desirable properties of the working medium, the practical generator to date has employed compressed air as the energy source because of its availability, ease of control, and general convenience. This method of operation has proved adequate for determining experimental procedures and establishing experimental trends in spite of the fact that a far from ideal gas was being used.

This paper is a report on the work done both theoretically and experimentally to determine the medium most suited for the EFD process. In particular, it describes an investigation carried out with the purpose of increasing the dielectric strength of the low molecular weight gases hydrogen and helium so as to yield a medium of high dielectric strength and low mass density.

THEORETICAL CONSIDERATIONS

A number of ARL reports have dealt with the theoretical and practical aspects of electrofluid dynamic machines (von Ohain, 1964; Lawson,

1964; Lawson et al, 1961; Hasinger, 1964; and Hawes, 1964). They show that thermodynamic, aerodynamic, and electrical considerations must be combined to achieve attractive values of output power and efficiency. They also point out the importance of selecting the most suitable working medium.

The pertinent performance relationships developed for the viscous EFD energy conversion process assuming a one dimensional geometry are as follows:

Slip Between Ions and Working Medium

$$S = \text{Slip Ratio} = \frac{\text{drift velocity}}{\text{gas velocity}}$$

Negligible Slip  
(Charged Aerosols)

$$S = \frac{kE}{v} \sim 0$$

Power Flux

$$L_e = \frac{\epsilon v^3}{2k_n} S^2 \left(1 - \frac{2}{3} S\right) \frac{\rho}{\rho_n}^2 \quad L_e = \frac{\epsilon v E_{b,n}}{2} \frac{\rho}{\rho_n}^2$$

Stage Efficiency

$$\eta_{st} = \frac{1 - \frac{2}{3} S}{1 + \frac{\xi \rho k}{\epsilon S^2} \frac{\rho_n}{\rho}} \quad \eta_{st} = \frac{1}{1 + \frac{\xi \rho v}{\epsilon E_{b,n}} \frac{\rho}{\rho_n}}$$

where the properties of the working medium are permittivity  $\epsilon$ , velocity  $v$ , density  $\rho$ , mobility  $k$ , and dielectric strength  $E$ . Subscript  $n$  refers to normal atmospheric conditions and  $\xi$  is an overall drag loss coefficient. The function  $\frac{\epsilon}{\rho k^2}$  is known as the Figure of Merit,  $K$ , of the medium.

Other geometries such as the two dimensional and axisymmetric cases yield similar equations which indicate that the medium parameters enter in the same way.

For generator action, it is always necessary that the drift velocity,  $kE$ , of the charges be less than the gas velocity  $v$ . There is a concurrent requirement that the field strength at any point must not exceed the breakdown strength of the gas at that point. Thus, depending on the value of  $k$  of the gas, it may or may not be possible to submit the gas to a field strength approaching its breakdown value. A high value of  $k$  places a severe limitation on the process as it means that the maximum electric pressure of the medium is not being utilized. The power and efficiency expressions indicate that for optimum performance, the medium should have the properties of low mobility, low mass density, and high dielectric strength. In particular, assuming that charged aerosols can be produced by, for example, a condensation process, and that these aerosols are of sufficient size that the difference in velocity between them and the flowing gas is negligible (in other words, the mobility  $k$  has been drastically reduced) the important results are that  $L_e$  is proportional to  $\frac{\epsilon}{2} E_b^2 v$  and  $n_{st}$  is proportional to  $\frac{1}{1 + \frac{\epsilon \rho v}{\epsilon E_b^2}}$ . In these ex-

pressions, the "n" subscripts and the density level terms have been combined to yield the actual values of density and dielectric strength at the density in question. It is seen that the ratio  $\frac{\epsilon E_b^2}{\rho v}$  should be as

large as possible to achieve strong interaction between electrical and fluid flow effects. It is not practicable to make  $v$  very small, however, because this would adversely affect output power; thus, there appears to be a conflict in the velocity requirements as seen from the power and efficiency expressions, while the desirability of high dielectric strength and low mass density is obvious.

That the property of low density is desirable also follows from a consideration of the two-component, two-loop energy conversion system previously mentioned in the AGARDograph, which has the function of uncoupling the thermodynamic and electrofluid dynamic processes so that each can be designed to perform most effectively. In such a system the thermodynamic cycle fluid may expand through a nozzle and impart energy to the EFD working gas (see Fig. 1); the high pressure ratio necessary for an efficient thermodynamic cycle implies a high Mach number flow through the nozzle. At the same time in the EFD cycle it is necessary to maintain a low Mach number flow to minimize the aerodynamic losses in the ducts. Consideration of the efficiency of the energy transfer due to the mixing of the thermodynamic and EFD fluids indicates that the two velocities should be comparable (one approximately twice that of the other). This can be done by making the molecular weight of the EFD gas lower than that of the thermodynamic fluid so that it flows at a subsonic Mach number while the thermodynamic fluid flows at a high supersonic Mach number.

In a constant area, adiabatic duct for fixed stagnation conditions, the electrical parameters depend only on the Mach number of the flow; therefore, for the EFD process the Mach number is of paramount importance and is selected to yield the desired electrical conditions. As the Mach number



corresponds to the ratio  $\frac{v}{a}$ , where  $a$  is the local speed of sound, then for a particular Mach number in the conversion section the requirements for the EFD working medium can be reduced to the following:

1. From the power output standpoint  $L_e$  is proportional to  $\frac{1}{2} \epsilon E_b^2 a$ . Hence the product  $E_b^2 a$  should be as large as possible.

2. From the stage efficiency standpoint, as the product  $\rho v^2$  is principally only a function of the Mach number (for a given total pressure), it becomes invariable when the Mach number of the flow is selected. Hence, to optimize the stage efficiency the highest possible value of  $E_b^2$  is desired.

3. From the overall two-fluid cycle efficiency standpoint, the mass density of the EFD gas should be low, in other words, the speed of sound in this gas should be high.

Thus the magnitudes of the terms  $E_b^2 a$  and  $E_b^2$  for a gas yield a method of comparison with other gases, and therefore may be referred to as "Relative Merit" indicators for power and efficiency, respectively.

The question now arises: Is it possible, by adding to hydrogen or helium a small percentage of breakdown inhibitor gas so that the molecular weight is not appreciably increased, to produce a mixture of improved relative merit values? Unfortunately, dielectric strength values are not amenable to computation - they must be determined experimentally for each particular gas or mixture. Furthermore, inasmuch as pressurization of a gas normally increases the dielectric strength and is highly desirable for the EFD process (as can be seen from the power and efficiency equations) knowledge of dielectric strength values at high pressures is required. Thus, the breakdown strengths of the selected mixtures must be determined experimentally over the range of conversion section pressures that are of

interest. Such mixtures would have the properties of low molecular weight and high dielectric strength which would make them well suited for use in the EFD generator employing charged aerosols as the particles transported by viscous interactions with the working medium. In such a generator, the highest possible value of dielectric strength can always be utilized. If the nature of the working medium, or of one of its components in the case of a mixture, was such that condensation could be induced under controlled conditions, so as to form aerosols for the process, the value of the medium would be further enhanced. Additional properties, such as surface tension and vapor pressure, become increasingly important in this case.

#### Selection Of Working Fluid Components

Hydrogen and helium have the lowest molecular weight; however, neither hydrogen nor helium has a high dielectric strength; hydrogen usually being quoted as about 60% that of air, with helium much more inferior (about 20%). The list of possible breakdown inhibitor or "quench" additives is extensive; there is a large amount of data on gases of relatively high dielectric strength in the literature. Many of the reported investigations have been carried out for the purpose of obtaining an insulating fluid for high voltage apparatus (Narbut, et al, 1959; Howard, 1956; Camilli, et al, 1952). Families of gases, such as the fluorocompounds and hydrocarbon compounds, have been studied quite extensively over a wide range of pressures. Their electronegative character and their high molecular weights have been used to explain, in part, their high dielectric values, and they have gained widespread use as insulating media, particularly since they have some

attractive and practical advantages over oil.

But other properties as well as dielectric strength must be taken into account before a compound can be considered as an additive for EFD purposes. It is, of course, necessary that the substance be a gas or vapor at the operating temperature. Ambient room temperature, about 72<sup>o</sup>F, was considered the operating temperature for the purpose of the present investigation, and though this is an over-simplification of the problem, the results yield comparative figures among the mixtures tested.

A selected list of the more common high dielectric strength gases, together with their relative (to air) dielectric strengths and vapor pressures at 25<sup>o</sup>C, is given below (Liao, 1962).

Gas	Mol. Wt.	Relative Dielectric Strength	Vapor Pressure (atm)
Trichloromonofluoromethane CCl <sub>3</sub> F, (Freon 11)	137.4	3	1.02
Dichlorodifluoromethane CCl <sub>2</sub> F <sub>2</sub> (Freon 12)	121	2.4	6
Monochlorotrifluoromethane CClF <sub>3</sub> (Freon 13)	104.5	1.4	25
Dichlorotetrafluoroethane C <sub>2</sub> Cl <sub>2</sub> F <sub>4</sub> (Freon 114)	171	2.8	1.1
Sulfur Hexafluoride, SF <sub>6</sub>	146	2.4	22
Carbon Tetrachloride, CCl <sub>4</sub>	153.8	6.3	0.14

The list is comprised mainly of fluoro-compounds, some of which have been investigated as breakdown inhibitors for a long time both by themselves and as mixture components. Initial experimentation showed that mixtures had higher dielectric strengths with increasing concentration of these substances as additives. Closer investigation revealed that small concentrations of additive

caused a disproportional increase in the dielectric strength of the mixture. It is this disproportional increase that holds interesting possibilities in the present application as it implies large increases in strength at small additive concentrations, i.e., small density increases. A number of curves have been published which confirm this fact (Charlton, et al, 1937; Hudson, et al, 1937; Rodine, et al, 1937). More recently, the same anomaly has been observed for the mixture perfluoromethylcyclohexane ( $C_7F_{14}$ ) and nitrogen (Berberich, et al, 1955). All curves indicate the rather dramatic increase in breakdown strength on injecting the first small fraction of additive.

It was decided to investigate both sulfur hexafluoride and Freon-12 as the breakdown inhibitors to be added to hydrogen and helium. Their other properties enhance their selection. Sulfur hexafluoride is colorless, odorless, tasteless, and inert; it produces no harmful physiological effects. It is very stable chemically; however, breakdown by an electric arc leads to products which are toxic but can be absorbed by solid materials such as pellets of sodium hydroxide or activated alumina. If the sparking is performed in the presence of hydrogen, complete decomposition of the  $SF_6$  results, with the formation of hydrogen fluoride and hydrogen sulphide (Schum, et al, 1949). This could be looked upon as constituting a possible disadvantage of using a hydrogen- $SF_6$  mixture. For the present investigation it called for frequent purging of the test vessel, as will be described later.

Dichlorodifluoromethane, ( $CCl_2F_2$  or Freon-12), is a colorless, odorless, nonpoisonous, noncorrosive, chemically stable gas. When exposed to an electrical discharge in the presence of hydrogen, it also yields corrosive discharge products.

### Experimental Apparatus And Procedure

The maximum pressure level that has been used in the conversion section of the experimental EFD generator at ARL is approximately 600 psia. To enable data to be available for possible operation at higher pressure and to keep the present maximum roughly in the middle of the test pressure range, it was decided to extend the dielectric tests on gases and mixtures up to 1,000 psia.

Dielectric strength was determined from the voltage necessary to cause breakdown between two spherical electrodes. The electrodes were mounted in a pressure chamber- a stainless steel flanged cylinder, six inches inside diameter and twelve inches long, with provisions for the introduction of gases and for their exhaust. Pressure and temperature probes were also installed. In order to prevent alteration of mixture proportions during a test, it was absolutely essential that the vessel and fittings be leaktight. High voltage DC was applied to one (fixed) electrode through a resin-impregnated fiberglass electrical bushing from a 0-60kv continuously variable power supply. The other electrode was electrically connected to the pressure vessel (ground potential) and was mounted on a depth gauge micrometer shaft. This permitted easy positioning relative to the fixed electrode with the aid of a temporarily connected ohmmeter circuit, micrometer graduations being in .001 inch, so that readings to .0001 inch were possible by interpolation; it also permitted the interelectrode spacing to be set independently of any variations in chamber dimensions due to pressurization.

The electrodes were aluminum bronze spheres (1-3/8 inch in diameter, diameter tolerance 0.0002 inch, hardness 225-275 Brinell) mounted at a spacing of .01 inch. For such a small spacing to radius ratio, an essentially uniform field results in the gap so that dielectric strength is readily obtained from a knowledge of the breakdown voltage. This value of

spacing was compatible with the expected breakdown values, considering the pressures involved and the supply voltage available, thus eliminating the need of manufacturing more elaborate electrodes, for example, Rogowski contours (Cobine, 1958), or Stephenson contours (Stephenson, 1933), which would be needed if a much larger spacing was involved. A further advantage of using a small spacing is that some experimental results are available at the same gap dimensions which can be used for comparison purposes. The relative dimensions of the spheres and supporting shanks compared to those of the chamber were within the requirements of AIEE No. 4 (American Standard for Measurement of Voltage in Dielectric Tests), which was probably an over-rigorous requirement at such small spacing, particularly at the lower pressures. Figure 2 is a drawing of the chamber and electrode arrangement.

Although the field strength distribution in the EFD generator is not uniform, the uniform field breakdown voltage of the various gases was thought to be the best indication of suitability from the dielectric strength consideration. Furthermore, as the spacing was kept constant for all tests at .01 inch, no difficulty is involved in comparing the results. For a nonuniform field, the breakdown voltages in general show a much greater degree of scatter or variation, and it is difficult to select the most representative value. Comparisons are consequently more difficult also. With nonuniform fields, the effects of corona stabilization and the anomalous electric strength decrease with pressure increase make true dielectric strength determination very difficult.

Breakdown voltages were determined for the parent gases of the investigation, hydrogen and helium, at various pressures and additive concentrations. None of the gases used were of more than commercial purity. An analysis of

cylinder contents was in no case obtained; gas purity and analysis probably varied slightly between different cylinders of the same gas, but the effects were not noticeable. Breakdown voltage was read on the power supply voltmeter, which was calibrated against a Sensitive Research Instrument Company electrostatic voltmeter, accuracy 1% of full scale (30kV). As comparative values of dielectric strength were of more importance in this investigation than absolute values, no attempt to improve the accuracy of voltage reading was made beyond this calibration, which was repeated a number of times during the course of the experiments and always found to be satisfactory.

Breakdown voltage was taken as the mean of a number of close readings, generally within 0.5 kV of each other. Occasionally, an attempt at a breakdown determination resulted in a breakdown value of about 3 kV too low. With repeated sparking, this voltage increased and a breakdown value could be assigned. The probable explanation of this occurrence is that a heavy spark causes some roughness on an electrode surface which lowers the breakdown voltage; repeated sparking removes the offending protrusion. The low readings were therefore discarded.

It is of interest that breakdown voltage was found throughout to be almost independent of the rate of application of voltage. Originally, the voltage was increased manually at about 1 kV/second; later, a slow speed motor was used to give a more uniform rate of increase, about 0.5 kV/second. At random points within a series of experiments, the rate of application was varied widely, sometimes making pauses of 30 seconds between each increase of 0.5 kV over the last about 5 kV before breakdown. In all cases, the breakdown voltage was found to be essentially the same. This is consistent with

the fact that the time of application of voltage is much greater than the breakdown statistical and formative time lags which are of the order of microseconds. Having established this fact, the procedure usually followed was that the voltage was quickly raised manually to about 50% of the anticipated breakdown value and then continued by means of the motor.

In the course of time, a slight pitting of the spherical electrode surfaces occurred. Rechecking with former values showed that this effect changed (reduced) the breakdown value slightly. To eliminate such discrepancy, at intervals the spheres were removed and repolished.

Before a new gas was admitted, the chamber interior, including walls and flanges, was cleaned with distilled water. In the cases where hydrogen gas was involved, an initial purging cycle with nitrogen was performed before the hydrogen was admitted, to eliminate the possibility of having an explosive hydrogen-air mixture. Gas was then admitted to a pressure of about 100 psia and exhausted. This was repeated a number of times until it could be assumed that the chamber contained only the gas of interest. The apparatus was allowed to stand overnight under about 100 psi gas pressure so that the chamber became fully "saturated" with the gas, and further exhausted and refilled the next morning. The contents were now considered as 100% parent gas.

Mixture proportions were all by volume percentage, the additive being admitted to the chamber until it exerted the desired partial pressure, and then injecting the parent gas to the required total pressure. Each time a mixture test was made, a small fan was put into operation, to assure a good mixing of the components. The fact that the fan was effective was easily demonstrated by determining the breakdown voltage before and after it



was set in operation. Without it, the large density difference between the parent and additive gases apparently led to a natural separation, so that the gas in the interelectrode gap contained little of the heavier additive.

Due to the possibility that the percentage of each component might change if the total pressure was reduced by as much as 100 psi, rather than compounding a mixture at the highest pressure (1000 psia) and then exhausting to achieve the lower levels, after testing the mixture at any pressure, the chamber was exhausted and purged thoroughly with the parent gas (hydrogen or helium) until it could be assumed that no additive was present. This fact was verified by determining the breakdown voltage of the contents and comparing with the results for the parent gas. The mixture was then compounded again to the new partial pressures.

Some general observations made during the course of the tests on the different gases may be of interest to the reader. Although in all cases it was possible to assign a breakdown voltage, in some cases this was simpler to do than in others. Both hydrogen and helium exhibited a good constancy of breakdown at each pressure level so that specific voltages were easily assigned. In the tests involving mixtures an increased scatter in the results was exhibited. This was most pronounced in the hydrogen-freon-12 mixtures, and could probably be partly explained by the fact that a slight discoloration of the spheres occurred in the neighborhood of the spark. As mentioned previously, this mixture yields corrosive electric discharge products. The discoloration effect was minimized by frequent polishing of the electrodes.

In all cases where there was a scatter of results, a voltage was finally

chosen which was on the conservative side; test data may therefore be considered as somewhat pessimistic, perhaps by about 1 or 2 kV, especially at the higher pressures above 500 psia.

### Results And Discussion

The results of the investigation are presented in graphical form in Figures 3 through 8. In the curves showing breakdown voltage values, all of which are drawn on the same scale, the curve for air is repeated each time to establish a reference. The data for air from this investigation permitted comparison with results of a similar test at the same spacing (.01 inch) by other investigators (Skilling, et al, 1941), and very close agreement was exhibited. Further seeking to establish a confidence level in the overall apparatus by checking the test results for air, one of the most recent publications on the subject of breakdown furnishes a formula for breakdown voltage for the region in which the streamer theory of breakdown is thought to be valid ( $pd > 500 \text{ mm Hg} \times \text{cm}$ , i.e., greater than about 380 psia in this investigation) (Kontaratos, et al, 1965). This formula is used to calculate theoretical breakdown voltages at a number of points, and they fit very closely to the experimental curve.

It is seen from the curves, Figures 3 through 6, that the addition of the breakdown inhibitor,  $\text{SF}_6$  or freon-12, has a much larger percentage effect on the dielectric strength of helium than on that of hydrogen. For example, at 500 psia total pressure, the addition of 1%  $\text{SF}_6$  raises the breakdown voltage of helium from about 3.1 kV to 6.75 kV, an increase of 118%, while at the same pressure and additive percentage, the breakdown voltage of hydrogen

is raised from 13.25 kV to 16.7 kV, an increase of 26%. The previously mentioned disproportional increase in dielectric strength with small additive percentage is also exhibited in these curves and at all pressures. Considering the hydrogen-freon-12 mixture at a total pressure of 300 psia, the breakdown voltages for 0, 1, 2, 5, and 10 per cent freon-12 are 9.3 kV, 10.3kV, 10.8 kV, 11.5 kV, and 12.3 kV, or expressed as percentages of 9.3 kV, 100%, 111%, 117%, 124%, and 132%. Thus, although 1% additive gives an 11% increase in strength, 2% additive gives only 17% increase, or considerably less than if the mixture dielectric strength increased linearly with additive concentration.

It is interesting to note that although there is only a minute difference between the dielectric strengths of the two additive gases, this is reflected into a considerable difference in strengths of the mixtures, depending on which additive is used. The  $SF_6$  mixture at any pressure was of consistently higher strength than the corresponding freon-12 mixture. Similarly, these curves left no doubt but that the hydrogen-sulfur hexafluoride combination, because of the low molecular weight of hydrogen, was best suited to yielding desirable EFD working media. Tests of a mixture with lower additive concentrations of 1/2% and 1/5% accordingly seemed to be desirable and were performed.

In Figure 7 the relative merits of the various hydrogen- $SF_6$  mixtures as EFD media, based on the power consideration, are shown. The values of the expression  $E_{B-a}^2$  are divided throughout by the corresponding value for air at the same pressure to achieve a non-dimensionalized parameter, thus the curve for air would be a horizontal line through 1.0. Variations in  $\gamma$ , the ratio of specific heats, are taken as being in proportion to the mass percentage of each constituent; the effect of this parameter is small. The curve for  $SF_6$

is also given, up to the vapor pressure at test conditions. Below 400 psia, the pressure range of immediate interest for the EFD application, both the  $SF_6$  and the mixtures of hydrogen with low concentrations of  $SF_6$  yield power outputs about 60% higher than are indicated for air. Recalling, however, that from the overall two-fluid cycle efficiency standpoint the EFD medium should have a low molecular weight, it is evident that the mixtures are vastly superior to the heavy  $SF_6$  gas. It is interesting that the  $H_2$ -1/2%  $SF_6$  mixture is more desirable than air except for the extreme high pressure end where the dielectric strength of air outweighs its high molecular weight disadvantage.

The relative merits for efficiency of some mixtures of gases, again non-dimensionalized by comparing with air at the same pressure, are shown in Figure 8. As dielectric strength is the only parameter to be maximized for efficiency purposes, it is evident that the heavy  $SF_6$  gas will appear attractive on this plot also. At the lower pressures  $SF_6$  is over 4 times better than the best mixture. However, it is important to note that this does not represent a factor of 4 improvement in efficiency, as can be seen by referring to the stage efficiency equation.

In this pressure range it is also interesting to note that  $H_2$ -10%  $SF_6$  mixture is almost as good as air but its molecular weight is reduced almost by a factor of 2, (16.4 compared to 28.9 for air), this lower density indicating a much more desirable EFD cycle medium.

### Conclusions

This investigation has yielded the constituents of some mixtures with properties desirable in an EFD working medium. Other gases and mixtures may

also be suitable; they remain to be investigated. It is evident from the results here given, however, that, as there is little possibility of achieving a mixture of molecular weight below that of hydrogen-1/2% SF<sub>6</sub> (2.72) due to the generally high molecular weights of the breakdown inhibitors, the greatest improvement must come from increased dielectric strength values. As can be seen from Figure 7, a sufficiently high breakdown voltage value can offset even order of magnitude increases in molecular weight.

The ARL experimental generator has, up to the present, employed high pressure air as a working medium, mainly because of its availability and convenience of use. Figures 7 and 8 show how it compares with other possible media from power density and efficiency considerations. Added to these there is the very important matter of overall cycle efficiency and in this respect the relatively high molecular weight of air is a serious disadvantage. At present operating pressures of the generator, 100 to 400 psi in the conversion duct, it is seen that either the H<sub>2</sub>-1/2% SF<sub>6</sub> mixture or H<sub>2</sub> alone has attractive possibilities compared to air, and that there are good reasons to justify the use of one of these media. Some increase in power would result, and though the stage efficiency would decrease to an extent governed largely by  $\xi$ , the drag coefficient, conditions for the overall system efficiency would be enhanced. Thus the lower mass density substance would be preferable as the driven gas, the working medium in the two-fluid EFD process.

In conclusion it should be stated that the disadvantage of hydrogen-SF<sub>6</sub> mixtures in forming hydrogen fluoride and hydrogen sulphide as discharge products would not be a limitation on their employment in EFD generators. Operating voltages, in any event, have to be kept low enough that the dielectric strength of the duct gases are not exceeded at any point so that transients and output fluctuations are eliminated.

## REFERENCES

1. Berberich, L.J., Works, C. N., and Lindsay, E.W., "Electric Breakdown of Perfluorocarbon Vapors and Their Mixtures with Nitrogen", Transactions AIEE 74, 660, 1955.
2. Camilli, G., Gordon, G.S., and Plump, R.E., "Gaseous Insulation for High Voltage Transformers", Transactions AIEE, 71, 348, 1952.
3. Charlton, E.E., Cooper, F.S., "Dielectric Strength of Insulating Fluids", General Electric Review, 40, 438, 1937.
4. Cobine, J.D., "Gaseous Conductors", (Book), Dover Publication, Inc. New York.
5. Hasinger, S., "Performance Characteristics of Electro-Ballistic Generators", Aerospace Research Laboratories Technical Report ARL 64-75.
6. Hawes, M., "Experimental Techniques in Electro-Fluid Dynamic Energy Conversion Research", Aerospace Research Laboratories Technical Report ARL 64-77.
7. Howard, P.R., "Insulation Properties of Compressed Electronegative Gases", Proceedings IEE, 104 (Part A), 123, 1956.
8. Hudson, C.M., Hoisington, L.E., and Royt, L.E., "Dielectric Strength of  $CCl_2F_2$ -Air and  $SO_2$ -Air Mixtures", Physical Review 52, 664, 1937.
9. Kontaratos, A.N., Demetriades, S.T., "Electrical Breakdown of Gases at Elevated Temperatures", Physical Review, 137, No. 6A, A 1685, 1965.
10. Lawson, M.O., "Performance Characteristics of Electro-Fluid Dynamic Energy Conversion Processes Employing Viscous Coupling", Aerospace Research Laboratories Technical Report ARL 64-75.
11. Lawson, M.O., von Ohain, H.J.P., and Wattendorf, F.L., "Performance Potentialities of Direct Energy Conversion Processes Between Electrostatic and Fluid Dynamic Energy", Aerospace Research Laboratories Technical Report ARL 178.
12. Liao, T.W., "Compressed Gas as a High Voltage Insulant", Central Electricity General Board, London, Publication, "Gas Discharges and the Electricity Supply Industry", (BOOK), London, Butterworths, 1962.
13. Narbut, P., Berg, D., Works, C.N., Dakin, T.W., "Factors Controlling Electric Strength of Gaseous Insulation", Transactions AIEE, 78, (Part 3), 545, 1959.
14. von Ohain, H.J.P., Wattendorf, F.L., "Potentialities of Direct Electro-Fluid Dynamic Energy Conversion Processes for Power Generation", Aerospace Research Laboratories Technical Report ARL 64-73.

15. Rodine, M.T., Herb, R.G., "Effect of  $\text{CCl}_4$  Vapor on the Dielectric Strength of Air", Physical Review 51, 508, 1937.
16. Schum, W.C., Trump, J.G., Priest, G.L., "Effect of High Voltage Electrical Discharges on Sulfur Hexafluoride", Industrial and Engineering Chemistry, 41, 1348, 1949.
17. Skilling, H.H., Brenner, W.C., "The Electric Strength of Air at High Pressure". Transactions AIEE, 60, 112, 1941 and Discussion, 677.
18. Stephenson, J.D., "Corona and Spark Discharge in Gases", Journal IEE, 73, 69, 1933.

### RECIRCULATORY EFD GENERATOR, (CLOSED CYCLE SIMULATION) SCHEMATIC VIEW

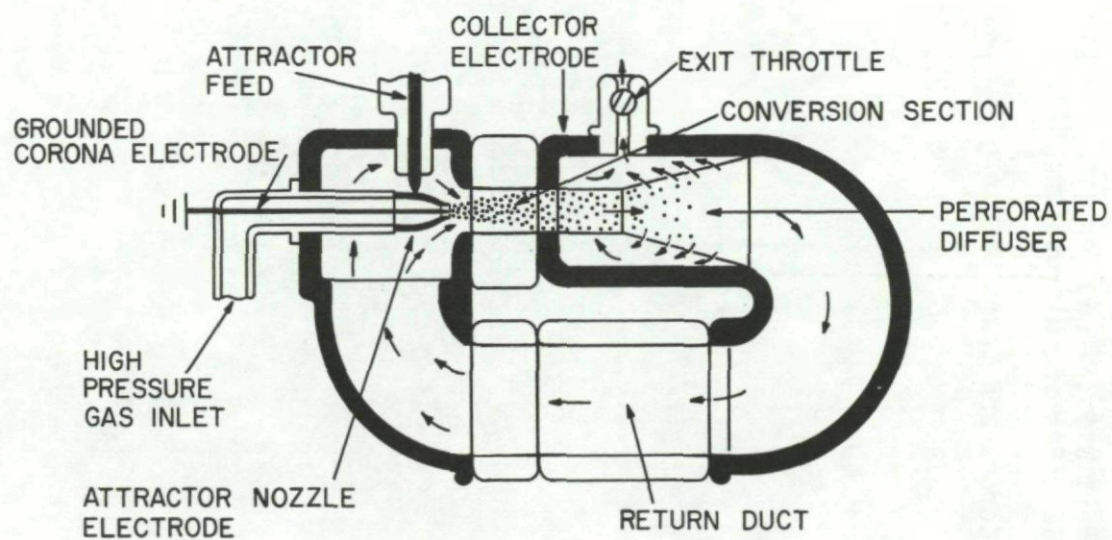


FIGURE 1.



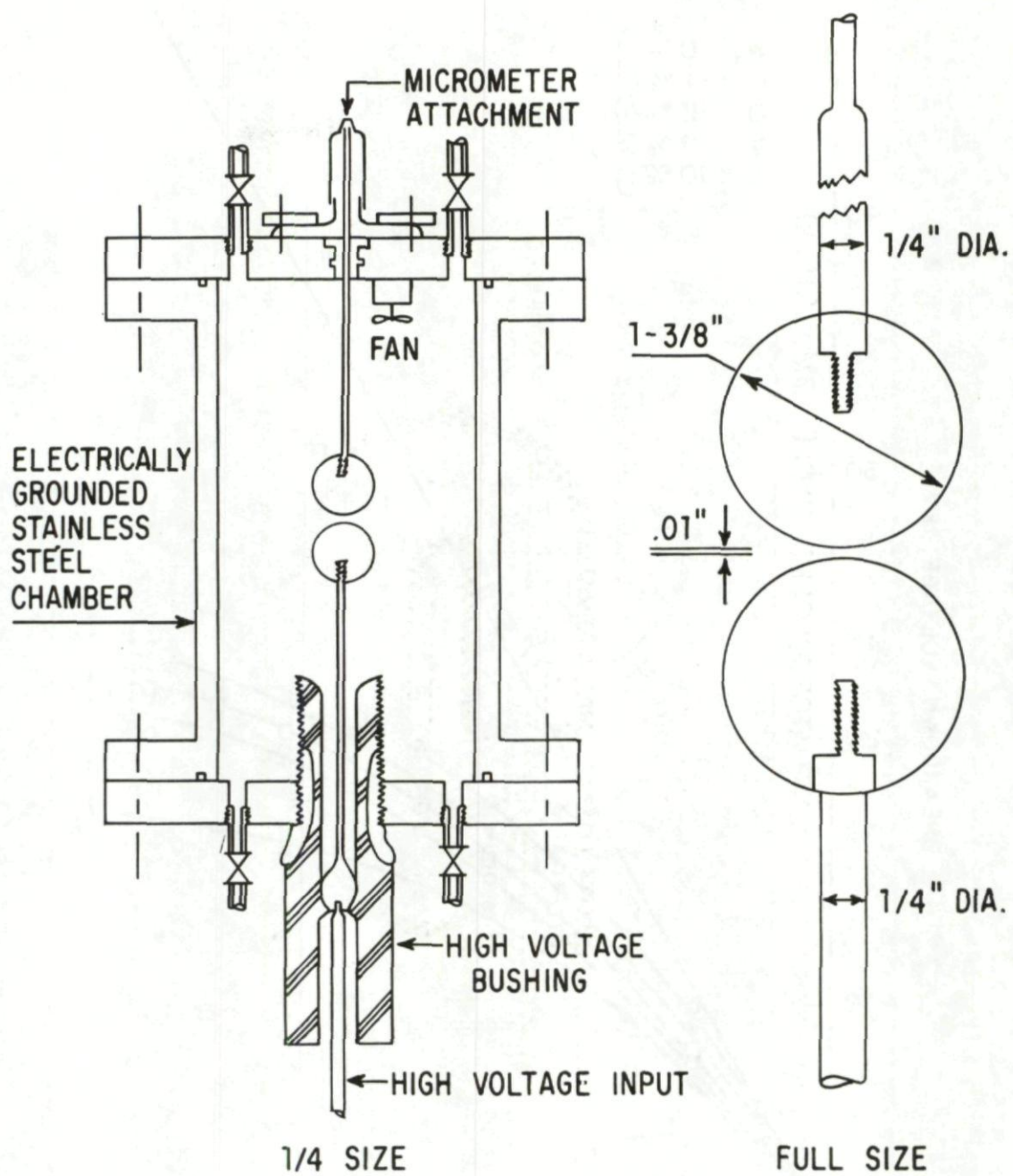


FIG. 2 BREAKDOWN CHAMBER and ELECTRODES

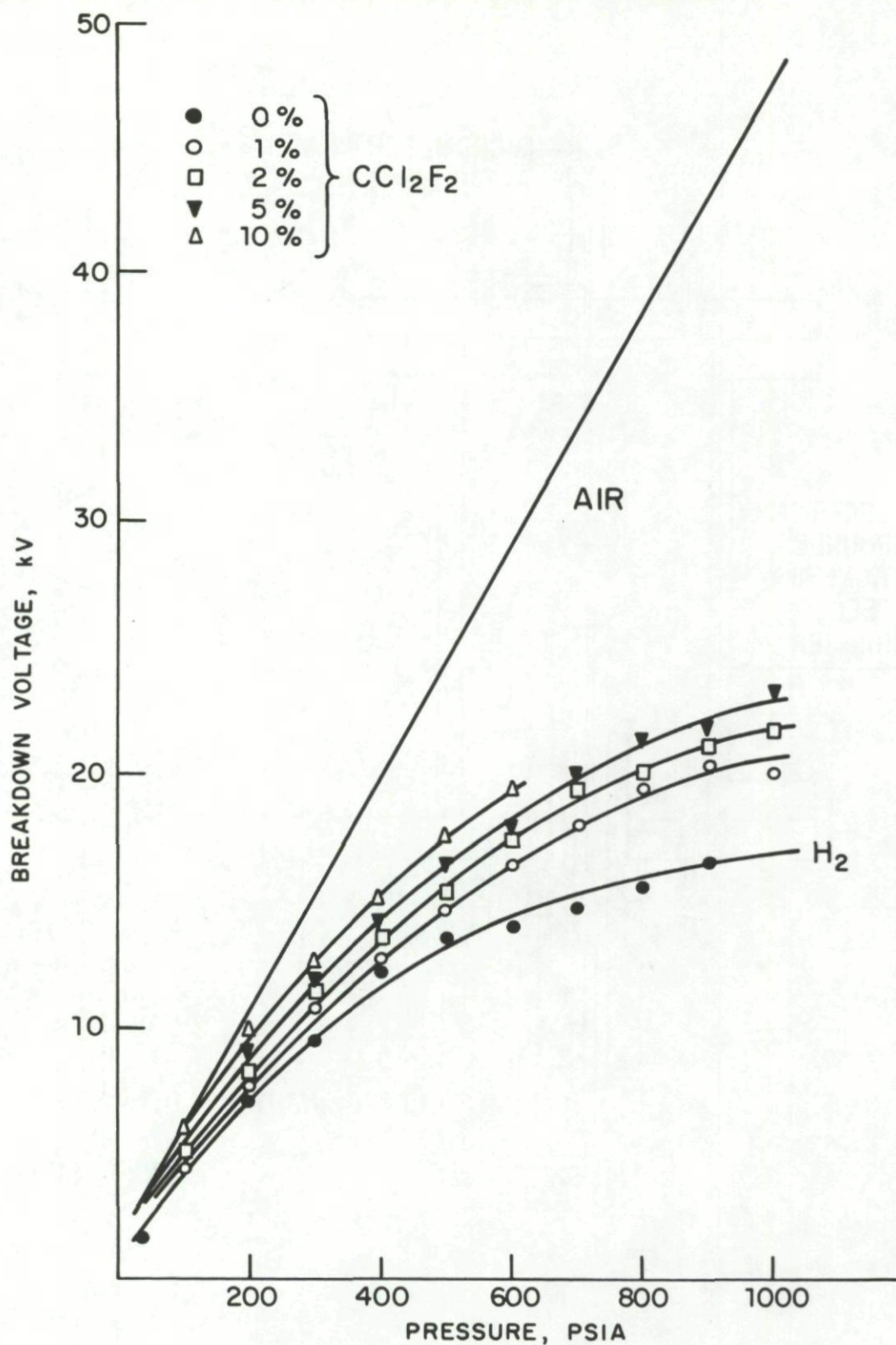


FIG. 3 EFFECT OF ADDING VARIOUS PERCENTAGES OF FREON-12 ON THE BREAKDOWN VOLTAGE OF HYDROGEN

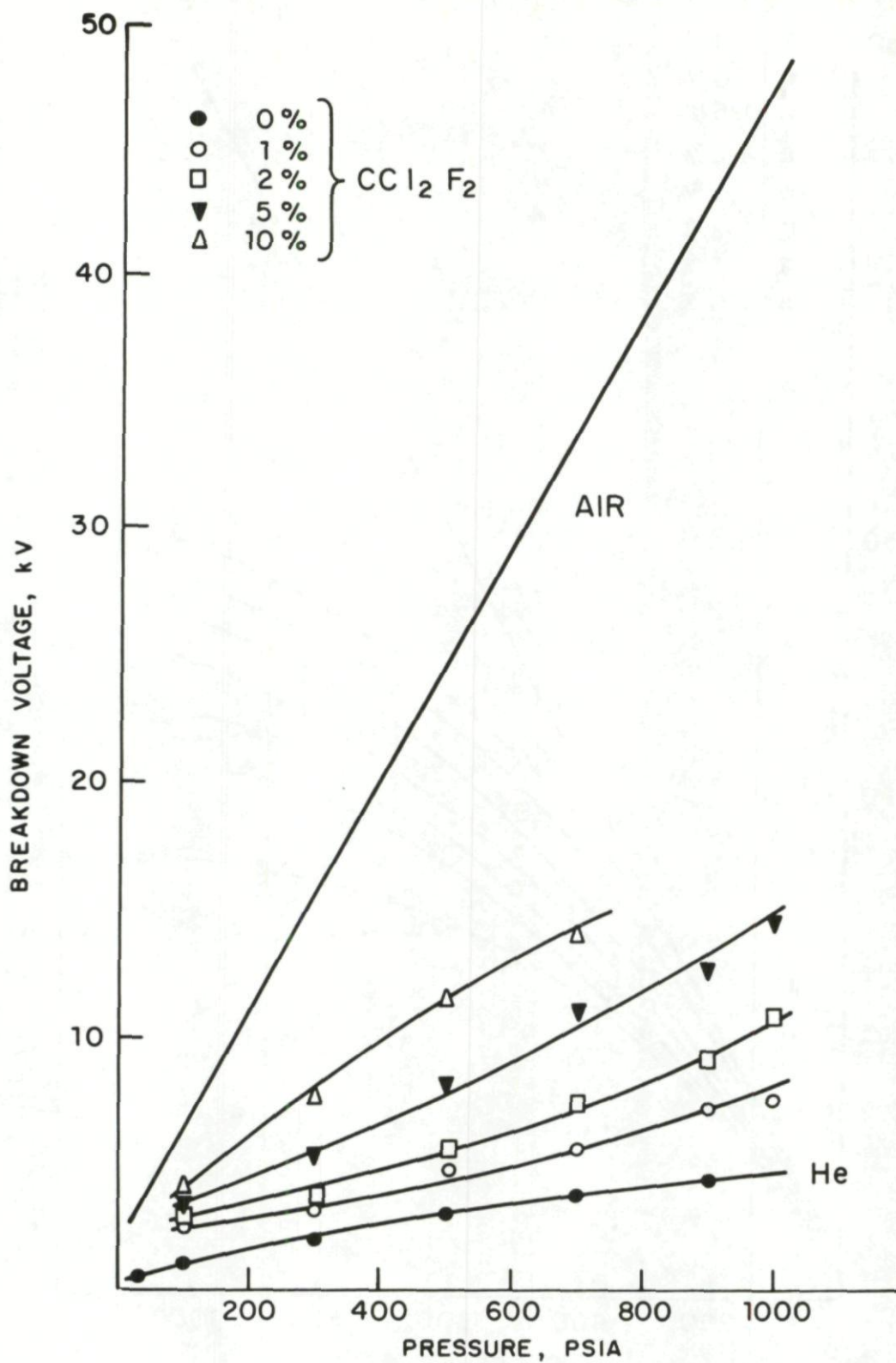


FIG. 4 EFFECT OF ADDING VARIOUS PERCENTAGES OF FREON-12 ON THE BREAKDOWN VOLTAGE OF HELIUM

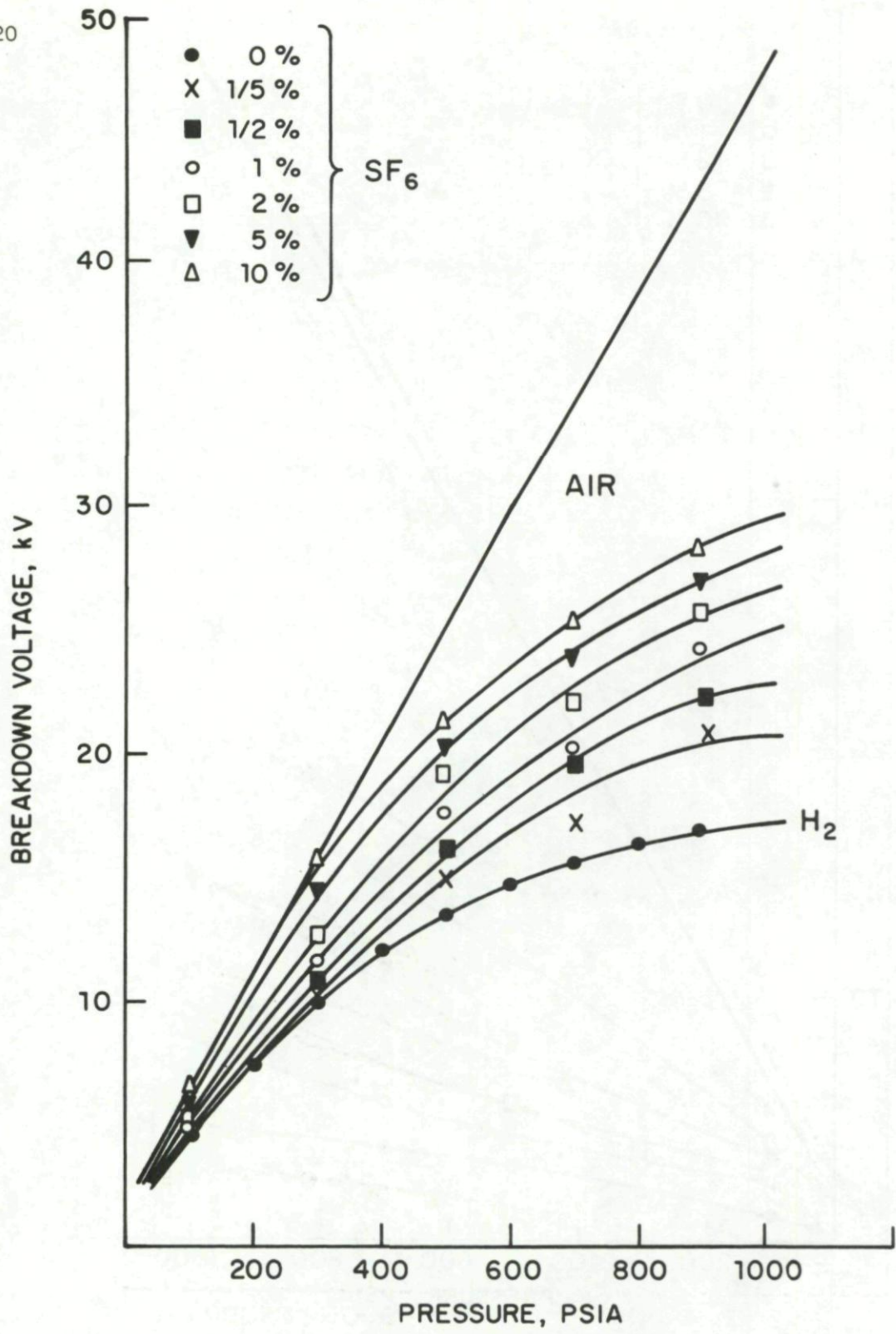


FIG. 5 EFFECT OF ADDING VARIOUS PERCENTAGES OF SF<sub>6</sub> ON THE BREAKDOWN VOLTAGE OF HYDROGEN

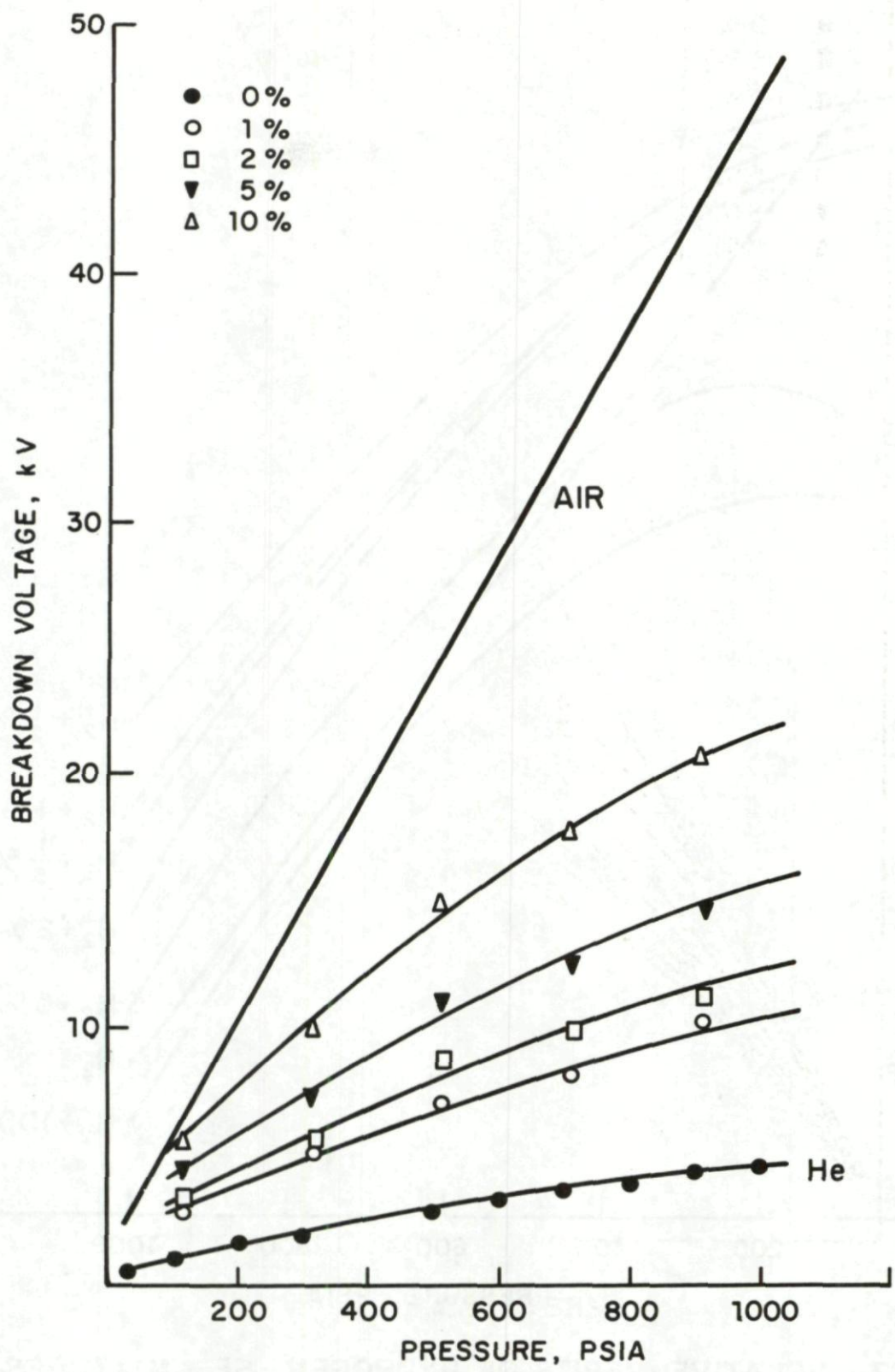


FIG. 6 EFFECT OF ADDING VARIOUS PERCENTAGES OF SF<sub>6</sub> ON THE BREAKDOWN VOLTAGE OF HELIUM

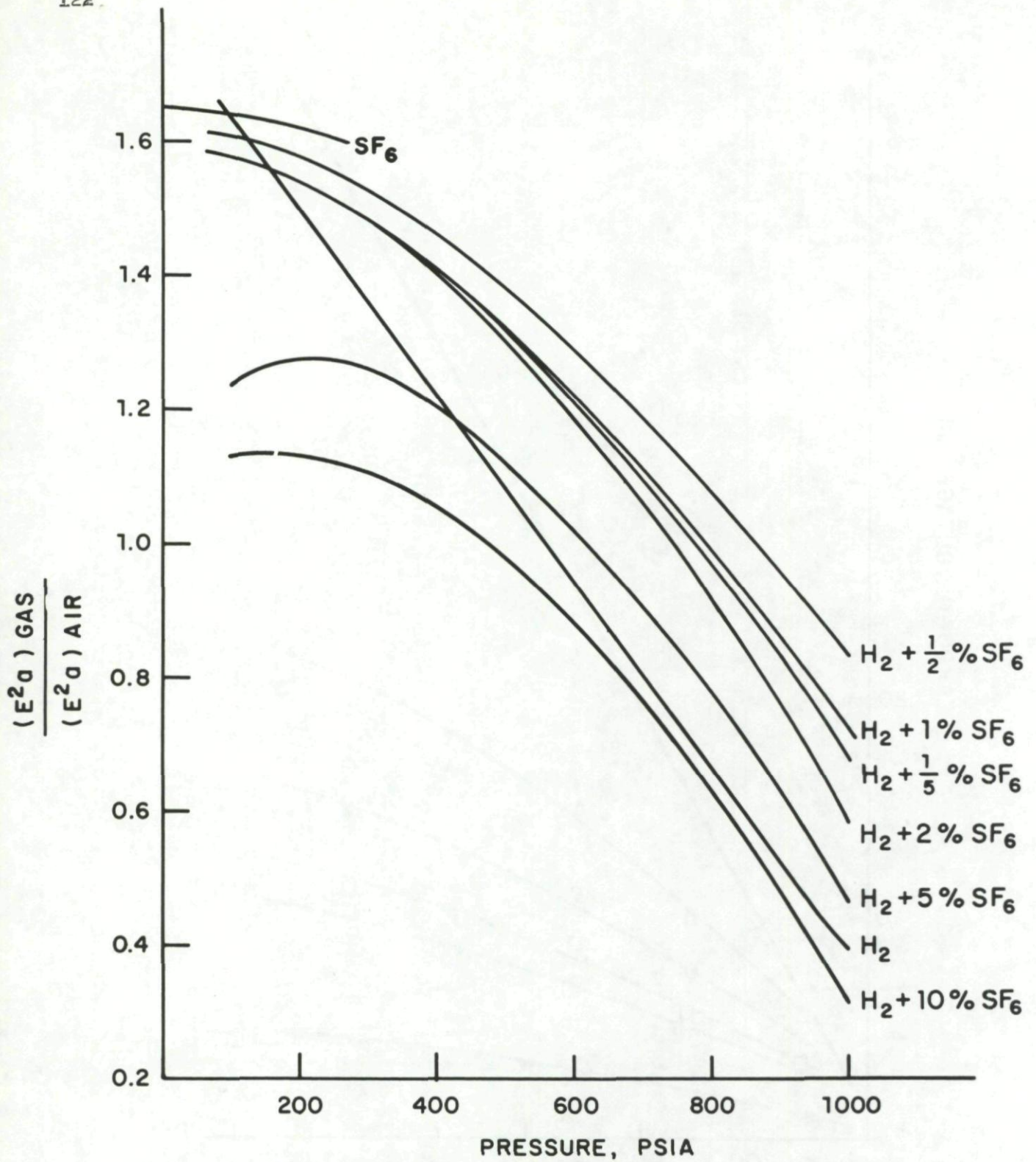


FIG. 7 RELATIVE MERITS OF HYDROGEN - SF<sub>6</sub> MIXTURES  
( POWER CONSIDERATIONS )

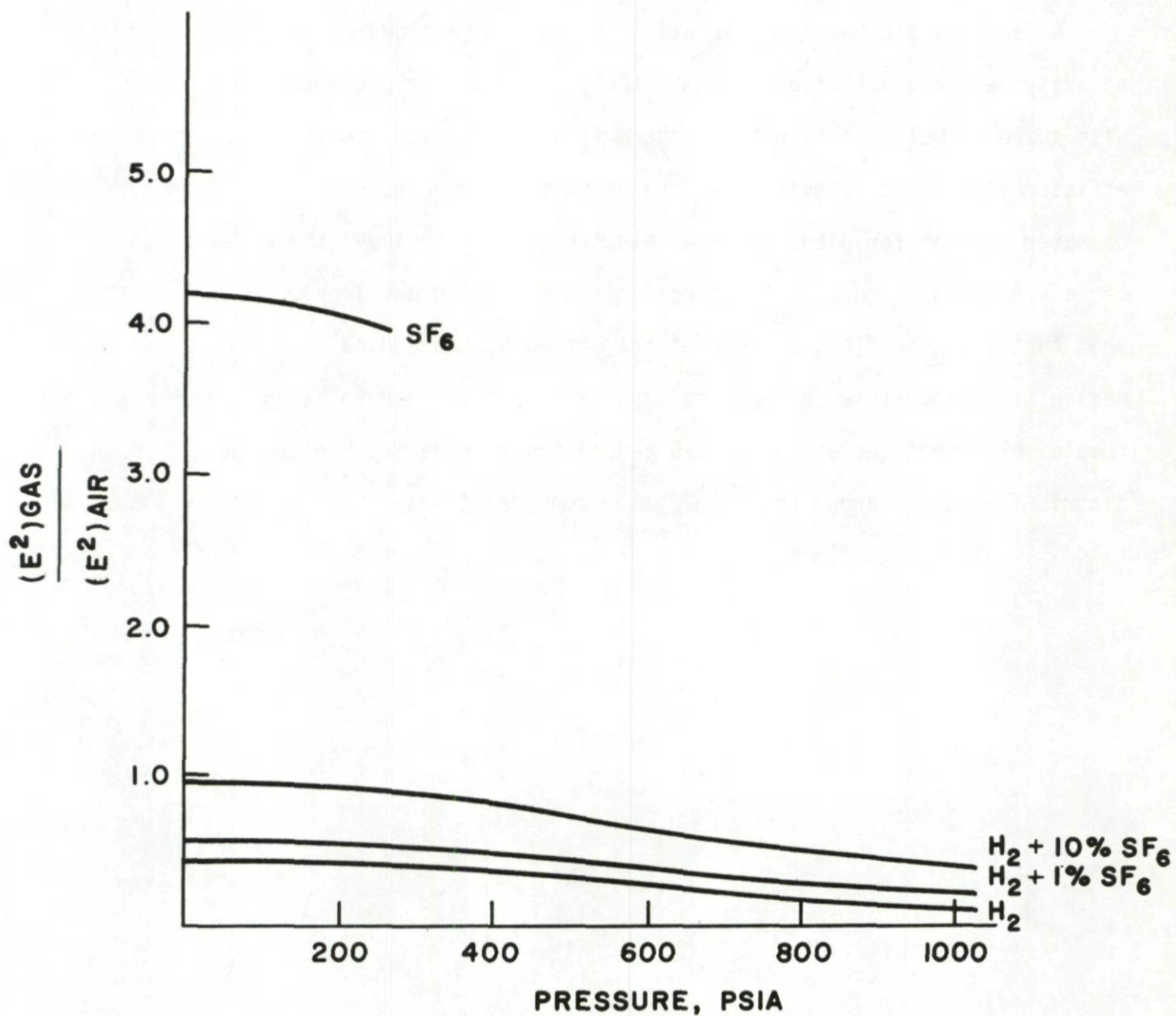


FIG. 8 RELATIVE MERITS OF VARIOUS GASES  
(EFFICIENCY CONSIDERATIONS)

SOME ANALYTICAL TREATMENTS OF  
EFD PROCESSES

Summary

An approximate, analytic solution to the charge cloud growth in an axisymmetric electrofluid dynamic (EFD) generator is presented. With these formulas, a computer program is used to calculate the efficiency and power density over a wide range of parameters. A computer program for plane parallel electrodes that includes the effects of charge spreading due to the electric field is also developed. Results show that electric field effects on the motion of charged colloids are negligible. Therefore, a numerical approach is developed to study complex electrode geometries of EFD generators considering the charge distribution to be known from fluid flow considerations.



SOME ANALYTICAL TREATMENTS OF  
EFD PROCESSES

John E. Minardi  
University of Dayton Research Institute  
Dayton, Ohio

Aerospace Research Laboratories  
Office of Aerospace Research  
United States Air Force  
Wright-Patterson Air Force Base, Ohio

Introduction

Research at the Aerospace Research Laboratories in the area of electrofluid dynamic (EFD) energy conversion processes has shown promise of being an effective means of producing power. Theoretical studies have been chiefly one-dimensional since explicit solutions were available; however, the experimental geometry has been axisymmetric in character. Hence, the need arose for axisymmetric theoretical studies where an explicit solution without serious simplifying assumptions did not exist. This paper reports the first portion of the planned study which includes an approximate solution to the axisymmetric equations which enables one to make general studies of efficiency and power flux. Also reported are several specially designed computer programs which, it is hoped, will ultimately lead to a capability of computer-assisted design of EFD generators, either axisymmetric or two dimensional.

General Considerations

An EFD generator consists of a neutral working medium which drives unipolar charged particles (ions or colloids) against an electrostatic field to produce direct current electrical power. Such devices are characterized by very high voltage and very low current density. The most

successful method to date of producing the charged particles has been by corona discharge at a needle point. For purposes of this chapter, it will be assumed that charges of constant density over a circular cross-section enter the conversion section at a grounded infinite plane electrode. The charges are then transported to the collector electrode, also an infinite plane, at some voltage  $V$ . Since the pressure drop in the conversion section is small, the working fluid is assumed to be incompressible and the velocity constant in the conversion section.

The assumed model is shown in Fig. 1.

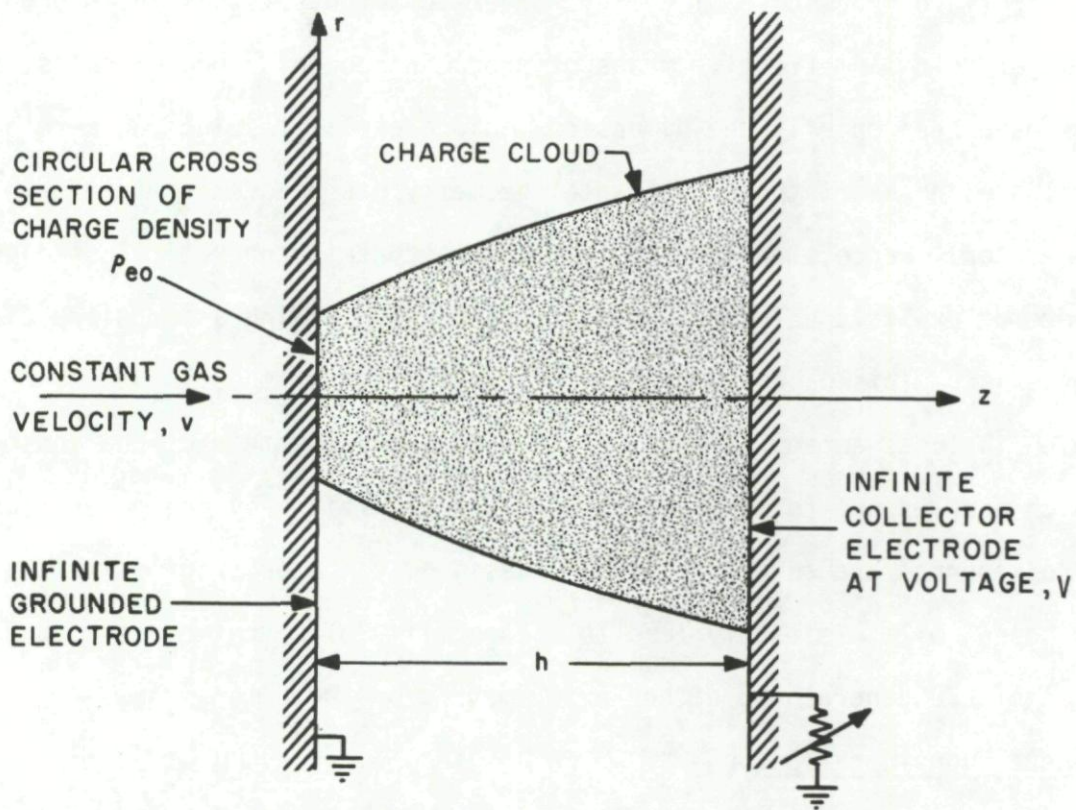


Figure 1. Assumed generator model.

It is desired to calculate the charge cloud shape and the charge

density,  $\rho_e$ , as a function of position in the conversion section. Knowledge of the charge cloud shape is important, since an actual generator must be designed so that the charges first touch the walls of the conversion section at the collector electrode. If the charges come into contact with the dielectric walls of the conversion section before they reach the collector electrode, extraneous electric fields will result in the conversion section which could lead to electric breakdown of the working medium, as well as increase the losses in the generator. Also, as the expanding charge cloud enters the fluid boundary layer near the walls, the charges can return to the grounded electrode, causing increased losses in the generator. Hence, knowledge of the charge cloud shape is important in the design of an axisymmetric EFD generator.

The velocity of the charged particles,  $v_e$ , is dependent on the neutral gas velocity,  $v$ , the charged particle mobility,  $k$ , and the electric field,  $E$ .

$$\bar{v}_e = \bar{v} + k \bar{E}$$

Further, the flow is considered steady and magnetic effects negligible; consequently, the conservation of charges requires

$$\nabla \cdot \rho_e (\bar{v} + k \bar{E}) = 0 \quad (1)$$

Also for a homogeneous medium

$$\nabla \cdot \bar{E} = \frac{\rho_e}{\epsilon_0} \quad (2)$$

and finally

$$\nabla \times \bar{E} = 0 \quad (3)$$

Assuming the flow to be incompressible, Equation (1) can be expanded to yield

$$\rho_e k \nabla \cdot \bar{E} + (\bar{v} + k \bar{E}) \cdot \nabla \rho_e = 0 \quad (4)$$

Substitution of Equation (2) into Equation (4) yields

$$\frac{k \rho_e^2}{\epsilon_0} + (\bar{v} + k \bar{E}) \cdot \nabla \rho_e = 0 \quad (6)$$

In the particular case of axisymmetric flow with only a  $z$ -component of the fluid velocity,  $v$ , Equation (6) becomes

$$\frac{k \rho_e^2}{\epsilon_0} + (v + k E_z) \frac{\partial \rho_e}{\partial z} + k E_r \frac{\partial \rho_e}{\partial r} = 0 \quad (7)$$

Now the axisymmetric form of Equation (1) under the same assumptions as above is

$$\frac{1}{r} \frac{\partial (r \rho_e k E_r)}{\partial r} + \frac{\partial \rho_e (v + k E_z)}{\partial z} = 0 \quad (8)$$

Equation (8) clearly admits of a stream function,  $\psi$ , defined as

$$\begin{aligned} -\frac{1}{r} \frac{\partial \psi}{\partial r} &= \rho_e (v + k E_z) \\ \frac{1}{r} \frac{\partial \psi}{\partial z} &= \rho_e k E_r \end{aligned} \quad (9)$$

Along a stream line  $\psi = \text{constant}$  and  $d\psi = 0$ , therefore

$$\left. \frac{dr}{dz} \right|_{\psi = \text{const}} = -\frac{\partial \psi / \partial z}{\partial \psi / \partial r} = \frac{k E_r}{v + k E_z} \quad (10)$$

Further, consider the density along a stream line. Since

$$d\rho_e = \frac{\partial \rho_e}{\partial z} dz + \frac{\partial \rho_e}{\partial r} dr \quad (11)$$

then along a stream line the expression for  $d\rho_e$  is obtained by combining Equation (10) with Equation (11) to obtain

$$d\rho_e \Big|_{\psi=\text{const}} = \left( \frac{\partial \rho_e}{\partial z} + \frac{kE_r}{v+kE_z} \frac{\partial \rho_e}{\partial r} \right) dz \quad (12)$$

which in view of Equation (7) yields

$$- \frac{d\rho_e}{\frac{k}{\epsilon_0} \rho_e^2} = \frac{dz}{v+kE_z} \quad (13)$$

In a similar way it can be shown that

$$- \frac{d\rho_e}{\frac{k}{\epsilon_0} \rho_e^2} = \frac{dr}{kE_r} \quad (14)$$

Equation (3) admits of a potential  $\phi$  such that  $\vec{E} = -\nabla\phi$ , therefore Equation (2) in the axisymmetric form is

$$\frac{1}{r} \frac{\partial \phi}{\partial r} + \frac{\partial^2 \phi}{\partial r^2} + \frac{\partial^2 \phi}{\partial z^2} = - \frac{\rho_e}{\epsilon_0} \quad (15)$$

and Equation (7) becomes

$$\frac{k\rho_e^2}{\epsilon_0} + (v-k \frac{\partial \phi}{\partial z}) \frac{\partial \rho_e}{\partial z} - k \frac{\partial \phi}{\partial r} \frac{\partial \rho_e}{\partial r} = 0 \quad (16)$$

which, as was shown above, has the associated total differential equations

$$\frac{dz}{v - k \frac{\partial \phi}{\partial z}} = \frac{dr}{-k \frac{\partial \phi}{\partial r}} = \frac{d\rho_e}{\frac{k}{\epsilon_0} \rho_e^2} \quad (17)$$

For Figure 1 the boundary condition would be:

$$\begin{aligned}
 \phi(r,0) &= 0 \\
 \phi(r,h) &= V \\
 \rho_e(r,0) &= \rho_{e0} \quad r \leq r_a \\
 \rho_e(r,0) &= 0 \quad r > r_a
 \end{aligned}
 \tag{18}$$

There are, in addition, other constraints on the solution; in particular, the field strength must be less than the breakdown field strength,  $E_b$  of the working gas, i.e.,  $|E| < E_b$  and the z component of velocity for the charge particles must be greater than zero, i.e.,  $v - kE_z > 0$ .

The solution of Equations (15) and (16) with boundary conditions (18) would then give the charge cloud shape through the Equations (17). An exact analytic solution to these equations has not been obtained, but an approximate solution using just the Equations (17) was obtained and used in equations for efficiency and area power density. The following section discusses these results.

#### The Approximate Charge Cloud Shape

An approximation to the density profile can be obtained from Equation (13) for those cases where the drift velocity induced by the space charge effects is small compared to the velocity of the charges in the absence of the field resulting from the space charges. The magnitude of the applied field will be defined to be the constant field obtained by the ratio of the applied voltage to the channel width, h. The applied field, which acts in the z direction only, is

$$E_a \equiv -V/h \tag{19}$$

Hence the total field acting in the z direction is

$$E_z = E_a + E_{sc} \quad (20)$$

Substitution of Equation (20) in Equation (13) yields

$$\int_{\rho_{e0}}^{\rho_e} \frac{d\rho_e}{\rho_e} - \frac{k}{\epsilon_0} \frac{\rho_e}{\rho_e} z = \int_0^z \frac{dz}{v + kE_a + kE_{sc}} \quad (21)$$

The integration of Equation (21) is simple for those cases where it is valid to assume that

$$v + kE_a \gg kE_{sc} \quad (22)$$

since  $v$ ,  $k$ , and  $E_a$  are constants. The result of the integration yields the density variation as a function of  $z$  only, i.e.,

$$\frac{\rho_e}{\rho_{e0}} = \left[ 1 + \frac{k\rho_{e0}z}{\epsilon_0(v+kE_a)} \right]^{-1} \quad (23)$$

To the same degree of approximation, the conservation of charges gives

$$\rho_{e0}(v + kE_a) \pi r_a^2 = \rho_e(v + kE_a) \pi r^2 \quad (24)$$

Hence,

$$r = r_a \sqrt{\rho_{e0}/\rho_e} \quad (25)$$

or

$$r = r_a \sqrt{1 + \frac{k\rho_{e0}}{\epsilon_0(v+kE_a)} z}$$

Equation (23) gives the approximate variation in density, while Equation (25) gives the outer profile of the charge cloud if  $r_a$  is the initial cloud radius (if  $r_a$  is replaced with smaller values, Equation (25)

would produce stream lines).

Since the performance of an EFD generator is sensitive to the breakdown field strength,  $E_b$ , of the working gas and to the mobility of the charged particles, it is convenient to normalize Equation (25). The mobility varies inversely with the gas density,  $\rho_g$ , and the breakdown field strength directly with  $\rho_g$  over a wide range of interest; their values at any density are related to the values at standard conditions (subscript n) by

$$E_b = E_{bn} \rho_g / \rho_{gn} \quad (26)$$

$$k = k_n \rho_{gn} / \rho_g \quad (27)$$

Hence, the value of the maximum possible slip velocity is constant, since

$$kE_b = k_n E_{bn} \quad (28)$$

It is convenient to use the following definitions to normalize the equations

$$\begin{aligned} \mu &= v / (kE_b) = v / (k_n E_{bn}) \\ \alpha &= E_a / E_b \\ Z &= z/h; R = r/h \\ \rho &= \rho_e / \rho_{e0} \\ K &= (\rho_{e0} h) / (E_b \epsilon_0) \end{aligned} \quad (29)$$

In the case of a generator,  $\rho_{e0}$  and  $E_b$  have opposite signs; also  $k$  and  $E_b$  have opposite signs. Therefore  $K$  and  $\mu$  are negative numbers. However, if the absolute values of  $\rho_{e0}$ ,  $k$ , and  $E_b$  are used Equation (25) becomes

$$R = R_a \sqrt{1 + \frac{K}{\mu - \alpha} Z} \quad (30)$$

In the next two sections the efficiency and the power per unit



area will be examined using Equation (30) along with the condition that the charges first contact the walls at the collector electrode. First the conditions of gas density and pressure will be fixed in the conversion section. Following that, a more interesting case is considered where the condition of gas density and pressure will be taken as fixed in a reservoir feeding the conversion section; also a more reasonable treatment of the initial charge density will be attempted.

#### Fixed Thermodynamic Conditions in the Conversion Section

In this section the power density, power per unit cross section area,  $Le$ , and the efficiency are investigated, assuming the approximate solution to be valid and that the charges initially contact the walls at the collector. Further, the initial charge density is considered constant for all velocities,  $v$ , and gas densities studied.

##### 1. Power flux

The power density based on the channel cross section area is simply the product of the current and voltage divided by the channel area; hence, for a generator using the absolute value of all parameters

$$Le = [\rho_{e0}(v - kE_a)\pi r_a^2] (E_a h) / \pi R^2$$

$$Le = \rho_{e0} h E_a (v - kE_a) (r_a/R)^2 \quad (31)$$

Since the charges initially contact the wall at the collector, the ratio of radii to be used in Equation (13) is obtained from Equation (30) by setting  $Z = 1$ . Substituting the result into Equation (31) and normalizing yields

$$\bar{L}_e \equiv \frac{L_e}{\epsilon_0 k_n E_{bn}^3} = \left(\frac{g}{\rho g n}\right)^2 \frac{K(\mu-\alpha)^2 \alpha}{K + (\mu-\alpha)} \quad (32)$$

In the case of an EFD generator, the domain of interest for Equation (32) is described by the following relations

$$\begin{aligned} & 0 \leq \alpha \leq 1 \\ \text{and} \quad & \mu \geq \alpha \\ & K > 0 \end{aligned} \quad (33)$$

Investigation of Equation (32) in the domain of interest indicates that the area power density always increases for increasing values of  $K$  or increasing values of  $\mu$ . However, for fixed  $K$  and  $\mu$  the function  $\bar{L}_e$  has a maximum (determined from the condition  $\frac{\partial \bar{L}_e}{\partial \alpha} = 0$ ) at

$$\alpha = (K+\mu) \left[ \frac{3}{4} - \frac{1}{2} \sqrt{\frac{9}{4} - \frac{2\mu}{K+\mu}} \right] \quad (34)$$

In the domain of interest, the maximum value of  $\bar{L}_e$  occurs at the largest available values of  $K$  and  $\mu$  with the corresponding value of  $\alpha$  obtained from Equation (34); however, if this value of  $\alpha$  is greater than 1, then the maximum would occur at  $\alpha = 1$ .

## 2. Stage Efficiency

The stage efficiency,  $\eta$ , of the EFD generator is developed in this section, considering losses resulting from slip and fluid friction on the walls of the conversion section. It is assumed that the approximate solution is valid and that the charge particles initially contact the walls at the collector. The efficiency is given by

$$\eta = L_e / (L_e + L_s + L_f) \quad (35)$$

where  $L_e$  is given by Equation (31) and the slip loss per unit cross

section area  $L_s$ , is

$$L_s = (\rho_{e_0} k E_a \pi r_a^2) (h E_a) / \pi R^2 \quad (36)$$

and the loss resulting from fluid friction,  $L_f$ , is

$$L_f = f \frac{h}{R} \rho_g v^3 \quad (37)$$

Combining Equations (31), (35), and (36) results in

$$\eta = (v - k E_a) / [v + f \frac{h}{R} \frac{\rho_g}{\rho_{e_0}} \frac{v^3}{h E_a} (\frac{R}{r_a})^2] \quad (38)$$

As before, the absolute values of the parameters were used in obtaining Equation (38). The condition that the charges initially contact the wall at the collector is again introduced by substituting for the radius ratio in Equation (38) the value obtained from Equation (30) by setting  $Z=1$ . Hence,

$$\eta = E_a (v - k E_a) / [(v - k E_a) v E_a + f \frac{h}{R} \frac{\rho_g v^3}{\rho_{e_0} h} (\frac{\rho_{e_0} h k}{\epsilon_0} + v - k E_a)] \quad (39)$$

If, in addition to the normalized parameters of Equations (29), the figure of merit of the working substance

$$\theta = \frac{4 \epsilon_0}{\rho_g k^2} = \frac{4 \epsilon_0}{\rho_{gn} k_n^2} \frac{\rho_g}{\rho_{gn}} = \theta_n \frac{\rho_g}{\rho_{gn}} \quad (40)$$

and a friction parameter

$$\zeta = 2f \frac{h}{R} \quad (41)$$

are introduced into Equation (39), the result is

$$\eta = \frac{(\mu - \alpha)^2 \alpha}{(\mu - \alpha) \mu \alpha + \frac{2\zeta}{K\theta} \mu^3 (K + \mu - \alpha)} \quad (42)$$

The significance of the figure of merit was first recognized by Dr. Hans von Ohain of ARL and it depends only on properties of the working medium and the charge carriers. Clearly, in view of Equation (42), a large value of the figure of merit results in higher stage efficiencies.

Analysis of Equation (42), considering it a function of  $\mu$  and  $\alpha$ , indicates that the stage efficiency is multivalued at the origin,  $\mu=\alpha=0$ . The analysis also shows that in the domain of interest ( $0 < \alpha < 1$  and  $\mu > \alpha$ ), the maximum value of  $\eta$  occurred at the origin. An upper limit to the stage efficiency can be determined at the origin as follows:

$$\begin{aligned} \text{Let} \quad \alpha &= a\mu \\ \text{where} \quad a &\leq 1 \end{aligned} \tag{43}$$

then substitution of Equation (43) into Equation (42) yields

$$\eta = \frac{a(1-a)^2}{a(1-a) + \frac{2\zeta}{K\theta} [K + \mu(1-a)]} \tag{44}$$

At the origin  $\mu = 0$ , and therefore Equation (44) gives for the stage efficiency

$$\eta_{\max} = \frac{a(1-a)^2}{a(1-a) + \frac{2\zeta}{\theta}} \tag{45}$$

In the usual way it can be shown that the roots of the equation

$$a^3 - a^2 - 3 \frac{2\zeta}{\theta} a + \frac{2\zeta}{\theta} = 0 \tag{46}$$

yield the value of  $a$  that maximizes  $\eta$ . Equation (46) always has a root such that  $0 < a < 1$ , this root will give the upper limit to the efficiency.

### 3. Discussion and Results

In this section, some numerical results of the equations are presented. Equations (45) and (46) can be combined to give a curve of the theoretical maximum stage efficiency as a function of the parameter  $2\zeta/\theta$ . For a given value of the parameter "a", Equation (46) is solved to obtain a value of  $2\zeta/\theta$  and this pair of values is used in Equation (45) to determine  $\eta_{\max}$ . Figure 2 is the result of this calculation and gives the maximum efficiency as a function of  $2\zeta/\theta$ . Figure 2 also includes various ranges of  $2\zeta/\theta$  for a number of gases; air,  $\text{CCl}_4$ , steam, and  $\text{CHCl}_3$ . The extent of the improvement in efficiency afforded by operation at higher gas densities is shown by the reduction in  $2\zeta/\theta$  for each gas. The numbers marked on the lines are the values of gas density ratio required to yield the indicated value of  $2\zeta/\theta$ .

The group of values at the right of Figure 2 were calculated for ions in the various gases with  $\zeta=0.1$ . The gas properties used for the calculations are given in Table 1. The improvement afforded by reducing  $\zeta$  to 0.01 is shown by the next group of values. In  $\text{CHCl}_3$ , the efficiency could go as high as 74%, while for air it is still less than 20%.

The final group of values is for colloids in place of ions with  $\zeta=0.1$ . The mobility was assumed to be  $1 \times 10^{-6} (\text{m/s}) / (\text{v/m})$  for each gas. The relative merit of each gas is, therefore, only dependent on the gas density. Hence, steam and air are better than  $\text{CCl}_4$  or  $\text{CHCl}_3$ . The reason for the relatively poor position of air in the other groups is, of course, due to its high value of mobility.

Figure 2 clearly points out the need to operate with colloids in order

to obtain high values of efficiency. It also points out the improvement that results from high density ratios, low values of  $\rho_{gn}$  (for a given mobility), and the sensitivity to drag losses.

However, since the maximum efficiency occurs at the origin ( $\mu=\alpha=0$ ) the power output would be zero and, therefore, for finite power outputs the efficiency would be lower than the maximum. In order to determine the performance throughout the  $\mu, \alpha$  domain, a computer program was written to solve the various equations and constant values of power density and efficiency determined. Figures 3,4,5, and 6 show typical results for several gases at  $\rho_g/\rho_{gn}$  of 17.

#### Performance for Constant Reservoir Conditions

In the last section, performance was developed for constant density in the conversion section; hence, increases in velocity (i.e., the parameter  $\mu$ ) would require increases in stagnation conditions. Also, no consideration was given to the method of producing the space charge. It was only assumed that some space charge density and initial radius were available and that these conditions were constant for all gas densities.

In order to obtain a more useful view of the performance, in this section the conditions in the conversion section will be assumed to result from the expansion of a gas from a reservoir of constant stagnation conditions. Variation in charge densities will also be treated.

##### 1. Charge Density Variations.

The procedure of using a constant charge density does not account for the inherent ability to produce higher charge densities at higher gas densities or gas velocities, or the ability to produce higher charge densities

with different gases, nor does it account for the fact that higher charge densities can be produced with colloids.

The corona discharge from a needle point is an extremely complex phenomena which is not completely understood (at least quantitatively). However, a simplified analysis may serve to indicate the effect of the ion generation process.

If, as a limiting case, a cylindrical space charge is assumed with the field strength at the edge of the cylinder equal to the breakdown value, then the formula for the charge density is

$$\rho_{eo} = \frac{2\epsilon_o E_b}{r_a} \quad (47)$$

If the limiting density given by equation (47) is multiplied by a function of  $\mu$ , say  $f(\mu)$ , where  $f(\mu)$  is a monotone increasing function such that

$$0 < f(\mu) < 1$$

then a formula for charge density would be obtained that could account for density variations due to velocity changes, different particle mobilities (ions or colloids) and different gas densities.

The result is

$$\rho_{eo} = 2\epsilon_o E_{bn} \frac{\rho_g}{\rho_{gn}} f(\mu) / r_a \quad (48)$$

At this time no satisfactory function of  $f(\mu)$  has been determined; however, a function of the form

$$f(\mu) = \left( \frac{a\mu}{b+\mu} \right)^n \quad (49)$$

would have the desired properties and has been shown to do an adequate

job of fitting a restricted amount of experimental data. Further work is required to determine an empirical form of  $f(\mu)$ , therefore, the function form of  $f(\mu)$  will be left open at this time.

## 2. Estimation of Performance

If it is assumed that a gas reservoir is available with fixed gas conditions,  $P_0, T_0$ , and  $\rho_{g0}$ , a set of equations can be determined which gives the EFD performance. The gas is assumed to expand isentropically to a specified value of velocity  $v$  and the associated values of static pressure  $P$ , static temperature  $T$ , and the static density  $\rho_g$ . The equations that govern the flow are

$$I = 2\pi\epsilon_0 k_n E_{bn}^2 \frac{\rho_g}{\rho_{gn}} R_a \mu f(\mu) \quad (50)$$

$$\rho_{e0} = 2\epsilon_0 E_{bn} \frac{\rho_g}{\rho_{gn}} f(\mu)/R_a \quad (51)$$

$$R = R_a \sqrt{1 + \frac{\rho_{e0} h}{\epsilon_0 E_{bn} \rho_g / \rho_{gn}} \cdot \frac{Z}{\mu - \alpha}} \quad (52)$$

$$Le = \frac{\rho_{e0} h}{\epsilon_0 E_{bn} \frac{\rho_g}{\rho_{gn}}} \cdot \epsilon_0 k_n E_{bn}^3 \cdot \left(\frac{\rho_g}{\rho_{gn}}\right)^2 \cdot \alpha(\mu - \alpha) \left(\frac{R_a}{R}\right)^2 \quad (53)$$

$$\dot{m} = \frac{\mu - \alpha}{\mu + f} \frac{h}{R} \cdot \frac{k_n^2 \rho_{gn} \rho_{gn}}{\epsilon_0 \rho_g} \cdot \frac{\epsilon_0 E_{bn} \rho_g}{\rho_{e0} h \rho_{gn}} \cdot \frac{\mu^3}{\alpha} \cdot \frac{R}{R_a} \quad (54)$$



$$\frac{\rho_g}{\rho_{g0}} = \left( 1 + \frac{\gamma-1}{\gamma+1} M^*2 \right)^{\frac{1}{\gamma-1}} \quad (55)$$

with the definitions

$$\mu = \frac{v}{k_n E_{bn}} ; \alpha = \frac{E_z}{E_b} ; M^* = \frac{v}{C^*} \quad (56)$$

Using Eqs. (51), (53), (55), and (56) it can be shown that

$$Le' \equiv \frac{Le}{\epsilon_0 k_n E_{bn}^3 \left( \frac{\rho_{g0}}{\rho_{gn}} \right)^2} = 2f(\mu) \frac{h}{R} \left[ 1 - \frac{\gamma-1}{2} \left( \frac{k_n E_{bn}}{C_0} \right)^2 \mu^2 \right]^{\frac{2}{\gamma-1}} \alpha(\mu-\alpha) \frac{R_a}{R} \quad (57)$$

Equation (57) holds on a closed region bounded by  $\alpha=0$ ,  $\mu=\alpha$  and  $\mu=\mu_{\max}$ .

The value of  $\mu_{\max}$  is determined from fluid mechanics. Since

$M^*_{\max} = \sqrt{\frac{\gamma+1}{\gamma-1}}$  it is easy to show that

$$\mu_{\max} = \sqrt{\frac{2}{\gamma-1}} \frac{C_0}{k_n E_{bn}} \quad (58)$$

Assuming  $f(\mu)$  to be a monotone increasing function such that  $0 < f(\mu) < 1$

it can be determined by inspection that

- if  $\mu=\alpha$  then  $Le' = 0$
- if  $\alpha=0$  then  $Le' = 0$
- if  $\mu=\mu_{\max}$  then  $Le' = 0$
- within the interior of the triangle  $Le' > 0$
- $Le'$  is bounded

Hence,  $Le'$  has a maximum within the triangle (note  $\alpha$  may be greater than 1 at the maximum).

The condition that the charges just touch the wall at the collector ( $Z=1$  and  $R=R$  in Eq. 52) has not been introduced into Eq. (57). This can be accomplished either through the  $h/R$  ratio or through the  $R_a/R$  ratio. In this section it is assumed that  $R_a/R$  is held constant and that  $h/R$  is varied in order to satisfy the condition that the charges just touch the wall at the collector. Setting  $R=R$ ,  $Z=1$  and using Eq. (57) in Eq. (52) yields

$$R = R_a \sqrt{1 + 2f(\mu) \frac{h}{R_a} \frac{1}{\mu - \alpha}}$$

which yields after some algebra

$$\frac{h}{R} = \left( \frac{R}{R_a} - \frac{R_a}{R} \right) \left[ \frac{\mu - \alpha}{2f(\mu)} \right] \quad (59)$$

Substituting Eq. (59) into Eq. (57) yields

$$Le' = \left[ 1 - \left( \frac{R_a}{R} \right)^2 \right] \left[ 1 - \frac{\gamma - 1}{2} \left( \frac{k_n E_{bn}}{C_0} \right)^2 \mu^2 \right]^{\frac{2}{\gamma - 1}} \alpha (\mu - \alpha)^2 \quad (60)$$

Once the experimental geometry, type of gas, and stagnation conditions are chosen, Eq. (60) is a function only of  $\mu$  and  $\alpha$ ; hence, the maximum occurs

$$\frac{\partial Le'}{\partial \alpha} = \frac{\partial Le'}{\partial \mu} = 0$$

The derivative with respect to  $\alpha$  yields

$$\frac{\partial Le'}{\partial \alpha} = \frac{Le'}{\alpha} - \frac{2Le'}{\mu - \alpha}$$

Rejecting  $Le' = 0$  and setting the partial derivative equal to zero yields the result

$$\alpha = \frac{1}{3} \mu \quad (61)$$

Substitution of Eq. (63) into Eq. (64) yields

$$M = \sqrt{3/2} = 1.225 \quad (65)$$

Therefore, for all gases and initial conditions, the maximum power per unit area is obtained at a Mach number of 1.225.

In the above derivation, the power density,  $Le$ , was the power per unit area of channel cross section, another useful index is the power per unit mass flow  $\tilde{Le}$ .

$$\tilde{Le} = \frac{\text{POWER}}{\dot{m}} = \frac{\text{POWER}}{\rho AV} = \frac{Le}{\rho V}$$

A useful normalized form  $Le''$  is

$$Le'' \equiv \frac{\tilde{Le}}{\frac{\epsilon_0 E_{bn}^2}{\rho_{gn}}} = \frac{Le'}{\frac{\rho_g}{\rho_{g0}} \mu}$$

Hence

$$Le'' = \left[ 1 - \left( \frac{R_a}{R} \right)^2 \right] \left[ 1 - \frac{\gamma-1}{2} \left( \frac{k_n E_{bn}}{C_0} \right)^2 \mu^2 \right]^{\frac{1}{\gamma-1}} \frac{\alpha}{\mu} (\mu - \alpha) \quad (66)$$

To determine the maximum, the same procedure as used for  $Le'$  is used.

The results are

$$\alpha = \frac{1}{3} \mu \quad (67)$$

$$\mu = \sqrt{\frac{2}{\gamma}} \frac{C_0}{k_n E_{bn}} \quad (68)$$

Eqs (67) and (68) yield the values of  $\mu$  and  $\alpha$  which give the maximum value of  $Le''$  (power per unit mass flow rate).

Eq. (68) can also easily be put in terms of the Mach number with the

Substitution of Eq. (61) into Eq. (60) gives

$$Le' = \left[ 1 - \left( \frac{R_a}{R} \right)^2 \right] \left[ 1 - \frac{\gamma-1}{2} \left( \frac{k_n E_{bn}}{C_0} \right)^2 \mu^2 \right]^{\frac{2}{\gamma-1}} \frac{4}{27} \mu^3$$

Taking the derivative with respect to  $\mu$  and setting the result equal to zero results in

$$\mu = \sqrt{\frac{6}{3\gamma+1}} \frac{C_0}{k_n E_{bn}} \quad (62)$$

Therefore, for the given rig, type of gas, and stagnation conditions, the values of  $\mu$  and  $\alpha$  which yield the maximum value of  $Le'$  (power per unit area of channel cross section) are determined from Eqs. (62) and (61) respectively. The maximum value of  $Le'$  can then be obtained from Eq. (60). The results for  $\mu, \alpha$  and  $Le'$  were independent of the function of  $f(\mu)$ , however, to determine the value of  $h/R$  from Eq. (59), the function of  $f(\mu)$  must, of course be known.

Since  $\mu = v/k_n E_{bn}$  Eq. (62) can be put in terms of the flow Mach number  $M$  and also  $M_*$  as follows:

$$M_* = \frac{v}{C_*} = \sqrt{\frac{6}{3\gamma+1}} \frac{C_0}{C_*}$$

$$\frac{C_0}{C_*} = \sqrt{\frac{\gamma+1}{2}}$$

$$\text{Therefore } M_* = \sqrt{\frac{3(\gamma+1)}{3\gamma+1}} \quad (63)$$

The equation relating  $M$  and  $M_*$  is

$$M^2 = \frac{\frac{2}{\gamma+1} M_*^2}{1 - \frac{\gamma-1}{\gamma+1} M_*^2} \quad (64)$$

result

$$M = \sqrt{2} = 1.414 \quad (69)$$

Hence, the maximum power per unit mass flow rate is achieved at a flow Mach number of 1.414 regardless of the type of gas or initial conditions.

If the value of  $\mu$  obtained from either Eq. (68) or (62) exceeds 3 then the value of  $\alpha$  given by Eq. (67) or Eq. (61) would exceed 1. In this case, breakdown would occur and the maximum could not be achieved. The physically realizable maximum would then occur on the  $\alpha = 1$  line. The value of  $\mu$  which yields a maximum in this case can be determined by substitution of  $\alpha = 1$  into either Eq. (60) or Eq. (66) and proceeding in the usual way.

The power densities discussed above were independent of the function  $f(\mu)$ ; however, the efficiency is dependent on the function  $f(\mu)$ . For the case of constant  $R_a/R$  and constant reservoir conditions, Eq. (54) can be put into the form

$$\eta = \frac{\alpha(\mu-\alpha) \left[ 1 - \frac{\gamma-1}{2} \left( \frac{k_n E_{bn}}{C_0} \right)^2 \mu^2 \right]^{\frac{1}{\gamma-1}}}{\mu \alpha \left[ 1 - \frac{\gamma-1}{2} \left( \frac{k_n E_{bn}}{C_0} \right)^2 \mu^2 \right]^{\frac{1}{\gamma-1}} + f \frac{k_n^2 \rho_{gn}^2}{2\epsilon_0 \rho_{g0}} \frac{R}{R_a} \frac{\mu^3}{f(\mu)}} \quad (70)$$

Inspection of Eq. (70) indicates that

if  $\alpha = 0$  then  $\eta = 0$

if  $\mu - \alpha = 0$  then  $\eta = 0$

if  $\mu = \mu_{\max}$  then  $\eta = 0$

if  $\mu$  and  $\alpha$  are in the interior of the triangle ( $\mu = \mu_{\max}$ ,  $\alpha = 0$   $\mu - \alpha = 0$ )  
then  $\eta > 0$

Hence, the efficiency has a maximum within the triangle (or at the origin for certain forms of the function  $f(\mu)$  which may cause  $\eta$  to be multivalued at the origin). The partial of  $\eta$  with respect to  $\alpha$  is

$$\frac{\partial \eta}{\partial \alpha} = \frac{\eta}{\alpha} - \frac{\eta}{\mu - \alpha} - \frac{\mu \eta^2}{\alpha(\mu - \alpha)} \quad (71)$$

Setting Eq. (71) equal to zero results in

$$\alpha = \frac{\mu}{2} (1 - \eta) \quad (72)$$

Substitution of Eq. (70) into Eq. (72) results in

$$\alpha = F(\mu) \left[ \sqrt{1 + \frac{\mu}{F(\mu)}} - 1 \right] \quad (73)$$

where

$$F(\mu) \equiv \frac{2f}{\sigma_n} \frac{\rho_{gn}}{\rho_{g0}} \frac{R}{R_a} \frac{\mu^2}{f(\mu) \left[ 1 - \frac{\gamma-1}{2} \left( \frac{k_n E_{bn}}{C_0} \right)^2 \mu^2 \right]^{\frac{1}{\gamma-1}}} \quad (74)$$

For various assumed values of  $f(\mu)$  the maximum value of efficiency can be determined numerically on a computer. For assumed values of  $\mu$  between 0 and  $\mu_{\max}$ ,  $F(\mu)$  can be determined from Eq. (74),  $\alpha$  from Eq. (73), and  $\eta$  from Eq. (70). An iterative computational scheme can easily be devised to determine the maximum value of  $\eta$  to a reasonable degree of approximation.

### Discussion and Results

A computer program was written to obtain quantitative results

from the theory developed in this section. In order to obtain quantitative results for the efficiency and length to diameter ratio, it was necessary to assume a form of  $f(\mu)$ . The function chosen for the examples is

$$f(\mu) = \frac{0.264\mu}{1.441+\mu} \quad (75)$$

This function approximates the data of reference 7.

Air was chosen as the working substance and calculations made for ions ( $k_n = 2.2 \times 10^{-4} \text{ m}^2/\text{volt-sec}$ ) and colloids (assumed  $k_n = 1 \times 10^{-6} \text{ m}^2/\text{volt-sec}$ ). The data for ions at gas density ratios of 1, 20, and 32.8 are given in figures 7, 8, and 9 respectively.

Curves of constant power density  $Le'$ , efficiency  $\eta$ , and length to radius ratio  $h/R$ , are presented as functions of normalized velocity  $\mu$  and applied field strength  $\alpha$ . The normalized power density and  $h/R$  ratio are independent of the gas density ratio. The efficiency, however, is not independent of the gas density ratio and therefore requires a separate chart for each density. Although the normalized power flux is independent of the gas density the normalizing factor ( $\epsilon_0 k_n E_{bn}^3 (\rho_{g0}/\rho_{gn})^2$ ) is not, and therefore, the actual power per unit area increases as the square of the gas density ratio.

In the case of ions (figures 7, 8, and 9) the maximum value of  $\mu$  is 1.15 (due to the large value of  $k_n E_{bn} = 660 \text{ m/sec}$ ) and hence nearly the entire triangular region ( $\alpha = 0, \mu = \mu_{\text{max}}, \alpha = \mu$ ) is usable. In the case of colloids (figures 10, 11, and 12) the maximum value of  $\mu$  is 253 ( $k_n E_{bn} = 3 \text{ m/sec}$ ) and only a narrow strip of the triangular region is usable since  $\alpha$  must be less than 1. Since only the usable portion of the  $\mu, \alpha$  plane

is shown in the figures, the curves for the colloids appear entirely different than the curves for the ions.

The peak value of  $Le'$  is clearly shown in the case of ions and occurs on the interior of the region but is outside the region of interest in the case of colloids (i.e., the usable peak value occurs on the boundary  $\alpha = 1$  in the case of colloids).

The peak value of power density from Figure 9 ( $\rho_{go}/\rho_{gn} = 32.8$  with ions) is  $36 \text{ w/cm}^2$  at an efficiency of 0.2%. The peak value of power density from Figure 12 ( $\rho_{go}/\rho_{gn} = 32.8$  with colloids) is  $4100 \text{ w/cm}^2$  at 28% efficiency. From Figure 10 ( $\rho_{go}/\rho_{gn} = 1.0$  with colloids) the maximum power is  $3.8 \text{ w/cm}^2$  at 1% efficiency. Clearly operation with colloids at high stagnation pressure is required for reasonable efficiencies and high power.

One of the chief deficiencies in the approximate solution is the assumption that the axial field is constant. This means that the results near the  $\mu = \alpha$  boundary are poor. This is of little consequence for the colloid case and should not be too serious at the interior of the triangular region for ions. However, the upper limit of  $\alpha$  equal to 1 is unrealistic even for colloids since the breakdown field strength depends on the radial field as well as the axial; a more realistic limit on  $\alpha$  would be 1/2. In order to determine the region of validity of the approximate theory, a computer program has been written to solve the partial differential equations numerically for the axisymmetric case.

#### Computer Program

Equations (15) and (17) along with the boundary conditions,



Equation (18), have been programmed for a high speed digital computer (IBM 7094). The equations were normalized and put into the following form:

$$(RU_R)_R + (RU_Z)_Z = -RC\rho \quad (76)$$

$$dR = [ -U_R/(A-U_Z) ] dZ \quad (77)$$

$$-d\rho/C\rho^2 = dZ/(A-U_Z) \quad (78)$$

The boundary conditions for the above equations which are compatible for the assumed model (see Figure 1) are:

$$\begin{aligned} U(R,0) &= 0 \\ U(R,1) &= 1 \\ U(\infty,Z) &= Z & 0 < Z < 1 & \quad (79) \\ \rho(R,0) &= 1 & R < RI \\ \rho(R,0) &= 0 & R > RI \end{aligned}$$

In the above equations,

$$U = \phi/V; A = hv/Vk = \mu/\alpha; C = h^2 \rho_{e0}/V\epsilon = 2f(\mu)/\alpha RI$$

$$Z = z/h; R = r/h; \rho = \rho_e/\rho_{e0}; RI = r_a/h$$

$$U_R = \partial U/\partial R; \rho_Z = \partial \rho/\partial Z; \text{etc.}$$

A brief outline of the method of solution is:

- a) Values of  $RI$ ,  $\mu$  and  $\alpha$  are inputs to the program,  $C$  is calculated using Equation (75) for  $f(\mu)$ .
- b) The initial charge density distribution is calculated from the approximate solution.
- c) The finite difference form of Equation (76) is solved by the point successive over relaxation iterative method.

d) The potential obtained in step (c) is used to numerically integrate Equation (77) to obtain various stream lines.

e) The results from steps (c) and (d) are used to numerically integrate Equation (78) to obtain charge density variations along the stream lines.

f) Using the new density distribution, steps (c) to (e) can be repeated until the convergence criteria are satisfied (e.g., the maximum change in the density and the stream line is less than  $10^{-6}$ ). Some results of this program are presented in Figures 13 to 19.

Figures 14, 15, and 16 present data for colloids at three different values of applied field (i.e.,  $\alpha$ ) and the same value of gas velocity ( $\mu$ ) and initial radius (RI). The value of  $\mu$  was chosen to give approximately the maximum power per unit area for the colloid case. Using Figure 11, this value of  $\mu$  is seen to be 103. Since this value of  $\mu$  corresponds to a value of  $h/R_{\text{final}}$  of about 7.5 and the figure is calculated for a value of  $R_{\text{initial}}/R_{\text{final}}$  of 0.98 a value of  $RI = R_{\text{initial}}/h$  of  $0.98/7.5 = 0.1307$  was assumed for the computer runs. Figure 14 presents the data for colloids for  $\alpha$  of 0.2. It contains constant potential lines ( $U = \phi/V$ ) and lines of constant field magnitude ( $|\bar{E}| = E/E_{\text{appl}}$ ). Also shown is the outer radius of the charge cloud. Figures 15 and 16 contain the same type of data for  $\alpha=0.5$  and  $\alpha=0.7$  respectively. Each of these three figures is to scale geometrically. Since the total charge in the channel is approximately constant for a given  $\mu$  and RI, the distortion of the curves should be greatest for the lower value of  $\alpha$ , which implies a lower applied field and hence a greater relative effect of the space

charge.

Figure 13 is the result of a calculation for the case of ions. The values of  $\alpha$ ,  $\mu$ , and RI for Figure 13 are chosen to correspond to maximum power output for the ion case (see Figure 8), the values used were  $\alpha=0.1843$ ,  $\mu=0.553$  and  $RI=0.026315$ . Additional data were obtained for the same value of RI but at a value of  $\alpha=0.4$  and  $\mu=0.56$ .

### 1. Example Calculations

To present the output of the computer program in a more concrete form and to compare the results of the approximate theory, a specific example will be calculated.

#### a. Colloids

Assume that the working gas is air in a channel 10 cm long ( $h = 10$  cm) and that the gas density in the working channel is 20 atmospheres ( $\rho_g/\rho_{gn} = 20$ ). For the colloid case assume the mobility at standard conditions to be  $10^{-6} \text{ m}^2/\text{V-sec}$ . For these assumed conditions we have:

$$\begin{aligned} E_{bn} &= 3 \times 10^6 \text{ V/m}, k_n = 10^{-6} \text{ m}^2/\text{V-sec}, k_n E_{bn} = 3 \text{ m/sec}, \\ \epsilon_0 &= 8.854 \times 10^{-12} \text{ coul}/(\text{V-m}), \epsilon_0 k_n E_{bn}^3 = 23.9 \times 10^{-6} \text{ KW/cm}^2, \\ h &= 10 \text{ cm}, \rho_g/\rho_{gn} = 20, \mu = 103, RI = 0.13077. \end{aligned}$$

Therefore,

$$\begin{aligned} E_b &= 6 \times 10^7 \text{ V/m}, k = 5 \times 10^{-8} \text{ m}^2/(\text{V-sec}), \epsilon_0 k E_b^3 = 9.56 \times 10^{-3} \\ &\text{KW/cm}^2, r_i = 1.3077 \text{ cm}, v_{el} = 309 \text{ m/sec} \end{aligned}$$

Using the computer output and the approximate solution we can obtain the data of Table II at the various values of  $\alpha$ .

The normalized power given in the fifth row of Table II can be converted to  $Le'$  of Figure 11 by multiplying by the factor

$$\left[ 1 - \frac{\gamma-1}{2} \left( \frac{k_n E_{bn}}{C_0} \right)^2 \mu^2 \right]^{\frac{2}{\gamma-1}}$$

which is 0.406 for the conditions assumed to obtain the data of Figure 11 (e.g., at  $\alpha=0.5$   $Le' = 196.4 \times 0.406 = 80$ ).

It can be concluded that the approximate solution gives good agreement with the computer program for the case of colloids. Of course, since the approximate solution assumed a constant axial field, it could not predict the value of  $E_{max}$  which occurs in the channel. The data of Table II indicates that the channel will break down at a value of  $\alpha$  slightly larger than 0.5 at this value of  $\mu$ . The shaded region of Figure 16 exceeds the break down field strength.

b. Ions

For the case of ions in air at a density of 20 atmospheres and a 10 cm channel we have:

$$E_{bn} = 3 \times 10^6 \text{ V/m}, k_n = 2.2 \times 10^{-4} \text{ m}^2/\text{V-sec}, k_n E_{bn} = 660 \text{ m/sec}$$

$$\epsilon_0 = 8.854 \times 10^{-12} \text{ coul}/(\text{V-m}), \epsilon_0 k_n E_{bn}^3 = 52.5 \times 10^{-4} \text{ KW/cm}^2,$$

$$h = 10 \text{ cm}, \rho_g/\rho_{gn} = 20, \mu = 0.553, RI = 0.026315.$$

Therefore,

$$E_b = 6 \times 10^7 \text{ V/m}, k = 1.1 \times 10^{-5} \text{ m}^2(\text{V-sec}), \epsilon_0 k E_b^3 = 2.1 \text{ KW/cm}^2,$$

$$r_i = 0.26315, v_{el} = 365 \text{ m/sec}.$$

Using the computer output and the approximate solution we can obtain the

data of Table III at the two values of  $\alpha$ .

As expected the approximate solution in the ion case is not nearly as good as it was for the colloid case. However, the power per unit area estimate is fair with the greatest error being in the estimate of the final radius and consequently in the total power.

It is significant to note that the power per unit area did decrease as predicted at the higher value of  $\alpha$ . More data would be required to determine if the maximum occurs at  $\mu = 0.553$  and  $\alpha = 0.1843$ .

## 2. Effects of Surface Charge and Applied Voltage

Figure 17 shows the effects of impressing a linear voltage gradient at a radius of 0.2 for the case of colloids at  $\alpha = 0.2$ ,  $\mu = 103$ . Figure 18 shows the effects of assuming that a "surface charge" is located at a radius of 0.2. The total charge resulting from this surface charge was assumed to be equal to the total charge within the charge cloud. The "surface charge" could be the result of charged particles that have drifted into the boundary layer and then slowly drift toward the ground plate.

The distortion of the constant potential lines is reduced by the linear voltage gradient and it is increased by the "surface charge". Figure 19 is a comparison of the center line potential for the three cases; "surface charge", linear voltage, and charge cloud only. All the cases were for  $\alpha = 0.2$ ,  $\mu = 103$  and  $RI = 0.13$ . Since the maximum field strength in the channel occurs on the center line at  $Z = 0$ , it is clear from Figure 19 that the surface charge effects would induce breakdown at lower values of applied voltage and that the linear voltage gradient

would permit operation at higher values of applied voltage (i.e.,  $\alpha$ ).

### 3. Program for More Complex Electrode Geometry

The results of the program developed for the simplified geometry above indicated that the approximate solution yielded reasonable estimates of power for colloids and gives therefore reasonable estimates of generalized performance such as indicated by Figure 11. However, in order to reduce space charge distortion of the field and thereby delay breakdown in the channel, a program was required that could account for more complex geometry. In Reference 8 a program was presented for the design of ion engines. The method of solution used for Poisson's equation had been developed over a number of years to a high degree of sophistication and therefore it was decided to use this program with appropriate modifications for application to the EFD generator. In the course of the earlier study it was observed that in the case of colloids the effects of field distortion on the shape of the colloid cloud was negligible. Since a practical EFD generator would most probably use colloids, it is more reasonable to determine the shape of the colloid cloud from fluid flow considerations such as turbulent jet mixing.

Results of this program are shown in Figures 20, 21, and 22. Figure 20 gives the results for no space charge, i.e., a solution of Laplace's equation. Figure 21 shows the results for the same geometry but with space charge included. To obtain these results an initial charge density at the nozzle exit of  $0.0523 \text{ coul/m}^3$  was assumed. A turbulent spreading angle of  $\cot^{-1} 12$  was assumed for high gas density, high Reynolds number flow.

From Figure 21 we note that the 500,000 volt potential extends under the ground plate and that the peak voltage is nearly twice the value of the collector voltage. Figure 22 shows the potential on the center line and  $R = .4$  and  $R = 1.0$ . The high field strengths resulting from the space charge distribution is quite apparent. The program will be used to study various electrode geometries in order to determine those geometries which tend to minimize the maximum value of the electric field.

REFERENCES

1. Performance Potentialities of Direct Energy Conversion Processes Between Electrostatic and Fluid Dynamic Energy; Maurice O. Lawson, Hans von Ohain, and Frank Wattendorf, ARL 178, December 1961
2. Potentialities of Direct Electrofluid Dynamic Energy Conversion Processes for Power Generation; Hans von Ohain, and Frank Wattendorf ARL 64-73, October 1964
3. "Electrofluid Dynamic Energy Conversion Processes for Power Generation", Siegfried Hasinger, Michael Hawes, Maurice O. Lawson, Hans J.P. von Ohain, and Frank L. Wattendorf. Paper presented at Sixth AGARD Combustion and Propulsion Colloquium, Cannes, 16-20 March 64.
4. Performance Characteristics of Electrofluid Dynamic Energy Conversion Processes Employing Viscous Coupling, Maurice O. Lawson, ARL 64-74, October 1964.
5. Performance Characteristics of Electro Ballistic Generators Siegfried Hasinger, ARL 64-75, October 1964.
6. Experimental Techniques in Electrofluid Dynamic Energy Conversion Research, Michael Hawes, ARL 64-77, October 1964
7. Ion Generation by Corona Discharge for Electrofluid Dynamic Energy Conversion Processes, Maurice O. Lawson, ARL 64-76, October 1964
8. A Space-Charge-Flow Computer Program, Carl D. Bogart and Edward Richley, NASA TN D-3394, April 1966.



TABLE I Gas Data Used to Obtain Efficiencies of Fig. 1.

GAS	$k_n$ $m^2/V\text{-sec}$	$E_{bn}$ $V/m$	$k_n E_{bn}$ $m/sec$	$p_n$ $Kgm/m^3$	$\sigma = \frac{4\epsilon}{\rho_n k_n^2}$
AIR	$2.2 \times 10^{-4}$	$3.0 \times 10^6$	660	1.22	$6.03 \times 10^{-4}$
Sat. Steam Ions	$8.2 \times 10^{-5}$	$3.6 \times 10^6$	295	0.598	$8.86 \times 10^{-3}$
Sat. Steam Colloids	$1.0 \times 10^{-6}$	$3.6 \times 10^6$	3.6	0.598	59.6
CHCL <sub>3</sub>	$1.9 \times 10^{-5}$	$1.26 \times 10^7$	239	5.05	$1.95 \times 10^{-2}$
CCL <sub>4</sub>	$3.7 \times 10^{-5}$	$1.92 \times 10^7$	710	6.51	$4.00 \times 10^{-3}$

TABLE II

$\alpha =$	.2		.5		.7	
	Computer Output	Approximate Solution	Computer Output	Approximate Solution	Computer Output	Approximate Solution
$V = h\alpha E_b$	$1.2 \times 10^6$ Volts	$1.2 \times 10^6$	$3 \times 10^6$	$3.10^6$	$4.2 \times 10^6$	$4.2 \times 10^6$
$E_{app.} = \alpha E_b$	$1.2 \times 10^7$ V/m	$1.2 \times 10^7$	$3 \times 10^7$	$3 \times 10^7$	$4.2 \times 10^7$	$4.2 \times 10^7$
$E_{max} = \alpha  \bar{E} _{max} E_b$	$4.156 \times 10^7$ V/m	$1.2 \times 10^7$	$5.95 \times 10^7$	$3 \times 10^7$	$7.16 \times 10^7$	$4.2 \times 10^7$
$r_f = RFh$	1.3271348 cm	1.3327694	1.3271891	1.3328592	1.3272360	1.3329041
$Le/\epsilon_0 k E_b^3$	79.15	78.82	197.3	196.4	275.6	274.5
Le	.7567 KW/cm <sup>2</sup>	.7535	1.886	1.878	2.635	2.624
Total Power	4.187 KW	4.205	10.44	10.48	14.58	14.65

TABLE III

$\alpha =$	.1843		.4	
	Computer Output	Approximate Solution	Computer Output	Approximate Solution
$V = h\alpha E_b$	$1.11 \times 10^6$ V	$1.11 \times 10^6$	$2.4 \times 10^6$	$2.4 \times 10^6$
$E_{app} = \alpha E_b$	$1.11 \times 10^7$ V/m	$1.11 \times 10^7$	$2.4 \times 10^7$	$2.4 \times 10^6$
$E_{max} = \alpha  \bar{E} _{max} E_b$	$1.75 \times 10^7$ V/m	$1.11 \times 10^7$	$2.88 \times 10^7$	$2.4 \times 10^7$
$r_f = RFh$	0.8574 cm	1.056	1.040	1.581
$Le/\epsilon_0 k E_b^3$	0.02510	0.02350	0.01085	.009956
Le	0.0536 KW/cm <sup>2</sup>	0.0494	0.0228	0.0210
Total Power	0.122 KW	0.173	0.0776	0.166

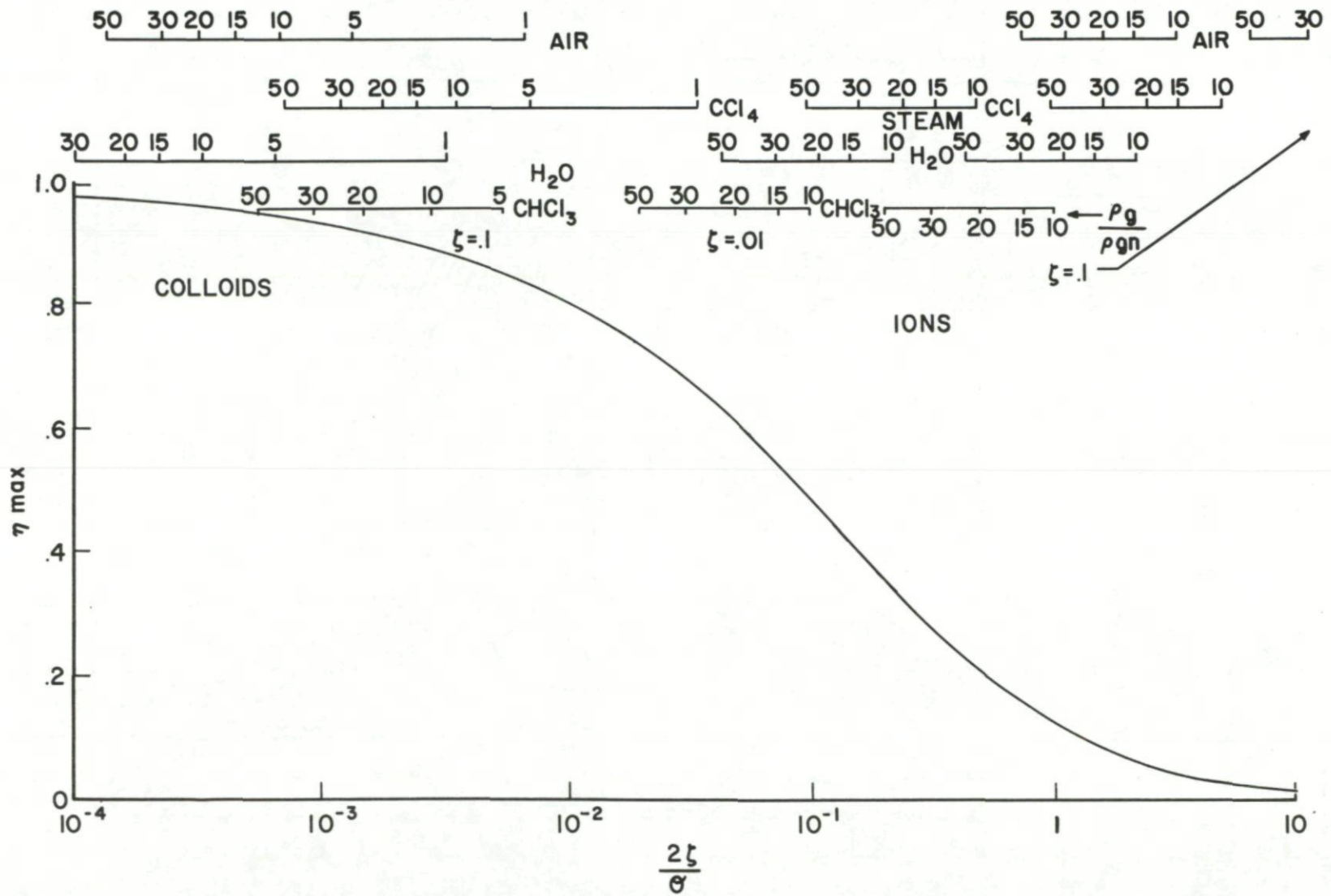


Figure 2. Maximum Theoretical Stage Efficiency vs  $2 \zeta/\theta$

RIG DATA	GAS DATA	DIMENSIONLESS RATIOS AT STD. CONDITIONS	SPECIFIC CONDITIONS
$h = 0.0254 \text{ m}$ $R = 0.0159 \text{ m}$ $f = 0.0313$ $\rho_0 = 0.16 \text{ (A-s)/m}^3$	<b>AIR</b> $\rho_n = 1.22 \text{ Kg/m}^3$ $k_n(-) = 2.2 \times 10^{-4} \text{ (m/s)/(v/m)}$ $E_{bn} = 3 \times 10^6 \text{ v/m}$ $k_n E_{bn} = 660 \text{ m/s} = 2165 \text{ fps}$ $F_n = \epsilon_0 k_n E_{bn}^3 = 5.29 \text{ WATTS/cm}^2$	$\sigma_n = \frac{4\epsilon_0}{\rho_n k_n^2} = 6.03 \times 10^{-4}$ $K_{In} = \frac{\rho_0 h}{\epsilon_0 E_{bn}} = 152$ $\zeta = 2f \frac{h}{R} = 0.100$ $C = \frac{2\zeta}{\sigma K_I} = 2.18$ $CK_{IN} = \frac{2\zeta}{\sigma_n} = 332$	$\frac{\rho_g}{\rho_n} = 17.0$ $K_I = 8.95$ $CK_I = 19.5$ $\eta_{max} = 0.0075$
$\mu = u/k_n E_{bn}$ ; $\alpha = E_z/E_b$ ; $\bar{L}e = Le/F_n$			

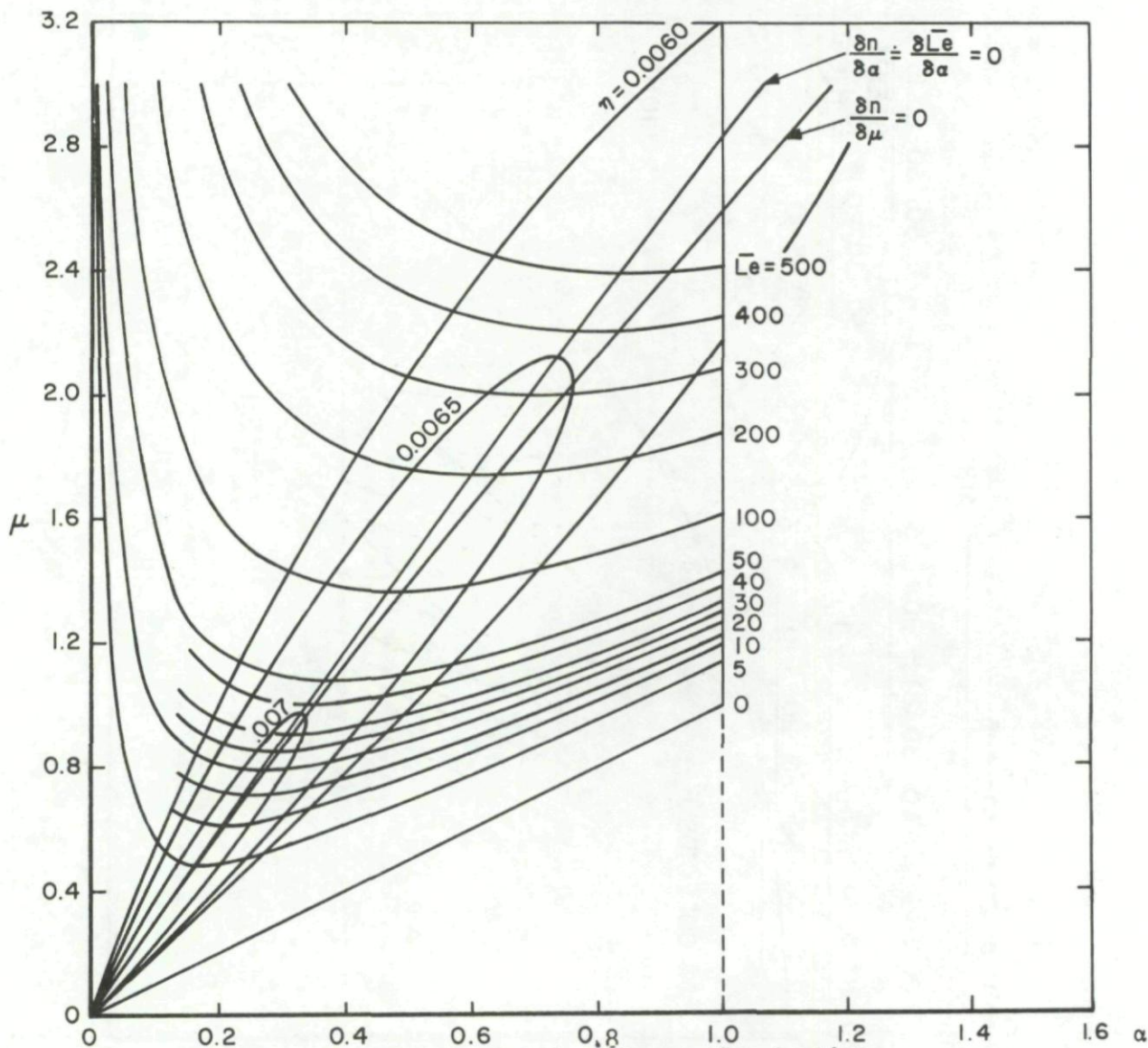


Figure 3. Performance for Constant Conversion Section Density: AIR IONS.

RIG DATA	GAS DATA	DIMENSIONLESS RATIOS AT STD. CONDITIONS	SPECIFIC CONDITIONS
$h = 0.0254 \text{ m}$ $R = 0.0159 \text{ m}$ $f = 0.0313$ $\rho_0 = 0.16 \text{ (A-s)/m}^3$	$\text{CCl}_4$ $\rho_n = 6.50 \text{ Kg/m}^3$ $k_n = 3.7 \times 10^{-5} \text{ (m/s)/(v/m)}$ $E_{bn} = 1.92 \times 10^7 \text{ v/m}$ $k_n E_{bn} = 710 \text{ m/s}$ $F_n = \epsilon_0 k_n E_{bn}^3 = 233 \text{ WATTS/cm}^2$	$\sigma_n = \frac{4\epsilon_0}{\rho_n k_n^2} = 3.99 \times 10^{-3}$ $K_{in} = \frac{\rho_0 h}{\epsilon_0 E_{bn}} = 23.78$ $\zeta = 2f \frac{h}{R} = 0.100$ $C = \frac{2\zeta}{\sigma K_1} = 2.10$ $CK_{in} = \frac{2\zeta}{\sigma_n} = 50.0$	$\frac{\rho_g}{\rho_n} = 17.0$ $K_1 = 1.39$ $CK_1 = 2.94$ $\eta_{max} = 0.046$

$\mu = u/k_n E_{bn}$ ;  $\alpha = E_z/E_b$ ;  $\bar{L}e = L_e/F_n$

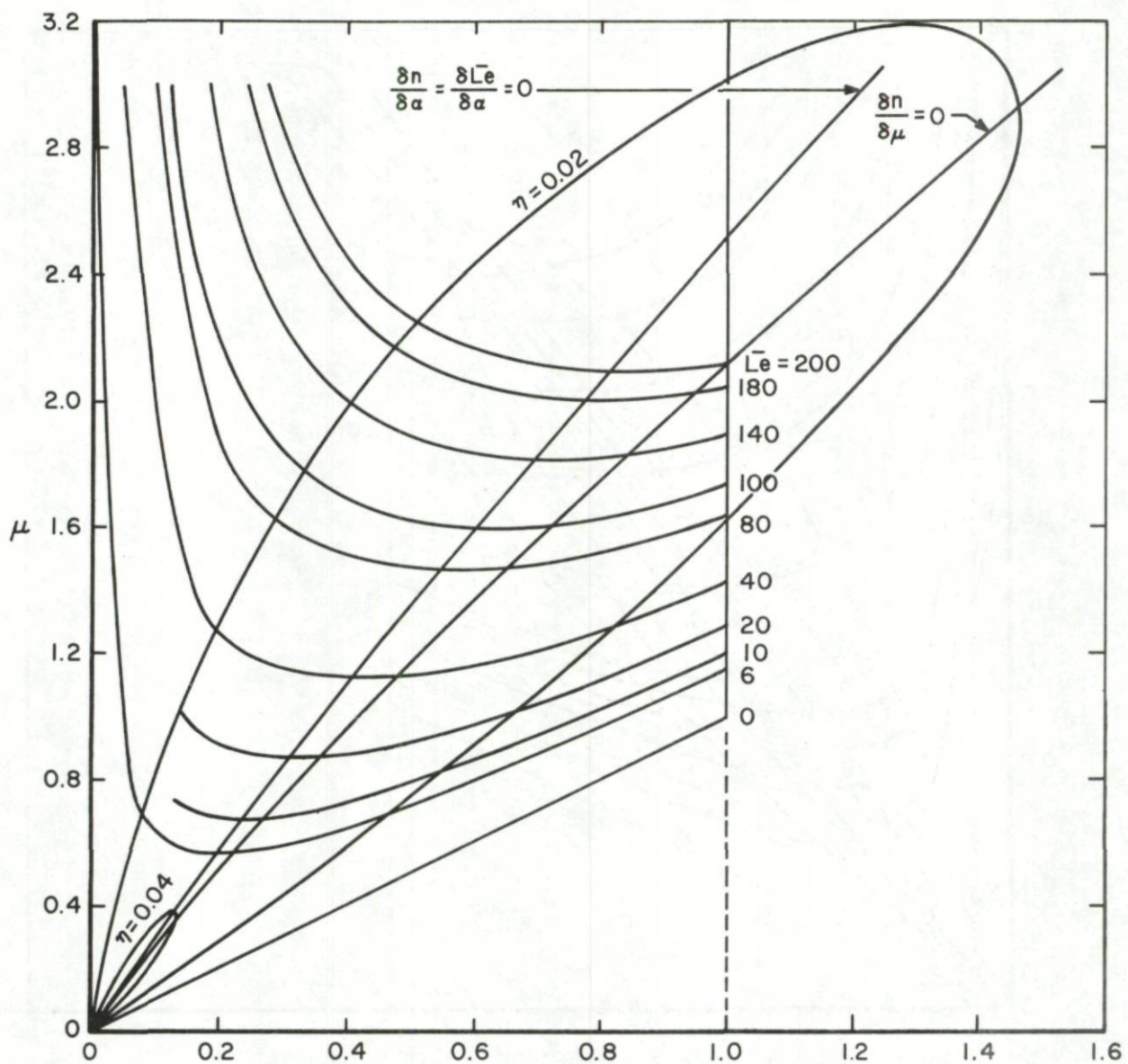


Figure 4. Performance for Constant  $\alpha$  Conversion Section Density:  $\text{CCl}_4$  IONS.

RIG DATA	GAS DATA	DIMENSIONLESS RATIOS AT STD. CONDITIONS	SPECIFIC CONDITIONS
$h=0.0254\text{ m}$ $R=0.0159\text{ m}$ $f=0.0313$ $\rho_0=0.16\text{ (A-s)/m}^3$	<u>H<sub>2</sub>O SAT. STEAM</u> $\rho_n = 0.59\text{ Kg/m}^3$ $k_n = 8.2 \times 10^{-5}\text{ (m/s)/(v/m)}$ $E_{bn} = 3.6 \times 10^6\text{ v/m}$ $k_n E_{bn} = 295\text{ m/s}$ $F_n = \epsilon_0 k_n E_{bn}^3 = 3.40\text{ WATTS/cm}^2$	$\sigma_n = \frac{4\epsilon_0}{\rho_n k_n^2} = 8.85 \times 10^{-3}$ $K_{in} = \frac{\rho_0 h}{\epsilon_0 E_{bn}} = 127$ $\zeta = 2f \frac{h}{R} = 0.100$ $C = \frac{2\zeta}{\sigma K_1} = 0.178$ $CK_{IN} = \frac{2\zeta}{\sigma} = 22.5$	$\frac{\rho_g}{\rho_n} = 17.0$ $K_1 = 7.46$ $CK_1 = 1.32$ $\eta_{max} = 0.095$
$\mu = u/k_n E_{bn}$ ; $\alpha = E_z/E_b$ ; $\bar{L}e = Le/F_n$			

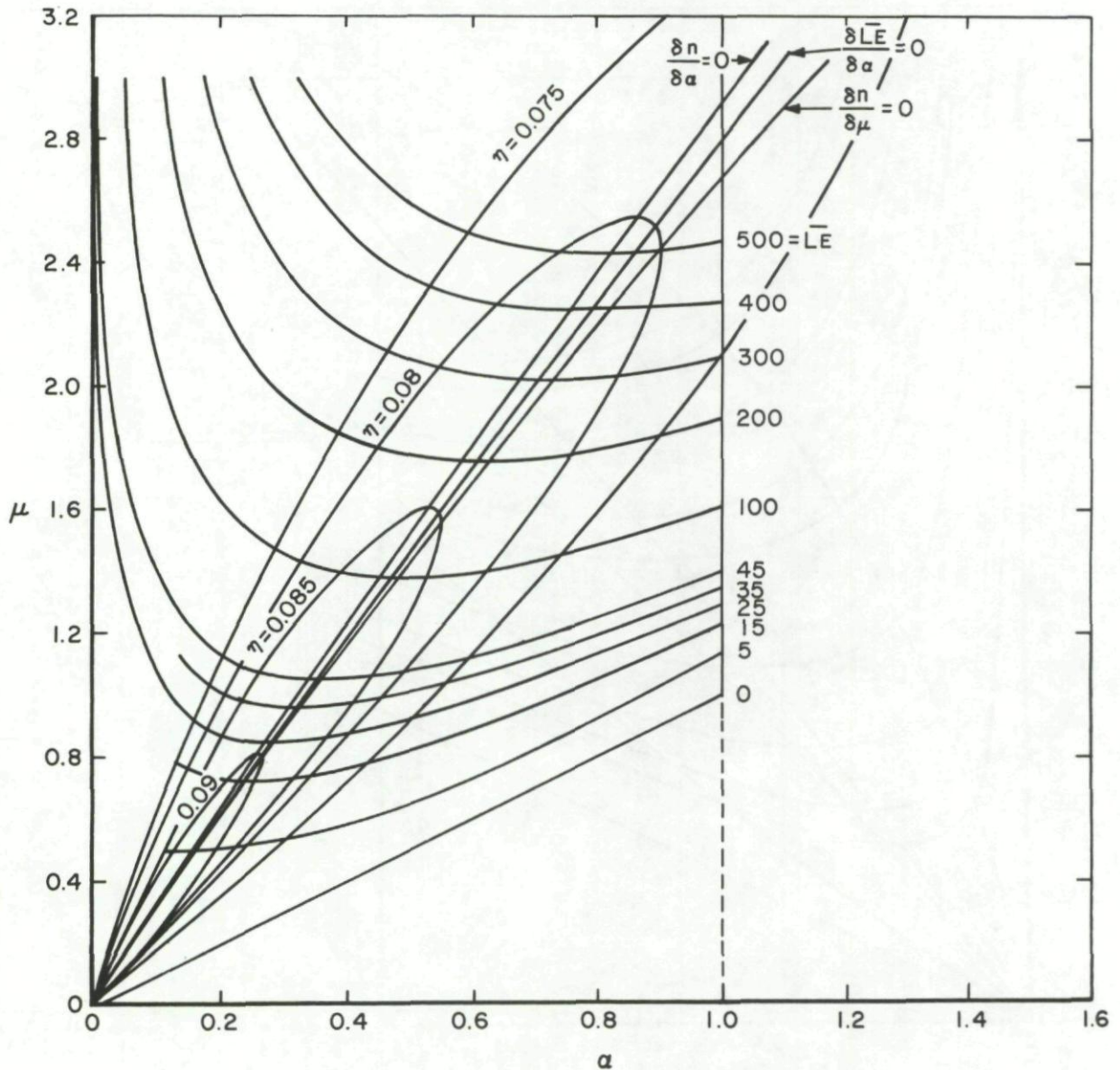


Figure 5. Performance for Constant Conversion  
 Section Density: Steam Ions

RIG DATA	GAS DATA	DIMENSIONLESS RATIOS AT STD. CONDITIONS	SPECIFIC CONDITIONS
$h=0.0254\text{ m}$ $R=0.0159\text{ m}$ $f=0.0313$ $\rho_0=0.16\text{ (A-s)/m}^3$	$\text{CHCl}_3$ $\rho_n=5.05\text{ Kg/m}^3$ $k_n=1.9\times 10^{-5}\text{ (m/s)/(v/m)}$ $E_{bn}=1.26\times 10^7\text{ v/m}$ $k_n E_{bn}=239\text{ m/s}$ $F_n=\epsilon_0 k_n E_{bn}^3=33.8\text{ WATTS/cm}^2$	$\sigma_n=\frac{4\epsilon_0}{\rho_n k_n^2}=1.95\times 10^{-2}$ $K_{In}=\frac{\rho_0 h}{\epsilon_0 E_{bn}}=36.2$ $\zeta=2f\frac{h}{R}=0.100$ $C=\frac{2\zeta}{\sigma K_I}=0.28$ $CK_{IN}=\frac{2\zeta}{\sigma_n}=10.2$	$\frac{\rho_g}{\rho_n}=17.0$ $K_I=2.13$ $CK_I=0.602$ $\eta_{\max}=0.181$

$$\mu = u/k_n E_{bn}; \quad \alpha = E_z/E_b; \quad \bar{L}e = L_e/F_n$$

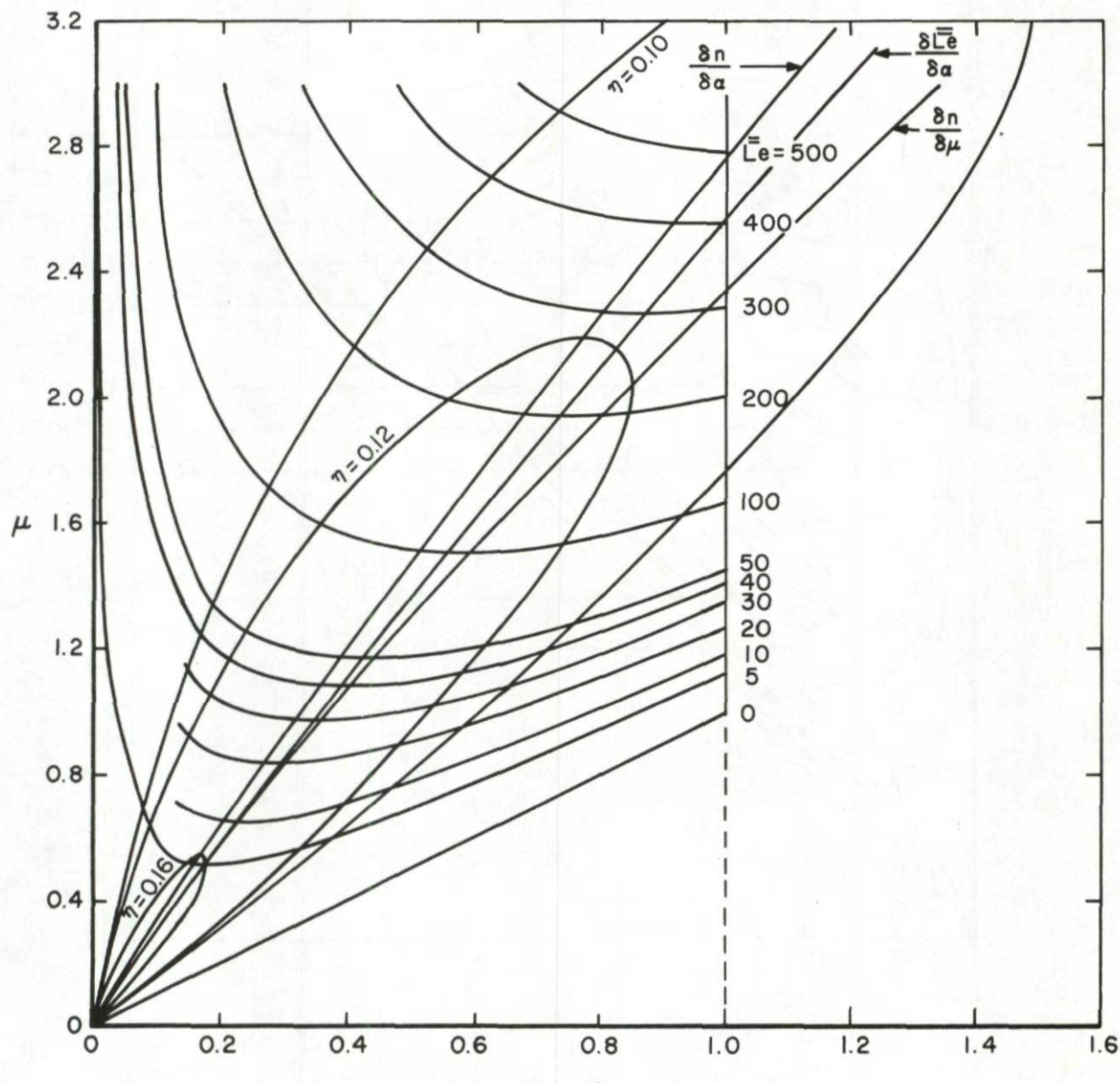


Figure 6. Performance for Constant Conversion

Section Density:  $\text{CHCl}_3$  Ions

AIR  $E_{bn} = 3 \times 10^6 \text{ v/m}$ ;  $k_n = 2.2 \times 10^{-4} \text{ m}^2/\text{v-s}$ ;  $C_0 = 340 \text{ m/s}$ ;  $\gamma = 1.4$

$$f(\mu) = \frac{.264 \mu}{1.441 + \mu}$$

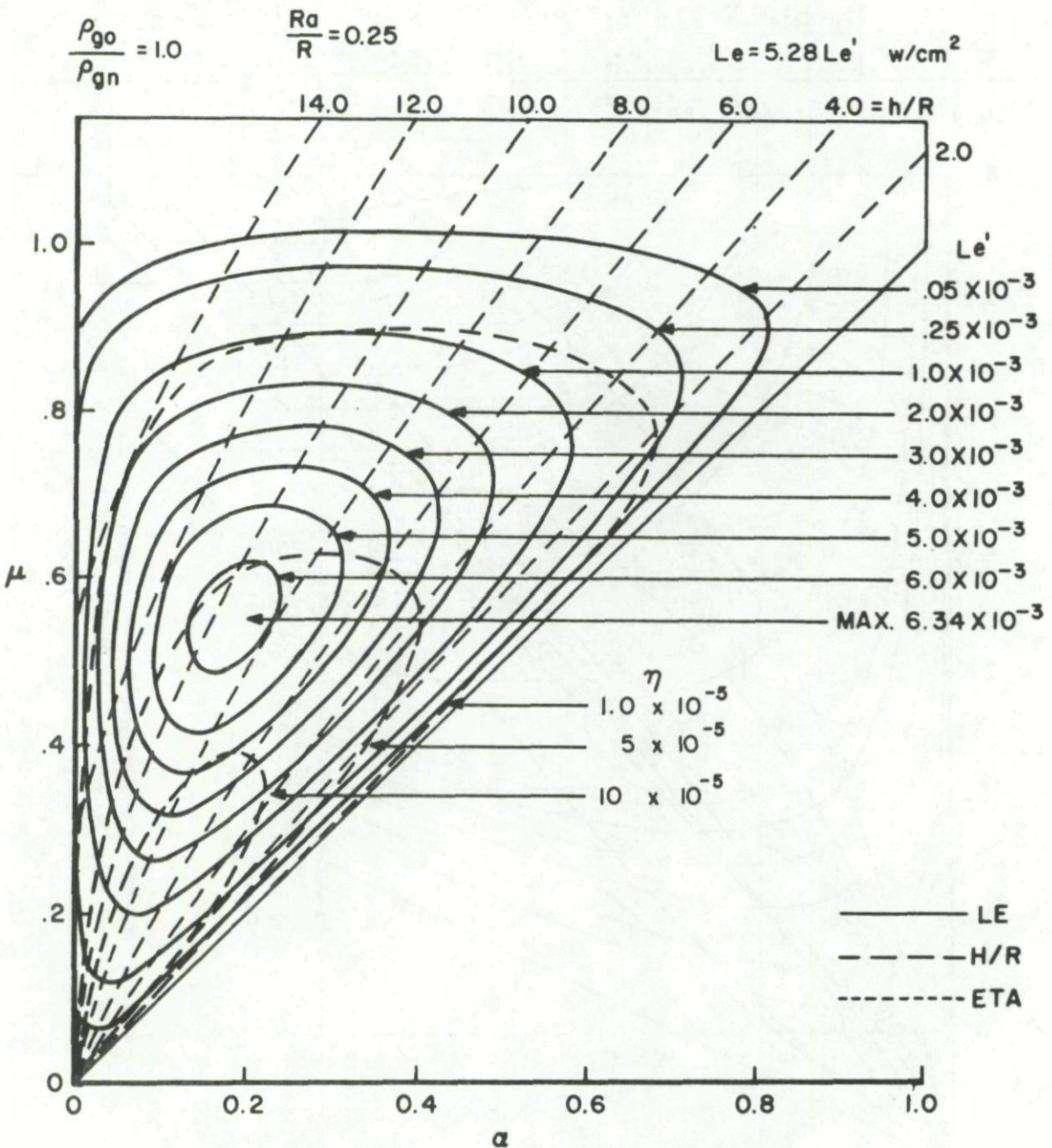


Figure 7. Performance for Constant Stagnation

Conditions: Air Ions,  $\rho_{go}/\rho_{gn} = 1.0$



AIR  $E_{bn} = 3 \times 10^6$  v/m;  $k_n = 2.2 \times 10^{-4}$  m<sup>2</sup>/v-s;  $C_0 = 340$  m/s;  $\gamma = 1.4$

$$f(\mu) = \frac{.264\mu}{1.441 + \mu}$$

$$\frac{\rho_{go}}{\rho_{gn}} = 20$$

$$\frac{Ra}{R} = 0.25$$

$$Le = 2115 Le' \sim w/cm^2$$

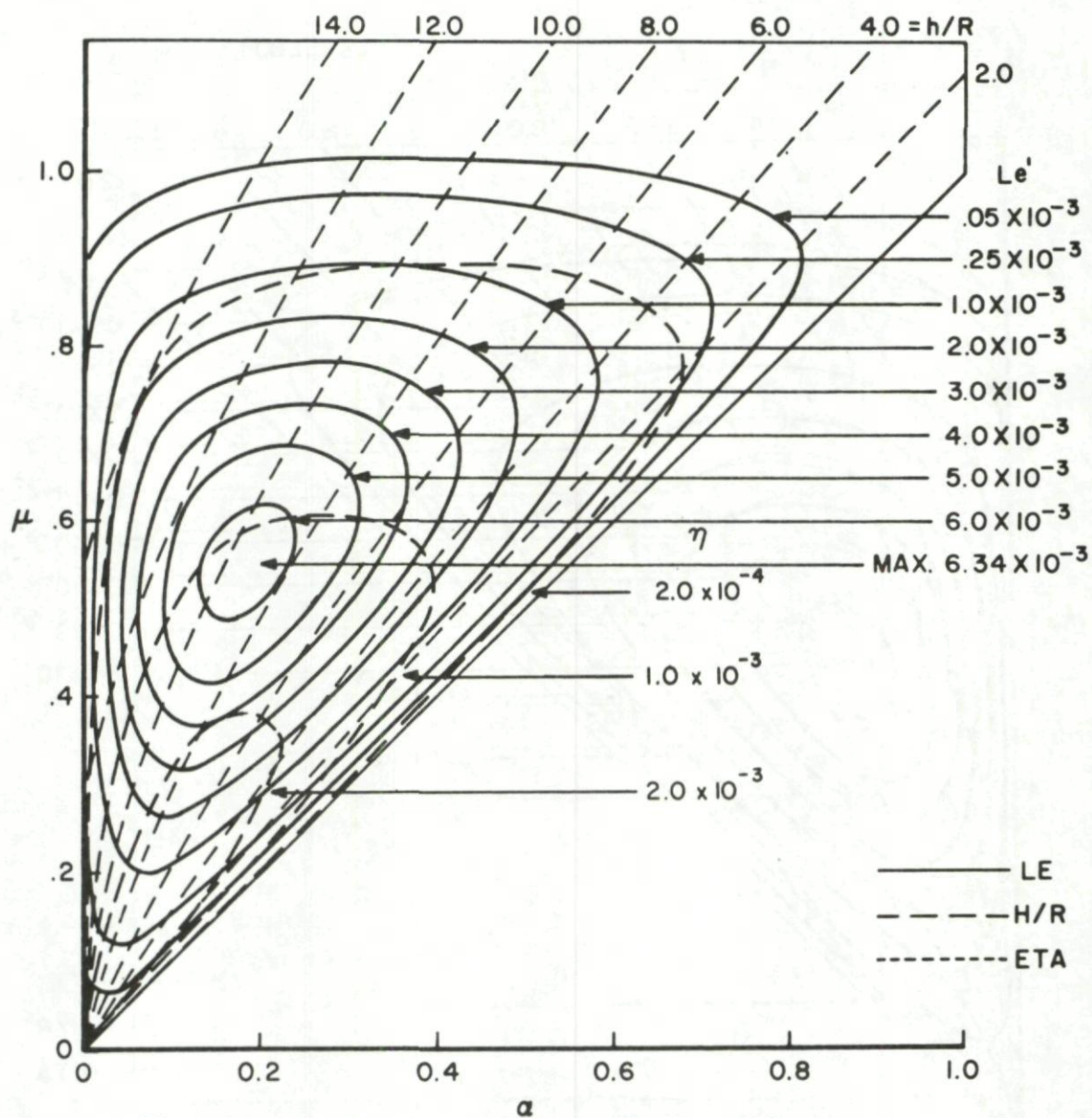


Figure 8. Performance for Constant Stagnation

Conditions: Air Ions,  $\rho_{go}/\rho_{gn} = 20$

**AIR**  $E_{bn} = 3 \times 10^6$  v/m;  $k_n = 2.2 \times 10^{-4}$  m<sup>2</sup>/v-s;  $C_0 = 340$  m/s;  $\gamma = 1.4$

$$f(\mu) = \frac{.264 \mu}{1.441 + \mu}$$

$$\frac{\rho_{go}}{\rho_{gn}} = 32.8$$

$$\frac{Ra}{R} = 0.25$$

$$Le = 5680 Le' \quad w/cm^2$$

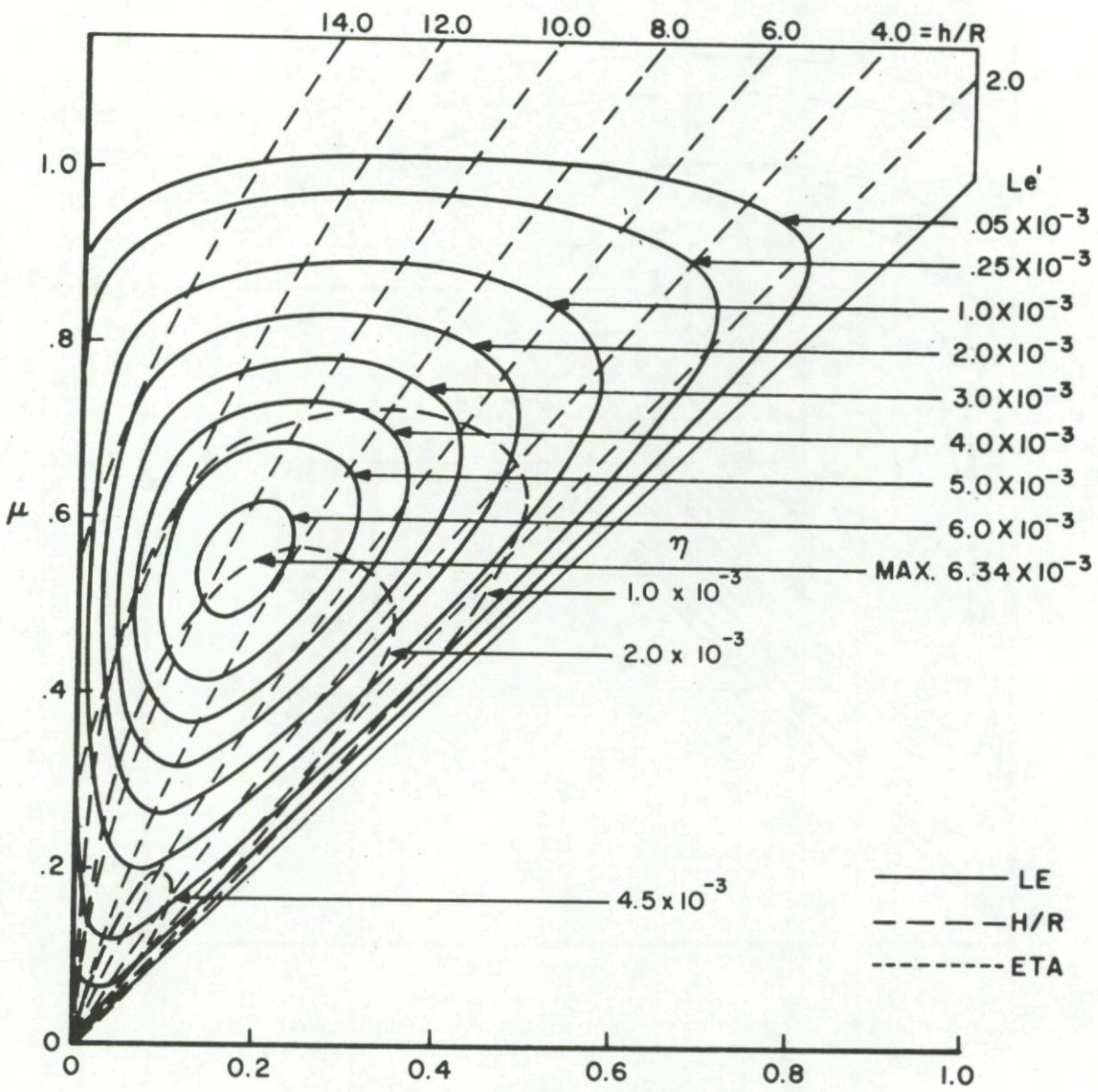


Figure 9. Performance for Constant Stagnation

Conditions: Air Ions,  $\rho_{go}/\rho_{gn} = 32.8$

AIR  $E_{bn} = 3 \times 10^6 \text{ v/m}$ ;  $k_n = 1 \times 10^{-6} \text{ m}^2/\text{v-s}$ ;  $C_0 = 340 \text{ m/s}$ ;  $\gamma = 1.4$

$$f(\mu) = \frac{.264 \mu}{1.441 + \mu}$$

$$\frac{\rho_{go}}{\rho_{gn}} = 1.0$$

$$\frac{Ra}{R} = 0.98$$

$$Le = 0.024 Le' \text{ w/cm}^2$$

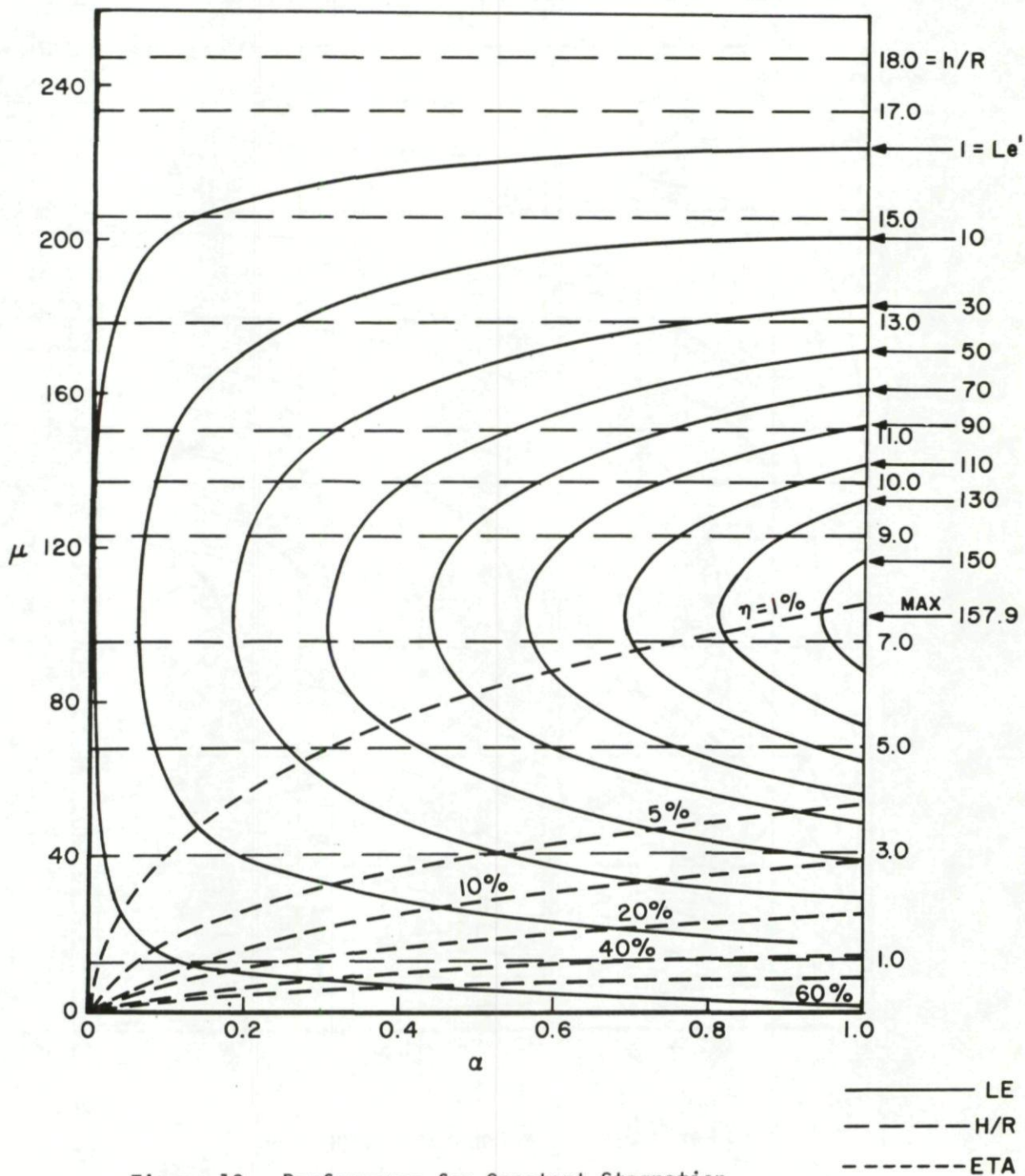


Figure 10. Performance for Constant Stagnation

Conditions: Air colloids,  $\rho_{go} / \rho_{gn} = 1.0$

**AIR**  $E_{pm} = 3 \times 10^6 \text{ v/m}$ ;  $k_n = 1 \times 10^{-6} \text{ m}^2/\text{v-s}$ ;  $C_0 = 340 \text{ m/s}$ ;  $\gamma = 1.4$

$$f(\mu) = \frac{.264\mu}{1.441 + \mu}$$

$$\frac{\rho_{go}}{\rho_{gn}} = 20.0 \quad \frac{Ra}{R} = 0.98$$

$$Le = 9.6 Le' \text{ w/cm}^2$$

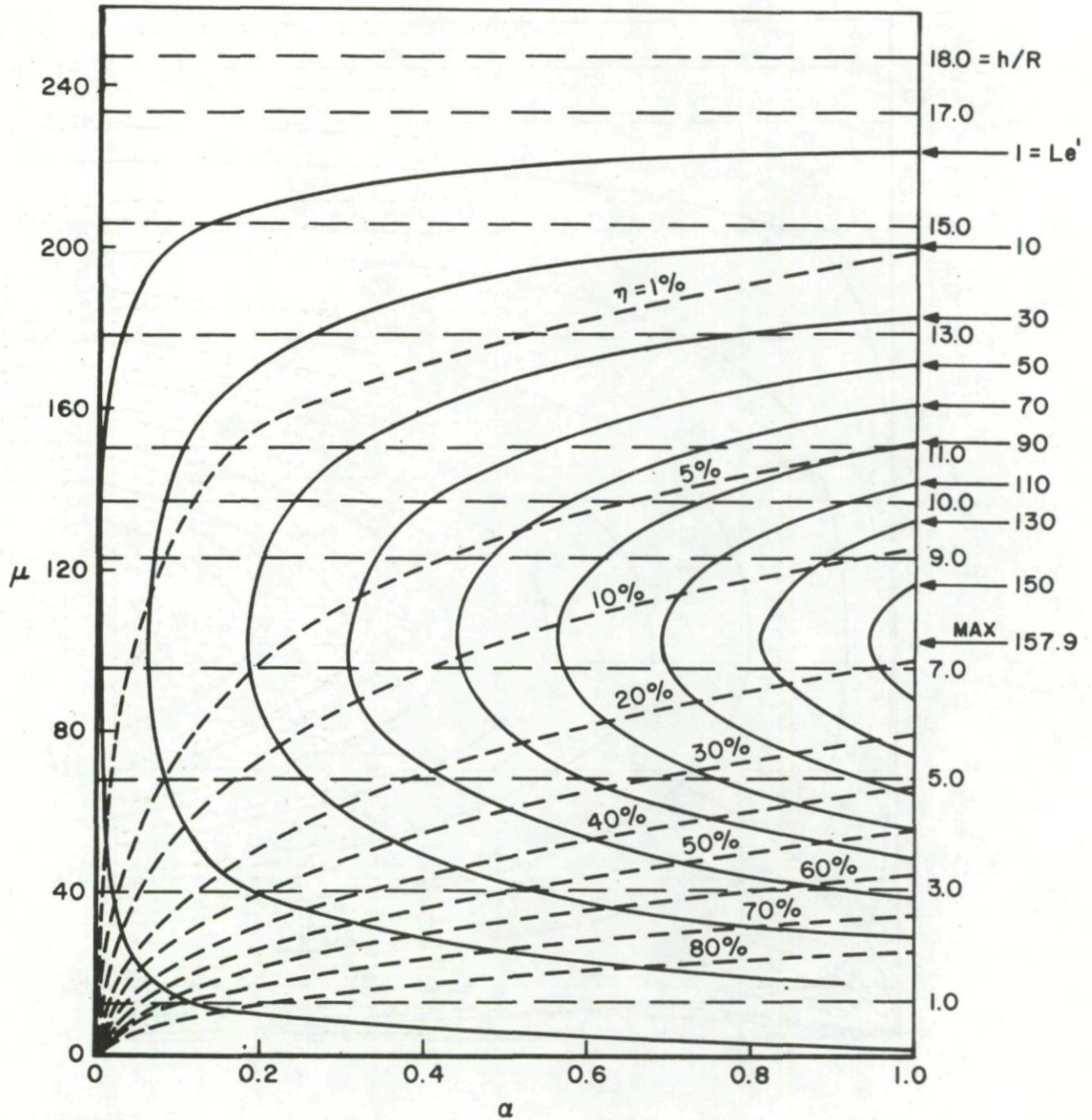


Figure 11 Performance for Constant Stagnation

Conditions: Air Colloids  $\rho_{go}/\rho_{gn} = 20$

- LE
- - - - - H/R
- · · · · ETA

AIR  $E_{bn} = 3 \times 10^6 \text{ v/m}$ ;  $k_n = 1 \times 10^{-6} \text{ m}^2/\text{v-s}$ ;  $C_o = 340 \text{ m/s}$ ;  $\gamma = 1.4$

$$f(\mu) = \frac{.264 \mu}{1.441 + \mu}$$

$$\frac{\rho_{go}}{\rho_{gn}} = 32.8 \quad \frac{Ra}{R} = 0.98$$

$$Le = 25.8 Le'$$

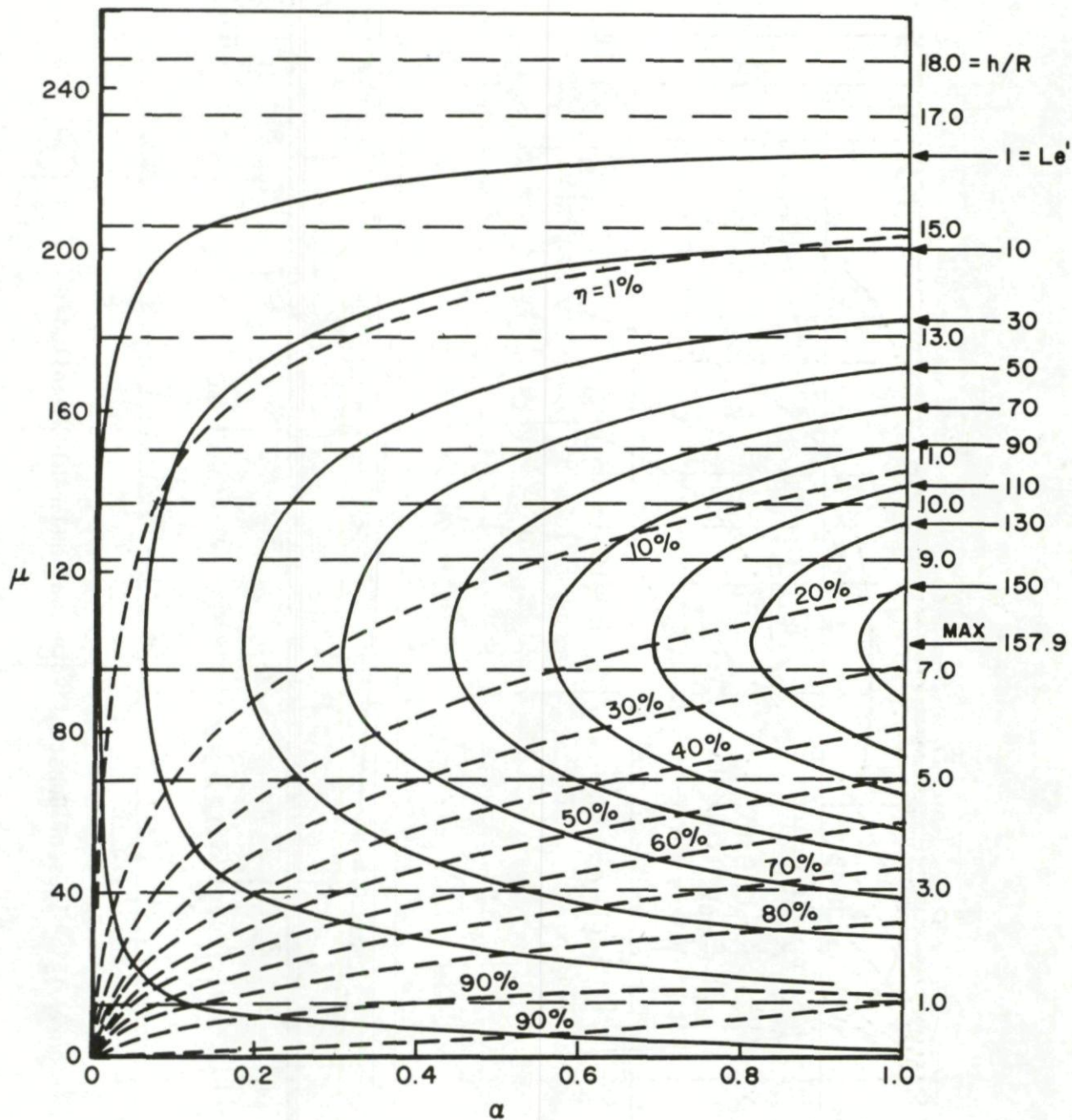


Figure 12. Performance for Constant Stagnation

Conditions: Air Colloids,  $\rho_{go}/\rho_{gn} = 32.8$

——— LE  
 - - - - H/R  
 . . . . . ETA

$$\alpha = .1843$$

$$\mu = .553$$

$$Rl = .026315$$

$$E_{max} = 1.58061$$

$$\phi = U\alpha E_b h$$

$$\frac{|\bar{E}_{Loc}|}{E_b} = \alpha |\bar{E}|$$

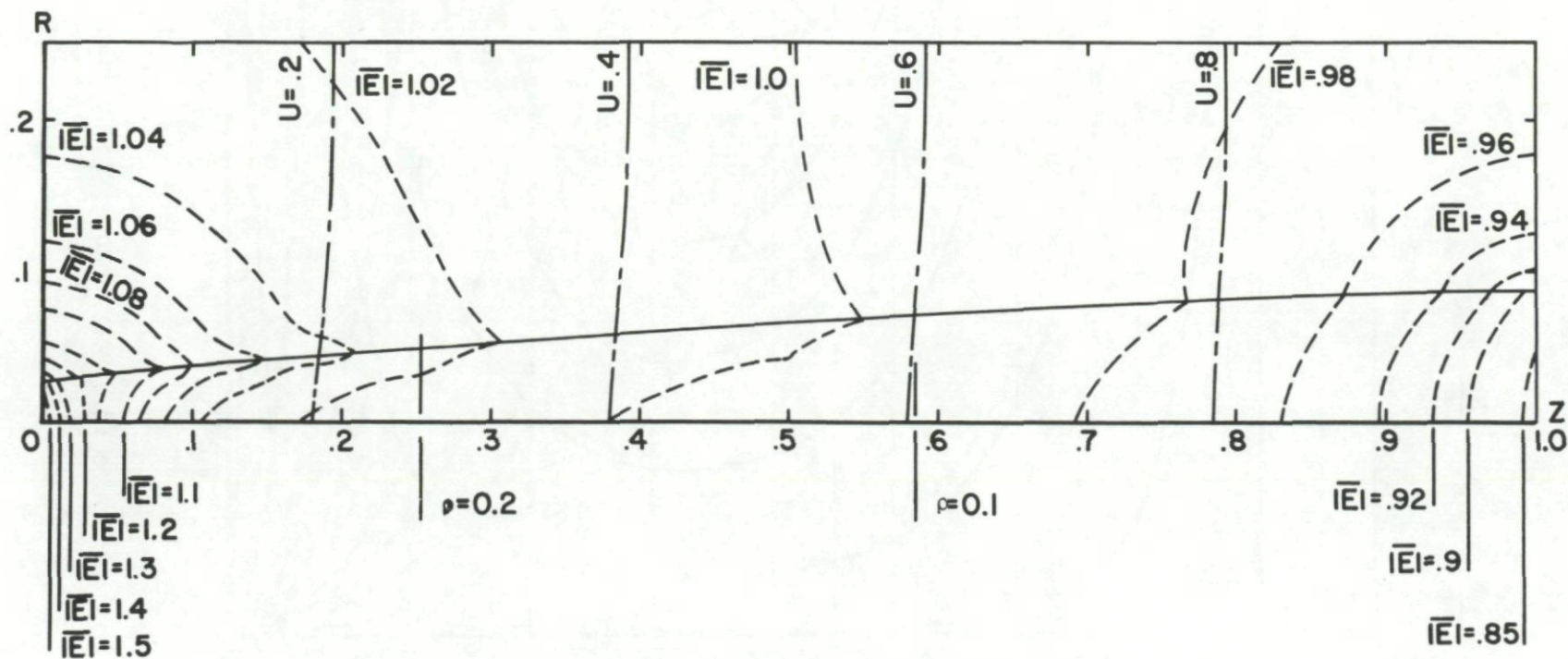


Figure 13 Lines of Constant Potential and Field Magnitude:  
Air Ions.

$\alpha = .2$   
 $\mu = 103$   
 $Ri = .13077$

$E_{max} = 3.4636$   
 $\phi = U\alpha E_b h$

$$\frac{|\bar{E}_{Loc}|}{E_b} = \alpha |\bar{E}|$$

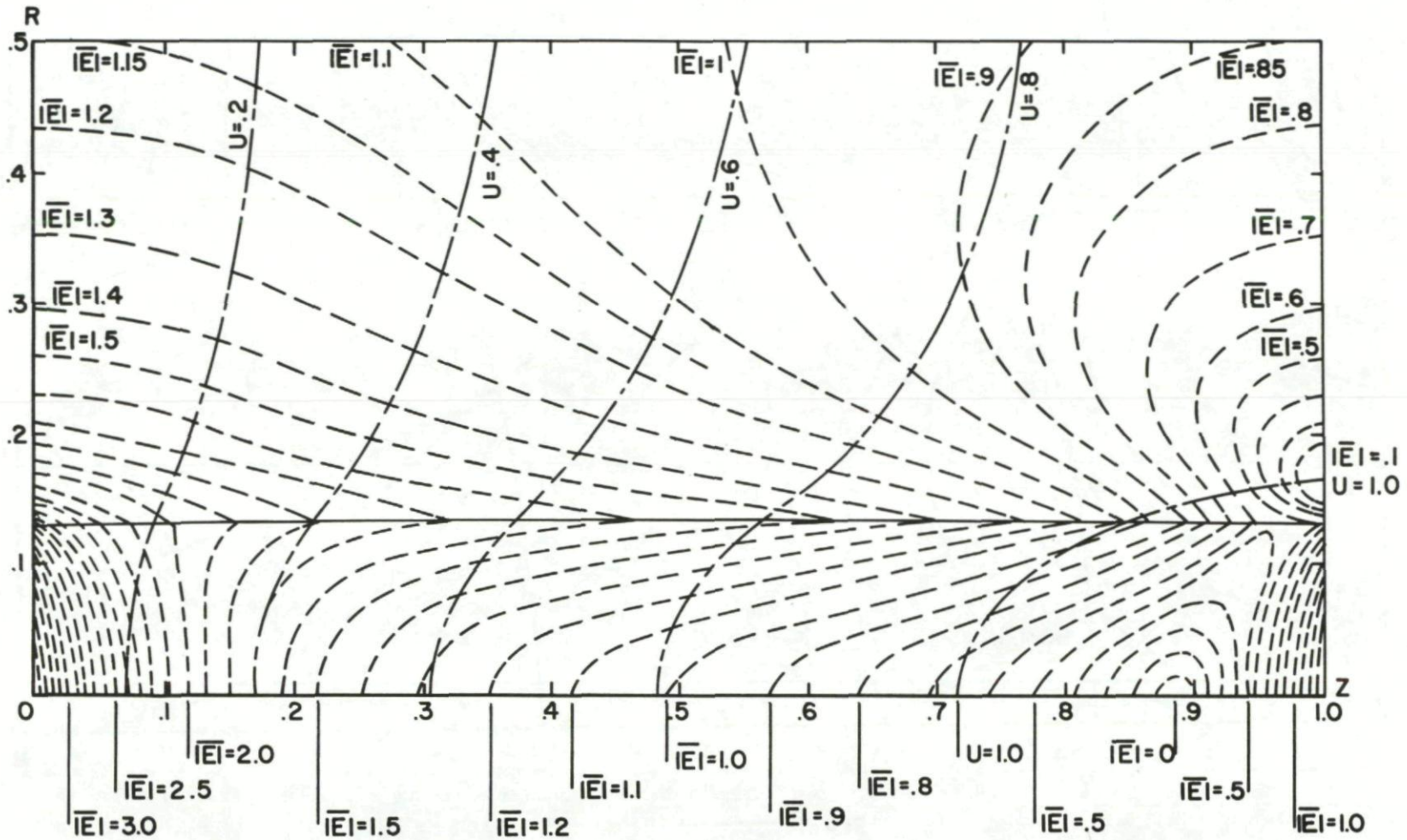


Figure 14. Lines of Constant Potential and Field Magnitude:

Air Colloids,  $\alpha = 0.2$

$\alpha = .5$   
 $\mu = 103$   
 $RI = .13077$

$\phi = U\alpha E_b h$   
 $\frac{|\bar{E}_{Loc}|}{E_b} = \alpha |\bar{E}|$

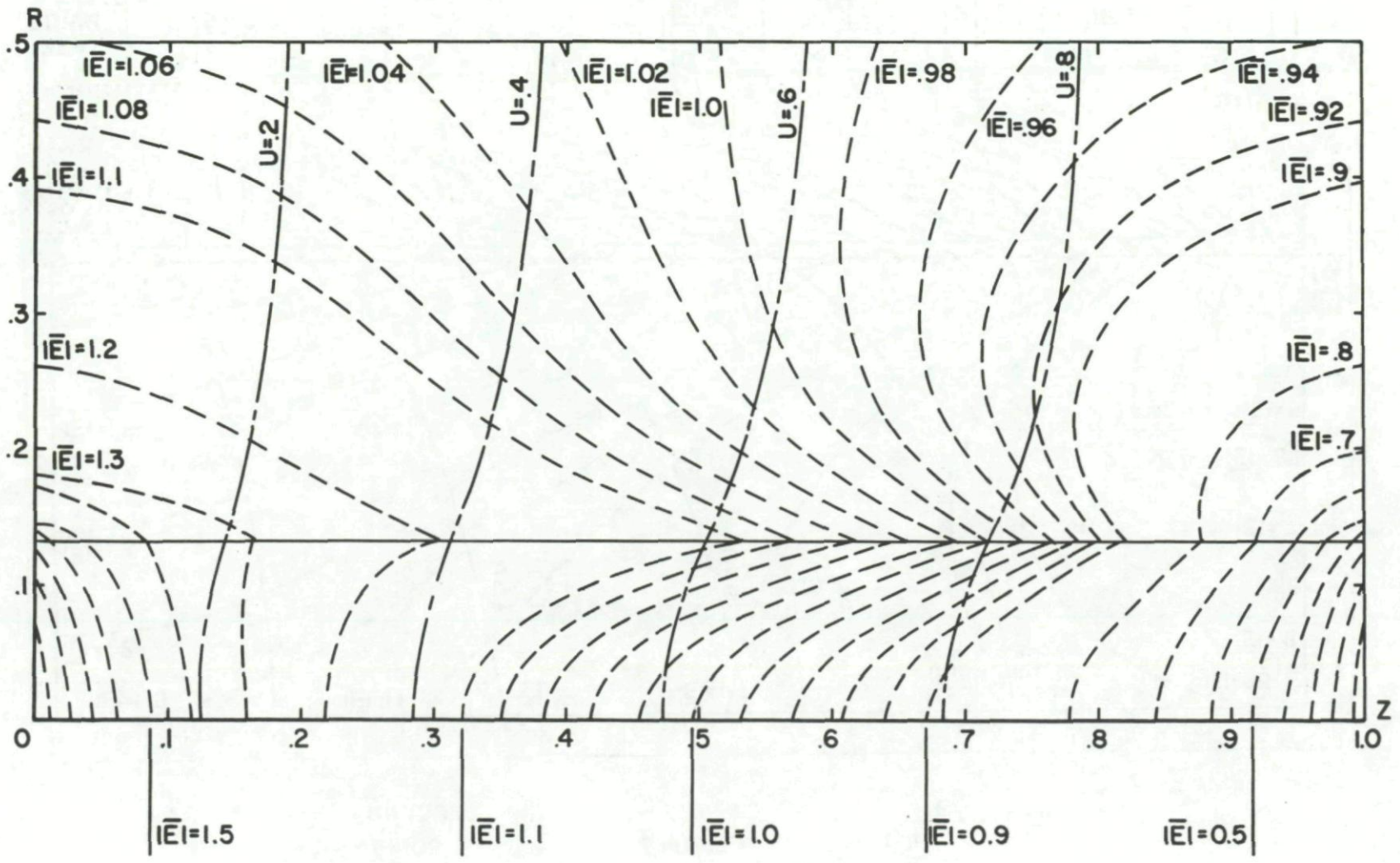


Figure 15. Lines of Constant Potential and Field Magnitude Air Colloids,  $\alpha=0.5$



$\alpha = .7$   
 $\mu = 103$   
 $RI = .13077$

$$\phi = U \alpha E_b h$$

$$\frac{|\bar{E}_{Loc}|}{E_b} = \alpha |\bar{E}|$$

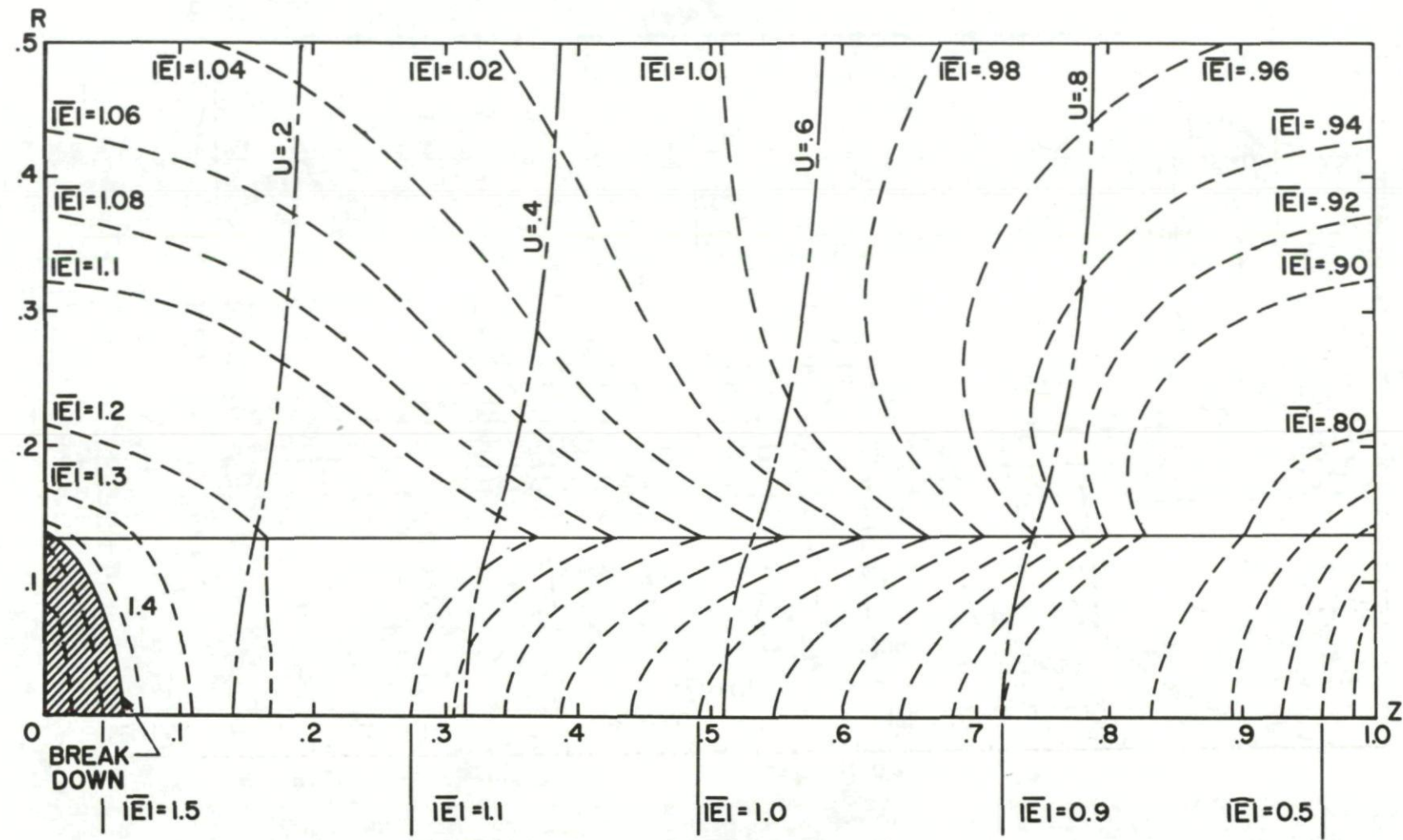


Figure 16. Lines of Constant Potential and Field Magnitude:  
 Air Colloids,  $\alpha = 0.7$

$$\phi = U\alpha E_b h$$

$$\frac{|\bar{E}_{Loc}|}{E_b} = \alpha |\bar{E}|$$

$$\alpha = 0.2$$

$$\mu = 103$$

$$R1 = .13077$$

$$U = Z \text{ at } R = 0.2$$

$$E_{MAX} = 2.84377$$

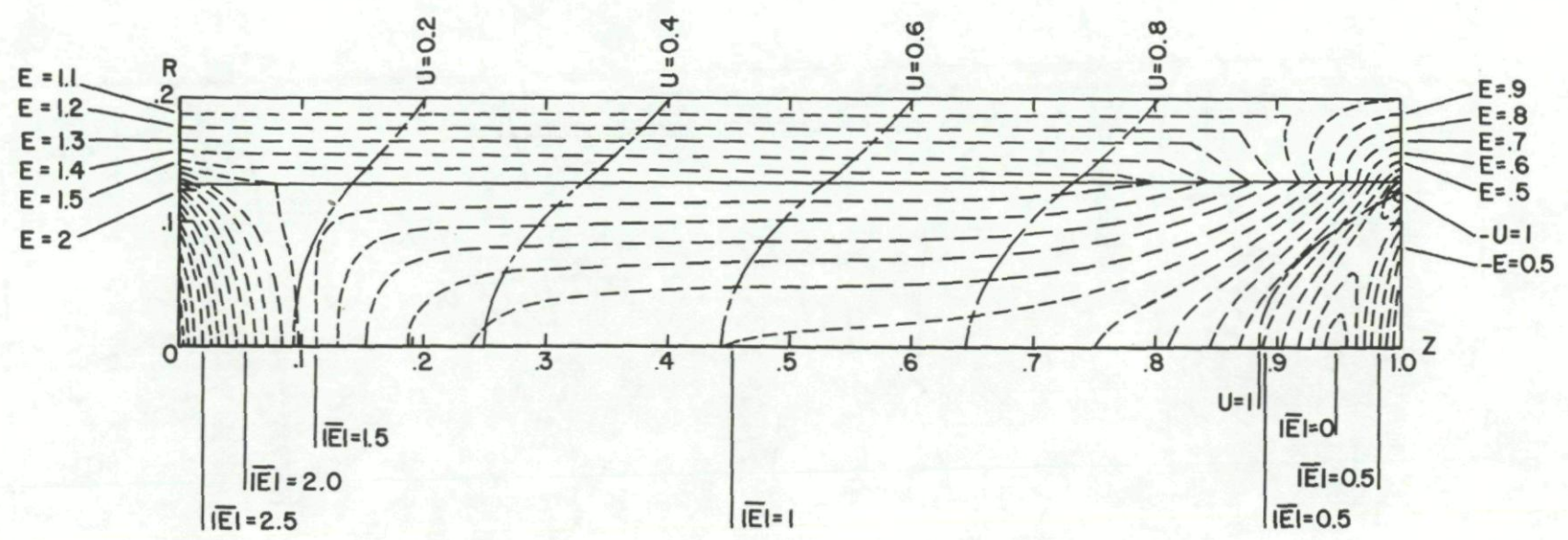


Figure 17. Lines of Constant Potential and Field Magnitude:  
 Air Colloids,  $\alpha = 0.2$  with Linear Potential at  $R = 0.2$

$\alpha = .2$   
 $\mu = 103$   
 $RI = .13077$

$E_{max} = 4.0394$   
 surface charge  
 at  $R = .2$

$\phi = U\alpha E_b h$   
 $\frac{|\bar{E}_{Loc}|}{E_b} = \alpha |\bar{E}|$

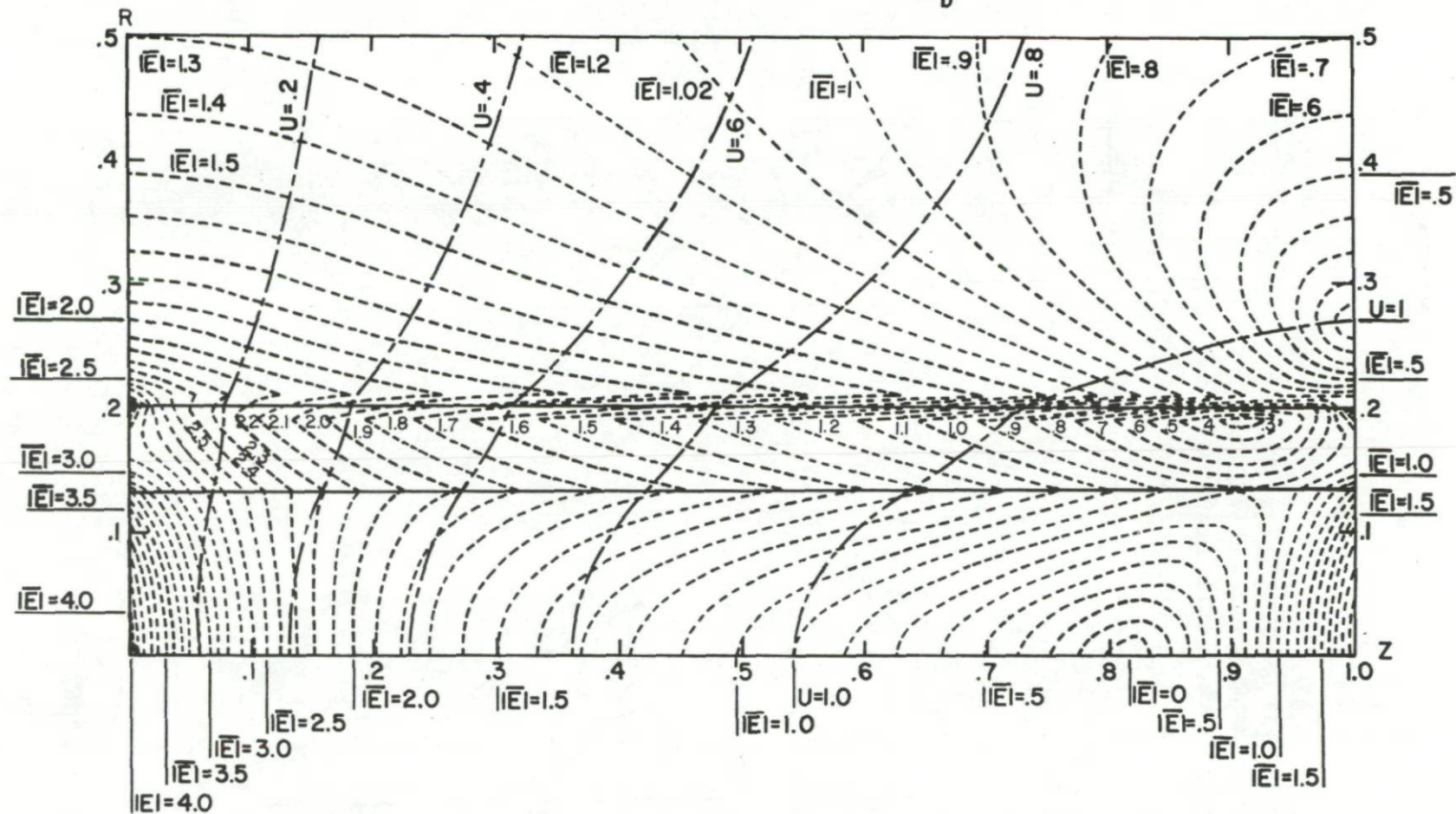


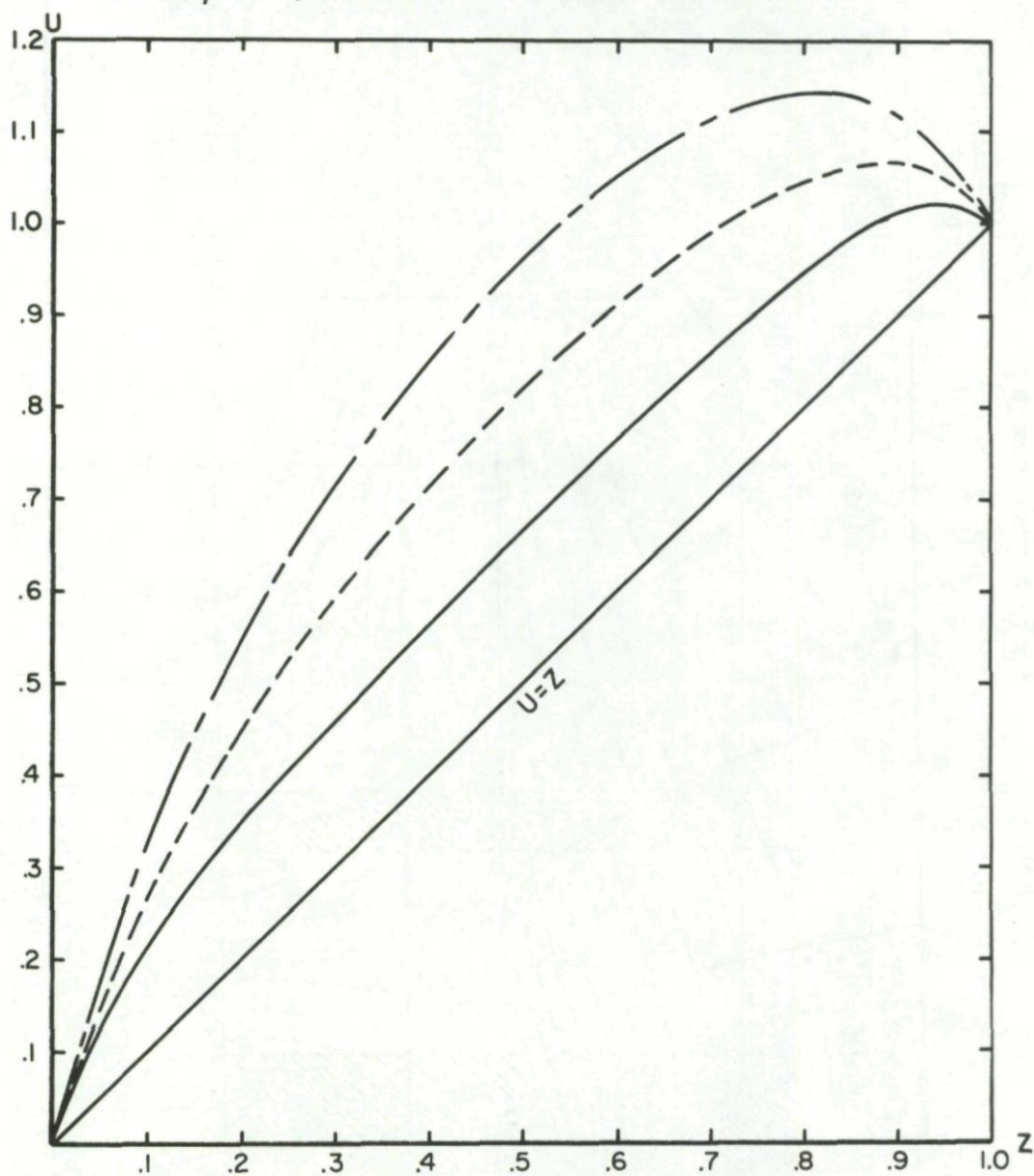
Figure 18. Lines of Constant Potential and Field Magnitude:  
 Air Colloids,  $\alpha = 0.2$  with "Surface Charge" at  $R = 0.2$

## COMPARISON OF CENTER LINE POTENTIAL

-----  $\alpha = .2, \mu = 103, RI = .13077$

————  $\alpha = .2, \mu = 103, RI = .13077$      $U = Z$  at  $R = .2$

-----  $\alpha = .2, \mu = 103, RI = .13077$     SURFACE CHARGE AT  $R = .2$



$R=0$  THROUGHOUT

Figure 19. Comparison of Center Line Potentials for  
Air with Colloids

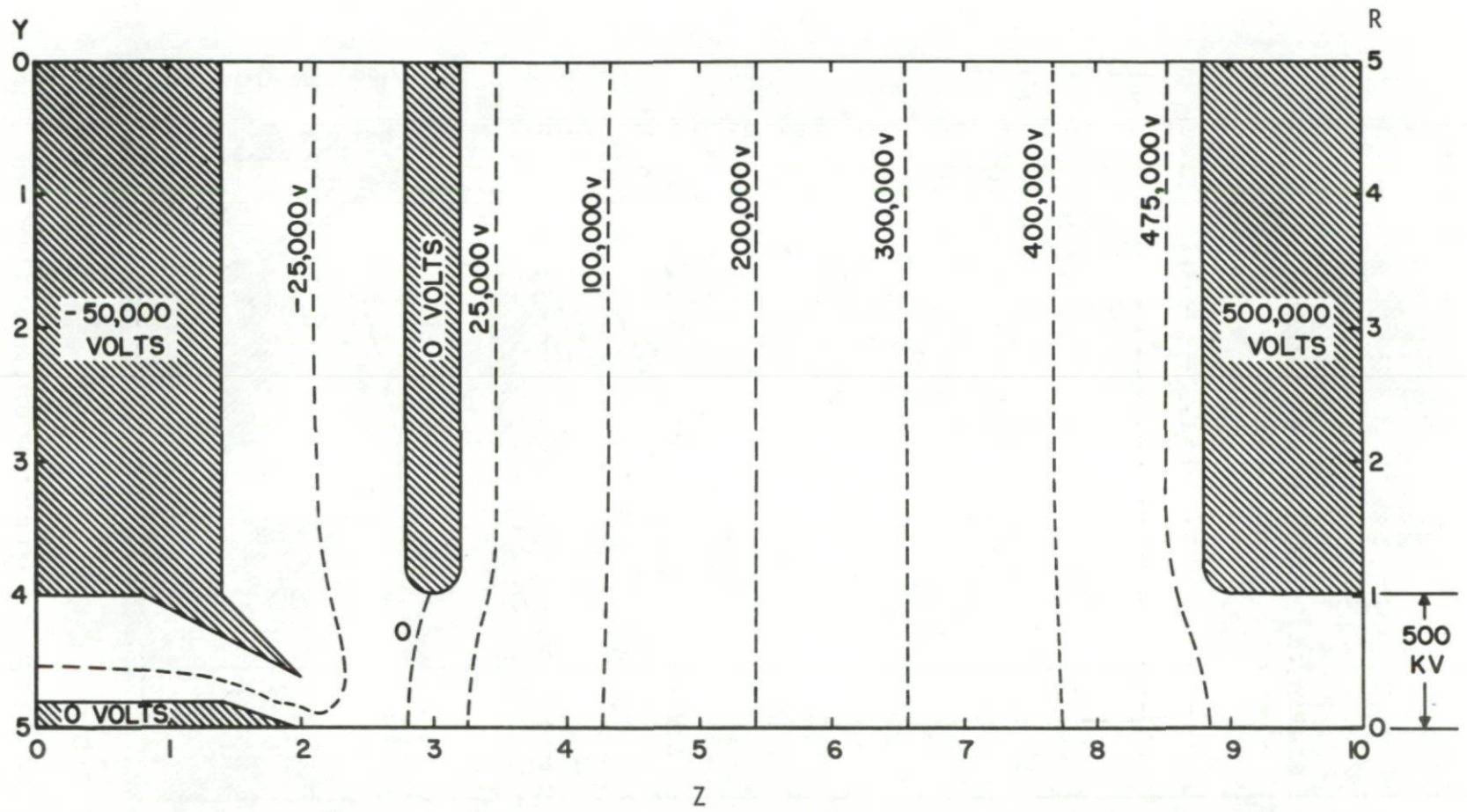


Figure 20. Laplace Solution of More Complex Geometry.

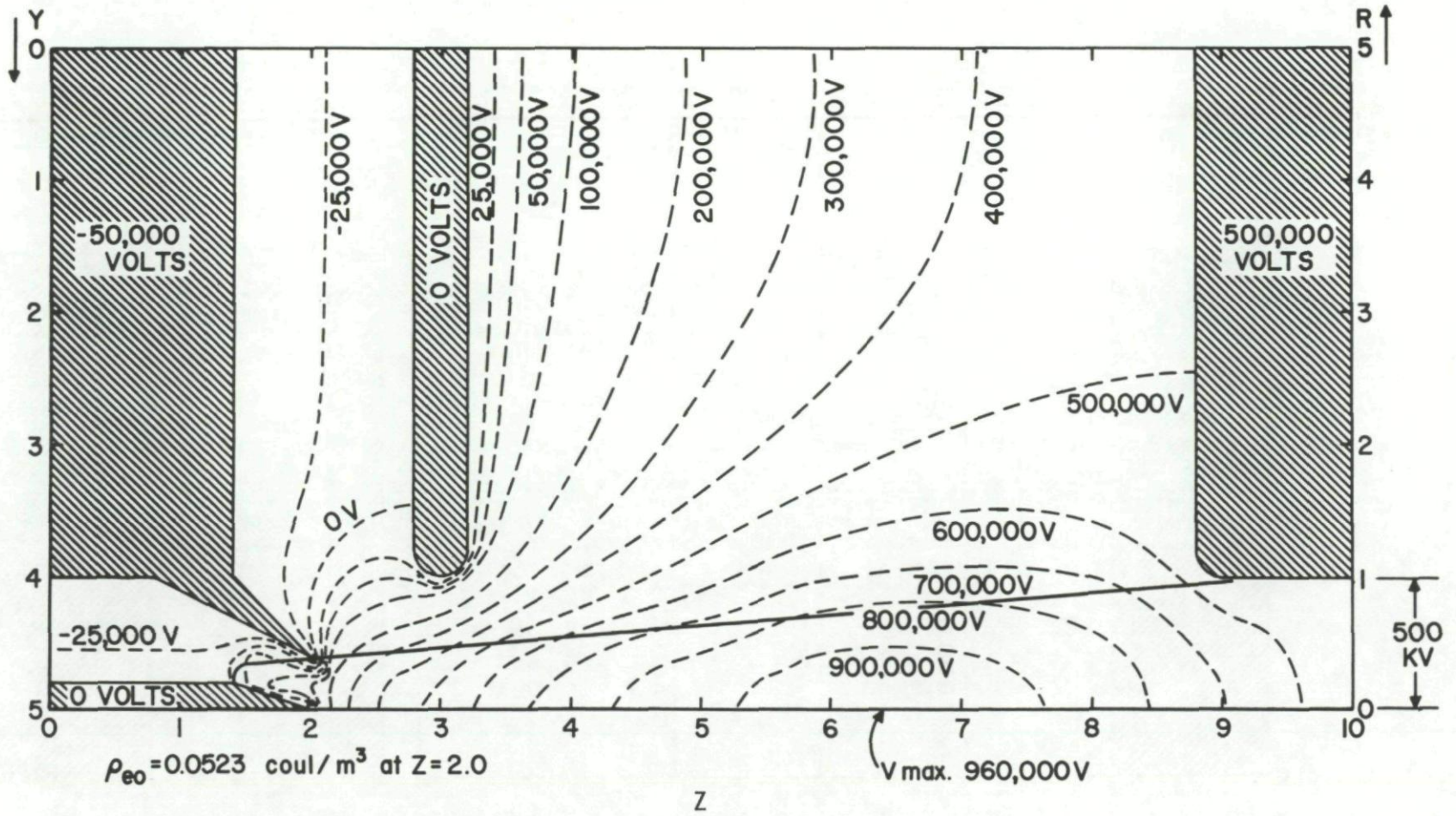


Figure 21. Poisson Solution of More Complex Geometry.

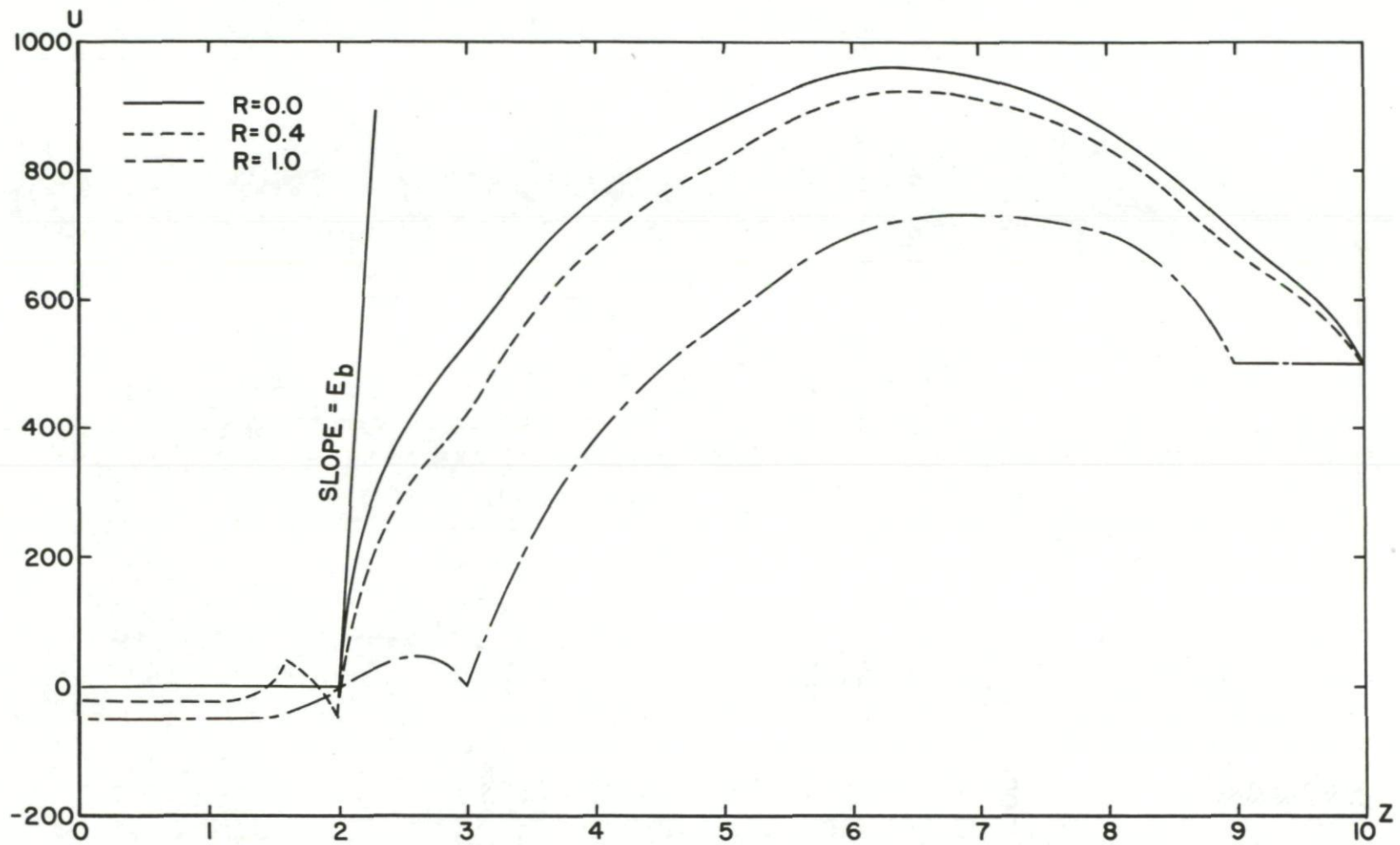


Figure 22. Potential vs Z at Various R for Poisson Solution.

## SOME REMARKS ON EFD ENERGY CONVERSION

## Summary

Some of the work carried out in Belgium in the field of fluid dynamics associated with electric or magnetic effects is briefly reviewed. The paper gives also some suggestions on possible applications of the EFD energy conversion process.



## SOME REMARKS ON EFD ENERGY CONVERSION

Jean-Pierre Contzen  
Belgium

Limited work is currently being done in Belgium in the field of plasma dynamics or more precisely in the field of fluid dynamics associated with electric or magnetic effects. Some research in this area is carried out at the two following places:

- The Institute of Applied Mechanics of the Free University of Brussels,
- the von Karman Institute for Fluid Dynamics at Rhode-St-Genese.

Work at the latter is concentrated around a 30 kW arc heater for use with a low density hypersonic wind tunnel; theoretical and experimental research is performed on velocity measurements at high Mach numbers, on the behaviour of Langmuir probes in high velocity rarefied ionized flows, and on plasma conductivity measurements. All this work is specifically aimed at determining the characteristics of the existing installation and not at developing new diagnostic methods.

The Free University of Brussels has oriented its work along the following lines:

#### Arc Heaters

A 20 kW plasma generator GP-1 (tangential injection, graphite cathode, red copper anode) has been used for extensive studies with argon. The influence of various parameters on operational characteristics and lifetime of the generator has been analyzed. A high temperature measurement system based on spectrum-lines inversion is being built. A second generator GP-2 with axial flow is in the construction stage.

### Mercury Loop

The University carries out a study of mercury flow in the presence of a magnetic field. (1), (2). Measurements of head losses have been performed on ducts of circular, square and triangular cross sections with nonconductive walls as well as on a circular duct with thin conductive walls (platinum). The laminar flow regime, the transition zone and the beginning of the turbulent flow regime have been investigated; Hartmann numbers under consideration are in the range of 20 to 80. A criterion for transition has been studied and for the case of the triangular cross section, a theoretical solution has been found.

It should also be mentioned that in 1965 private industry set up a joint Industrial Study Group on Direct Conversion Processes. This Group is currently performing exploratory studies in the field of MHD, the initial emphasis being on liquid metal systems.

As can be seen, all this work is not directly related to the EFD process but rather corresponds to the more general field of fluid dynamics associated with electric or magnetic effects.

Notice should also be taken of the activities of the Group of Experts on the Production of Energy from Radioisotopes set up by the European Nuclear Energy Agency with the participation of the various OECD countries and of international organizations - CETS, ELDO, ESRO, EURATOM. This Group is reviewing the possibilities of coupling radioisotope heat sources ranging from bulk fission products to high density  $\alpha$  emitters, with various conversion systems to produce electrical power for undersea, earth or space use, the power range under consideration going from microwatt to kilowatt. It appears from the ARL papers that the latter value is within the reach of the EFD conversion process, and this type of system-radio-isotope source-EFD converter

would certainly be worthy of assessment.

The survey of possible applications for the EFD process - taking into account, in particular, the production of high voltages - and the study of the integration of the EFD converter into a suitable thermodynamic cycle in order to achieve a practical system, appear essential at this stage of the work. The general feasibility of the EFD concept is now proved and it does not seem necessary to await further refinements to the converter, before undertaking general studies related to system engineering and fields of application.

As a contribution to this last problem, the following diagram (see Fig. 1) is an attempt to define most probable areas of interest for the EFD process, and to determine its position relative to other electrical power producing processes. It should be noted that the diagram is particularly biased towards space applications but that the areas of interest shown appear to be also valid for terrestrial applications.

The most promising areas, shown by cross-hatching on the diagram, are as follows:

- I Open cycle EFD system (blowdown systems ): short durations -  
power range: less than 1 kW to several tens of kW.
- II Closed cycle EFD systems: longer durations (months) -  
power range: 1 to 10 kW.

A possible application which lies outside the boundaries of the diagram (higher power and duration), and which should evidently be considered, is the power station application; in the same line of thought, the possibility of using the EFD process as a topping cycle in combination with other conversion processes, notably the Joule or Brayton cycle and the Feher cycle, should also

be investigated.

In a quite different field, a promising application for the EFD system would be its use as a "fluid" van de Graaff high-voltage generator; this may well prove to be commercially highly attractive.

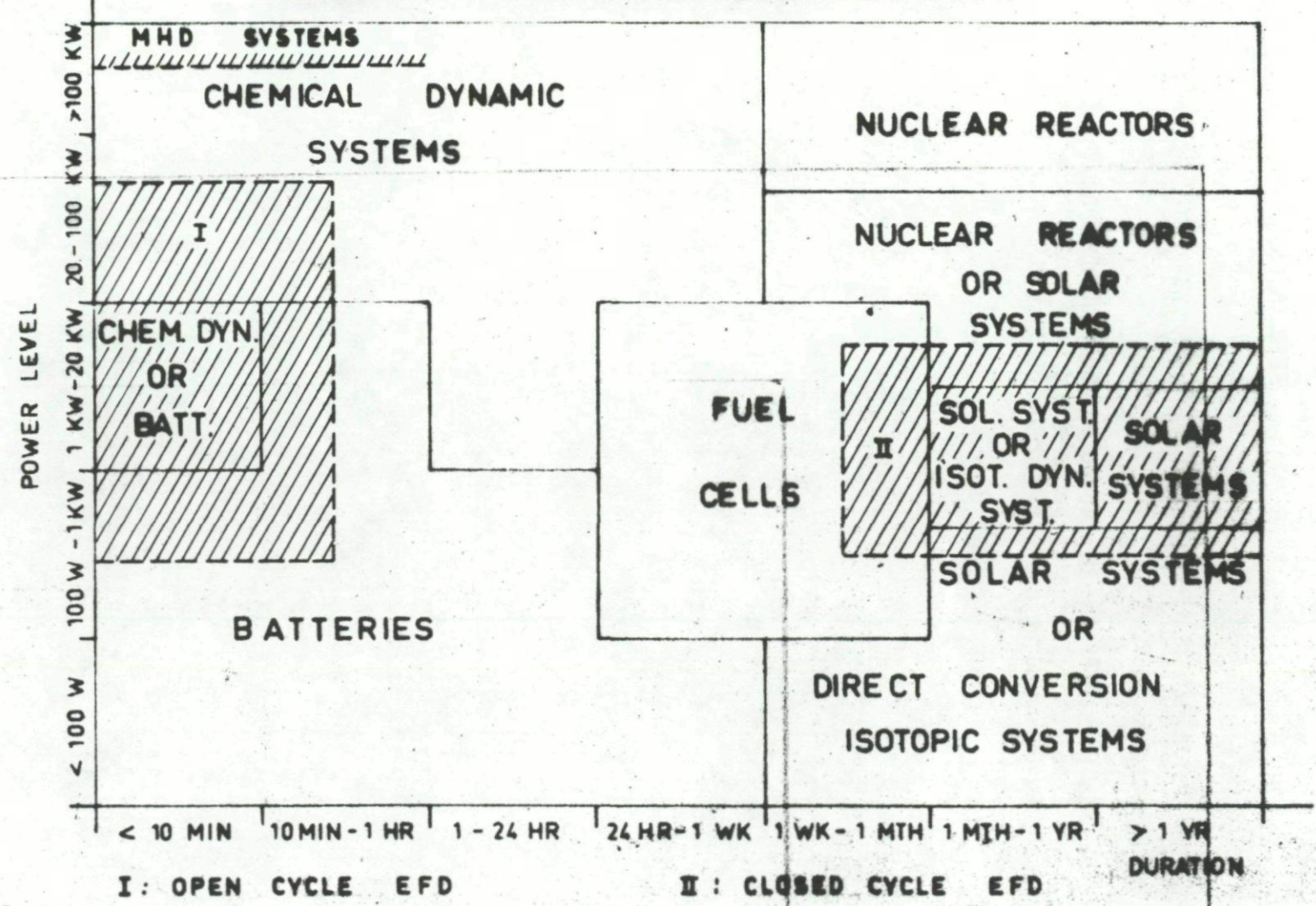
As far as space is concerned, colloidal particle propulsion constitutes an important potential use of EFD power generators; this type of electric propulsion requires high voltages and appears to be in the right range of specific impulse for many missions. Furthermore, the basic technological effort undertaken for the EFD generator appears to be of direct benefit to the development of the colloid thruster.

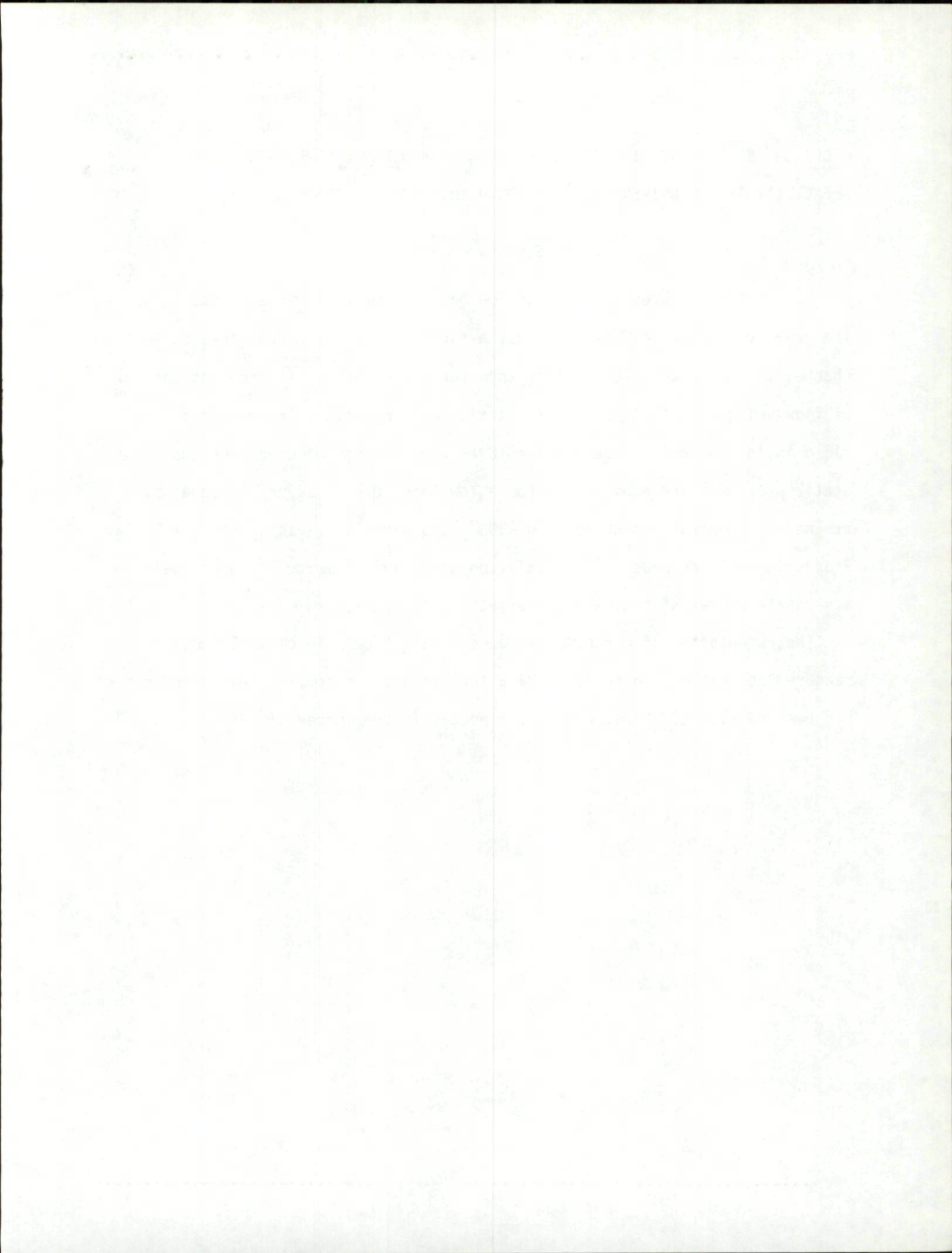
To obtain a more precise definition of the general pattern which has just been described, it would be necessary, as has been stated, to undertake preliminary design studies of complete systems including primary energy source, working fluid, converter and power conditioning equipment. These engineering studies should complement and not replace further development work on the basic conversion process; a carefully balanced progress along these two lines should, it is hoped, bring the EFD process to its maturity.

## REFERENCES

1. A. Jaumotte and C. Hirsch Acad. Roy. Belg. Cl. Sc. Séance du 7 octobre 1967.
2. C. Hirsch Pertes de charge en magnétohydrodynamique. Ecoulement laminaire permanent d'un fluide incompressible. Revue de Mécanique - M - to be published.

# POWER GENERATORS MATRIX





DESIGN AND CONSTRUCTION OF A 3-MW MAGNETOGASDYNAMIC POWER GENERATION  
FACILITY AT THE UNIVERSITY OF TORONTO INSTITUTE OF AEROSPACE STUDIES

Summary

The design features of a 3-MW, blow-down plasma facility are described. The primary aim has been to construct a facility having a large interaction channel to emphasize volume rather than surface effects. Independent control of flow velocity, static pressure, static gas temperature and magnetic field in the channel can be achieved over a wide range of operating conditions. Static pressures are achievable from a few Torr to over seven atmospheres, stagnation temperatures up to 2200-2500°K and magnetic fields up to 1.7 Tesla. Provision has been made for the addition of radial or vortex-flow channels on a separate outlet of the main heater at a later date.

Instrumentation of a constant-area channel, 5 cm x 10 cm x 120 cm, to measure the voltage and current characteristics of up to fifty electrode pairs has been completed. First runs are expected in the summer of 1968.



DESIGN AND CONSTRUCTION OF A 3-MW MAGNETOGASDYNAMIC POWER GENERATION  
FACILITY AT THE UNIVERSITY OF TORONTO INSTITUTE OF AEROSPACE STUDIES

by

Professor Stanley J. Townsend  
Institute for Aerospace Studies  
University of Toronto, Canada

Introduction

With the advent on the Canadian scene of nuclear power reactors producing electricity at costs below those of coal-burning stations, advanced power conversion schemes for nuclear reactors are worthy of increased attention. With the added incentive of the likely demand for large amounts of electrical power in space, particularly for propulsion purposes, it was decided to initiate a research program into magneto-hydrodynamic (MHD) power generation. The present study involves the simulation of a portion of a closed cycle system involving a high-temperature, gas-cooled reactor. More properly, then, we should call it magnetogasdynamic (MGD) power generation.

A large number of the earlier experiments in MGD power generation were performed in small scale devices dominated by surface effects such as boundary layers filling most of the channel and radiation losses to the walls from the hot plasma. Accordingly, it was decided to construct a facility which would simulate a small scale nuclear reactor at the megawatt level. This power level is adequate to study the behaviour of a dense, seeded flowing plasma in a rather large interaction channel; surface effects no longer predominate over volume effects. Hence, some rather basic studies can be performed on the plasma.

The use of nuclear reactors as heat sources will involve the use of non-equilibrium ionization to keep the plasma conductivity high. An elevated electron temperature must be maintained while keeping the carrier gas temper-

ature low to minimize heat transfer to the walls. Thus, a two-temperature plasma is involved. The relatively weak coupling of the electron gas to the atomic species can give rise to electrothermal instabilities, with large scale fluctuations in electron number density.

### Magnetogasdynamic Facility

Figure 1 is a schematic layout of the MGD facility. A blow-down system was chosen in order to provide a plasma flow through a channel having a large cross sectional area. Length of operating time was sacrificed in the interests of a larger power flow. Even so, one to two minutes of plasma flow gives ample time for almost all experimental procedures of interest to be performed. This is particularly true if one preheats the channel and electrodes to near operating temperature before the plasma flow starts.

The pressure gradient between the upstream heater and downstream vacuum sphere is used to accelerate the plasma to the desired Mach number.

The Mach number can be set subsonically by controlling the ratio of stagnation to static pressure. Supersonically, individual isentropic nozzles and proper diffuser recovery techniques must be employed. By choosing a particular value of stagnation pressure in the heater, which can be set independently by a regulator, any desired value of static pressure in the channel can be achieved. By choosing a particular value of the stagnation temperature in the heater, which can be set independently by a pyrometer, any desired value of static temperature in the channel can be achieved. Thus, in the gasdynamic sense, there is independent control of velocity, pressure, temperature and hence density, over a very wide range of operating parameters. Figure 2 shows the upper limit of mass flow rate and static

pressure through the 50 cm<sup>2</sup> initial channel. The calculations were done for  $T_0 = 2500^\circ\text{K}$ . The lower limit of static pressure is well below 76 Torr, since the vacuum sphere can be evacuated to at least 2 Torr. The possibility then exists for studies of ion slip at low pressures.

The MGD channel is situated between the pole faces of a large iron C-magnet that can be operated at any value of magnetic field from 0 to 1.7 Tesla.

The plasma exits from the interaction channel, enters a diffuser, and subsequently is cooled down in a pebblebed heat exchanger. The gas flow is then scrubbed of the alkali seed without any attempt at recovery. The cool, scrubbed gas is then discharged to the vacuum sphere. The sphere has a capacity of slightly less than 1000 m<sup>3</sup>.

Figure 3 shows a close-up view of the experimental region.

#### Inert Gas Heater

The inert gas heater was designed on the heat-sink principle, using a core of graphite. Figure 4 is a diagram of the stagnation heater. The outer steel shell, water-cooled, is 1.37m in diameter and 2.74 m in height and is designed to operate at a rated pressure differential of 100 psig, just under 8 atmospheres absolute. Within the steel shell there is 12.7 cm layer of alumina fibre insulation, surrounding another layer of 7.5 cm of graphite felt. These two layers of high-temperature insulation sheath the graphite core of the heater.

The core was machined from a solid rod of graphite 0.9 m in diameter and 1.8 m long. This graphite assembly contains an outer annulus in which three radiant-heating graphite electrodes are situated at 120° intervals. They radiate upon the inner core which is a pebble bed 0.45 m in diameter and 0.85 m high. 3-phase, AC power is supplied to the three electrodes in a Y-connection; the power dissipation is about 150 kW. The heater has been tested to 1700°K so

far. Since the temperature was climbing at  $200^{\circ}\text{K}$  per hour, it can be inferred that the thermal insulation is probably adequate for about  $2200^{\circ}\text{K}$ . With more graphite felt insulation,  $2500^{\circ}\text{K}$  is probably achievable.

The inner core houses a bed of pebbles made out of 1.9 cm diameter rod cut into right cylindrical chunks. The cost of this bed was about 1/20 that for spherical pebbles with no significant sacrifice in heat transfer ability.

The gas flow enters at the top and proceeds down the outer annulus, in through two 10 cm holes in the side of the bottom heater, up through a slotted grate, through the pebbles, into the top plenum chamber where it is mixed with the alkali seed and then accelerated to the desired Mach number in a nozzle.

Temperature control of the heater is accomplished by a two-temperature, infrared pyrometer viewing the bottom current-ring. This ring is the "unipoten-tial" junction connecting the three heater elements.

An emergency water recirculation cooling system capable of dissipating 145 kW has been constructed. It will allow safe cooling of the heater in the event of an unexpected interruption in water or electrical service to the laboratory.

A second outlet hole has been bored into the top plenum chamber to allow the addition of a second outlet pipe. A radial-flow or vortex-flow MGD channel could be installed on this outlet at a later date after a super-conducting magnet is acquired.

#### Seed Injection And Removal System

Figure 5 shows a schematic diagram of the seed injection system. The alkali seed is drawn into a stainless steel bellows from which it is driven

by positive-displacement into a boiler. The flow of liquid NaK is metered by controlling the speed of a variable-speed motor. The boiler is maintained at 1100-1200°K. The seed vapour is passed through a 2.5 cm stainless steel pipe into the plenum chamber of the inert gas heater. Care is taken that no seed condensation occurs in this line.

The seed injection system can use any of Cs, K, or NaK-90. The seeding ratio can be varied from zero to over 1 mole per cent for up to a 3 kg/sec argon flow. The operating time would be about one minute at this high rate and longer at lower rates.

Seed removal is accomplished by washing down the cold gas flow emerging from the downstream heat exchanger with alcohol (ethanol or preferably amyl alcohol for its low heat release) to form a harmless potassium compound. This compound is then flushed away with water to a settling tank. Because of the low cost of NaK-90 (90% potassium - 10% sodium liquid metal) no attempt is made to recover the seed. The primary interest lies in preventing embrittlement of the steel in the downstream piping and vacuum sphere.

### Electromagnet

Figure 3 is a photograph of the electromagnet and the MGD channel. A C-lamination was used in order to provide ease of access for spectroscopy experiments and for electrode and probe connections. The dimensions of the gap were set at 15 cm x 25 cm in a plane normal to the plasma flow. This accommodated the first channel of 5 cm x 10 cm inner dimensions. The length of the magnet was chosen to be 1.25 m, of which 1.0 m gives a uniform field region. The magnetic field of 1.7 T is uniform to  $\pm 0.25\%$  over the channel

area and to  $\pm 0.1\%$  over the one meter length. A long, uniform interaction region was desired to permit relaxation studies of non-equilibrium ionization.

The magnet body consists of a stack of twenty-five 5 cm thick mild steel plates flame cut to the desired cross section. The 10 cm thick pole faces are of machined, annealed mild steel and are removable. They can be replaced by thinner and/or tapered pole faces to allow for a larger channel.

The coils were wound from extruded aluminum conductor, 1.15 cm square with a 0.63 cm I.D. hole for water cooling. Electrical power requirements are 137 volts per coil at 834 amperes from a bank of heavy-duty truck batteries. The rate of collapse of the magnetic field is controlled by crowbarring with a large diode (IN4054R).

#### Initial Channel

Figure 6 shows a pictorial view of one of six sections of the MGD channel. Inner dimensions are 5 cm in the B-field direction and 10cm in the  $\underline{U} \times \underline{B}$  direction. A simple constant-area channel was chosen to be constructed first. Data gathered on boundary layer growth will be used to design a constant Mach number channel. Each section of channel is 30 cm long. Upstream and downstream sections are being instrumented for velocity profiles. One upstream section is being modified to operate as a pre-ionizer. One section of channel has been fitted with four voltage-sensing probes to measure Faraday and Hall voltage gradients.

#### Instrumentation

An electrical recording system has been constructed to record automatically voltages from up to fifty pairs of electrodes. A switching circuit can scan

all the electrodes over a period that can be varied from one to ten seconds. The output voltages are fed into a 100k buffer amplifier and are then recorded on a high speed oscillograph. During a 60 to 120 second run, there is ample time to achieve steady state conditions, perform all D.C. measurements, change load resistors or electrode configuration by relays and then to proceed with further measurements.

### Initial Research

In conjunction with the experimental work being performed, theoretical calculations of the electrical conductivity in the channel are being carried out. Calculations of electron number density and temperature for the bulk plasma are also being done. In addition, a detailed study of the variation of these quantities throughout the volume of the channel is proceeding.

Preliminary testing of most of the components has been carried out. The heater has been tested to 1700<sup>0</sup>K and has performed flawlessly. The magnet has been checked for proper crowbarring action. A preliminary field survey was performed at low field levels and the uniformity appears to be somewhat better than computer calculations predicted. The NaK boiler will be taken up to temperature shortly and tested out. The seed removal system is the only major sub-system yet to be tested.

### Acknowledgement

This work has been supported by the Defence Research Board and the National Research Council of Canada, the Ontario Department of University

Affairs, the University of Toronto and by the National Aeronautics and Space Administration of the United States.

The computer program for the calculation of the magnet distribution of current and iron was developed by K. Wakefield, Plasma Physics Laboratory, Princeton University. Its use is gratefully acknowledged by the author.



- Key:
- (1) Gas Flow
  - (2) Stagnation Temp. Monitor
  - (3) Electrode Voltage Monitor
  - (4) Magnet Control
  - (5) Shutoff Valve Control
  - (6) Generator Load Circuit
  - (7) Magnet Power Circuit

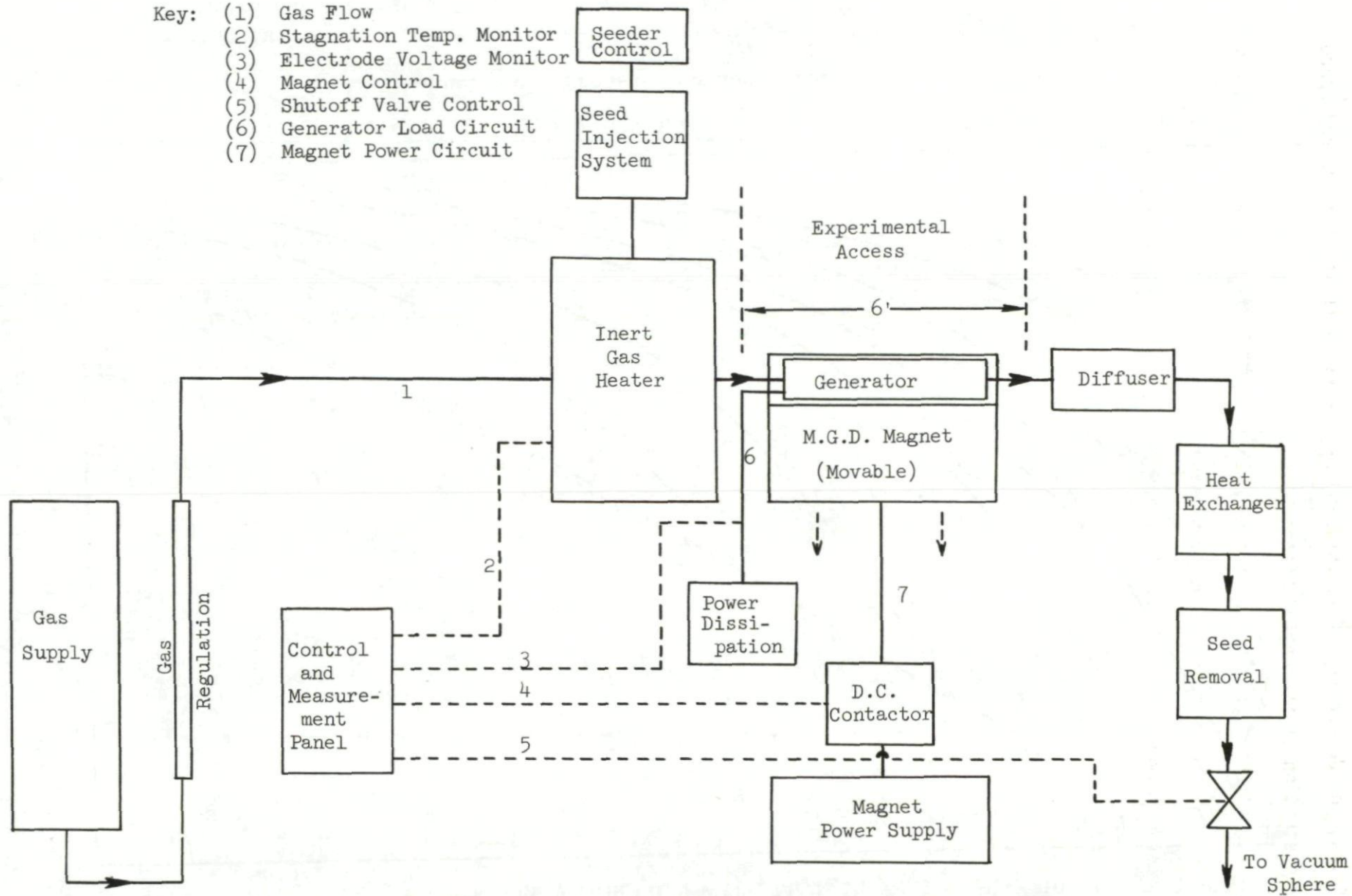


FIG. 1. LAYOUT SCHEMATIC OF M.G.D. GENERATOR FACILITY

MASS FLOW VARIATION WITH  $\dot{M}$  & P. IN A 5CM. X 10 CM. CHANNEL

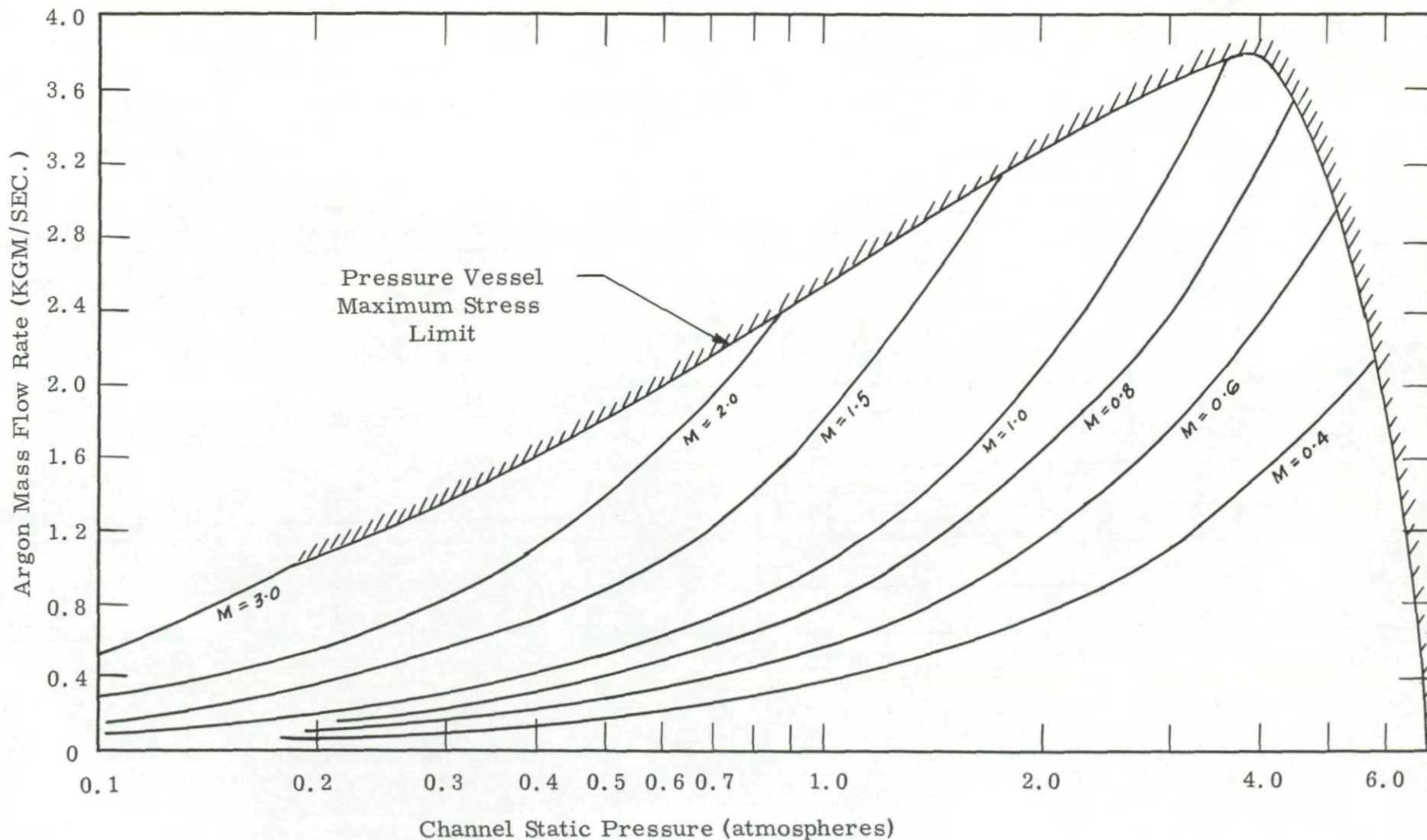


FIGURE 2 Mass Flow Variation With Static Pressure in MGD Channel for Operating Conditions Permitted By Stagnation Pressure Limitation

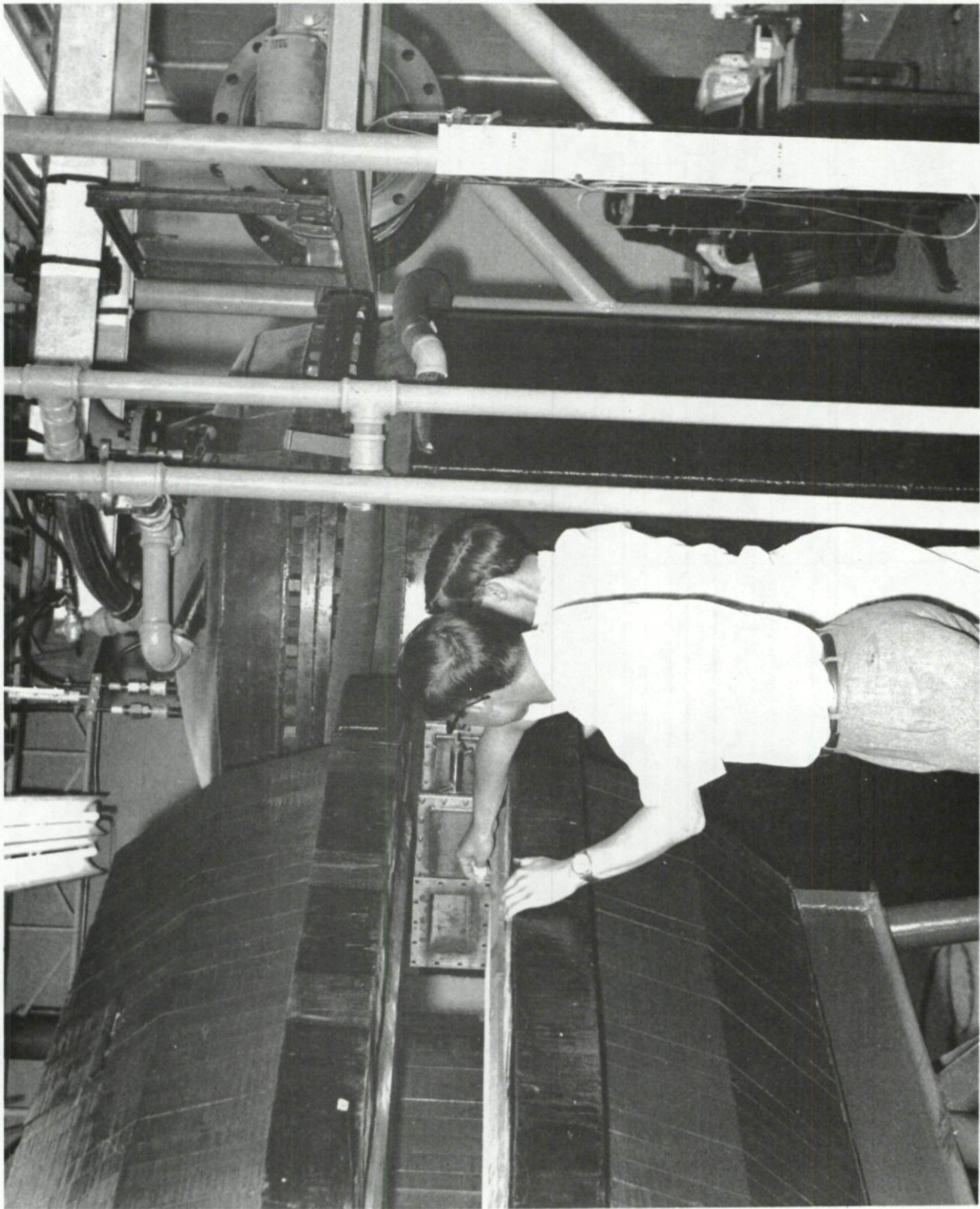


FIGURE 3

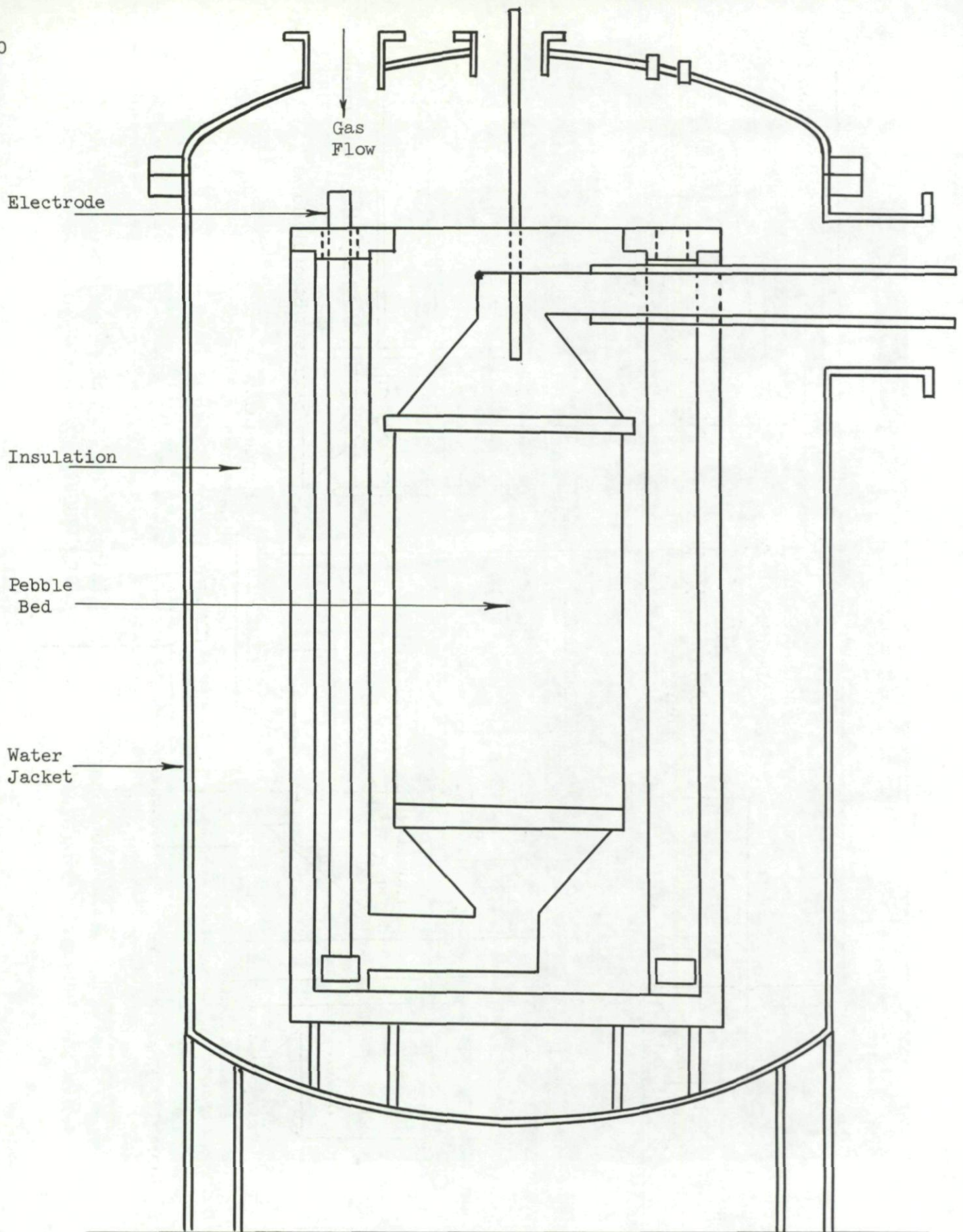


FIG. 4 CROSS-SECTIONAL VIEW OF THE INERT GAS STAGNATION HEATER

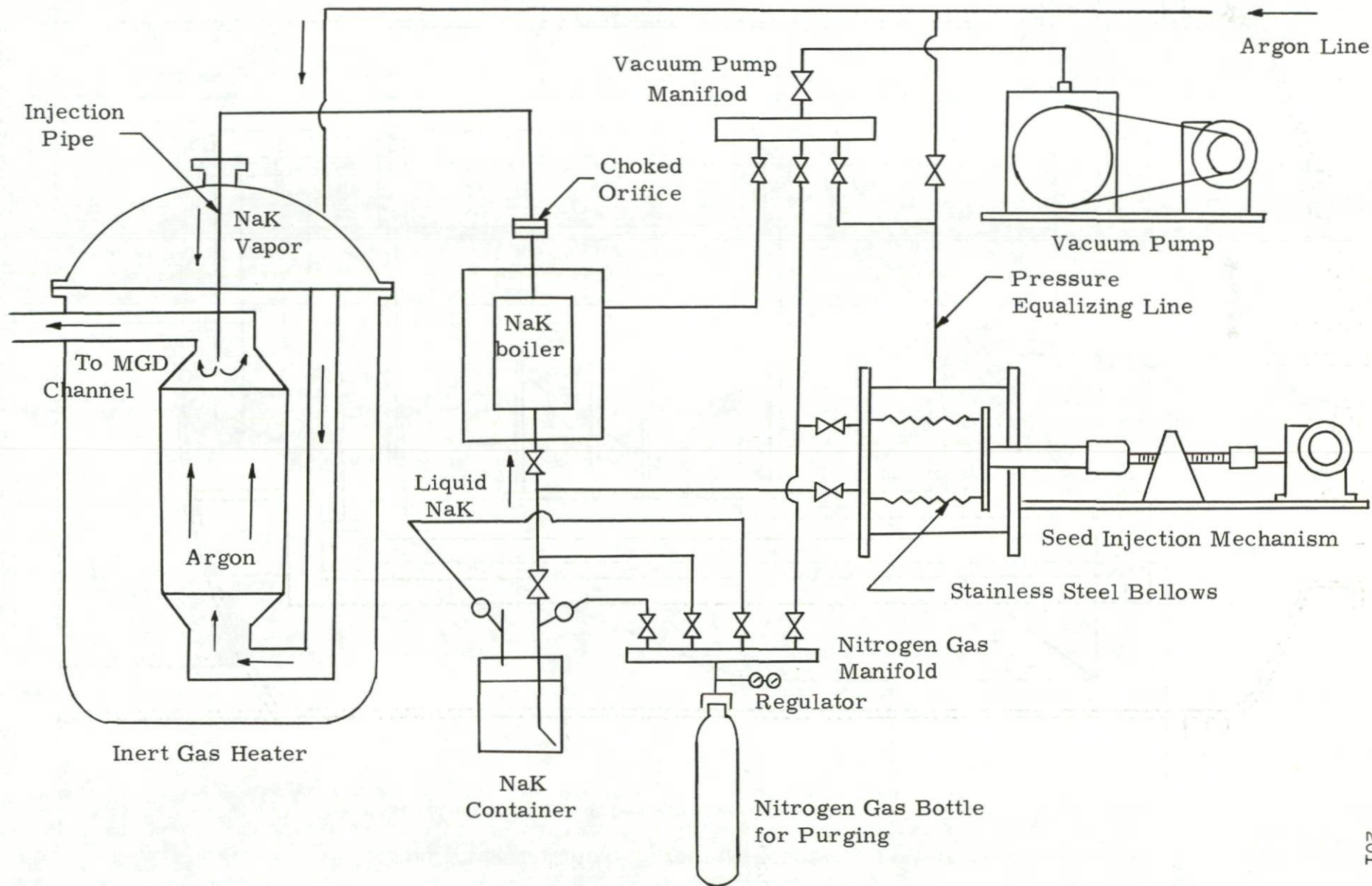
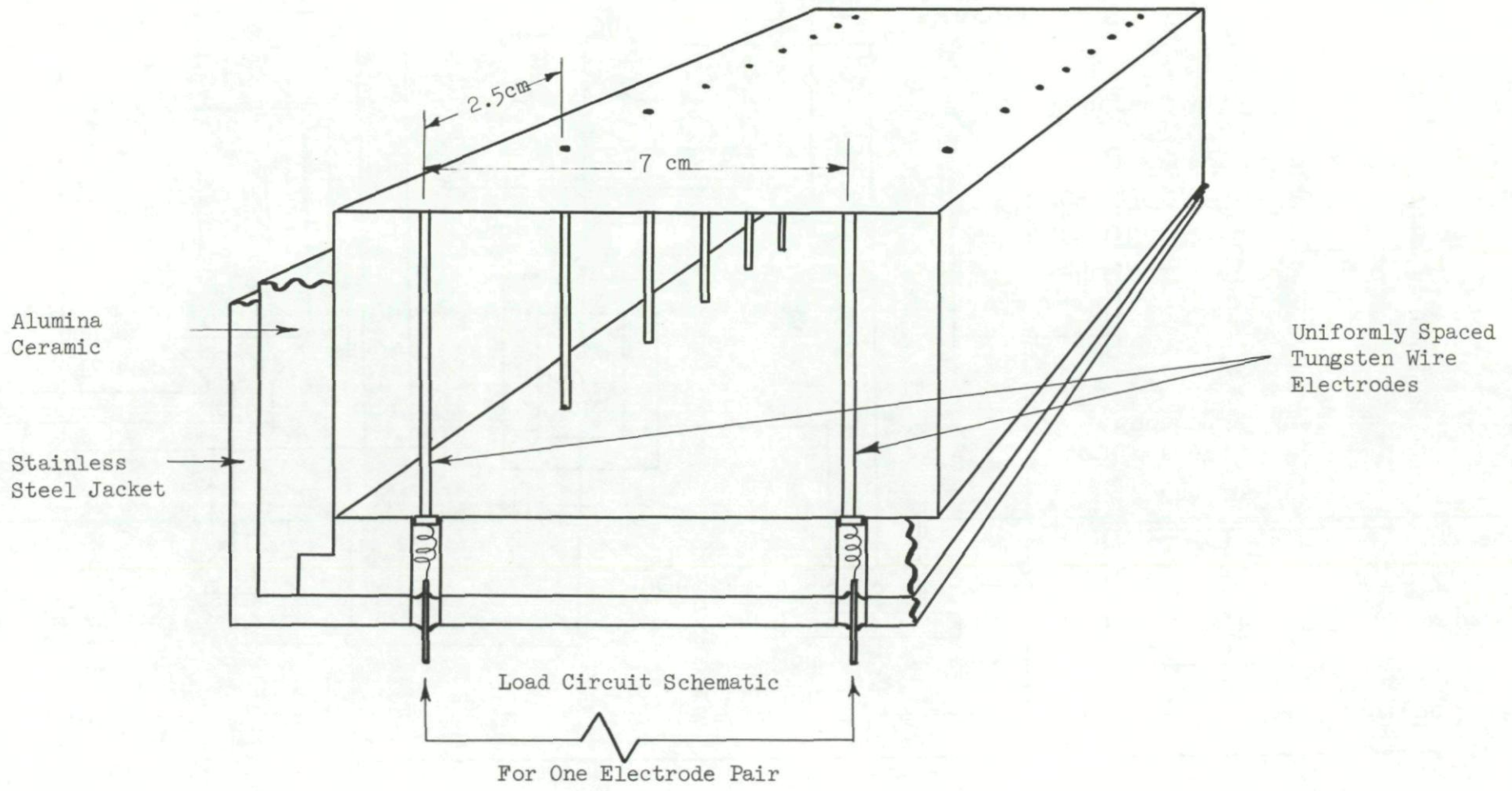


FIGURE 5 SEED INJECTION SYSTEM.

FIG. 6 INITIAL CHANNEL DESIGN: SEGMENTED ELECTRODE FARADAY GENERATOR  
(Composite View of One of Six Identical Sections)



## PLASMA RESEARCH IN DENMARK

Professor K. Refslund  
 Fluid Mechanics Department  
 Technical University of Denmark  
 Copenhagen, Denmark

Advanced plasma research in Denmark is concentrated in the Physics Department of the Danish Atomic Energy Station at Risø. Three important pieces of equipment are at present under test.

- a. A Q-machine is used for studying wave-instabilities in Ka-plasma. The parameters are measured by Langmuir-probes. Machine data: Magnetic field: 8-10 kGauss

Distance between emitters: 103 cm.

- b. Propagation of a spark-driven plasma shock.

The plasma is created by spark-shortening a capacitor-bank over two parallel slabs of brass placed in vacuum. Observations are made by smear camera and by mass-spectrometer. The following gases have been used: N<sub>2</sub>, Ne, Ar and He.

- c. A homopolar machine with a fast acting gas valve, called a "puffatron", is used for studying rotating high energy

plasma. Machine data:  $B_{\text{mirror}}$  : 60 kGauss

$B_{\text{intersection}}$  : 40 kGauss

$n$  :  $\sim 10^{21} / \text{m}^3$

$T_{\text{ions}}$  : 1 - 2 kev.

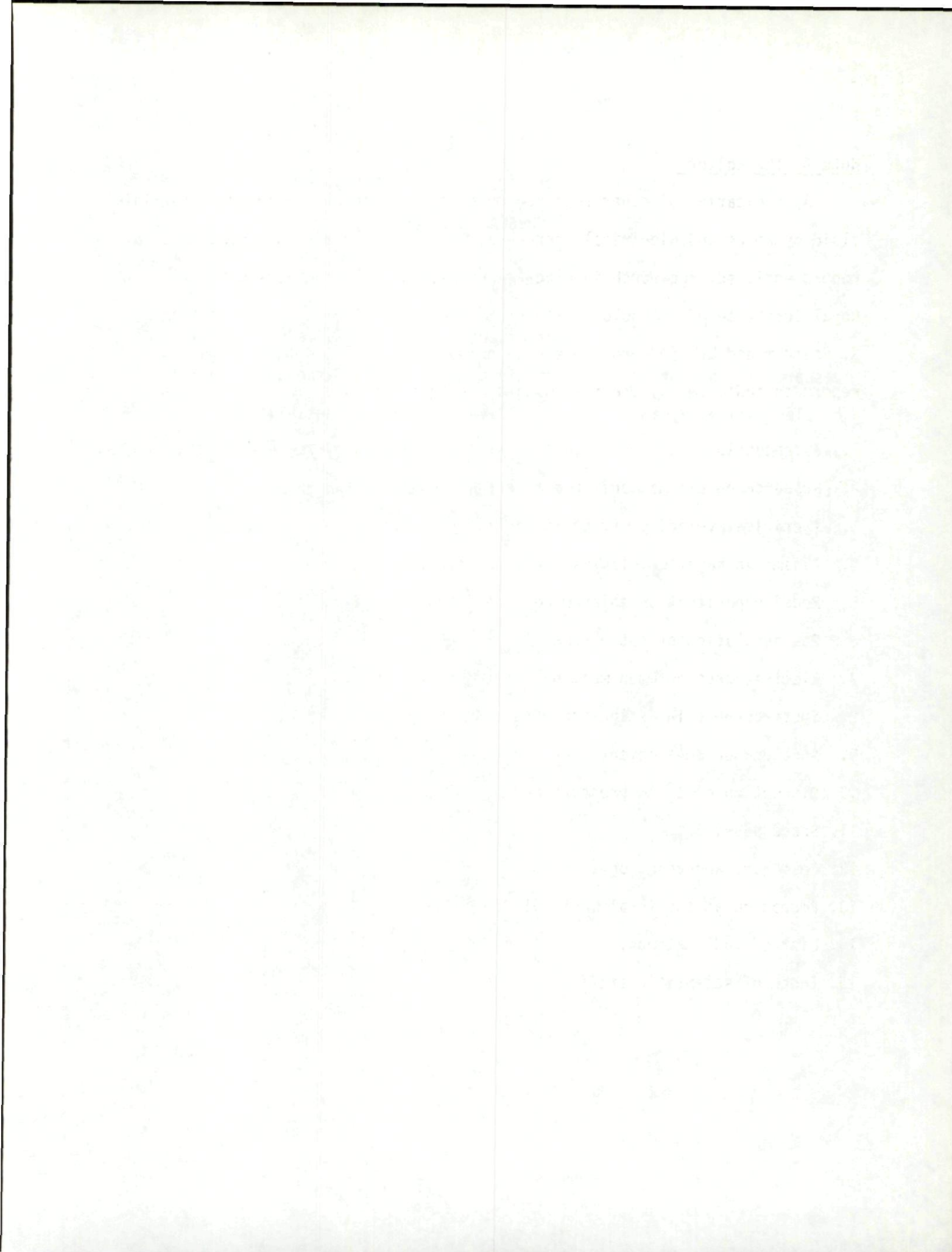
---

Note By The Editors

As indicative of other research going on in Scandanavia in areas combining fluid dynamics and electrical phenomena, Professor Refslund has sent us a report entitled: "Research in Electron Physics and Plasma Physics at the Royal Institute of Technology, Stockholm, Sweden" dated May 1967: Editors: R. Böstrom and L. Lindberg: Reference number 67-04. The nature of the report is indicated by the following table of contents:

1. Introduction.
2. Research on plasma confinement.
3. A critical velocity effect in partially ionized gases.
4. Plasma in parallel electric and magnetic fields.
5. Model experiment on solar-wind magnetosphere interaction.
6. Gas insulation of hot plasma.
7. Electric arcs between melting electrodes.
8. Spectroscopic investigation of a rotating plasma.
9. Accelerator development.
10. Disruption of a low pressure mercury plasma.
11. Space physics.
12. Cosmogony and cosmology.
13. Education at the Royal Institute of Technology.
14. List of publications.
15. Index of scientific staff.





COMMENTS ON ELECTROFLUID DYNAMICS  
AND RELATED RESEARCH IN FRANCE

Summary

In France various laboratories are working on plasmadynamics but the research is more of the magnetofluid dynamic type. Although the field of electrofluid dynamics is little developed, its potentialities seem very promising, in particular for space applications. Two French laboratories are working in the field of ion propulsion and this work is briefly described.

## COMMENTS ON ELECTROFLUID DYNAMICS AND RELATED RESEARCH IN FRANCE

Jean Fabri  
Chief, Non-Chemical Propulsion Division  
Office National d'Études et de Recherches Aérospatiales  
Chatillon-sous-Bagneux, France

In France various laboratories are working on plasmadynamics, but the experimental set-ups generally use magnetic fields, and the research is more of the magneto-fluid dynamic type. The field of electrofluid dynamics is not much developed in France, although the potentialities of EFD seem very large and promising, in particular for space applications.

The work that seems the most closely related to EFD is the research in progress on ion acceleration. Two laboratories are working in this field: the Centre d'Études Nucléaires de Saclay (CEN) where a very efficient team is studying the fundamental processes of ion acceleration and the possibilities of obtaining a uniform high speed neutral plasma beam; and the Office National d'Études et de Recherches Aérospatiales (ONERA) where more applied research is going on, the ultimate aim being the design of an attitude control thruster for space applications.

The ONERA ion engine is shown on Fig. 1: this is a conventional Kaufmann electron bombardment mercury ion source with extraction and acceleration grids. The engine was operated without any major difficulty for 100 hours in a low density chamber. The main results are shown on Fig. 2. The future development of this research will follow a more technical path; the long durations required for space attitude control call for solutions in which the wear of every element is reduced as much as possible. It appears however, that EFD

might be a very interesting field of research, due namely to the high efficiencies achieved and also to the low pressure level at which these propulsion devices operate and the small wear of the engine.

EFD energy conversion devices seem well fitted for space applications, and the high voltages obtained could be used directly in the ion thrusters, for example. It is hoped that EFD energy conversion will be developed during the coming years, and that space power of sufficient power level will be available on spacecraft of the future.

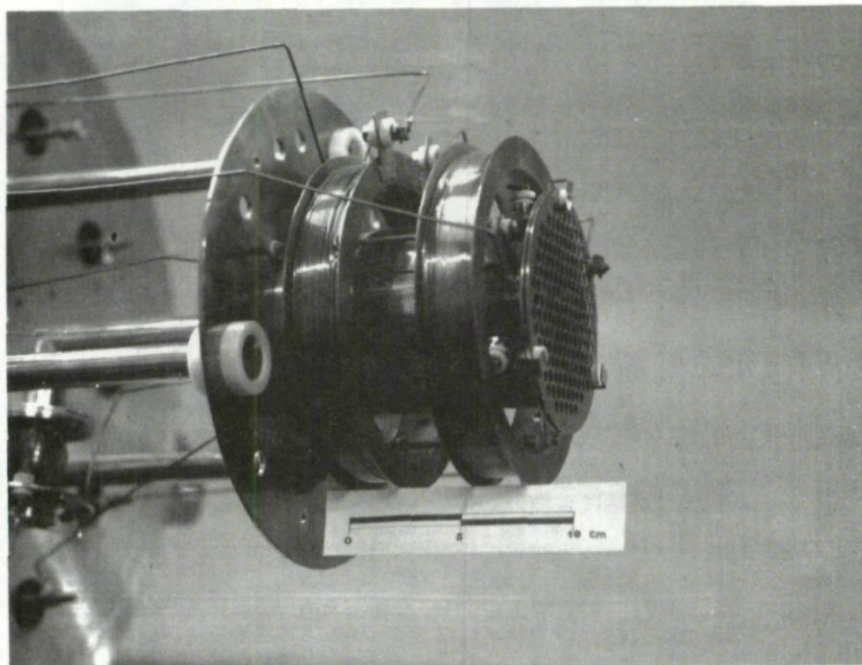


Fig. 1 - ONERA Mercury Ion Thrustor

Specific Impulse	4000 to 6000 sec
Estimated Thrust	$2.5 \cdot 10^{-3}$ N
Exhaust Velocity	50 km/sec
Mercury Mass Flow Rate	0.25 gr/hr
	$\frac{N_{\text{neutral}}}{N_{\text{ions}}} = 0.70$
Efficiency	$\frac{W_{\text{beam}}}{W_{\text{total}}} = 0.35$
Overall power requirement	180 w
Test Duration	100 hr

Fig. 2 - Performance of the ONERA Mercury Ion Thrustor.

THE ELECTROFLUID DYNAMIC ENERGY CONVERTER  
WITH SPACECHARGE NEUTRALIZATION

Summary

This paper is concerned with a device which would eliminate the biggest disadvantage of the electrofluid dynamic (EFD) converter, namely its operation at very high voltage. The question, in which the first-named author was interested about ten years ago, was whether one could get rid of the space charge and design a converter which has its space charge neutralized, and therefore would operate at any voltage desired. In recent years this idea was taken up in the Hall accelerator which can be considered a space charge neutralized ion engine. After a short introduction to the various types of EFD energy converters, the basic difference between the space charge limited and the space charge neutralized operation is pointed out. The importance of a magnetic field on the mechanism of space charge neutralization is described. The equation of flow and of the forces which act in a space charge neutralized converter are derived. Test results which prove that space charge neutralization is possible, are presented.

THE ELECTROFLUID DYNAMIC ENERGY CONVERTER  
WITH SPACECHARGE NEUTRALIZATION

Eugen Knoernschild and Peter A. Schoeck  
Institut für Energiewandlung und Elektrische Antriebe  
Deutsche Versuchsanstalt für Luft-und Raumfahrt  
Stuttgart, Germany

Introduction

In the field of direct conversion of flow energy into electric energy and vice versa, one distinguishes between two major types of converters: MHD converters and electrostatic converters. This classification is based on the concept that: in the first type electromagnetic forces; in the second type electrostatic forces are responsible for the conversion process. Actually, this conventional terminology is not quite accurate, for, depending on the approach, one may show that in certain types of MHD converters it is an electrostatic field which causes acceleration of ions and (because of momentum transfer by collisions) of the flow. Thus, perhaps the distinction between spacecharge neutralized and spacecharge limited converters would seem more exact. It is the objective of the present study to investigate the phenomenon of spacecharge neutralization in so-called fluid dynamic energy converters, i.e., electrostatic converters working on the principle of ion convection against an electric field (generator) or by an electric field (accelerator). This type of converter may be subdivided into ballistic devices and non-ballistic devices.

In the first species the charge carriers behave like individual

projectiles; in the second species their flow is governed by the laws of thermodynamics, i.e., collisions occur accomplishing, if not a statistical energy distribution, at least a random motion of the particles.

Ballistic generators suffer from the shortcoming that the kinetic energy of the individual particle is limited by the chemical energy of available fuels which is of the order of 1 eV. Hence, the voltage which can be obtained is limited to the order of 1 V unless many neutral molecules are clustered about one elementary charge. Ballistic accelerators on the other hand serve the purpose of achieving high particle velocities by applying excessive voltage; and have been successfully used, as has been demonstrated since decades in numerous laboratory experiments, and recently in the well-known ion engine.

The non-ballistic generator enables higher voltages than the ballistic generator provided a sufficient number of neutral particles are contained in the flow which transfer momentum to the ions to be dragged against the applied electric field. The application of this viscous drag principle is of course equally possible in the case of the accelerator.

Our present study considers only the non-ballistic converter. The approach starts with a brief consideration of the spacecharge limited electrostatic converter whereupon the implication of spacecharge neutralization on the performance is discussed. Then, the mechanism of spacecharge neutralization, the motion of the charge carriers, and the effect of a transverse magnetic field is investigated.

#### Ion Convection With and Without Space Charge

A simplified theoretical model shall be postulated:



1. The flow is frictionless and one-dimensional.
2. The current is carried by the convective flow of positive ions only.
3. The ion velocity is equal to the flow velocity.

The equations for conservation of charge, mass, momentum, and energy are:

$$\rho V A = I \quad (1)$$

$$\delta V A = \dot{M} \quad (2)$$

$$\delta V \frac{dv}{dx} + \frac{dp}{dx} - \rho E = 0 \quad (3)$$

$$\delta V \frac{d}{dx} \left( i + \frac{V^2}{2} \right) - jE = 0 \quad (4)$$

These equations shall first be applied to the spacecharge limited electrostatic generator. In this case  $\rho$ , which is the ion density responsible for the current, represents a positive spacecharge. It is connected with the electric field  $E$  through Poisson's equation:

$$\frac{dE}{dx} = \frac{\rho}{\epsilon} \quad (5)$$

From (3) and (4) it follows

$$\rho/\delta = \text{Const} \quad (6)$$

Integration of the momentum equation (3) becomes particularly simple for the case  $V = \text{const}$ . It yields with (5):

$$\frac{p_1 - p_2}{p_1} = \frac{\epsilon}{2p_1} (E_1^2 - E_2^2) \quad (7)$$

An upper limit for the pressure drop  $p_1 - p_2$  is given by the conditions  $E_1 = E_b$  and  $E_2 = 0$  where  $E_b$  corresponds to the breakdown field strength.

Since for gases at atmospheric pressure  $E_b = 10^6$  to  $10^7$  V/m we receive:

$$\frac{p_1 - p_2}{p_1} \approx 10^{-4}$$

a value which demonstrates the limitation of the non-neutralized electrostatic generator, namely too small a pressure drop to make the device attractive from the view point of thermodynamic cycle efficiency.

Because of this small permissible pressure drop the flow through the conversion section of a non-neutralized electrostatic generator may be treated as incompressible, i.e., constant thermodynamic state may be assumed. The output voltage for this case is

$$U (\ell) = \rho_1 \frac{\ell^2}{2\epsilon_0} \quad (8)$$

which with (1) yields for the power flux

$$\frac{UI}{A_1} = \frac{1}{2\epsilon_0} \rho_1^2 \ell^2 V_1 \quad (9)$$

The maximum possible value  $\rho_1 \ell$  is again limited by the break-through voltage through the relation

$$E_b = \frac{\rho_1 \ell}{\epsilon} \quad (10)$$

as may be derived from (1) to (5) assuming constant thermodynamic properties. If we assume an air flow of  $V_1 = 1000$  m/s which has been expanded through a nozzle to atmospheric pressure, the power flux in the generator is limited to approximately  $10^6$  W/m<sup>2</sup> as follows from (9) and (10) with  $E_b = 10^7$  V/m.

Next the spacecharge neutralized electrostatic generator shall be

considered. In addition to the above simplifying assumptions we conceive a mechanism by which electrons immersed in the fluid are held fixed in place relative to an outside observer. The number of electrons shall equal the number of positive ions which means that the spacecharge is zero. No interaction shall be assumed between the electrons and the particles which constitute the flow in this ideal model. Then equations (1) to (4) are still valid, however, with the understanding that  $\rho$  (ion density) does not generate a spacecharge. With this change of the meaning of the symbol  $\rho$ , equation (5) does not hold any more. It is replaced by

$$E = U/\ell \quad (11)$$

Considering again the special case  $v = \text{const.}$ , integration of the momentum equation (3) yields

$$\frac{p_1 - p_2}{p_1} = \frac{E}{p_1} \int_1^2 \rho dx \quad (12)$$

Contrary to the non-neutralized case,  $E$  is now independent of  $\rho$ . Hence, for a prescribed value of  $E$  - which of course is again limited by the breakdown field strength - the pressure drop  $p_1 - p_2$  is not limited. This implies that thermodynamic considerations are not prohibitive for the application of this type of generator, provided the latter is practically feasible. As is readily recognized, the power flux is also not limited, unlike the situation in the non-neutralized case.

While the foregoing discussion pertains to the generator, an analogous argument may be applied to the accelerator case. In the spacecharge limited accelerator the applied electric field is also limited by the breakdown

field strength value.

### The Mechanism of Spacecharge Neutralization

Let us first consider the situation for the short-circuit case of a spacecharge-neutralized converter. A neutral plasma may enter the conversion section (fig 1)

$$n_e = n_i \quad (13)$$

in which electrons and ions have the same velocity

$$V_i = V_e \quad (14)$$

from which follows

$$n_e V_e = n_i V_i \quad (15)$$

Beginning at the entrance of the conversion section the electrons may be slowed down by some imaginary external force about whose nature no statement shall be made at this point.

Because of the slowing down of the electrons, within the conversion section the inequality

$$V_e < V_i \quad (16)$$

holds, giving rise to a net current

$$j = en(V_i - V_e) \quad (17)$$

Obviously, inside the converter the net current is carried by positive ions. In the outside branch of the circuit the current is an electron current. The situation is schematically pictured in fig. 1. The assumed imaginary force denoted by  $K_1$  slowing down the electrons represents a flow resistance giving rise to an entropy increase of the flow, while the total flow enthalpy remains constant since no electric energy is extracted.

From the above it follows that the converter under discussion suffers a priori from an inevitable internal loss arising from the necessity of reducing the velocity of the electrons in order to produce a net positive current in the downstream direction.

Now we proceed to the generator case by putting a resistance into the external branch of the circuit, giving rise to an electric field pointing upstream inside the converter (fig.2). This resistance necessarily decreases the electron current in the outside branch and, because of the electric field, also the ion current in the converter. However, it increases the negative electron current inside the converter. If the resistance is increased to finally becoming infinite (open circuit) the positive ion current and negative electron current inside the converter equal each other in magnitude, i.e.,  $j = 0$ .

As long as the resistance in the outside branch has a finite value, electric power is generated. This fact requires the existence of a force  $K_{II}$  per unit volume acting in the upstream direction in the converter section such that (in the special case of constant velocity  $V_0$ )

$$K_{II} V_0 = IU \text{ (Watt)} \quad (18)$$

If we put a power source (instead of a resistance) into the outer branch, providing a negative potential downstream of the conversion duct, the ion flow is accelerated and the electron flow decelerated, forcing a large fraction of the electron flow into the outer branch, where it is lifted by means of the power source (battery) up to the negative potential downstream of the conversion duct (see fig. 3)

It may be mentioned that, if only the applied electric field  $E^*$  would act upon the ions and electrons contained in a volume element, no net force upon the center of gravity would result because

$$\begin{aligned} K_i &= enE^* \\ K_e &= -enE^* \end{aligned} \tag{19}$$

would cancel each other.

Obviously, since  $K_I$  and  $K_{II}$  are directed upstream in the case of the generator, the motion of the electrons due to the applied electric field  $E^*$  is slowed down. The resulting electron velocity is therefore

$$V_e = V - \mu_e E^* + \frac{\mu_e}{en_e} (K_I + K_{II}) \tag{20}$$

with  $\mu_e$  representing electron mobility and  $K_I/en_e$ ,  $K_{II}/en_e$ , respectively the fields corresponding to the forces  $K_I$  and  $K_{II}$ .

The result of the foregoing may be summarized as follows:

Decreasing the electron current below the value it would have due to the applied electric field  $E^*$ , is equivalent to a net force in the field direction upon a neutral plasma.

Applying this rule to the accelerator, where the field points downstream, a net force  $K_{II}$  is produced in the downstream direction by decreasing the electron current below the value it would have due to the applied field.

In the generator  $K_I$  and  $K_{II}$  both point in the same direction, namely upstream. In the accelerator, on the other hand,  $K_I$  points upstream while

$K_{II}$  points downstream. The case  $K_I = K_{II}$  in the accelerator represents the situation where the accelerating force  $K_{II}$  produced by a field in the downstream direction just compensates the retarding force  $K_I$  necessary to produce the outer circuit current as explained above. In other words, the applied power just compensates for the inevitable internal loss.

The change of the velocity vectors of ions and electrons in the generator and in the accelerator is qualitatively shown in fig. 4. It is noted that starting from the short-circuit condition, the magnitude of the electron velocity in the accelerator first decreases to zero with respect to an outside reference system. From there on it increases again after having changed its direction, giving rise to a now positive electron current. From a comparison of fig. 4b and 4f, it is seen that in the generator the net current is always caused by a surplus of ion current, while in the accelerator this is not necessarily the case, i.e., an excess of electron current is well possible.

#### The Effect of a Transverse Magnetic Field

In the previous section two forces  $K_I$  and  $K_{II}$  were introduced about whose origin no statement was made. However, anticipating their nature, we assumed that they are attached to the electrons rather than to the ions or to the neutrals. The first force  $K_I$  retards the electrons with respect to the flow of the neutral plasma. It acts even in the absence of an applied electric field. The second force  $K_{II}$  becomes effective only after the application of an external electric field, and opposes the motion of the electrons due to this field.

The question now arises as to how such forces may be produced. To our

present knowledge only a magnetic field transverse to the flow respectively to the applied electric field can give rise to forces acting solely - or more exactly - acting primarily upon the electrons (the effect upon the ions is negligible) contained in the plasma.

As is well understood, the electrons are deflected in perpendicular direction to the flow and to the applied magnetic field whereby the electron velocity transverse to the magnetic field is reduced. As is also well known, this peculiarity of the electrons is caused by their high mobility compared to that of the ions, which in connection with an applied magnetic field gives rise to the condition

$$\omega_e \tau_e \gg \omega_i \tau_i \quad (21)$$

This condition forms the basis for MHD power conversion. A complete discussion of the resulting motion of the charge carriers in the x-direction and y-direction, the production of secondary electric fields and currents whose self-magnetic field in connection with the applied magnetic field produces a magnetic pressure gradients etc., is not intended in connection with this treatise.

It may suffice to say that by calling upon a transverse magnetic field in order to achieve the effects required for power conversion, our spacecharge neutralized electrostatic converter has become the well-known Hall converter. In fact, the Hall converter has previously been recognized as a special form of an electrostatic converter.

Let us now identify the forces  $K_I$  and  $K_{II}$  appearing in the equations pertaining to the Hall converter.



The effective electric fields as experienced by electrons and ions respectively moved across a magnetic field  $B$  having velocities  $V_e$  and  $V_i$  respectively are:

$$(\bar{E}_{\text{eff}})_e = \bar{E}^* + [\bar{V}_e \times \bar{B}] \quad (22)$$

$$(E_{\text{eff}})_i = \bar{E}^* + [\bar{V}_i \times \bar{B}] \quad (23)$$

We assume a rectangular coordinate system:

$$E^* = (E_x^*, E_y^*, 0) \quad (24)$$

$$V_e = [V - \mu_e (E_{\text{eff}x})_e, -\mu_e (E_{\text{eff}y})_e, 0] \quad (25)$$

$$V_i = [V + \mu_i (E_{\text{eff}x})_i, +\mu_i (E_{\text{eff}y})_i, 0] \quad (26)$$

$$B = (0, 0, B_z) \quad (27)$$

Using the definition of  $\mu_e$

$$\mu_e = \frac{e}{m_e} \tau \quad (28)$$

and considering that

$$\beta = \omega\tau = \frac{eB}{m} \tau = \mu B \quad (29)$$

one obtains from (22) to (29) for the field acting on the electrons:

$$(E_{\text{eff}x})_e = E_x^* - \frac{\beta_e^2}{1+\beta_e^2} E_x^* + \frac{\beta_e}{1+\beta_e^2} VB - \frac{\beta_e}{1+\beta_e^2} E_y^* \quad (30)$$

$$(E_{\text{eff}y})_e = E_y^* - \frac{\beta_e^2}{1+\beta_e^2} E_y^* - \frac{1}{1+\beta_e^2} VB + \frac{\beta_e}{1+\beta_e^2} E_x^* \quad (31)$$

For the field acting on the ions, we have, since  $\beta_i \approx 0$  (no coupling

with the magnetic field)

$$(E_{\text{eff}x})_i = E_x^* \quad (32)$$

$$(E_{\text{eff}y})_i = E_y^* - VB \quad (33)$$

Since we intend to apply only an electric field in the x-direction,  $E_y^* = 0$ , and we obtain:

$$(E_{\text{eff}x})_e = E_x^* - \frac{\beta_e^2}{1+\beta_e^2} E_x^* + \frac{\beta_e}{1+\beta_e^2} VB \quad (34)$$

$$(E_{\text{eff}y})_e = -\frac{1}{1+\beta_e^2} VB + \frac{\beta_e}{1+\beta_e^2} E_x^* \quad (35)$$

$$(E_{\text{eff}x})_i = E_x^* \quad (36)$$

$$(E_{\text{eff}y})_i = -VB \quad (37)$$

Obviously the second term on the right side of (34) corresponds to a decelerating force which we may call  $K_{II}$

$$K_{II} = \frac{\beta_e^2}{1+\beta_e^2} neE_x^* \quad (38)$$

Similarly the third term on the right side of (34) represents a force  $K_I$

$$K_I = -\frac{\beta_e}{1+\beta_e^2} ne VB \quad (39)$$

The change of sign between (38) and (39) with respect to (34) occurs because  $K_I$  and  $K_{II}$  act on the electrons which have negative charge. For

a given  $V$  and  $B$  the factors  $\beta_e/1+\beta_e^2$  and  $\beta_e^2/1+\beta_e^2$  are indicative of the retarding forces  $K_I$  and  $K_{II}$ . As  $\beta_e \rightarrow \infty$ ,  $K_I \rightarrow 0$  and  $K_{II} \rightarrow n_e e E_x^*$ .

The fact that  $K_{II}$  becomes zero under this condition may be interpreted in such a way that for  $\beta_e = \infty$  the electrons do not undergo collisions. As a consequence, no force is required for retarding their motion with respect to the flow. The force  $K_{II}$ , on the other hand, compensates in the case  $\beta_e \rightarrow \infty$  for the electric field force completely. Thus  $(E_{\text{eff}x})_e = 0$ , i.e., the electron sees no electric field for  $\beta_e = \infty$ .

Note that our spacecharge neutralized converter, as conceived in the foregoing, is an electrostatic converter based on a differential convection of positive and negative charge carriers by means of a flow in the  $x$ -direction. Hence, the current in the  $y$ -direction is not used for obtaining power, respectively for adding power, as is the case with a Faraday converter. If the current in the  $y$ -direction is prohibited by providing insulating walls, polarization of the plasma entering the region of the magnetic field takes place. The accumulation of positive, respectively, negative charges on two opposing walls generates a field (according to the Poisson equation), which compensates for the Hall field in the  $y$ -direction. Hence,  $(E_{\text{eff}y}) \rightarrow 0$  and we obtain from

$$VB = \beta_e E_x^* \quad (40)$$

which, if introduced into (30) yields

$$E_{\text{eff}x} = E_x^* \quad (41)$$

In other words, preventing an electron drift perpendicular to the flow direction makes both forces  $K_I$  and  $K_{II}$  vanish.

#### Experimental Verification

In the Institut für Energiewandlung und Elektrische Antriebe of the Deutsche Versuchsanstalt für Luft- und Raumfahrt, Stuttgart, an electrofluid dynamic energy converter operating on the principle of spacecharge neutralization was tested in November 1967.

The plasma was generated in a Hall-accelerator, which is able to produce a plasma-jet of up to 30 km/sec velocity. The principle of operation of this accelerator can be seen from fig. 5. The plasma is generated at a pressure of  $10^{-2}$  torr by means of a low voltage discharge with a glow cathode, and is accelerated within an annular space, with the magnetic field oriented radially and the electric field along the axis of the device. At the end of the acceleration region an electron emitter is positioned which provides the electrons for space charge neutralization.

The accelerated plasma is decelerated in a device which is positioned after the accelerator. The electric power generated is equivalent to the decrease of kinetic energy of the working medium.

In Fig. 6 and 7 test results are presented. Fig. 6 shows power and current measured at the energy converter. Fig. 7 shows a relation between power consumed in the accelerator and power extracted in the decelerator. The maximum current measured in the accelerator was about 6 amperes, in the decelerator about 2 amperes. The spacecharge-limited current is only  $10^{-4}$  of these values, indicating the effectiveness of spacecharge neutralization. From the results of the experiments the conclusion can be drawn

that space charge neutralized energy conversion of a jet of ions is possible.

The maximum potential which the ballistic type of energy converter is able to sustain, follows from the energy equation:

$$eU = \frac{m}{2} v^2$$

If only thermal energy is available,  $U$  may be only 0.5 to 1.0 volt. However, very large currents should be obtainable.

In order to increase the potential above the purely thermal value of 0.5 to 1.0 volt, the drag effect of neutrals could be used. As is known, the ions can be dragged by collisions with neutrals and thus sustain a higher voltage. For instance, a potential of 20 or 50 volts requires that the degree of ionization does not exceed about 2% to 5%. Dragging the ions naturally requires the collision frequency, e.g., the gas pressure, to be sufficiently high, so that ion slip can almost be neglected. The question is now whether at pressures where ion slip is negligible, collisions with electrons can still be kept so small that the main feature of spacecharge neutralization, namely purely azimuthal motion of electrons, is at least to a large degree maintained.

For the preliminary tests discussed above, the pressure was so low (about  $10^{-2}$  torr), that the drag effect was probably very weak. Similarity considerations indicate that one condition for successful operation at higher pressures is to keep the  $\omega\tau$  value the same. In other words, an increased collision frequency has to be offset by a higher magnetic field. Since the presented experiments showed an optimum magnetic field of below 300 Gauss, a 20-fold increase of this field appears possible.

However, there may even be a field of application without using the drag effect of neutrals. Future high temperature gas-core reactors or fusion reactors will have a sufficiently high temperature that it is very likely to extract from the gaseous core of the reactor a beam of high-energy ionized atoms, whose energy could provide a considerable voltage at high currents in the energy converter.

## Symbols

A	Area
B	Magnetic Field
e	Electron Charge
E	Electric Field
E*	Applied Electric Field
h	Enthalpy
I	Electric Current
j	Current Density
K	Force
l	Length
M	Mass Rate
n	Particle Density
p	Pressure
U	Voltage
V	Velocity
x,y	Coordinates
$\beta$	Hall Parameter
$\delta$	Mass Density
$\epsilon$	Dielectric Constant
$\mu$	Mobility
$\rho$	Charge Density
$\tau$	Collision Frequency
$\omega$	Cyclotron Frequency

Subscript:

e	Electron
i	Ion
b	Breakdown

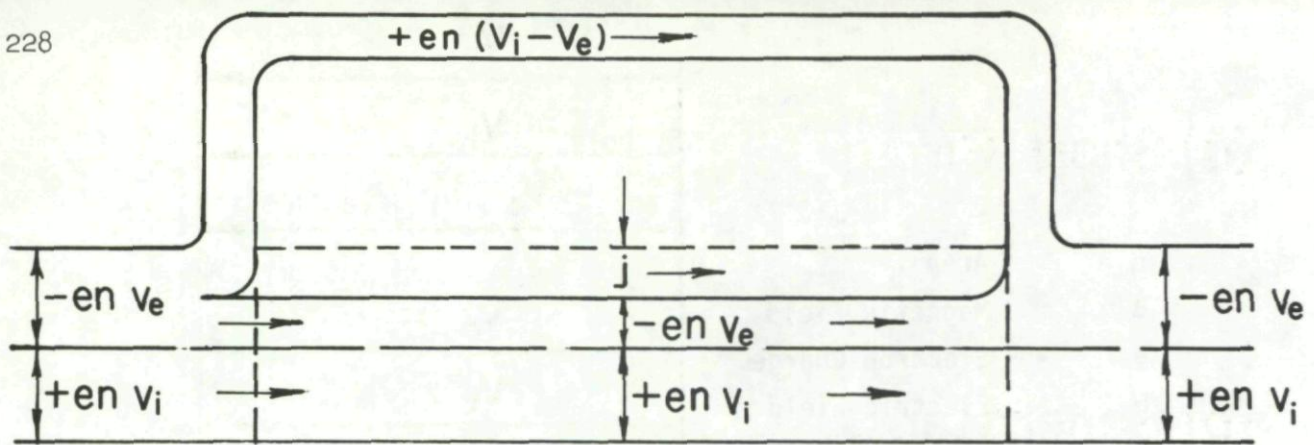


Fig. 1 Short Circuit

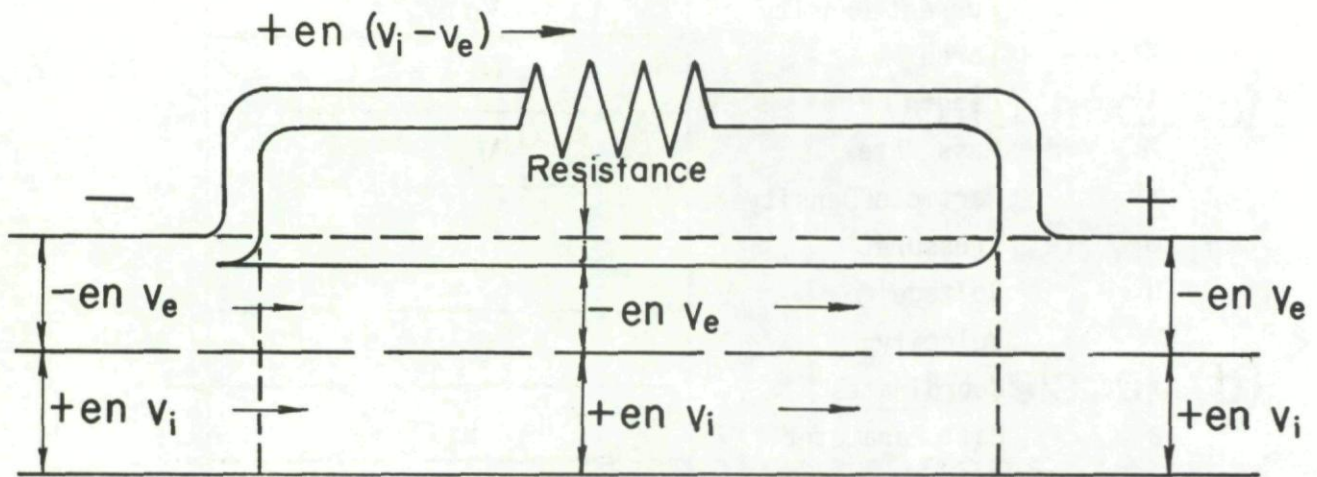


Fig. 2 Generator

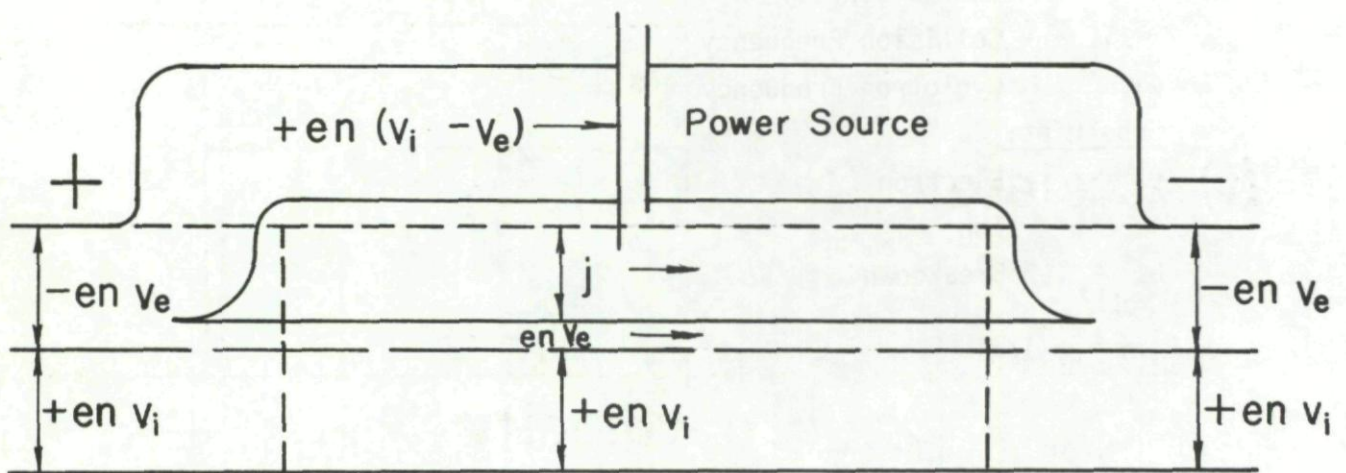


Fig. 3 Accelerator



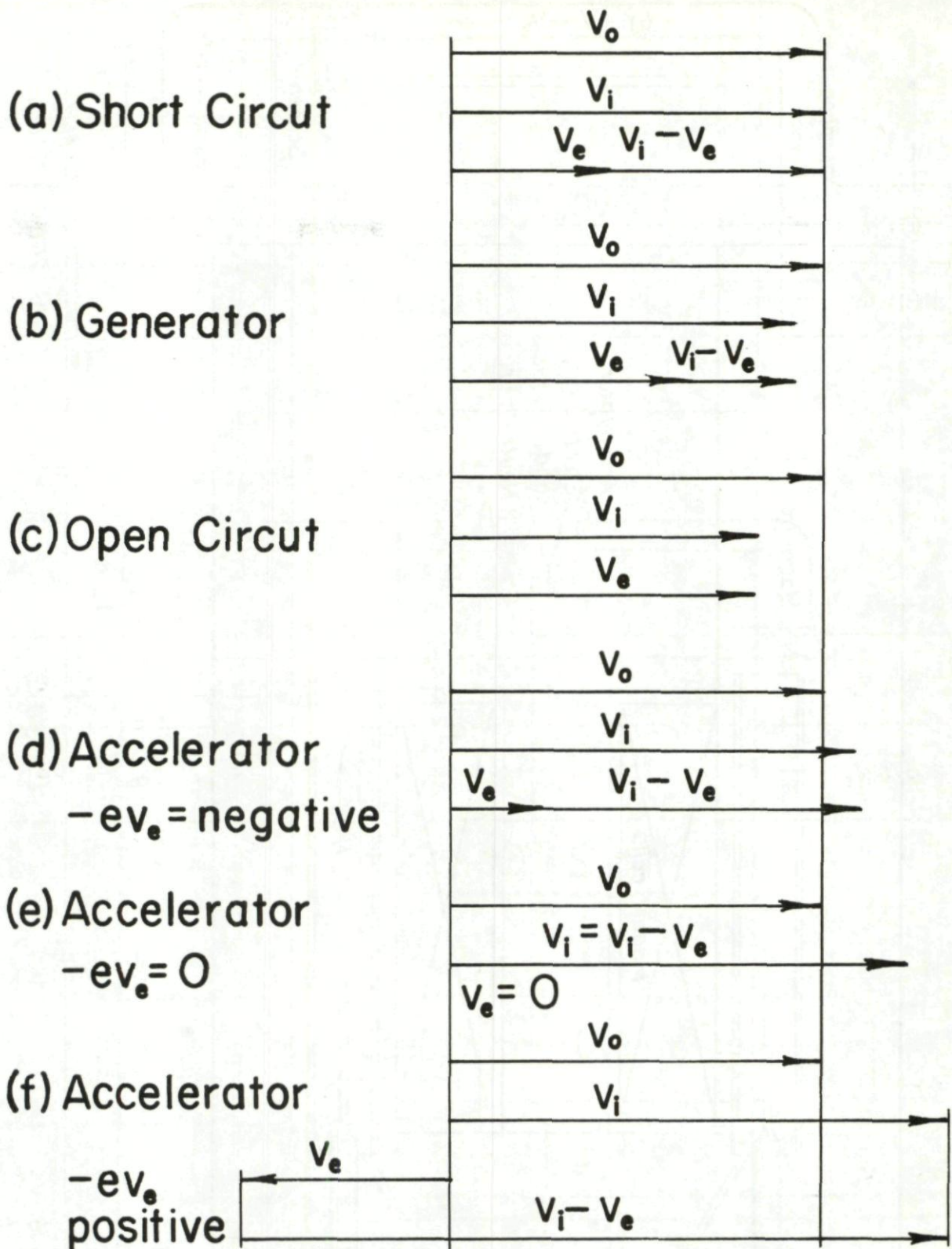


fig. 4 velocity vectors for various operating conditions

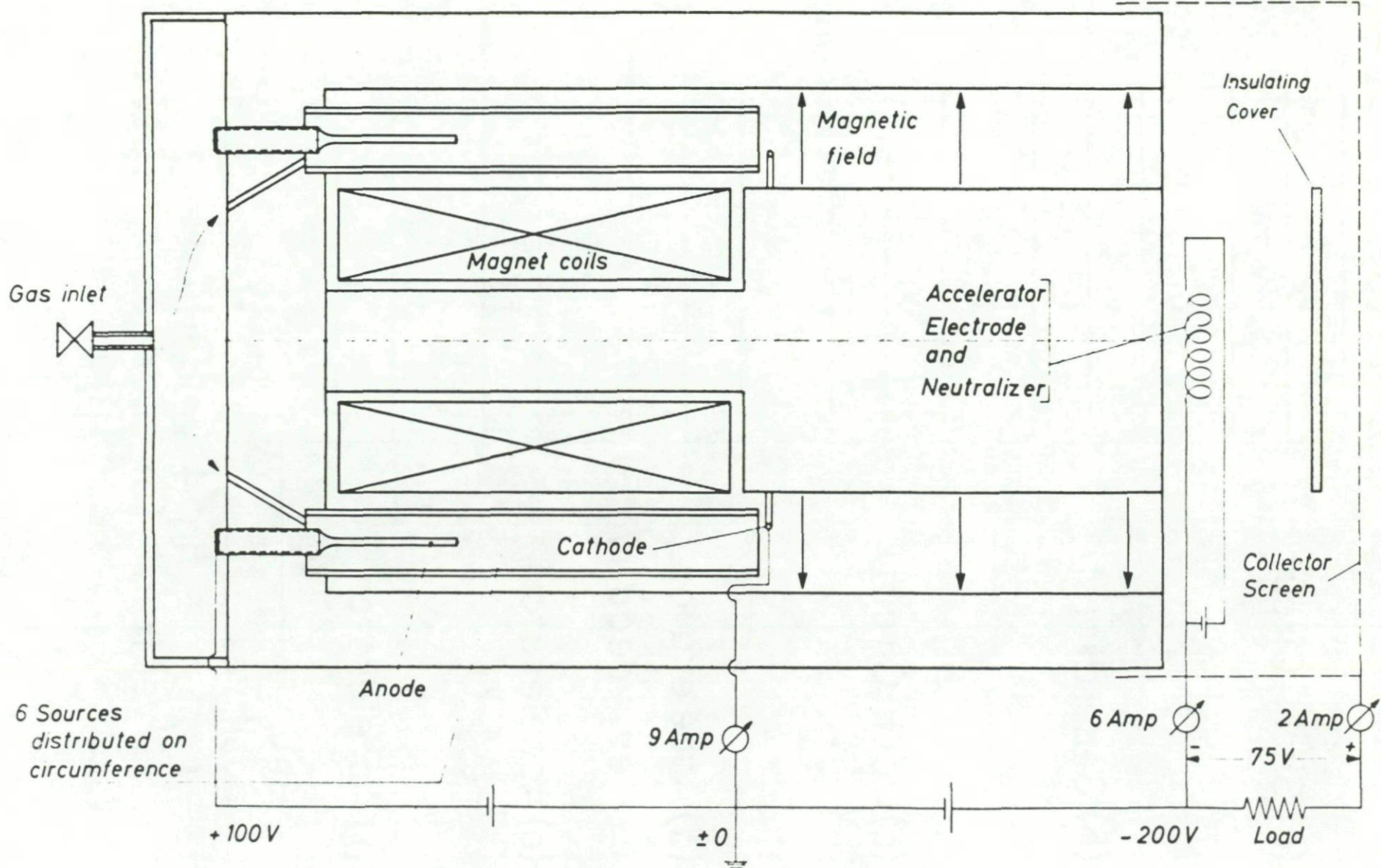


fig.5 schematic of test-set up

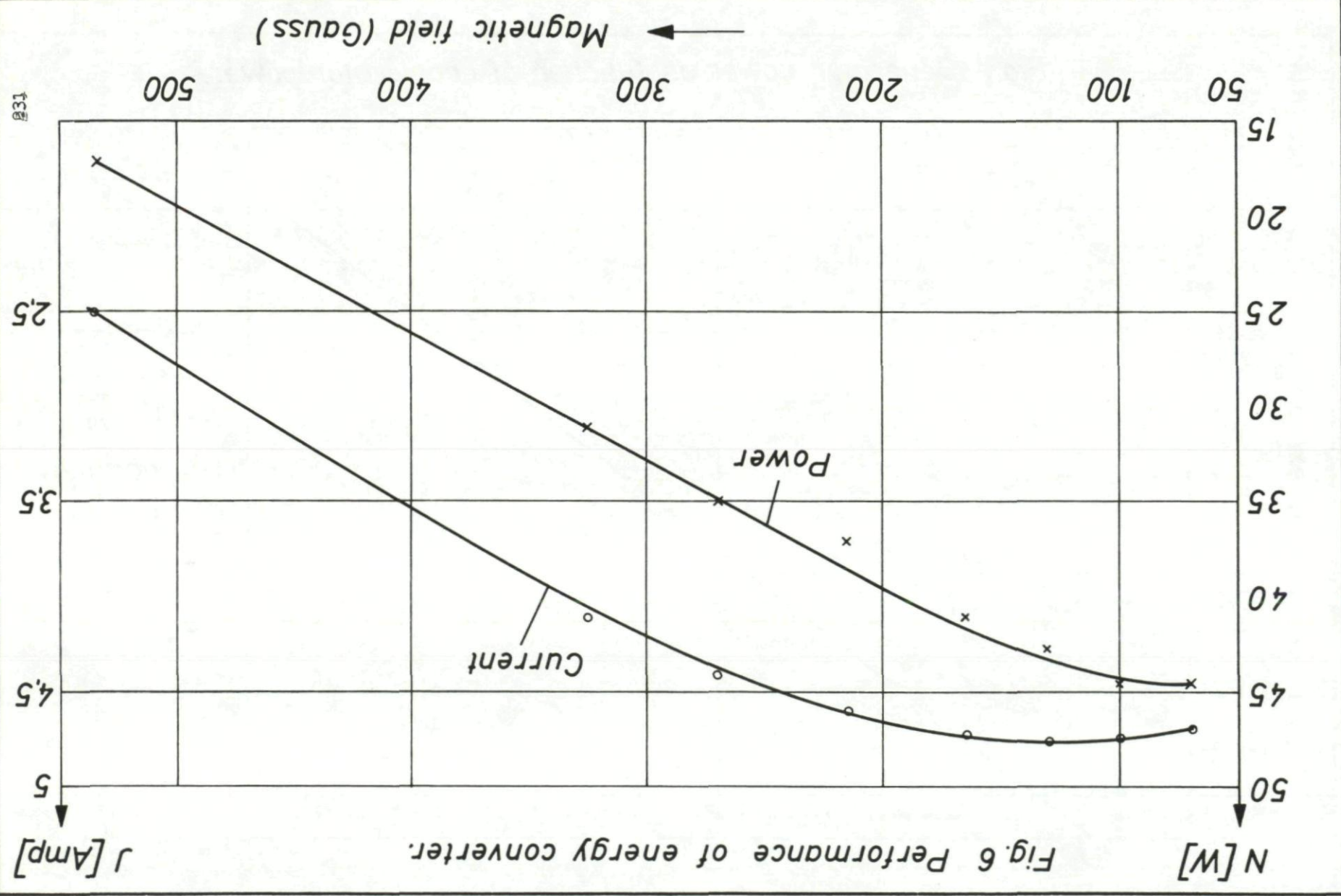


Fig. 6 Performance of energy converter.

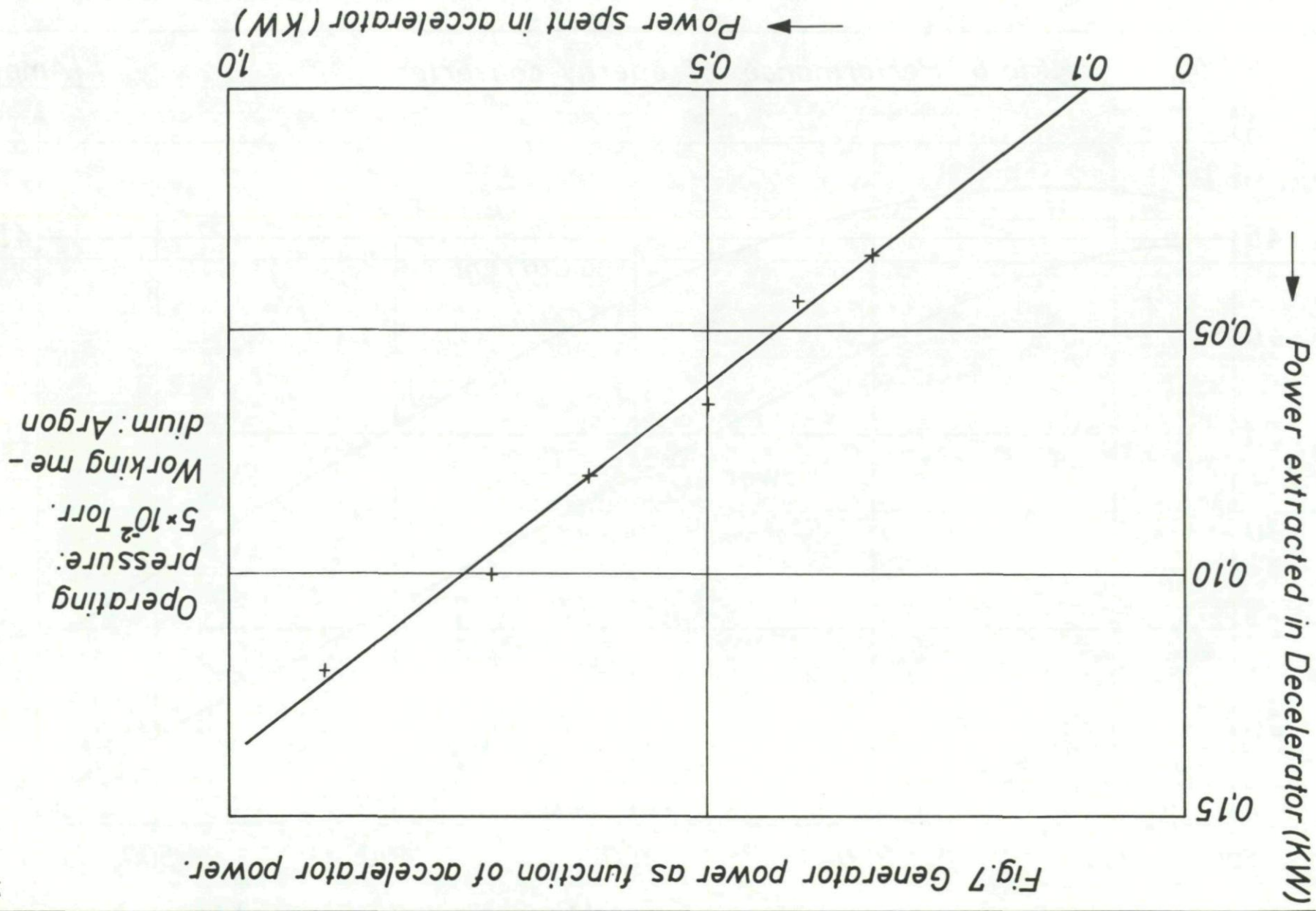


Fig.7 Generator power as function of accelerator power.

100

100

100

100

100

100

100

100

100

100

100

100

100

100

100

100

100

100

100

100

100

100

100

100

100

100

100

100

100

100

100

100

100

100

100

100

100

100

100

100

100

100

100

100

100

100

100

100

100

100

100

100

100

100

100

100

100

100

100

100

100

100

100

100

100

100

100

100

100

100

100

100

100

100

100

100

100

100

100

100

COMMENTS ON ELECTROFLUID DYNAMICS AND  
RELATED RESEARCHES IN ITALY

Summary

Although there is little research in electrofluid dynamics in Italy, there is growing interest. The author discusses broad interpretations of the complex phenomenology arising from the interaction between electric and fluid dynamic fields; and describes the approach of general studies that he and his group are doing.

COMMENTS ON ELECTROFLUID DYNAMICS AND  
RELATED RESEARCHES IN ITALY

by

L.G. Napolitano  
Director, Aerodynamics Institute  
University of Naples  
Naples, Italy

Before discussing briefly the nature of the researches which I am doing, I would like to make a few remarks from points of view which are somewhat different from those of the other European contributors.

We have been witnessing the presentation, illustration and discussion, from both the technical and technological points of view, of a new process of direct energy conversion. Much care has been exercised in the various presentations in clearly differentiating this process from others which may appear as competitors (such as the MFD process), and in even more clearly defining the place which it occupies in the spectrum of all possible energy conversion processes.

I believe that it is appropriate, at this stage, to point out that the work done by the group led by Dr. von Ohain, like all good pioneering work, opens up new areas of basic, applied and development research which go far beyond the original scope and motivation. You start playing with the possibility of balancing, in a fluid, inertia forces and forces resulting from a stress tensor with body forces of electrostatic origin; and soon you find yourself in the midst of a complex, multifaced phenomenology due to the interaction of

fluid dynamic and electrostatic field.

The initial idea of getting energy converted directly into electric energy gives new momentum to a new science: electrofluid dynamics. This science, which purports to study the interaction between fluid dynamic and electrostatic fields, has many other applications. One immediate instance is the process, so to speak, "opposite" to the energy conversion; when electric energy is fed into, rather than drained from, the fluid (and one could thus think of all applications related to fluid pumping or fluid acceleration). Other instances are given by the problems falling within the realm of what is sometimes called "ionospheric aerodynamics" (although the name may be misleading) (Ref. 1); by all those problems connected with the electrical behavior of weakly ionized gases flowing along solid boundaries [when electrical interaction between the gas and the solid accompanies the conventional interaction due to exchange of momentum and energy, (see Ref. 2, for instance)]; and so on. Of course there are many differences among these applications, and the range of values of pertinent non-dimensional parameters may differ widely. Yet the point that I am trying to make is that they have enough in common (the basic physical facts) to warrant closer connections, frequent exchanges and osmosis of fruitful ideas and techniques (both theoretical and experimental), and unified approaches which may lead to better understanding of the basic phenomena to mutual advantage. It is true, as Dr. von Ohain said, that the study of EFD is simpler than that of a plasma in a magnetic



field. However, as the very same Dr. von Ohain also said, it is not "that" simple and the complex phenomenology arising from the interactions between electric and fluid dynamic fields is certainly not yet well understood, nor, even less, mastered. Thus there are definite advantages for everybody in getting together and discussing the common fundamental facets of this new science.

And it is when one tries to emphasize the basic aspect of the science that the second point which I try to make comes out naturally.

I believe that the fine experimental rig at the Aerospace Research Laboratories has great potential applications for basic research outside and beyond the energy conversion process. We have indeed already seen some instances: basic research in the field of breakdown at higher pressure, or breakdown with seeding and/or additives, has been carried out already by the group of Dr. von Ohain and Mr. Lawson. But I am sure that much more can be done (and, of course this only goes to prove, again, how much merit the designers of the experimental rig have gained in the scientific community).

For instance, I believe that the rig could be exploited to measure transport coefficients (of mass, momentum energy and electric charges) in mixtures (even multiphase ones); and the influence thereupon of large electrostatic fields. That such type of information is badly needed, that its importance is invaluable, that it could foster, motivate and substantiate theoretical approaches, are all such self-evident facts that I do not need to further dwell on the subject.

Now I would like to briefly mention some of the researches which have been sponsored by the group of Dr. von Ohain and Mr. Lawson. They are essentially basic in nature and are concerned with the thermodynamic and fluid dynamic aspects of EFD. The principal aim is to be as general and as fundamental as possible, for the reasons already implied in what I have said above.

The first, and simplest, problem approached is that of quasi one-dimensional flow. Some particular cases of this problem had been treated already, however it was felt that it was not done with a sufficiently unified and general approach, which I had already proved to be useful and powerful in MFD (Ref. 3).

In short, the idea is that the study of the actual dynamic evolution of a fluid system should be preceded, as often as possible and feasible, by a thorough study of the properties of particular, relevant families of fluid dynamic states.

These properties are very interesting and may be very useful but, most important of all, are very general since they are independent of any specific dynamic evolution of the system. A harvest of a priori knowledge can thus be made available to any one who undertakes to study a particular evolution of the system, and very often, makes possible embedding it into a wider class of evolutions.

This general approach, obviously, is not always possible; we have shown, however, that it is so for electrofluid dynamics quasi-one-dimensional constant area flow.

Of special interest is the limiting case of isentropic trans-

formations, and I wish to elaborate a little upon the hypothesis of isentropicity and its practical implications.

Consider the number  $(v/kE)$  which has appeared again and again during this AGARD-graph and which has been interpreted either as the ratio of two characteristic velocities (the convective velocity  $v$  and the drift velocity  $(kE)$ ), or as the ratio of two electric fields. Those with a fluid dynamic background like to call it the electrical Reynolds number because it has the same structure and the same properties and features of the Reynolds number of classical fluid dynamics. From my point of view, which is more thermodynamically flavoured, I like to think of this number as a measure of the efficacy of entropy production. According to this interpretation, then, when this number is very large there is not "enough time" to produce an appreciable amount of entropy, and you will not have to "pay" anything for the transformation. One will thus have the maximum ideal efficiency for any such a transformation, for it will be isentropic.

The electrical Reynolds number is, in normal conditions, very large for the cases of charged colloid particles, because in that case the drift velocity is a small fraction of the mass velocity. Hence you have here a thermodynamic a posteriori proof of the validity of Dr. von Ohain and Mr. Lawson's initial idea to investigate the use of charged colloidal particles for the energy conversion process. Thermodynamics implies that this is the right direction to go because, everything else being equal, the electrical Reynolds number

will be much larger, the entropy production much smaller and the transformation itself will tend toward the ideal isentropic one.

By the above mentioned general approach one can also study the case when the electrical Reynolds number effects cannot be neglected and the states of the family have no longer the same entropy. As mentioned already, when the energy goes from the fluid into the electric field one may call the process "energy conversion". When it goes from the electric field into ordered kinetic energy of the fluid one may call the system an accelerator. If, finally, it goes from the electric field into "disordered" (i.e. thermal) kinetic energy of the fluid one may call the system a compressor or a diffuser or a pump. The subject approach will give thermodynamic ranges of existence and of good operating conditions for all of these processes in a general and unifying framework.

One can also discuss, in a most general way, choking conditions. Those familiar with fluid dynamics know that there would be some choking phenomena, that the Mach number is still an important parameter, and that at Mach number one some peculiar behaviour is expectable; all these aspects can be investigated thoroughly. Finally, last but not least, the same approach lends itself to studies of the properties of shock-waves in electrofluid dynamics. Such studies are of great importance also per se, as basic knowledge.

A second line of research tries to lay down the basic fundamental equations for a more accurate and more realistic study of the structure of the flow field. We have had some examples of

problems connected with the study of such a structure in Prof. Minardi's discussion. There are several interactions between the fluid dynamic and the electrostatic fields which all combine together to originate a complex flow field structure. Before attempting, however, any description of these flow fields one should be very careful and should not leave out important phenomena. One must start from the beginning and describe, adequately and appropriately, the exchanges of matter, energy and momentum between the two fluids (the charged fluid and the neutral one), and the exchanges of momentum and energy between the fluid dynamic and electrostatic fields (not to speak of the ionization process and of the possibility of "non-equilibrium ionization").

This complex and multifaced phenomenology is much too new (also because of the range of parameters within which one is operating). It is to be subject to intensive, detailed studies also in view of the several coupling effects which may be present and whose effects cannot be discarded, light-heartedly and a priori, without adequate justification.

Thus the work that one must do (and which we are presently carrying out) presents itself in three typical stages. First one derives, according to the principle of irreversible thermodynamics, a general formulation of the basic equation which takes into account all possible processes. Second, one individualizes and characterizes the parameters (é. g., the ratios of suitable transport coefficients) which measure the relative importance of the several effects

(including coupling effects). Third, one evaluates the orders of magnitude of these parameters, possibly in the several ranges of interest, in order to be subsequently able to determine, exactly, which phenomena may be neglected and under which conditions.

Let me conclude by expressing the wishes that a workshop be organized again in the future; that it include researchers from other related areas of this new and fascinating science, electrofluid dynamics; and, finally, that this initiative be taken by appropriate panels of AGARD.

## REFERENCES

1. R.N. Cox: "Some Aspects of Ionospheric Aerodynamics" Proceedings of the Third International Symposium on Rarefied Gas Dynamics, Academic Press, 1963.
2. P.M. Chung: "Electrical Characteristics of Couette and Stagnation Boundary Layer Flows of Weakly Ionized Gases" Physics of Fluids, Vol.7, n. 1, Jan. 1964.
3. L.G. Napolitano: "One-dimensional Motions in the Presence of Electromagnetic Fields" (In Italian) - La Termotecnica, n.3, 1966.

INTEREST AND PROGRESS IN ELECTROFLUID DYNAMICS  
AND RELATED RESEARCHES IN ENGLAND

Summary

In the United Kingdom there has been a small sustained interest in electrofluid dynamics over a long period of time, but the main effort has been on plasma research and MHD. Activities in these fields of the Central Electricity Generating Board; the Central Electricity Research Laboratories; the MHD Discussion Group; the Imperial College of Science; and the General Electric Company are discussed. There are by-products of such research of interest to electrofluid dynamics; and some work on EFD is continuing at Reading University and at the Rutherford High Energy Laboratory, Berkshire.



INTEREST AND PROGRESS IN ELECTROFLUID DYNAMICS  
AND RELATED RESEARCHES IN ENGLAND

R. G. Voysey  
Scientific Counsellor  
British Embassy  
Washington, D. C.

In the United Kingdom there has been sporadic interest in electrofluid dynamic generation for over a century. Industrialists, from Lord Armstrong onwards, hoped for practical electrical generation from simple gas or steam flow devices but their experiments produced only small experimental currents. Steam-jet 'electrostatic' generators remained a Victorian drawing-room novelty or a lecture room demonstration. The sparse publication of early work I have seen, suggests that the fundamental problem was usually not realized. A particle of charge (Kelvin's electrion) had not been demonstrated to exist but the electrical field theory was existent which could have explained the severe limitations on output current obliged by the high-voltage gradients which attend a high, non-neutral, space-charge density. The early experiments also showed clearly that high voltage outputs were easily achieved but that currents remained small; also that two-phase fluids gave better results. Yet there seems to have been no clear conception of the device's difficulty.

Thus the last large but unsophisticated experiments, made by Sir Charles Parsons soon after 1930 and reported in the house-journal of his company, showed that only wet steam gave measurable electrical outputs. Sir Charles realized only a subsidiary reason for this. His device injected the required priming of space charge by placing a simple target in a wet steam stream. The water droplets impinging and flung off this

target were electrified, by friction and by induction, and were collected, at much higher potential, further along the steam-pipe. The explanation of the generation of potential in this way was almost certainly familiar in physical terms to Sir Charles from many sources, e.g., through Lord Kelvin's lecture room demonstration of the high-potential generated by zinc-dust falling from a copper funnel. Kelvin is clear that this "gravity-electric" generator depended on two principles. Firstly that initial charging of the zinc-dust took place by the "galvanic potential difference" between zinc and copper (a work-function difference in modern conception). Secondly, that the subsequent climb in potential of the falling dust was due to its enforced separation from the bottom of the funnel by gravity. The viewpoint that the movement of the charge from the earthed funnel generates the voltage by "electrostatic induction", is simple to grasp, but tends to obscure the importance of space-charge effects out in the stream when high currents are sought. There seems no evidence that Sir Charles Parson saw that the space-charge effects in his steam-jet could limit its electrical output and its break-down; nor that a two-fluid medium opened up possibilities of packing more charge, e.g., on to particles of material of high specific inductive capacity, before voltage gradients became intolerable.

Perhaps it is true that most investigators of EFD are attracted by its simplicity and apparent promise before they realize the extreme difficulty of its fundamental snag. Certainly that is how I was drawn into the matter after reading of Parson's work in the archives of his company in 1947 and my conceptions were still optimistic in 1959 when I wrote of it in July 1959 "Research" and thereby encountered the practical work of

W.E. Bennett who had just concluded some experiments which were described in December 1959 "Research", Bennett had the genius and sufficient laboratory resources to construct a small but useful device while being fully aware of the space charge problem. He hoped, as I did, that further experiment might uncover some idea, or construction, that would resolve the problem. Bennett's achievements stimulated some practical interest. The Harwell establishment of the U.K. Atomic Energy Authority made a rather similar apparatus but, it proving the space charge difficulty and suggesting no remedy, their findings were not published. A few theoretical analyses were made in the U.K., e.g. those published by Lawton of the Imperial College of Science in the British Journal of Applied Physics in 1964, but all such were despondent about the limit on the electrical conversion efficiency.

There has, of course, been a general interest in plasma research in the U.K. but it is not very relevant to EFD, because it is more concerned with the very hot and electrically neutral plasmas that are of interest for MHD and nuclear research. Very common, of course, has been work on shock tubes; and there has been a considerable effort on MHD. There is a small but continuing amount of work on plasma jet processes and on electrically augmented flames.

We mounted a fairly large program on MHD in the U.K. It would be misleading to say that we were ever very optimistic about it in the context of large scale generation at which we were aiming.

The largest single program was that of the Central Electricity Generating Board which was to cost in total something over six million dollars,

spread over three years, and was about half spent in 1966. This was rather a bold attempt to make an MHD generator capable of some tens of megawatts output and of a long life compatible with the Central Electricity Board's interest. This resulted in some interesting by-researches including some high intensity combustion chambers, working on various fuels, including coal and oil. These were oxygen assisted in part, but they also ran quite well without. Some work was done on heat exchangers. This was perhaps the most discouraging aspect because the temperatures, of course, had to be very high. There seems very little chance of making such devices cheaply.

The project involved difficult decisions by the Electricity Generating Board. While they did embark, and had a lot of support to do so, I think that most people who were involved in the decision had pretty clearly in mind that by-product research was more likely to be the outcome, rather than a successful MHD duct. Dr. Chester of the Central Electricity Research Laboratories at Leatherhead, Surrey, reported on this work at the Salzburg Conference in June, 1966.

Besides the Electricity Generating Board, the U.K. firms which make large boilers and turbo generators also had a program of their own. In the main, it was a cooperative program on a scale of perhaps a million dollars a year, contributed in kind, not in money. The program was divided among various components like combustion chambers and heat exchangers of various sorts. Each company took on an item, did the work, and made its information freely available to other countries in the group. It is an interesting pattern that is followed also for other things, like alternator

development and transmission line development; but it matured earliest perhaps, in the MHD context where people had more to gain by sharing information on such a speculative matter. I think it is fair to say that if superconductivity had not come along in 1965 and offered a prospect of distinctly better efficiencies for MHD, the MHD project might have been abandoned in 1966. As it is, the super-conductivity prospect was stimulating and itself stimulated by MHD. It still may be true but now seems unlikely that the superconductivity development will ultimately make possible large MHD devices sufficiently cheap and efficient for large scale power generation.

During the past few years there existed an MHD Discussion Group in the U.K. This was started as an informal group by Dr. Ian Fells of the Chemical Engineering Department of Newcastle-in-Tyne, following Symposia at Sheffield University, and originally intended as a university discussion group. It soon became so popular that a number of companies, like oil companies and small companies engaged on MHD and direct generation projects, sought membership. Other people like myself and a representative of the National Research and Development Corporation were also included. The committee had some official blessing, meeting four times a year with expenses paid by the Department of Education and Science. The members of this group leaned toward engineering rather than physics. That is to say, they tended to come out of chemical-technical departments and most of them had physicist's training but, of course, this is not uncommon in technology now. On the other hand, the Chairman, Dr. Fells, took care that the purer physics departments of the country were circulated with information and not

left out. When I had the 1966 visit to the Aerospace Research Laboratories in prospect, I visited some of these other laboratories. They were naturally not much interested in EFD and the publications of related sort which they had made on their plasma work up to that time are well reported in the standard physical literature.

Before I left for the ARL meeting in 1966, I sought an EFD discussion at a meeting of the MHD discussion group. At that meeting, besides seeing MHD progress at the Central Electricity Research Laboratories, we had an hour's discussion of EFD. This discussion was primed with some simple analyses and the general judgment was that EFD seemed unlikely to be very rewarding to large scale electricity generation.

That EFD discussion made clear that gradients of over 40,000 volts per millimeter were needed in order to convert useful fractions of power, and that high gas pressures were then indicated. The only immediate special application of interest seemed to be to take small amounts of power from rocket exhausts. I also felt that it might just be possible to take the very simple sort of device that Bennett made (which was little more than a point-and-ring ionization producer), and to adapt this in assemblies of large numbers to make a cheap EFD wind power generator. One of the defects of EFD is that it can offer very little generation-resistance to the gas-stream. Yet this characteristic is well-matched to wind power. The problem in wind power is to make very cheap structures of large interception area which can take power from low wind velocities yet not be vulnerable to high wind velocities. It is just possible that there is something in this and that some very light and cheap sort of "chicken net" structure

may be constructable in huge areas to take power economically from the wind. Such a device might be so connected as to prime itself firstly from the very low positive ionization normally in the atmosphere, divert the first portion of its output to further self-excitation of ionization from its points and thereafter generate a useful power output from moderate winds (the case of most economic interest). There was also some conjecture at the meeting about alternating current from EFD, and Gourdine's work was discussed but it was then not very well understood in the U.K. The EFD discussion remained pessimistic on the whole.

There were people who were interested in its theoretical facets or in special applications and the University Grants Committee in the U.K. had a number of requests from the universities for grants for this purpose.

Professor Knoernschild at the 1966 ARL meeting mentioned the linear Hall accelerator with a solenoid and an annulus outside carrying a discharge. At that time, in England, in the Physics Department of the Imperial College of Science, they had a slightly different apparatus, a solenoidal RF coil and a DC discharge tube. This, devised by Dr. Haynes, was first put in hand in 1961 and you will find in the Physical Review letters in June 1965 a description of the initial experiment - a meter long tube carrying a centralized, solenoidally-squeezed core discharge. The radio frequency solenoid current interacts with the direct current axial discharge; whichever direction the discharge is going, a net axial thrust comes on the arc and is quite considerable. The device was first suggested as a possible type of ion rocket but this laboratory is rather more interested in nuclear research. The laboratory also has developing a

"plasmatron". This is essentially a large toroid designed to accelerate a discharge and pinch it to try and secure conditions near those of thermonuclearfusion. There is, of course, much thermofusion research going on in the U.K. and I need not refer to it further here.

Since May 1966, the U.K. researches on MHD and EFD have confirmed the difficulties and the unpromising costs for central electricity generation.

The large scale MHD development sponsored by the Central Electricity Generating Board nevertheless yielded some interesting subsidiary experience on combustion and heat exchange, particularly on the subject of superconducting magnets.

In the case of EFD, despite the clear realization of the space-charge problem, practical work is continuing at Reading University (with financial support from the Royal Aircraft Establishment, Farnborough) and at the Rutherford High Energy Laboratory, Berkshire. (Dr. W.D. Allen.) The latter work has included experiments on a rig provided by Gourdine and, more recently, a closed-circuit rig with modest pressure drops and currents, which allows useful studies of fields and breakdown strengths. Otherwise most U.K. interest in EFD is at the level of paper study and discussion.



BIBLIOGRAPHY

Research papers concerned with electrofluid dynamic power generation have appeared widely scattered throughout technical publications and meetings. Because of this great diversification, the following bibliography of EFD power generation "literature" has been compiled as an aid to the person unfamiliar with the field. No special attempt has been made to be absolutely complete, however, the list is believed to include the vast majority of papers, particularly those which have appeared in the United States in recent years. Additionally, some references pertaining to the converse process of EFD pressure generation are included.

1. T. Gunzler, K. Martinot, and M.C. Gourdine, "Electrogasdynamic Power Generation-II", 1968 Intersociety Energy Conversion Engineering Conference, Boulder, Colorado (13-16 August 1968).
2. J.E. Minardi, "Computer Study of Electrofluid Dynamic Colloid Generator", 1968 Intersociety Energy Conversion Engineering Conference, Boulder, Colorado (13-16 August 1968).
3. J.E. Minardi, "Theoretical and Analytical Research Study of Axisymmetric Electrofluid Dynamic Energy Conversion Processes", Final Report, Contract AF 33(615)-3203, Aerospace Research Laboratories, WPAFB, Ohio (August 1968).
4. M.C. Gourdine, "Electrogasdynamics", Science and Technology, pp 50-56, (July 1968).
5. H. Brandmaier, "Electrofluid Dynamic Generator Performance Limits", AIAA Journal, Vol 6, Nr 6, pp 1166-1168 (June 1968).
6. Marks Polarized Corporation, "Experimental Investigation of a High Pressure, High Voltage Electrogasdynamic Generator", Final Report, Contract NOW-0582-c, Bureau of Naval Weapons, Washington, D.C., (December 1967).

7. E.M. Walsh, "Electrostatic Energy Conversion", IEEE Spectrum, Vol 4, Nr 12, pp 57-62, (December 1967).
8. K.K. Joshi, "Electrical Charging of Liquid Sprays in High Pressure Gas Flows for Electrofluid Dynamic Processes", IEEE International Electron Devices Meeting, Washington, D.C. (18-20 October 1967).
9. G. Kvitek, "Fundamental Limitations of EHD Energy Converters", IEEE International Electron Devices Meeting, Washington, D.C. (18-20 October 1967).
10. J. Decaire and M. Lawson, "Outlook for Electrofluid Dynamic Power Generation", ASME Paper 67-PWR-11, ASME-IEEE Joint Power Generation Conference, Detroit, Michigan, (24-28 September 1967).
11. H.E. Brandmaier, "The Major Problem in Electrofluid Dynamic Power Generation", Advances in Energy Conversion Engineering-ASME pp 457-464 (1967) (Papers presented at 1967 Intersociety Energy Conversion Engineering Conference, Miami Beach, Florida, 14-17 August 1967).
12. P.L. Cowan, T. Gunzler, R. Kulka, and M.C. Gourdine, "Electrostatic Power Generation", Advances in Energy Conversion Engineering-ASME pp 435-455 (1967) (Papers presented at the 1967 Intersociety Energy Conversion Engineering Conference, Miami Beach, Florida, 14-17 August 1967).
13. J. Decaire and M. Lawson, "Investigation on Power Generation Using Electrofluid Dynamic Processes", Advances in Energy Conversion Engineering-ASME pp 473-483 (1967) (Papers presented at the 1967 Intersociety Conversion Engineering Conference, Miami Beach, Florida, 14-17 August 1967).
14. J. Decaire and J. Wifall "Charge Generation by Corona Discharge in Electrofluid Dynamic Energy Conversion Processes", Advances in Energy Conversion Engineering-ASME pp 465-471 (1967) (Papers presented at the 1967 Intersociety Energy Conversion Engineering Conference, Miami Beach, Florida, 14-17 August 1967).
15. G. Kvitek, "Feasibility of Colloidal Electrostatic Energy Converters for Space Use", 1967 Intersociety Energy Conversion Engineering Conference (14-17 August 1967).
16. H.E. Brandmaier and T.H. Dimmock, "Factors Influencing Electrofluid Dynamic Power Generation", Journal of Spacecraft and Rockets, Vol 4, Nr 8, pp 961-966, (August 1967).
17. W. Stevenson Bacon, "Electricity From a Stream of Air And Water", Popular Science, Vol 192, Nr 2, pp 80-81 (August 1967).

18. A.G.Bailey, "Charged-Particle Production in the Electrodynamic Generator", Electronic Letters, Vol 3, Nr 6, (June 1967).
19. H. Brandmaier, "Radial Space Charge Fields in Electrofluid Dynamic Generators", AIAA Journal, Vol 5, Nr 5, pp 1037-1039 (May 1967).
20. P.L. Cowan, M.C. Gourdine, and D. H. Malcolm, "Developments in Central Station EGD Power Generation", Eighth Symposium on Engineering Aspects of Magnetohydrodynamics, Stanford University, Stanford, California, (28-30 March 1967).
21. J. Decaire and M. Lawson, "Electrofluid Dynamic Power Generation: Trends and Expectations", Eighth Symposium on Engineering Aspects of Magnetohydrodynamics, Stanford University, Stanford, California, (28-30 March 1967).
22. H. Brandmaier, T.H. Dimmock, and B. Kahn, "Research on Power Generation Electrodynamic Energy Conversion", ARL Report 67-0008, Aerospace Research Laboratories, WPAFB, Ohio (January 1967).
23. A.M.Marks, "Heat Electrical Power Transducer", U.S. Patent Nr 3,297,887 (10 January 1967).
24. C.W. Tan, "The Prospects for Electrodynamic for Terrestrial Applications", AIAA Paper Nr 66-1008, AIAA Third Annual Meeting, Boston, Massachusetts (29 November - 2 December 1966).
25. E. Herzog, "Electrofluid Dynamic Generator Supplying an A.C. Electric System-A Feasibility Study", Final Report, Contract AF 33(615)-1915, Aerospace Research Laboratories, WPAFB, Ohio (November 1966).
26. J. Decaire, "The Effects of Partial Condensation Around Ions in Electrofluid Dynamic Energy Conversion Processes", ARL Report 66-0187, Aerospace Research Laboratories, WPAFB, Ohio (September 1966).
27. E.L. Daman and M.C. Gourdine, "Electrodynamic Power Generation", International Symposium on Magnetohydrodynamic Power Generation, Paper SM-74/197, Salzburg, Austria (July 1966).
28. H.E. Brandmaier and B. Kahn, "Recent Advances in Electrofluid Dynamic Power Generation", IEEE International Convention Record, IEEE Vol 14, Part 7, pp 28-37 (1966).
29. Maremont Corporation, "Charged Particle Power Generation and Propulsion Final Report Contract N0w 64-0594-f, Bureau of Naval Weapons, Washington, D.C. (15 July 1966) AD488253.
30. Invitational Working Electrofluid Dynamic Energy Conversion Conference, Aerospace Research Laboratories, WPAFB, Ohio (24-26 May 1966). AGARDO-graph 122, "Selected Topics in Electrofluid Dynamic Energy Conversion (1968).

31. J.F. Hughes and P.E. Secker, "Liquid Filled Electrostatic Generator" Electronics Letters, Vol 2, Nr 5, pp 174-175, (May 1966).
32. F.D. Yeaple, "Electrogas dynamics - A Bold New Power Source", Production Engineering, Vol 37, pp 90-92 (May 1966).
33. H.H. Chiu, H. Brandmaier, and B. Kahn, "Two-Dimensional Electro Fluid Dynamic Channel Flow", Seventh Symposium on Engineering Aspects of Magnetohydrodynamics, Princeton University, Princeton, New Jersey, (30 March-1 April 1966).
34. M. Hawes, "Electrofluid Dynamic Working Media for Direct Energy Conversion Processes", OAR Research Review, Vol V, Nr 1, pp 5-9, (March 1966).
35. M.O. Lawson, "Electrofluid Dynamic (EFD) Power Generation Processes", OAR Research Review, Vol IV, Nr 12, pp 17-18, (February 1966).
36. F. Wattendorf, H. von Ohain, M. Lawson, and S. Hasinger, "High Voltage Electrostatic Generator", U.S. Patent Nr 3,225,225 (21 December 1965).
37. M. Hawes, "Relative Dielectric Strengths at High Pressures of Selected Gases and Mixtures Suitable as Transport Media in Electrofluid Dynamics", Unpublished Thesis, Department of Electrical Engineering, The Ohio State University, Columbus, Ohio (1965).
38. M.C. Gourdine and D. H. Malcolm, "Propect for Electrogasdynamic Power", Engineering Developments in Energy Conversion-ASME pp 58-75, (Papers presented at International Conference on Energetics, University of Rochester, Rochester, New York, 18-20 August 1965).
39. J.C. Shiue, B. Kahn, and H. Brandmaier, "An Experimental Investigation of the Performance Characteristics of an Electrogasdynamic Power Generator", Engineering Developments in Energy Conversion-ASME pp 76-93 (Papers presented at International Conference on Energetics, University of Rochester, Rochester, New York, 18-20 August 1965).
40. K. Wang, "Analytic Solution for a Two-Dimensional, Axisymmetric EGD Conversion Channel", Engineering Developments in Energy Conversion-ASME pp 95-109 (Papers presented at International Conference on Energetics, University of Rochester, Rochester, New York, 18-20 August 1965).
41. J. Decaire and M. Lawson, "Experimental Investigations on Power Generation Using Electrofluid Dynamic Processes", AIAA Sixth Biennial Gas Dynamics Symposium, Northwestern University, Evanston, Illinois, (25-27 August 1965).
42. M.C. Gourdine and D.H. Malcolm, "Feasibility of an EGD High Voltage Power Source", 19th Annual Power Sources Conference, Atlantic City, New Jersey (May 1965).

43. A. Maciulaitis, "A Theoretical Investigation of Electrofluid Dynamic Propulsion in the Earth's Atmosphere", Grumman Research Department Report RE-204, Grumman Aircraft Engineering Corporation, Bethpage, New York (March 1965).
44. B. Kahn, "A Continuation of the Basic Study of Slender Channel Electrogasdynamics", ARL Report 65-4, Aerospace Research Laboratories, WPAFB, Ohio (January 1965), AD 614907.
45. M.P. Khan, "High Voltage Electrogasdynamic Generators", ASME Winter Annual Meeting, New York, New York, ASME Paper 64-WA/ENER-11 (29 November - 4 December 1964).
46. J. Mantel, "Der gegenwärtige Stand der E.H.D.-Forschung", Institut für Plasmaphysik-IPP 4/17, Garching bei München (December 1964).
47. M. Lawson and H. von Ohain, "Direct Electrofluid Dynamic Energy Conversion Processes for Power Generation", 11th Annual Air Force Science and Engineering Symposium, Brooks Air Force Base, Texas (20-22 October 1964)
48. M.C. Gourdine and B. Kahn, "Electrogasdynamic Power Generation", AIAA Journal, Vol 2, Nr 8, pp 1423-1427 (August 1964).
49. J.R. Roland, "Performance and Fluid Flow Characteristics of an Electrofluid Dynamic Generator", Unpublished Thesis GA/ME/64-5, Air Force Institute of Technology, WPAFB, Ohio (August 1964).
50. J.R. Wifall, "Ion Cloud Shape and Potential Distribution in an Electrofluid Dynamic Generator", Unpublished Thesis GAM/ME/64-22, Air Force Institute of Technology, WPAFB, Ohio (June 1964).
51. J.E. Collins, Jr. and A.J. Wilson, III, "Determination of the Ion Producing Scaling Trends for an Electrofluid Dynamic Generator", Unpublished Thesis GAM/ME/64-4, Air Force Institute of Technology, WPAFB, Ohio (June 1964).
52. J. Lawton, "The Generation of Electricity by Aerodynamic Conveyance of Space Charge", British Journal of Applied Physics, Vol 15, pp 935-939 (1964).
53. M.C. Gourdine, E. Barreto, and M.P. Khan, "On The Performance of Electrogasdynamic Generators", Fifth Symposium on Engineering Aspects of Magnetohydrodynamics, Massachusetts Institute of Technology, Boston, Mass. pp 161-171 (1-2 April 1964).
54. H. von Ohain and F. Wattendorf, "Potentialities of Direct Electrofluid Dynamic Energy Conversion Processes for Power Generation", Sixth AGARD Combustion and Propulsion Colloquium, Cannes, France (16-20 March 1964). ARL Report 64-73, Aerospace Research Laboratories, WPAFB, Ohio (October 1964). AGARDograph 81, "Energy Sources and Energy Conversion", pp 539-630 (1967).

55. M.O. Lawson, "Performance Characteristics of Electrofluid Dynamic Energy Conversion Processes Employing Viscous Coupling", Sixth AGARD Combustion and Propulsion Colloquium, Cannes, France (16-20 March 1964). ARL Report 64-74, Aerospace Research Laboratories, WPAFB, Ohio (October 1964). AGARDograph 81 "Energy Sources and Energy Conversion" pp 539-630 (1967)
56. M.O. Lawson, "Ion Generation by Corona Discharge for Electrofluid Dynamic Energy Conversion", Sixth AGARD Combustion and Propulsion Colloquium, Cannes, France (16-20 March 1964). ARL Report 64-76, Aerospace Research Laboratories, WPAFB, Ohio (October 1964). AGARDograph 81 "Energy Sources and Energy Conversion" pp 539-630 (1967) AD 455870
57. S. Hasinger, "Performance Characteristics of Electro Ballistic Generators", Sixth AGARD Combustion and Propulsion Colloquium, Cannes, France (16-20 March 1964). ARL Report 64-75, Aerospace Research Laboratories, WPAFB, Ohio (October 1964). AGARDograph 81 "Energy Sources and Energy Conversion" pp 539-630 (1967)
58. M. Hawes, "Experimental Techniques in Electrofluid Dynamic Energy Conversion Research", Sixth AGARD Combustion and Propulsion Colloquium Cannes, France (16-20 March 1964). ARL Report 64-77, Aerospace Research Laboratories, WPAFB, Ohio (October 1964). AGARDograph 81 "Energy Sources and Energy Conversion" pp 539-630 (1967) AD 455788
59. S. Hasinger, M. Hawes, M. Lawson, H. von Ohain, F. Wattendorf, "Electrofluid Dynamic Energy Conversion Processes for Power Generation", Sixth AGARD Combustion and Propulsion Colloquium, Cannes, France (16-20 March 1964).
60. A. Marks, E. Barreto, C.K. Chu, "Charged Aerosol Energy Converter" AIAA Journal, Vol 2, Nr 1, pp 45-51 (January 1964)
61. Marks Polarized Corporation, "The Conversion of Heat to Electrical Power by Means of a Charged Aerosol", Final Report on Contract N0w 63-0225-c, Bureau of Naval Weapons, Washington, D.C. (30 December 1963) AD 429304
62. M.C. Gourdine and B. Kahn, "A Basic Study of Slender Channel Electro-gasdynamics", ARL Report 63-205, Aerospace Research Laboratories, WPAFB, Ohio (November 1963), AD427967
63. A.L. Cox, "Colloidal Electrohydrodynamic Energy Converter", AIAA Journal, Vol 1, Nr 11, pp 2491-2497 (November 1963), ARS Space Power Systems Conference, Santa Monica, California (25-28 September 1962)

64. A.M. Marks, "State of the Art Paper on the Charged Aerosol (EHD) Generator", Prepared for Executive Office of the President, Office of Science and Technology, Washington, D.C. (August 1963).
65. P.J. Butkewicz, "Pressure and Geometry Effects on an Electrohydrodynamic Generator", Unpublished Thesis GAE/ME/63-3, Air Force Institute of Technology, WPAFB, Ohio (August 1963)
66. A.J.Dobrzelecki, "Efficiency Characteristics of a Recirculating Ejector", Unpublished Thesis GAE/ME/63-4, Air Force Institute of Technology, WPAFB, Ohio (August 1963)
67. L.K.McCallon, "Effect of Diffuser Configuration on Fluid Dynamic Energy Transfer in Recirculating Ejectors", Unpublished Thesis GAE/ME/63-9, Air Force Institute of Technology, WPAFB, Ohio (August 1963)
68. J.G. Rutter, "Study of Electrofluid Dynamic Energy Conversion Using a Recirculating Ejector", Unpublished Thesis GAE/ME/63-10, Air Force Institute of Technology, WPAFB, Ohio (August 1963)
69. J.P. Sutherland and J.W. Storr, "The Electrical Characteristics of an Electrohydrodynamic Generator for an Alternating Input", Unpublished Thesis GA/Phys/63-11,12, Air Force Institute of Technology, WPAFB, Ohio (August 1963)
70. O.M.Stuetzer, "Fundamentals of EHD Power Generation", Proceedings of the Symposium on Electrostatic Energy Conversion, PIC-ELE 209/1, Interagency Advanced Power Group (May 1963) AD 406990
71. M.C. Gourdine, "Slender Channel EGD Power Generation", Proceedings of the Symposium on Electrostatic Energy Conversion, PIC-ELE 209/1, Interagency Advanced Power Group (May 1963) AD 406990
72. A.M. Marks, "The Charged Aerosol Generator", Proceedings of the Symposium on Electrostatic Energy Conversion, PIC-ELE 209/1, Interagency Advanced Power Group (May 1963) AD 406990
73. A.L. Cox and S. Harrison, "High Voltage Colloidal Energy Converter", Proceedings of the Symposium on Electrostatic Energy Conversion, PIC-ELE 209/1, Interagency Advanced Power Group (May 1963) AD 406990
74. M.R. Merriman, "Investigations on Particle-Type Electrostatic Generators", Proceedings of the Symposium on Electrostatic Energy Conversion, PIC-ELE 209/1, Interagency Advanced Power Group (May 1963) AD 406990
75. J.M. Smith, "Performance Criterion for EHD Generators", Proceedings of the Symposium on Electrostatic Energy Conversion, PIC-ELE 209/1, Interagency Advanced Power Group (May 1963) AD 406990

76. Marks Polarized Corporation, "The Conversion of Heat to Electrical Power by Means of a Charged Aerosol", Final Report on Contract N0w 62-0644-C, Bureau of Naval Weapons, Washington, D.C. (April 1963) AD 403536
77. Marks Polarized Corporation, "The Conversion of Heat to Electrical Power by Means of a Charged Aerosol", Final Report on Contract N0w 60-0831-C, Bureau of Naval Weapons, Washington, D.C. (November 1962)
78. H.P. Wheeler, Jr., "The Volt-Ampere Characteristics of an Electrohydrodynamic Generator", Unpublished Thesis GAE/ME/62-8, Air Force Institute of Technology, WPAFB, Ohio (August 1962)
79. T.N. Lauritsen, "Ion Production and Flow in an Electrohydrodynamic Generator", Unpublished Thesis GAE/ME/62-3, Air Force Institute of Technology, WPAFB, Ohio (August 1962)
80. O.M. Stuetzer, "Magnetohydrodynamics and Electrohydrodynamics", The Physics of Fluids, Vol 5, Nr 5, pp 534-544 (May 1962)
81. K. Janner, S. Magun, and E. Schopper, "A Van de Graaff High Voltage Generator Using Liquid Charge Carrier", Technical Note FRL-TN-97, Feltman Research Laboratories, Picatinny Arsenal, Dover, New Jersey, (March 1962) AD273127
82. J.M. Smith, "Electrohydrodynamic Power Generation-Experimental Studies", GE Space Sciences Laboratory Report R62SD27 (March 1962)
83. A. Sherman, et.al., "Study of Electrical Energy Conversion Systems", Technical Report Nr ASD-TR-61-704, Aeronautical Systems Division, WPAFB, Ohio (February 1962) AD 274923
84. G.V. Jorgenson and E. Will, "Improved Ion Drag Pump", Review of Scientific Instruments, Vol 33, Nr 1, pp 55-56, (January 1962)
85. M. Lawson, H. von Ohain, and F. Wattendorf, "Performance Potentialities of Direct Energy Conversion Processes Between Electrostatic and Fluid Dynamic Energy", ARL Report 178, Aerospace Research Laboratories, WPAFB, Ohio (December 1961) AD 273015
86. J.M. Smith "Theoretical Study of the Electrohydrodynamic Generator" GE Space Sciences Laboratory Report R61SD192 (November 1961) AD 271768
87. A. Sherman, et. al., "Study of Electrical Energy Conversion Systems", ASD Technical Report 61-370, Aeronautical Systems Division, WPAFB, Ohio (1961)



88. M. Pauthenier, "Generators with Streams of Electrified Particles" Technical Note FRL-TN-41, Feltman Research Laboratories, Picatinny Arsenal, Dover, New Jersey, (1961) AD 257487
89. O.M. Stuetzer, "Ion Transport High Voltage Generators", Review of Scientific Instruments, Vol 32, Nr 1, pp 16-22, (January 1961)
90. M.C. Gourdine, "One-Dimensional Electrogasdynamics", Report Nr PLR-76, Plasmadyne Corporation, Santa Ana, California (August 1960)
91. M.C. Gourdine, "Power Addition and Extraction from Gas Flow by Means of Electric Wind", JPL Report Nr 32-18, Jet Propulsion Laboratory, California Institute of Technology, Pasadena, California (June 1960)
92. M.C. Gourdine, "Power Generation by Means of the Electric Wind", JPL Report Nr 32-6, Jet Propulsion Laboratory, California Institute of Technology, Pasadena, California (April 1960)
93. O.M. Stuetzer, "Ion Drag Pumps", Journal of Applied Physics, Vol 31, pp 136-146, (1960)
94. M.C. Gourdine, "Electrogasdynamic Channel Flow", JPL Report Nr 32-5, Jet Propulsion Laboratory, California Institute of Technology, Pasadena, California (January 1960)
95. W.E. Bennett, "The Generation of Direct Current at High Potentials", Research Applied in Industry, Vol 12, Nr 12, pp 455-459, (December 1959)
96. S. Krapf, "Ein Neues Prinzip eines Gleichstromgenerators", Energie Vol 4, pp 297-300 (1959)
97. O.M. Stuetzer, "Instability of Certain Electrohydrodynamic Systems" Physics of Fluids, Vol 2, pp 642-648 (1959)
98. O.M. Stuetzer, "Ion Drag Pressure Generation", Journal of Applied Physics, Vol 30, Nr 7, pp 984-994 (July 1959)
99. N.L. Petruzzella, "Corona Discharge-Aerodynamic Ion Flow Study", Senior Independent Study, P 383-4, Antioch College, Yellow Springs, Ohio (1959)
100. W.P. Smith, "Electrostatic Voltage Power Generator", U.S. Patent Nr 2,643,349 (23 June 1953)
101. A.M. Marks, "Heat-Electrical Power Conversion Through the Medium of a Charged Aerosol", U.S. Patent Nr 2,638,555 (12 May 1953)
102. M. Morand, A. Raskin, and L. Winand, Comptes Rendus Academie des Sciences, Paris, Vol 234, p 2450 (1952)

103. M. Moreau-Hanot, Comptes Rendus Academie des Sciences, Paris, Vol 206, p 1168 (1939)
104. M. Morand and A. Raskin, Bulletin of the Royal Society of Sciences of Liege, Vol 3-4, p 176 (1938)
105. M.M. Pauthenier, M. Moreau-Hanot, Le Journal de Physique et le Radium, Vol 8, p 193 (1937)
106. M. Moreau-Hanot, Comptes Rendus Academie des Sciences, Vol 204, p 1549 (1937)
107. R.E. Vollrath, "A High Voltage Direct Current Generator", Physical Review, Vol 42, pp 298-304 (October 1932)

<p>AGARDograph 122 North Atlantic Treaty Organization, Advisory Group for Aerospace Research and Development SELECTED TOPICS IN ELECTROFLUID DYNAMIC ENERGY CONVERSION 1968 264 pages Editors: M.O. Lawson and F.L. Wattendorf</p> <p>Electrofluid dynamic (EFD) energy conversion processes have only in recent years received renewed interest as an area of research. EFD processes are of particular interest for directly converting fluid dynamic energy into electrical energy without the use of moving parts. This AGARDograph is based largely on presentation of EFD research or related research being conducted in each NATO nation represented at the Electrofluid Dynamic "Workshop" Conference which was held at the Aerospace Research Laboratories, Wright-Patterson Air Force Base, Ohio, 23-25 May 1966; subsequently, many of the papers were updated at an editorial conference held at AGARD, Paris, 30-31 October 1967, while others still later, were updated by correspondence.</p>	<p>538.4: 533.95</p> <p>Electrofluid Dynamics Energy Conversion Conferences</p>	<p>AGARDograph 122 North Atlantic Treaty Organization, Advisory Group for Aerospace Research and Development SELECTED TOPICS IN ELECTROFLUID DYNAMIC ENERGY CONVERSION 1968 264 pages Editors: M.O. Lawson and F.L. Wattendorf</p> <p>Electrofluid dynamic (EFD) energy conversion processes have only in recent years received renewed interest as an area of research. EFD processes are of particular interest for directly converting fluid dynamic energy into electrical energy without the use of moving parts. This AGARDograph is based largely on presentation of EFD research or related research being conducted in each NATO nation represented at the Electrofluid Dynamic "Workshop" Conference which was held at the Aerospace Research Laboratories, Wright-Patterson Air Force Base, Ohio, 23-25 May 1966; subsequently, many of the papers were updated at an editorial conference held at AGARD, Paris, 30-31 October 1967, while others still later, were updated by correspondence.</p>	<p>538.4: 533.95</p> <p>Electrofluid Dynamics Energy Conversion Conferences</p>
<p>AGARDograph 122 North Atlantic Treaty Organization, Advisory Group for Aerospace Research and Development SELECTED TOPICS IN ELECTROFLUID DYNAMIC ENERGY CONVERSION 1968 264 pages Editors: M.O. Lawson and F.L. Wattendorf</p> <p>Electrofluid dynamic (EFD) energy conversion processes have only in recent years received renewed interest as an area of research. EFD processes are of particular interest for directly converting fluid dynamic energy into electrical energy without the use of moving parts. This AGARDograph is based largely on presentation of EFD research or related research being conducted in each NATO nation represented at the Electrofluid Dynamic "Workshop" Conference which was held at the Aerospace Research Laboratories, Wright-Patterson Air Force Base, Ohio, 23-25 May 1966; subsequently, many of the papers were updated at an editorial conference held at AGARD, Paris, 30-31 October 1967, while others still later, were updated by correspondence.</p>	<p>538.4: 533.95</p> <p>Electrofluid Dynamics Energy Conversion Conferences</p>	<p>AGARDograph 122 North Atlantic Treaty Organization, Advisory Group for Aerospace Research and Development SELECTED TOPICS IN ELECTROFLUID DYNAMIC ENERGY CONVERSION 1968 264 pages Editors: M.O. Lawson and F.L. Wattendorf</p> <p>Electrofluid dynamic (EFD) energy conversion processes have only in recent years received renewed interest as an area of research. EFD processes are of particular interest for directly converting fluid dynamic energy into electrical energy without the use of moving parts. This AGARDograph is based largely on presentation of EFD research or related research being conducted in each NATO nation represented at the Electrofluid Dynamic "Workshop" Conference which was held at the Aerospace Research Laboratories, Wright-Patterson Air Force Base, Ohio, 23-25 May 1966; subsequently, many of the papers were updated at an editorial conference held at AGARD, Paris, 30-31 October 1967, while others still later, were updated by correspondence.</p>	<p>538.4: 533.95</p> <p>Electrofluid Dynamics Energy Conversion Conferences</p>



